(NASA-CR-143374) ANALYSIS AND DESIGN OF A CAPSULE LANDING SYSTEM AND SURFACE VEHICLE CONTROL SYSTEM FOR MARS EXPLORATION Progress Report, 1 Jul. 1974 - 30 Jun. 1975 (Rensselaer Polytechnic Inst.) 167 p HC

N75-30243

Unclas
G3/18 34268

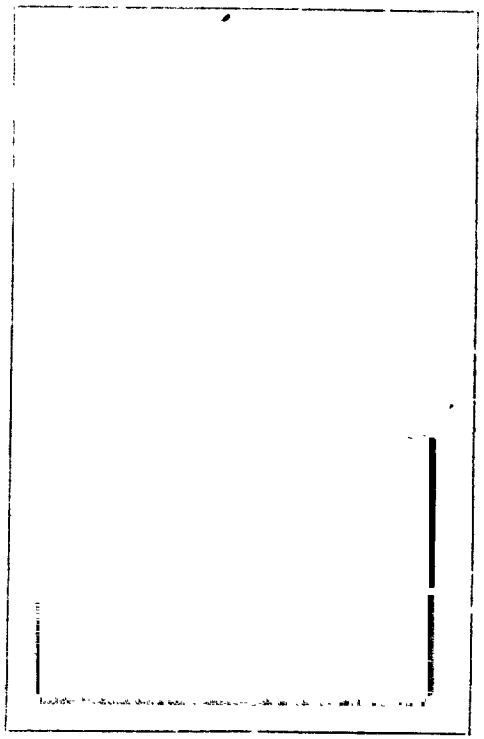

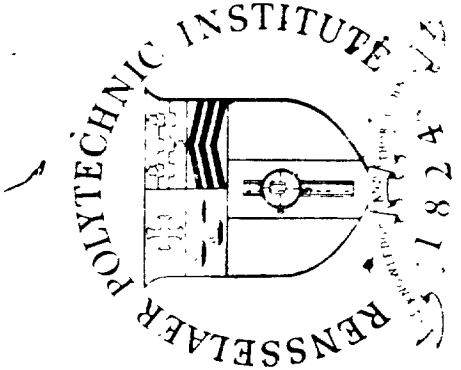

ABSTRACT

Problems related to an unmanned exploration of the planet Mars by means of an autonomous roving planetary vehicle have been investigated. These problems include: design, construction and evaluation of the vehicle itself and its control and operating systems. More specifically, vehicle configuration, dynamics, control, propulsion, hazard detection systems, terrain sensing and modeling, obstacle detection concepts, path selection, decision-making systems, and chemical analyses of samples have been studied.

Although earlier work along these lines had been focused on a vehicle which would house, transport and service scientific equipment for on-site analysis, more recent work has been directed to a vehicle capable of gathering specimens and data for an Augmented Viking Mission or to provide the basis for a Sample Return Mission.

The following tasks have been under active study: design, construction and testing of a dynamic vehicle, (weight exclusive of scientific payload of 150-200 pounds); mathematical modeling and experimental measurement of the vehicle dynamics; propulsion and deployment systems; electro-mechanical control systems; telemetry systems to permit autonomous off-board control; collapsibility concepts and hardware; design, construction and evaluation of double-hoop toroidal wheels; design and evaluation of a triangulation-based hazard detection system; obstacle perception by edge enhancement techniques; terrain modeling based on gradients; obstacle classification; path selection systems simulations and evaluations; gas chromatograph systems design concepts; experimental gas chromatograph separation measurements; and gas chromatograph model developments.

These tasks and other subtasks are defined in detail and the progress which has been achieved during the period July 1, 1974 to June 30, 1975 is summarized.

The educational impact of this project for the year has been assessed. A detailed report on the education implications of this NASA project at Rensselaer over the past eight years is included as Appendix A.

TABLE OF CONTENTS

Analysis and Design of a Capsule Landing System and Surface Vehicle Control System for Mars Exploration

I. Introduction

Current national goals in space exploration include a detailed study and examination of the planet Mars. The effectiveness of Mars exploration missions would be enhanced according to the extent to which the investigative devices which are landed are mobile, to the range of their mobility, and to the ability to control their motion. In order to achieve basic mission objectives, and beyond that, to maximize the return on the commitment of resources to the mission, formidable technical problems must be resolved. The major factor contributing to these problems is the round trip communications time delay between martian and earth control stations which varies from a minimum of about 9 minutes to a maximum of 25 minutes. This time delay imposes stringent requirements on the vehicle, on its control and communication systems and on those systems included on board to make the scientific measurements, in terms of their ability to function autonomously. These systems must be able to operate with a high degree of reliability and must be capable of calling for earth control under appropriate circumstances.

A number of important problems originating with these factors and relating directly the basic mission objectives of an unmanned exploration of Mars have been and are currently being investigated by a faculty-student project team at Rensselaer Polytechnic Institute with the support of NASA Grant NGL 33-018-091.

In addition to the technical objectives, the project is intended to involve students in meaningful design and problem-solving activities and by so doing to enhance their formal education in the area of design.

This progress report describes the tasks which have been undertaken and documents the progress which has been achieved in the interval July 1, 1974 to June 30, 1975 in addition to appraising the educational implications of the project.

II. Overview of the Project

For a number of years, the thrust of the project was derived from the objective of autonomous roving laboratory capable of a range of at least 1000 kilometers and a minimum operational life of one year. More specifically, Rensselaer's goal was to conceive, design and evaluate a roving vehicle concept together with the necessary hazard detection and control systems which could house, protect, service and transport the scientific instruments required to gain the desired biological, chemical and geological data.

However, the Viking project experience has cast considerable doubt on the feasibility of a sophisticated roving laboratory for purposes of a thorough unmanned exploration of Mars. This is not to say that the Viking project will not meet the prime mission objectives but rather to suggest that the far higher level goals anticipated for subsequent rover missions may well be met far better by alternative strategies.

The basic problem orginates with the extreme difficulty of miniaturizing scientific instruments and apparatus and of building in the minimal level of adaptability required to deal with unforeseen or unanticipated situations.

Two strategies which appear to have significant potential have been identified: (a) a series of Viking-type landers each of which would contain specialized equipment for a particular set of scientific studies but none of which would attempt to house all of the equipment required for a thorough exploration, and (b) sample return missions which would bring back specimens to earth for detailed analysis in earth laboratories. At this time, the preference of the scientific community appears to be a sample return mission which has the advantage of using the very superior capabilities of earth-based laboratories for martian samples analysis.

However, for either of these strategies to be viable, it has been concluded that some kind of a roving vehicle capable of gathering samples and returning them to the stationary lander will be required. Although the minimum capabilities of such a sample gathering rover have not been established an estimate of the range can be made. The size of the two sigma landing site footprint is of the order of 100 x 200 kilometers. Furthermore the areas considered attractive by scientists after analysis of the Mariner Orbitor Missions are too dangerous for landing either of a Viking-type of lander or a sample return vehicle. Thus it would appear that a sample-gathering rover capable of a 300 kilometer radial displacement would be required. Depending on the nature of the terrain between the landing site and the sample procurement locations, the displacement distance between these two, the capabilities of the rover and the effectiveness of hazard detection and path selection systems, the total distance to be traversed could be as high as 1500 to 2500 kilometers.

Given this overall situation, the thrust of the project was redirected in January of 1975 with the concurrence of the Office of Planetary Studies and the Jet Propulsion Lab towards the conception, design and evaluation of a mini-rover capable of augmenting Viking-type lander missions or enabling a sample return mission. The redirection of the project is more a matter of emphasis than of substance since the basic goals remain to develop a vehicle of exceptional mobility and reliability together with the hazard detection and path selection systems required for autonomous roving. A sample gathering mission imposes stringent requirements on a vehicle in terms of its ability to negotiate hazardous terrain, its maneuverability in avoiding truly hazardous situations, its hazard detection systems and its path selection decision making system.

Since January 1975 the major emphasis has been directed to tasks relating directly to a vehicle designed for a sample and data gathering mission. Beyond this emphasis, work has continued in the area of gas chromatographic systems analysis and design. The following major tasks have been under study:

A. Vehicle Configuration, Control, Dynamics, Systems and Propulsion
The objective of this task is to conceive, design and evaluate a roving vehicle for data and sample gathering during an unmanned exploration of Mars. Included are the aspects of vehicle configuration, collapsibility for launch configuration, deployment, dynamics, and motion and attitude control. One goal is to develop a vehicle concept capable of operating within the constraints of a Mars mission involving an augmented Viking or a sample return vehicle and of adapting to changes in the mission as a result of the information gathered during the exploration. The second goal is to construct a rover which can serve as a test bed for the evaluation of hazard detection and avoidance systems.

B. Hazard Detection Systems. The objective of this task is to conceive, develop, construct and evaluate a short range (0.5 to 2.5 meter) hazard detection system to provide data for an onboard path selection decision making system.

C. Path Selection Systems. The objective of this task is the simulation and evaluation of path selection systems with particular emphasis on the development of path selection algorithms. This task is also responsible for providing guidance for the design of hazard detection hardware.

D. Obstacle Detection and Terrain Modeling. This task is concerned with the problem of detecting obstacles and modeling terrain for the purpose of path selection.

E. Chemical Analysis of Specimens. A major objective of martian surface exploration will be to obtain chemical, biochemical or biological information. Many experiments proposed for the mission require a general duty, gas chromatograph-mass spectrometer system for chemical analysis. The objective of this task is to generate fundamental data and concepts required to optimize this chemical analysis system.

The project milestones for the past year and as planned for the period July 1, 1975 to June 30, 1976 are shown in Figure 1.

III. Summary of Results

Task A. Vehicle Configuration, Control, Dynamics, Systems and Propulsion

This broad task has been subdivided into the following subtasks: experimental and analytical studies of vehicle dynamics; detailed design of structural components; design of deployment hardware; motor drive and mechanical transmission details; development of a deployment procedure; detailed wheel design and construction; on-board controls for steering, motor drive for levelizing, deployment and emergency maneuvers; radio link for remote operation; and remote control station and transmitter design.

A.1. Vehicle Dynamics

On the basis of observed dynamical behavior of the vehicle during extensive field testing, a review of dampening alternatives was undertaken. A two-dimensional, two-degree of freedom dynamic model was used to select parameters for rotational dampening of the rear struts. The vehicle dynamical response has been much improved by the addition of rotational dampers.

A.2. Structural Aspects Including Propulsion

Following extensive field testing during the summer and early fall of 1974, the vehicle was disassembled and the components were examined for wear and failure indications. It was determined that design changes in the front end and torsion bar assembly were desirable. These changes have been implemented. Sensors have also been mounted such that the orientation of all major structural members will be known relative to the payload box. The data provided by these sensors in concert with the attitude gyro data will provide unambigious vehicle state parameters to the remote controller. A laboratory obstacle course has been constructed and can be used to evaluate the vehicle's ability to negotiate special terrain features and the validity of the structural component position sensors.

RENSSELAER MARS PROJECT ASK ORGANIZATION AND MILESTONES (FEBRUARY 1975 - JULY 1976)

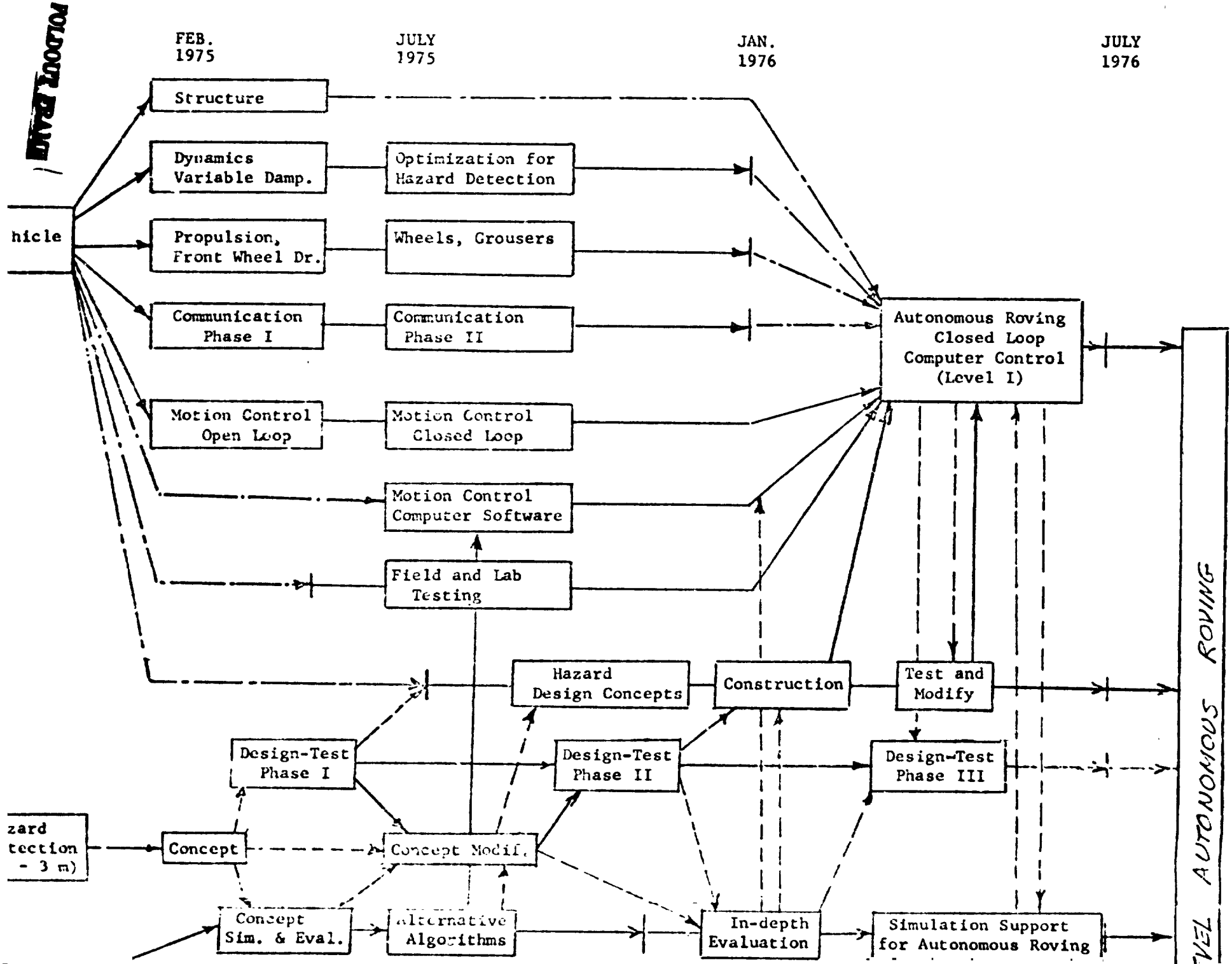

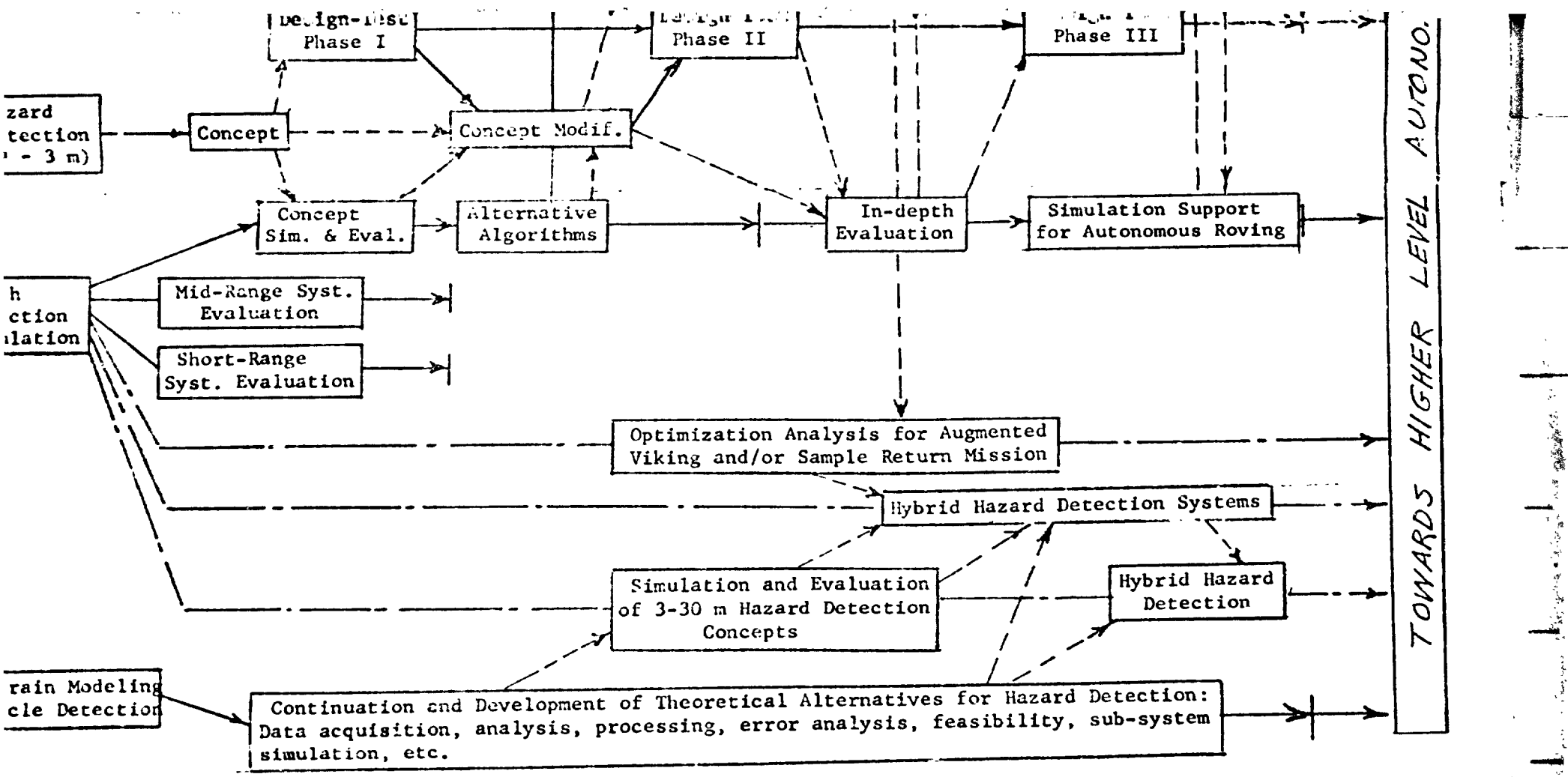

Figure 1. Rensselaer Mars Project Milestones to July 1976

Early hopes that rear wheel drive would suffice were unsupported by field testing. Analysis of the vehicle mobility indicated that a substantial advantage could be gained with front wheel drive. Front wheel drive was added and its advantages in increasing the vehicle's mobility in difficult terrains was demonstrated.

A.3. Wheel Design and Testing

The toroidal wheel, which had been redesigned during the previous year to increase lateral stiffness was further modified to decrease the footprint pressure and to increase its traction relative to irregular surfaces. A double-hoop toroidal wheel meeting design objectives was constructed but has not yet been field tested on the vehicle.

A.4. Telemetry Systems and Vehicle Electronics

Three tasks were pursued during the past year. Vehicle electronic systems were updated and modified to achieve desired operational characteristics. A control system for four-wheel drive was designed and implemented. The most significant effort was in the design and construction of a data link to be interfaced ultimately to a computer for autonomous vehicle roving.

A 50 Kbit/sec telemetry link from the vehicle to the controller receiver has been constructed, installed on the vehicle and tested. At the present time, this link transmits the strut sensor, steering angle, motor speed, latch and attitude gyro data to the off-board receiver for display. This link will be able to handle the hazard detection system data required for hazard avoidance decisions by a computer.

The original manual control box was modified to permit more effective remote control by an observer. This system is required for the extensive field testing program planned prior to autonomous roving studies.

Some of the software required for autonomous roving has been developed. CRT display of the front, side and top view of the vehicle including its pitch and roll is one of the software objectives.

Task B. Hazard Detection Systems

With the new objective of achieving a minimal level of autonomous roving by April 1976, the effort was directed to a short range (0.5 - 3.0 meter) hazard detection system. A concept employing a solid state laser and a solid state detector and using triangulation was constructed and demonstrated to be feasible as a detector of hazards to be avoided.

Task C. Path Selection Systems Simulation, Development and Evaluation

Two potential path selection systems received in-depth simulation and evaluation. The Mid-Range System which employs two or three body-fixed scanners has indicated real potential for the detection of positive obstacles. The Short Range System (1.0 to 2.0 meters range) has demonstrated an ability to detect craters providing therefore means for avoiding negative obstacles. Although it is not now planned to implement either of these concepts directly, the knowledge gained will aid the implementation of the hazard detection concept developed under Task B. Modeling of the latter concept has been initiated along with more detailed terrain simulation capabilities so as to permit a full scale evaluation of this concept as a potential hazard detection system.

Task D. Obstacle Detection and Terrain Modeling

This task deals with the problems of obstacle detection, terrain modeling, and scanning schemes for data acquisition.

D.1.a. Obstacle Detection and Picture Enhancing

The Four Directional Ratio Algorithm developed previously was able to detect only the tops of boulders and the leading edges of craters. A new algorithm making use of a Kalman Filter has been developed which not only detects the tops of boulders and leading edges of craters but also the bottom edges of boulders and the far edges of craters.

D.1.b. Minicomputer Simulation of Obstacle Edge Detection Systems

A computer program has been developed for use with a graphics terminal minicomputer to simulate and display the output of obstacle edge detection systems. The program allows the investigator to perceive visually the effects of data density and accuracy, obstacle shape and location on the identification of obstacles by edge detection and to adjust parameters readily.

D.2. Obstacle and Terrain Feature Classification

The problem of identifying the minimum number of terrain parameters required to deduce the passability or impassability of terrains has been examined. It is concluded that at least four parameters and three inequality conditions which must be met simultaneously are required. These results will be valuable input to the groups working on hazard detection hardware alternative and path selection algorithms.

D.3. Terrain Modeling

A two-dimensional spline function procedure has been developed for the modeling on terrain using range and pointing angle data such as may be provided by a laser scanning system. The modeling procedure

fits low order two dimensional polynomials to two adjacent terrain elements and provides a basis for minimizing discontinuities in height and slope at the common boundary. Once the first two terrain elements are modeled, a third adjacent element can be modeled without change in the parameters describing the first two elements. This process can now be extended to any number of terrain elements and ultimately yields gradient information to be used in a path selection algorithm. This terrain modeling procedure is intended to complement the obstacle detection concepts, Task C.1.a.

D.4.a. Measurement Scanning Concepts

Three alternative concepts have been considered: (a) Terrain and Zoom Scan, (b) Obstacle Scan and (c) Corridor Scan. The number of data points required for each method have been determined and the length of time required assuming one millisecond per measurement has been estimated. The relationship between vehicle velocity, maximum scanning range and time for data acquisition has been studied. It appears that the time for data acquisition can vary from about 6 to 15 seconds assuming a one millisecond data acquisition interval. At high vehicle speeds of the order of 1 meter/second, a scan range of 30 or so meters may be required for a timely detection of hazards. At low speeds of 0.1 meter/second, the scan range and concomitant data requirements can be reduced significantly without exposing the vehicle to hazardous situations.

D.4.b. Laser Rangefinder Errors

The implications of spreading of the laser beam and of the resulting reflections being sensed by a detector as possessing different times of flight and therefore different ranges have been investigated. It is shown that for a laser mounted 3 meters above the ground that the optimum laser aperture at the 30 meter range is 0.78 centimeters. For this set of parameters, the range error due to beam spreading on a horizontal terrain is 6.27 cm. Although this error is predictable for a level terrain and could conceivably be corrected, the fact that a rover would encounter terrains of all possible orientation excludes this simple correction.

Task E. Chemical Analysis of Specimens

E.1. Chromatograph System Characteristics

These studies are intended to provide chromatograph design techniques and guides using simulation models currently under development. Specific studies include: (1) development of a generalized simulation procedure; (2) determination of the effect of design parameters upon the degree of separation; and (3) characterization of realistic sample injection pulses. The simulation procedure treats a maximum of five components and uses actual sample sizes, carrier gas flow rates, and real time so results can be related to real systems. A method for quickly predicting degree of separation was developed by using a Gaussian-type approximation to the chromatograms. Input pulse data

were obtained on the experimental test facility. First and second time moments were correlated to provide a means of predicting gross characteristics of such pulses.

E.2. Chromatograph Simulation Development

Models developed previously to explain nonlinear composition-dependent effects appear too complicated to be solved efficiently by numerical methods. A simpler model involving the nonlinear Langmuir isotherm was derived and was solved numerically by the Crank-Nicolsen algorithm. This model represented well a chromatogram of n-heptane on Chromosorb C-102 previously simulated poorly by the linear model because of much tailing in the data. The numerical procedure was inefficient, requiring 25 to 60 minutes of IBM 360/67 time to fit a set of chromatographic data, so future work will involve development of a more practical numerical procedure.

IV. Educational Implications

As noted earlier, one of the objectives of the project is to involve engineering students in meaningful design and problem-solving activities enhancing, therefore, their overall education. Over the past year, this project has been successful in attracting many students over and above those attracted by financial support. These students, who participate on the project in this fashion, not only gain academic credit but also share in the challenge and the stimulation offered by the program. This past year is no exception with a total of 37 students actively involved in the project, only 12 of whom received some financial support. Of this total, two were doctoral level, twelve were master's level and twenty-three were undergraduate level students.

The students' reactions regarding the educational value continue to be very positive as evidenced by the number of new students attracted each year. The faculty appraisal of value is also very high. The project provides a unique learning experience in an academic setting for a number of reasons. These and other aspects of the educational impact are discussed in detail in Appendix A.

First, all of the problems addressed by the students are relevant and significant. The student realizes that the problem must be solved within the constraints that apply and not within artificial constraints which would make the solution relatively straightforward. Faculty attitudes and guidance are very important in this regard as are those of the technical monitors from Jet Propulsion Laboratory whose role is described below.

Second, the project is so organized and administered as to create a meaningful industrial climate. The students are aware of the short and long-term technical objectives and of their role in the project. The problem of interfacing their task with those tasks on which it impinges becomes painfully clear. They realize that interfacing with other tasks is just as crucial a constraint as are the direct technical objectives. The students are expected to plan their task, to formulate a milestone schedule and to achieve their stated objectives. Even though the students tend to be overly optimistic, they learn from this experience how to go about planning and executing their assignments. The students are required to make periodic progress reports and to prepare such progress and technical reports as are necessary. All in all, the students are experiencing the responsibilities of practicing engineers.

Third, progress review meetings involving the project technical monitors from JPL and invited guests are held at approximately ten week intervals. These review meetings are one of the most vital aspects of the project both from the technical and educational points of view. Students make presentations of progress to the group of monitors, guests, faculty and the other participating students. The progress is reviewed critically by all participants with appropriate comments and discussion. These meetings develop the student's ability to prepare his materials, including visual aids and demonstrations, to deliver his presentation and to react to questions and suggestions. The monitors and guests frequently provide additional information, knowledge and guidance which promotes the progress of the work. The progress review meetings are of considerable value in maintaining steadyand coordinated progress.

In summary, the project has contributed substantially to the education of engineering students and the professional growth of faculty interested in advanced study in the area of desi n.

V. Detailed Summaries of Progress

Task A. Vehicle Configuration, Control, Dynamics, Systems and Propulsion

The objectives of this task are two-fold: (a) to design,construct and evaluate a data and sample gathering rover to augment a second generation Viking lander or to enable a sample return mission for an extensive Mars exploration, and (b) to provide a test bed for the evaluation of alternative hazard detection and path selection systems for an unmanned autonomous rover.

Towards the accomplishment of these objectives, this group has addressed the following areas: vehicle dynamics, vehicle structure and propulsion, wheel design, and telemetry and control systems. These efforts are described in more detail below.

Task A.1. Experimental and Analytical Studies of Vehicle Dynamics - P. Marino
Faculty Advisor: Prof. G. N. Sandor

The objective was to analyze the vehicle's dynamic behavior and modify the vehicle's suspension so as to improve stability and reduce shock on the payload.

A two degree of freedom model of the vehicle's dynamics was developed and was used to choose appropriate rotational dampers for the rear wheel struts, Figures 2 and 3. These dampers have non-linear characteristics, and a mathematical model of the dampers was incorporated into the dynamic analysis program. It was found that the dampers must be geared to the rear torsion bar in such a way as to reduce the torque load on the dampers and increase their rotational velocity. A chain drive reduction was chosen because of light weight, high torque capability, and relative immunity to dust and foreign particles. A ratio of 6 to 1 was chosen and an appropriate chain drive installed. In addition to implementation of rotary dampers, it was found that a slightly stiffer torsion bar would improve the vehicle's dynamic behavior. A suitable torsion bar was designed, fabricated and installed on the vehicle model. Future work includes dynamic testing of the improved vehicle model so as to verify the mathematical model and analysis.

Task A.2. Vehicle Structure - J. Harrison and B. Musits
Faculty Advisor: Prof. G. N. Sandor

This task involved: redesign of the front end of the vehicle to overcome

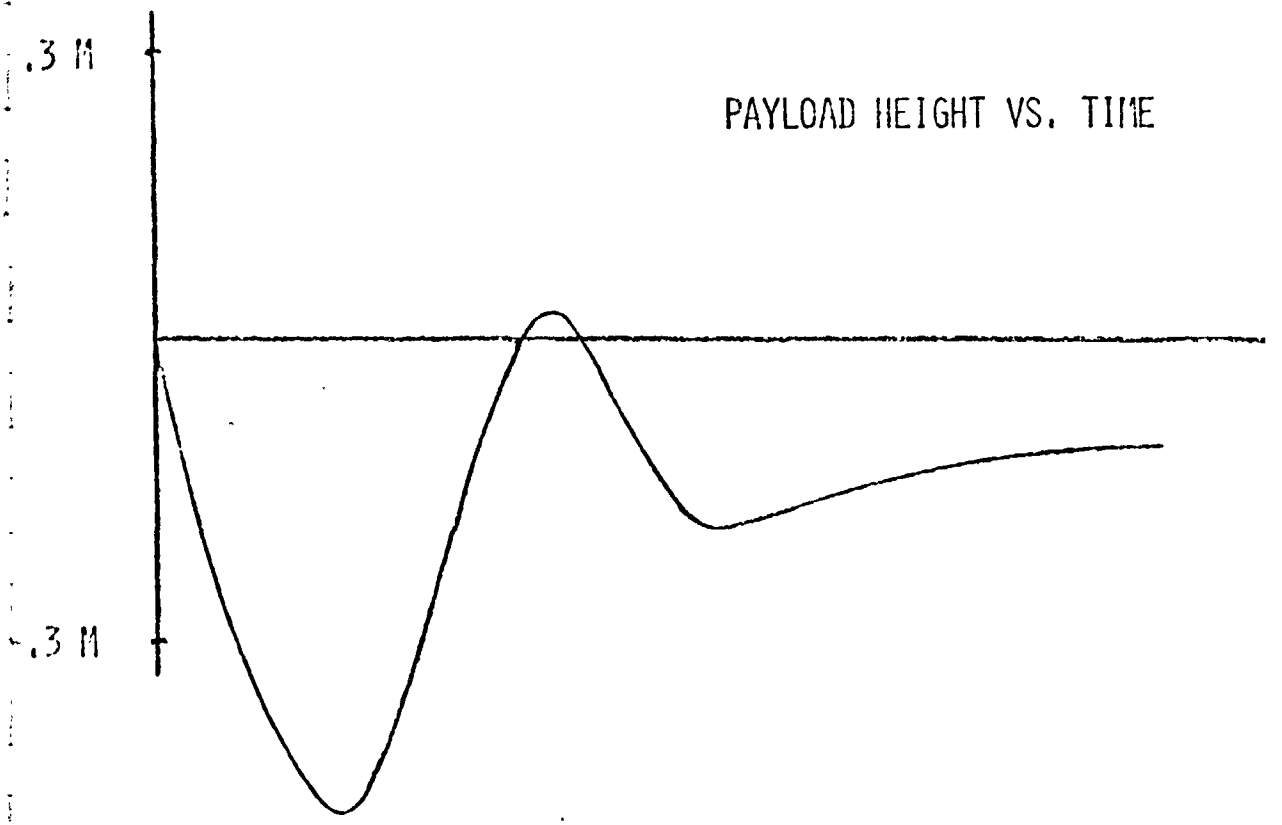

Fig. 2. Typical Dynamical Response with Rotation Dampening of Torsion Bar

EF-DYN CONTINUOUS ROTATION DAMPER- TYPE S-CRD

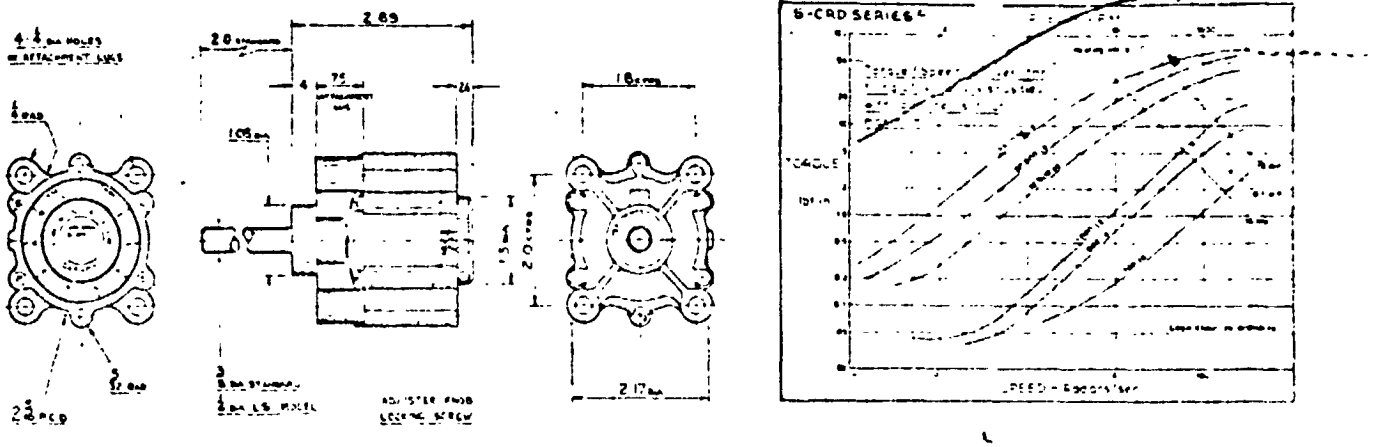

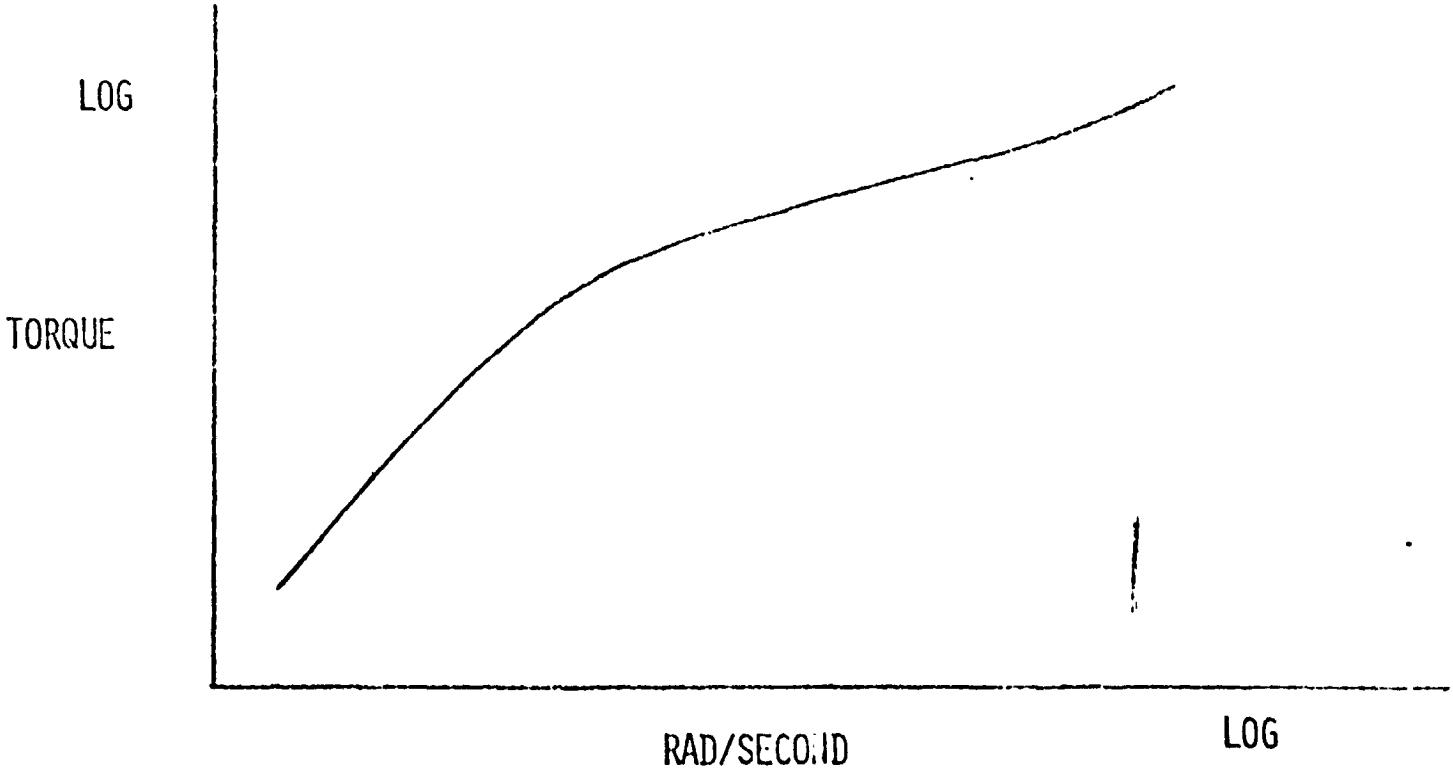

Fig. 3. Rotation Damper Characteristics

structural defects and weakness observed during the field testing; implementation of front wheel drive; implementation of strut sensors to provide vehicle configuration data; latch sensors to insure locking of members on completion of deployment; redesign of the torsion bar system and payload box; and construction of a laboratory obstacle course.

Front End Structural Revisions

Field testing of the vehicle and subsequent examination of components indicated that a number of structural improvements to strengthen the components were required. These have been made and results to date are satisfactory. The ability of the front end to withstand shock has been increased substantially.

Front Wheel Drive

Field testing indicated that the anticipated obstacle negotiating capability of a vehicle relying solely on powered rear wheels did not materialize. Analytical studies indicated that a significant improvement in step climbing ability could be expected with the addition of front wheel drive, Figure 4. A front wheel drive system was designed, constructed and implemented. Preliminary testing indicates that front wheel drive will add substantially to the vehicle's ability to negotiate potentially hazardous terrain situations. The vehicle's ability to overcome step obstacles depends not only on the torque applied to the wheels but also the traction between the wheel and the terrain. The new wheels described under Task A.3 are expected to provide a substantial increase in performance beyond that shown in Figure 4.

The addition of front wheel drive has also resulted in an improved reliability of the deployment maneuver.

Strut Sensors

Successful autonomous roving requires not only an effective hazard detection system but also knowledge of the state of the vehicle such as pitch and roll. For example, a terrain feature which may be entirely negotiable if the vehicle is essentially on a horizontal plane may be a severe hazard if the vehicle is climbing a 15^{o} slope. In order to provide the necessary vehicle "state" data, sensors which can detect the orientation of the rear and front struts relative to the payload have been installed along with sensors detecting the inclination of the front axle as well as the steering angle. Arrangements have been made, Task A.5, to transmit the sensor data to the remote control station.

Latch Sensors

The launch configuration requires the unfolding, extension and latching of both the rear and front struts. Four latch sensors, one for each rear wheel strut and two for the front strut were installed. Arrangements have been made to transmit the signal that the latches have been driven home.

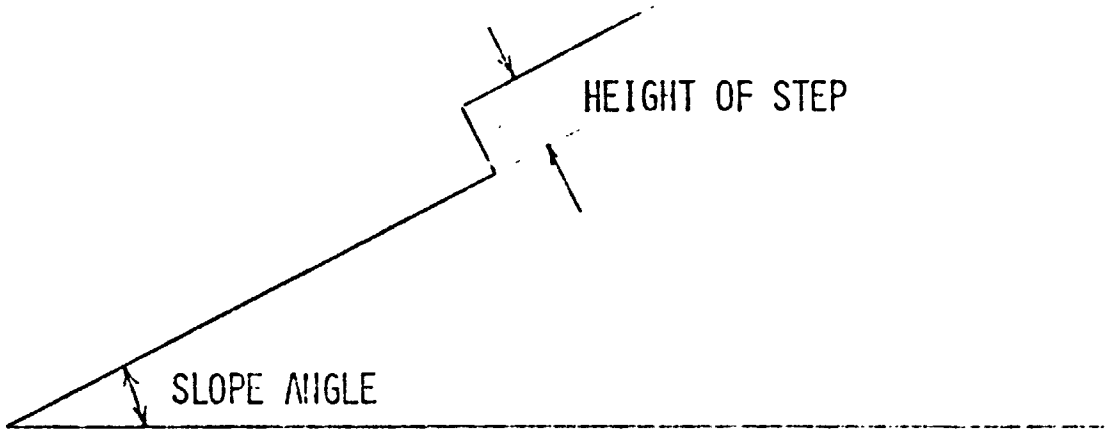

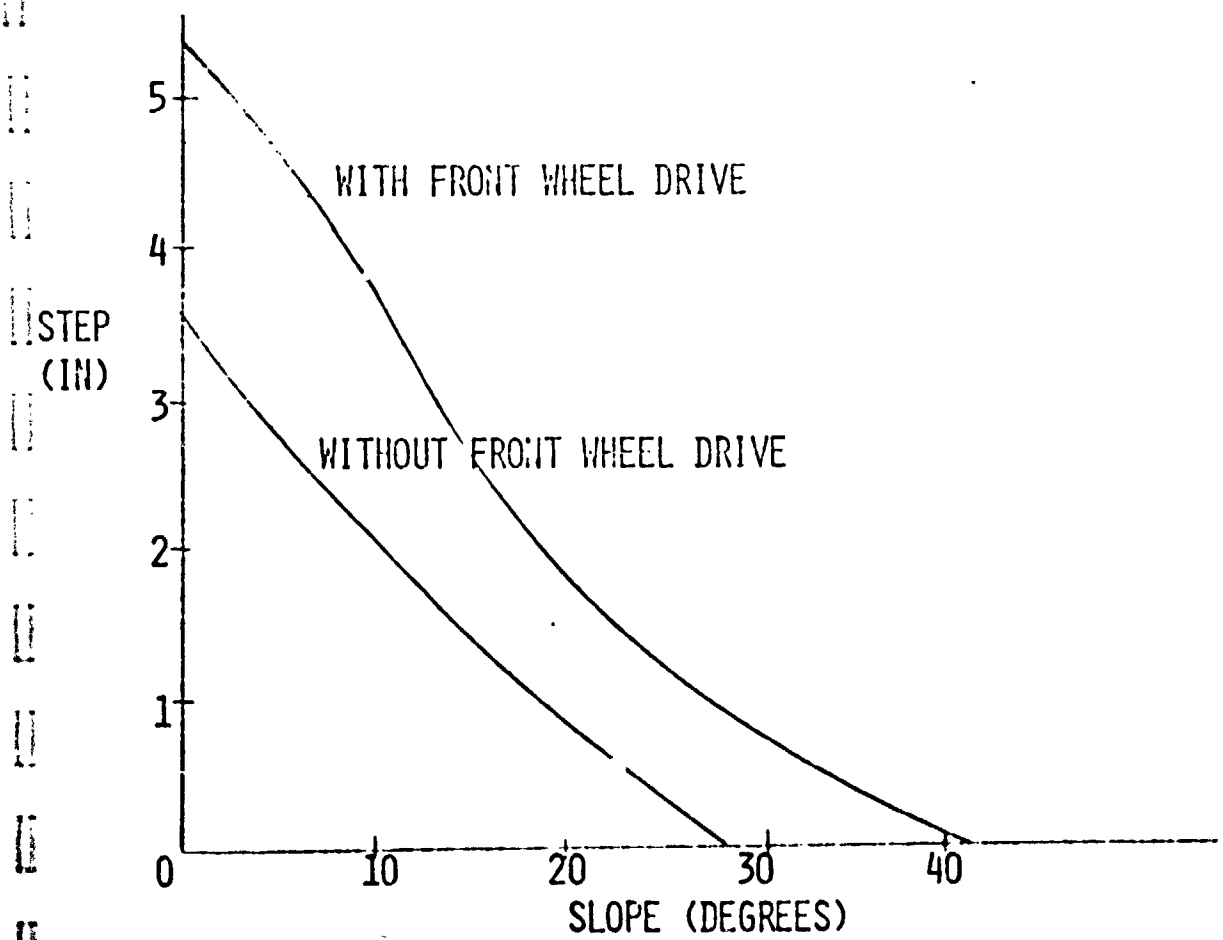

Fig. 4. Effects of Adding Front Wheel Drive on a Combined Slope-Step Obstacle

Torsion Bar and Payload Box Design

The torsion bar and gearbox were redesigned to eliminate observed structural weaknesses and to permit modification of the payload box. The previous design, Figure 5, can be compared with the current design, Figure 6. Not only has the torsion bar gearbox and assembly been improved structually but its reduction in size has increased the payload volume available for necessary on-board systems and reduced the payload weight by 40%.

Laboratory Obstacle Course

Although field testing is the ultimate test site which can reflect the realities to be overcome by the vehicle, it does not provide the quantitative data required for an in-depth appraisal of the vehicle's capabilities. Such an appraisal can lead to design changes which can result in significant improvements in vehicle performance. To this end, a laboratory obstacle course has been constructed. This system, Figure 7, is very flexible and provides the project group with the ability to create special terrain features according to the indicated needs. The present course which measures some eight feet by sixteen feet can be extended without difficulty.

Task A.3. Wheel and Grouser Analysis and Design - P. Marino

A.3.a. Wheel Tester and Grouser Design

The objective was to find an optimum tread for use on the RPI MRV vehicle model while examining grouser behavior in general.

Last year's tread design, while yielding good traction, proved to lack durability. A more durable tread material, commercially available for use on conveyor belts, was tested and chosen for use on the vehicle model. This tread material was applied to the stiff-rim type wheels in use last year and yielded satisfactory results. Current changes in wheel design at this time required a wrap-around type tread with reasonable backing stiffness to be used on a soft-rim design wheel. A search was then conducted for suitable tread material. The best readily available grouser was found to be the outside rim of an all-terrain-vehicle type motorcycle tire. One of these tires was obtained and modified for use on the new soft-rim type wheel. Future work includes testing of this new type grouser on the RPI wheel tester to determine its effectiveness on varied surfaces.

A.3.b. Wheel Analysis

The objective was to analyze the existing RPI MRV model wheels and decrease footprint pressure while maintaining lateral stability and increasing traction.

In an effort to reduce footprint pressure a change to a soft-rim design was investigated, Figure 8. It was found that a split hoop design combined with a soft rim yields adequate lateral stability, low footprint pressure,

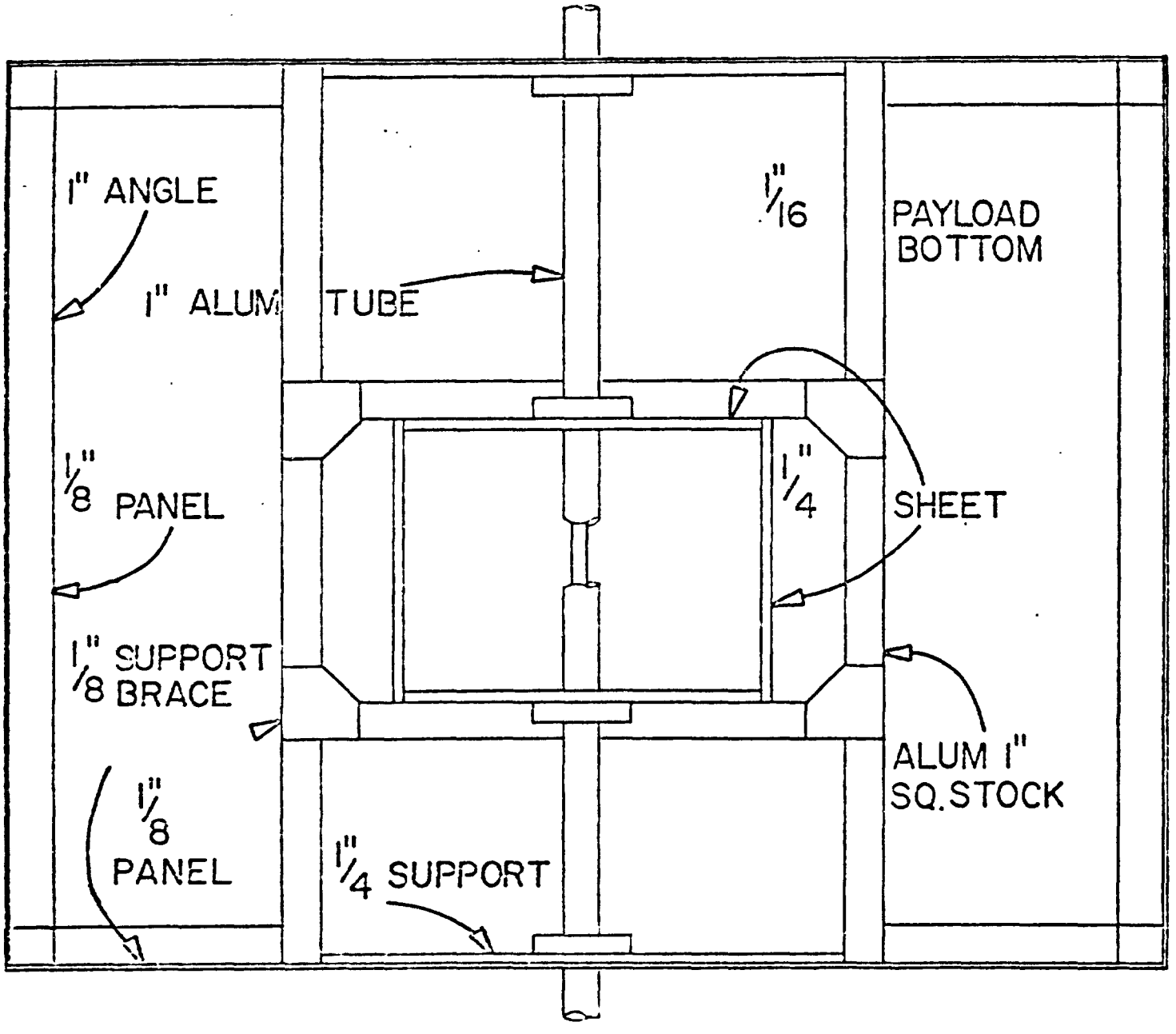

Fig. 5. Previous Payload Design

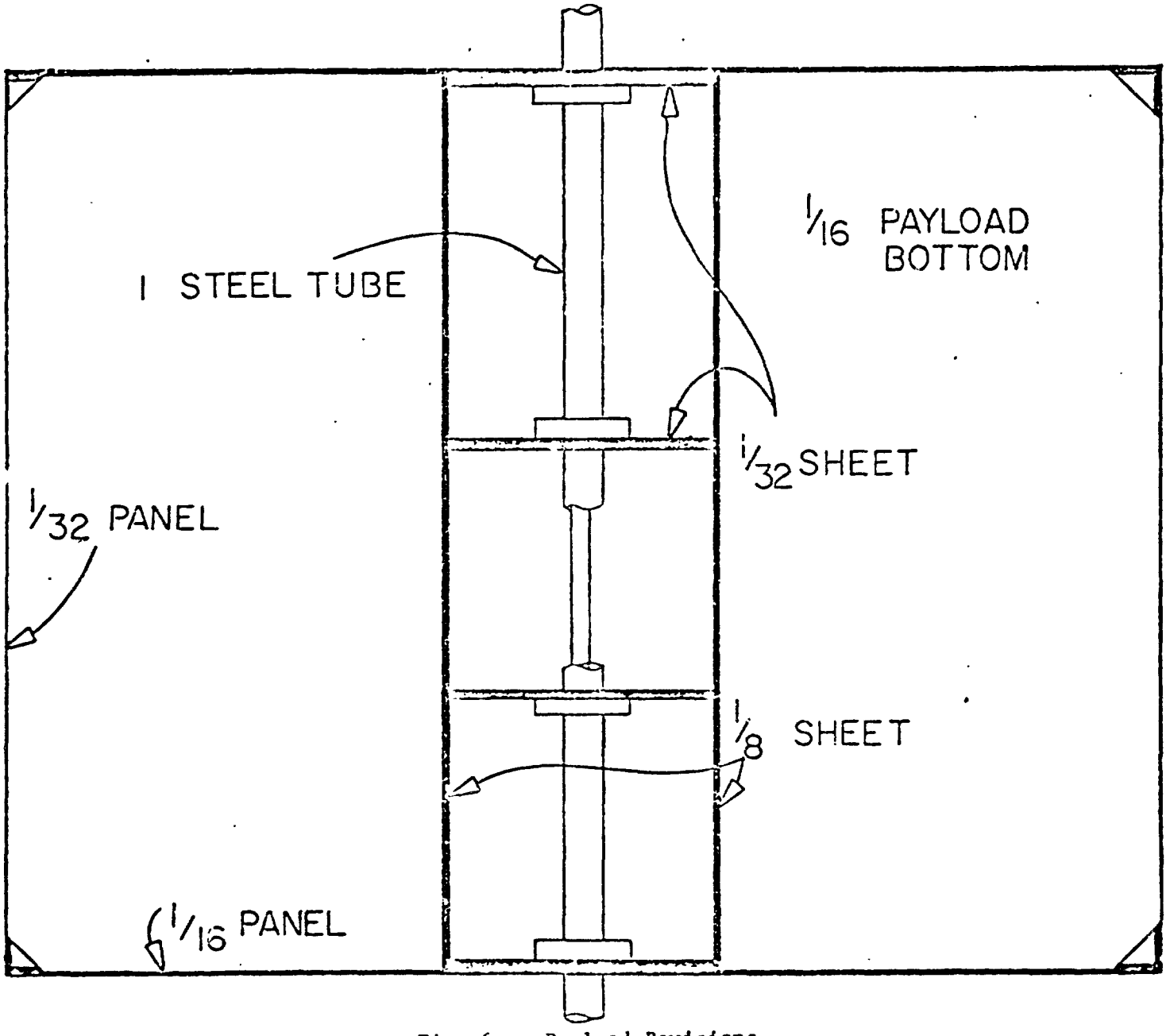

Fig. 6. Payload Revisions

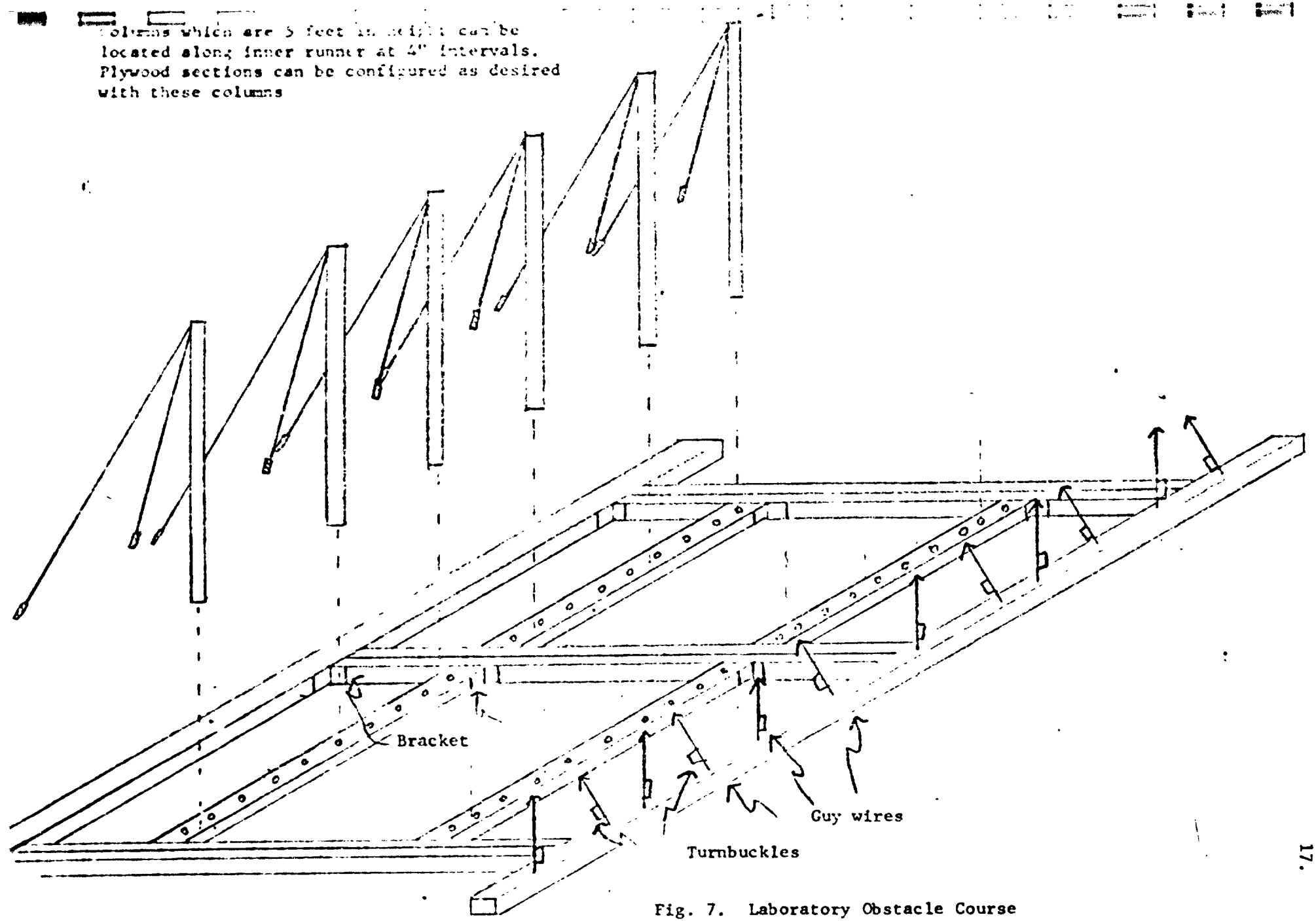

Fig. 7. Laboratory Obstacle Course

OBJECTIVES: TO MAXIMIZE TRACTION AND TERRAIN MOBILITY

DECREASE FOOTPRINT PRESSURE WHILE RETAINING LATERAL STABILITY

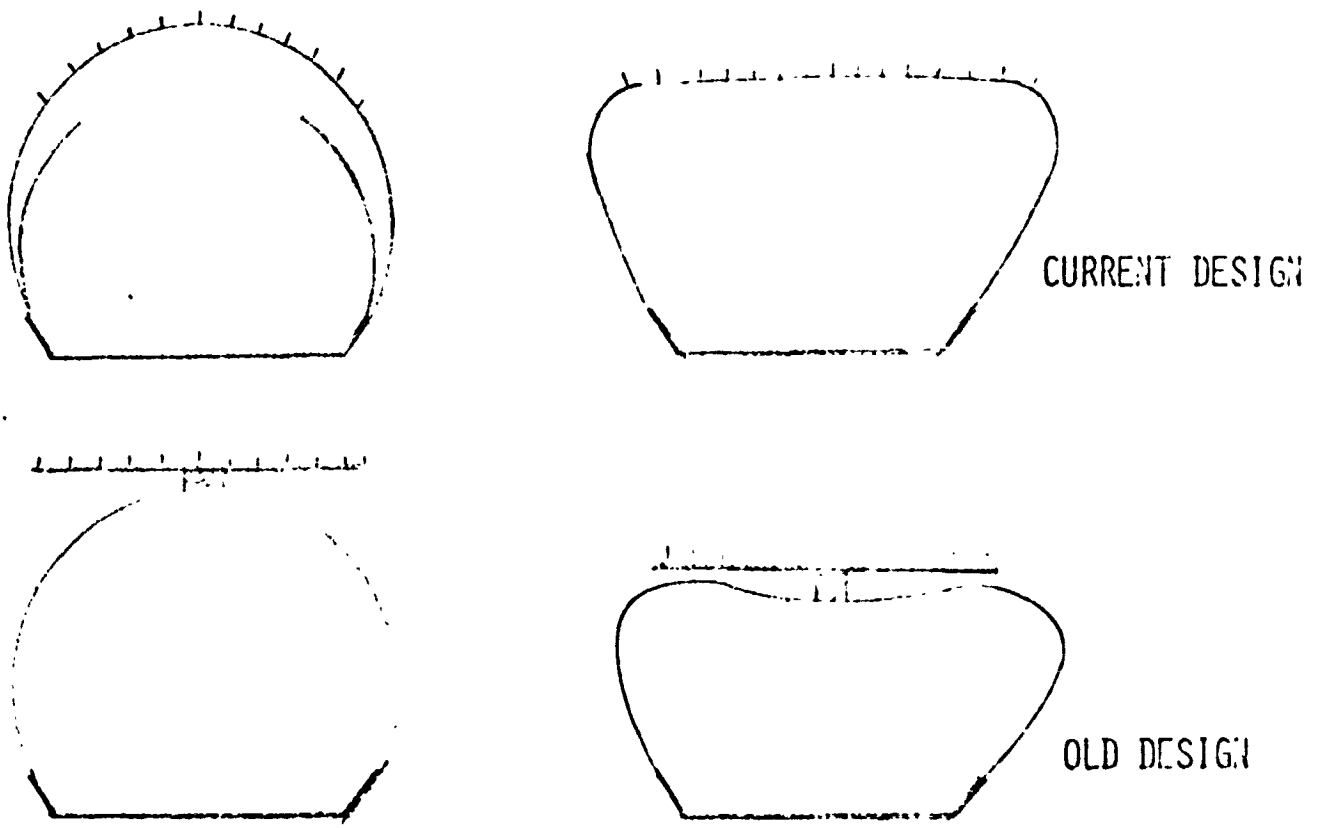

Fig. 8. Old and New Wheel Design

and high load capacity before overloading of the wheel hoops. This new design incorporates an inner split hoop and an outer grouser material. The soft outer hoop yields under low load and causes a large tread area in contact with the ground and thereby a low footprint pressure. Under higher loads, the outer hoop contacts the stiffer inner supporting steel and the the stiffer springs carry the additional load. In this way, the wheel combines two desirable characteristics: a low footprint pressure, and the ability to handle high loads due to the inner hoops, Figure 9.

The new wheel design offers a distinct advantage in the negotiation of hazardous terrain in that its softness will provide a better grippage and increased traction over the past steel rim wheel, (see Task A.2 Four Wheel Drive). It is hoped that step climbing ability will far exceed predictions for the stiff wheel.

Future work includes optimization of the design in terms of hoop stiffness, number of hoops, and spring hoop arrangement.

A.3.c. Detail Wheel Design and Construction

The objective was to combine the wheel structure and available grouser material and construct wheels for the RPI MRV vehicle model.

The new double hoop wheel design has been combined with the tire-type grousers and a new type wheel has been constructed. Plans include testing of this completed wheel and construction of four such wheels for use on the RPI MRV vehicle model.

Task A.4. Telemetry Systems and Vehicle Electronics - T. Barran, J. Cooley, K. Fell, T. Geis, T. Kasura, R. Richter, R. Pfeiffer
Faculty Advisors: Profs. G. N. Sandor and D. Gisser

Attention this year was focussed in three major areas: (a) update and modifications of the vehicle electronics, (b) implementation of front wheel drive, power and control systems, and (c) the construction of a data link from the vehicle to an off-board computer.

Modifications to Existing System

A new control system, found to be necessary during the testing of the previous summer, was designed and built this year. This control box, Figure 10, facilitates more rapid commands to the vehicle and a more effective human-machine interface than the previous design and hence more precise control of the vehicle. The control box is adaptable to interface with an offboard minicomputer to allow control of the entire system when under closed loop control.

Modifications were also made to the onboard vehicle electronics. A problem encountered during previous vehicle testing consisting of an overload in the steering drive circuitry was corrected by changing the function of steering motor control relays. Voltage fluctuations in the vehicle electronics power supply were found to be the cause of "creep" in the rear motor drives and variations in motor speed. To

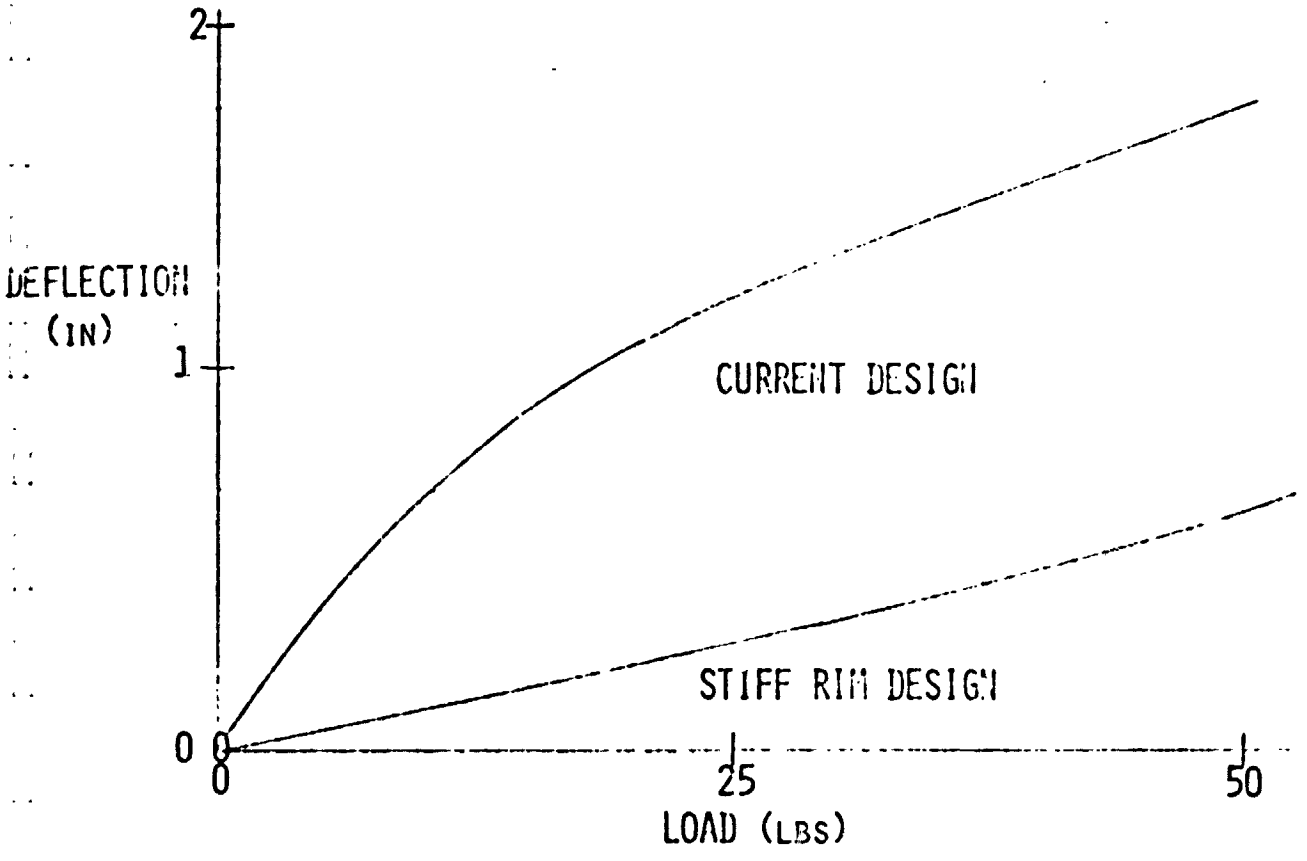

Fig. 9. Deflection Characteristics of the Double Hoop Toroidal Wheel

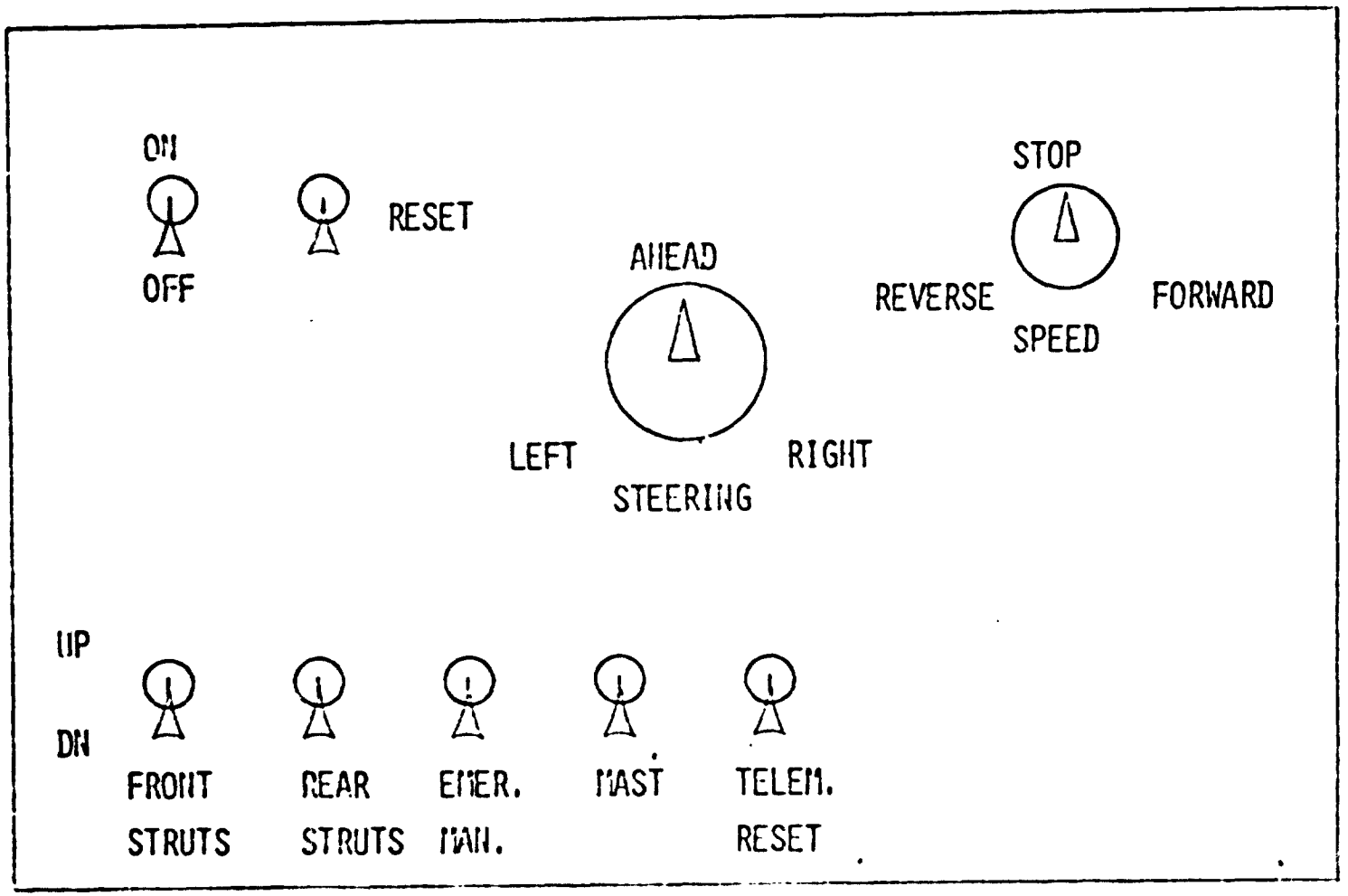

Fig. 10. New Remote Control Box Panel

minimize these fluctuations, a commercial power supply, capable of supplying 1 amp at both plus and minus fifteen volts with an input of twelve volts, was used instead of the unit built previously, which had been operating at near maximum ratings. This new power supply is working at about 1/3 capacity, allowing for a great deal of expansion while still maintaining well regulated output voltages.

Adoption of the mini rover concept this year necessitated the capability of much lower vehicle speeds in order to accommodate the laser hazard detection system, Task B, as opposed to the laser rangefinder system, Task D.1. To obtain these slower speeds, the motor drive circuitry was modified by adding gain to the feedback stage to allow the drive motors to turn more slowly.

Other modifications included a sensor to inform the vehicle electronics when the vehicle was in the "flipped" condition. This data was necessary to invert the differential action on the rear wheels to allow the vehicle to be driven in this mode. Mast control circuitry was added to allow a mast to be raised and lowered by remote control.

Front Wheel Drive

Electronic control for front wheel drive was implemented this year as a simple parallel or series connection over the main drive batteries. The parallel connection provided full power to the front wheels while the series connection provided a differential action to allow steering over large angles. This system provided adequate mobility but also showed that a four wheel speed control system would be desirable in terms of power consumption, precise speed control and steering at a standstill. Under consideration at this time is a four wheel speed control system that will achieve these benefits as well as have a fourfold increase in the accuracy of each wheel's speed as a function of steering angle. This new system is scheduled to be implemented by the middle of this summer.

Vehicle to Offboard Computer Data Link

The main objective this year was to send information concerning the state of the vehicle to an offboard computer. This is intended as a partial implementation of Phase II shown in Figure 11. Phase III which represents a fully autonomous, closed loop control of the rover is scheduled for implementation by March 1976.

Located on the vehicle are four latch sensors to verify the deployment of the vehicle, four tachometers to monitor the speed of each wheel, seven potentiometers to measure the positions of the front axle, emergency maneuver motor, steering angle, elevation of the front and rear struts, deflections in the torsion bar, and a gyroscope to monitor the pitch and roll of the vehicle, Figure 12.

Each sensor is sampled, converted into a 12 bit digital word, and presented with the latch sensor data to a digital multiplexor which selects this vehicle data or the data from any hazard detection system mounted on the vehicle. The multiplexor is capable of taking this vehicle data or hazard detection data any any desired "duty cycle" or having a "hazard detector override".

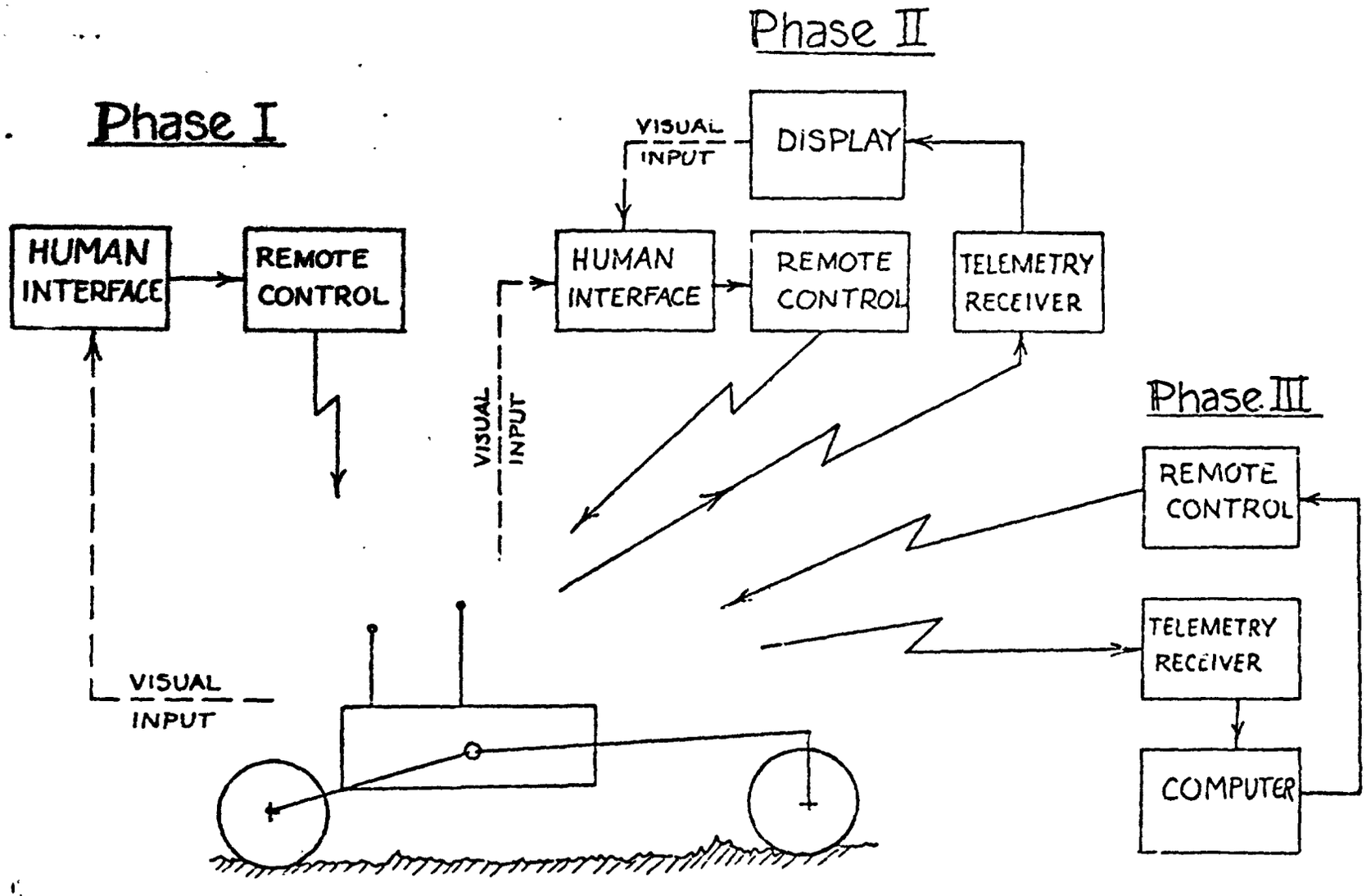

Fig. 11. Steps to a Completely Autonomous Ro[illegible] Vehicle

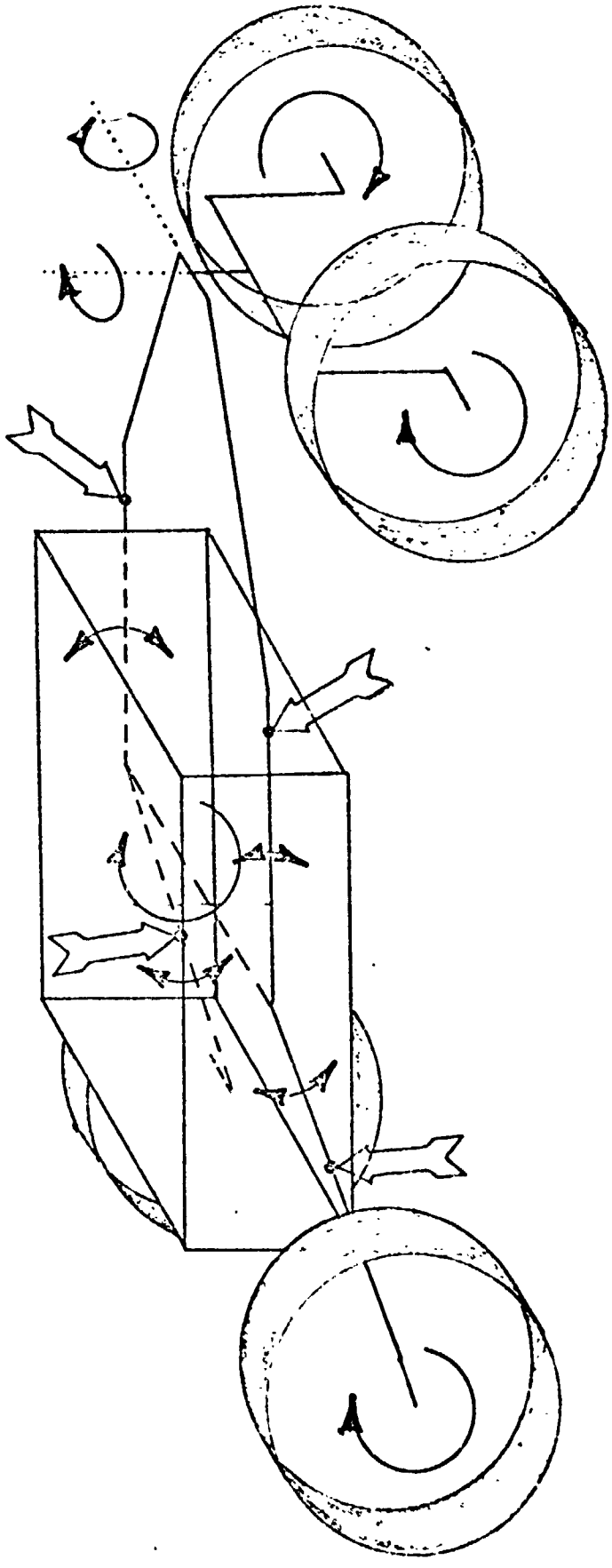

Fig. 12. Vehicle Attitude Sensors

A digital "word" is constructed which consists of a start bit, an address which locates the data word's origin to the hazard detector or the sensors, and if from the sensors, which one. The data is then put in serial form, followed by an error correcting code, four stop bits and one framing bit, Figure 13. The error correcting code is a combination of a five bit Hamming code and one parity bit. This code makes it possible to correct any single error and detect any multiple error. The system is currently sending 500 words per second and is capable of sending much more, if necessary.

The receiver unit, Figure 14, located at the computer, recognizes the start bit as the first zero received, and starts to count off the rest of the word changing it from serial to parallel. The start bit is verified to insure that the receiver didn't trigger on a noise pulse and finally, the four stop bits are verified to insure the first zero was indeed the start bit. If all is correct, the word is stripped of start and stop bits, any single errors are corrected (words with multiple errors are aborted), the word is fed into a register and a "data ready" pulse is created for the computer to use.

The lowpower telemetry transmitter uses direct carrier frequency shift keying in the VHF band, Figure 15. It is physically small and designed to handle at least 50 kilobits per second. It consists of two stages, a high frequency voltage controlled oscillator, fed by the serial digital data which drives a lower power output stage.

The receiver is a commercial unit chosen for its high overall bandwidth, Figure 16. It consists of a radio frequency amplifier, oscillator-mixer stage, and intermediate frequency amplifier section with an overall bandwidth of four megahertz. An FSK, Travis type detector was designed to derive the data from the received signal. Variations in carrier frequency are interpreted as digital symbols allowing the detector to be quite insensitive to amplitude variations and noise.

A display was built to show the data from the vehicle that samples the data at the computer interface. It displays at all times the state of the latches on light emitting diodes. In addition, the operator can select any sensor on the vehicle and watch the transmitted information from that sensor on a digital readout.

Also this year, preliminary work was done on a computer program which will use the information from the vehicle to create a graphical display of the state of the vehicle. This would show top, front, and side views, as well as the roll and pitch on the CRT display, Figure 17. This will assist operation of the vehicle from the computer.

Task B. Hazard Detection Systems - S. Cairns and D. Holly
Faculty Advisor: Prof. D. Gisser

The Mars Roving Vehicle must be capable of operating autonomously over varied terrain for extended periods, although a reasonable number of (automatic) stops with requests for human assistance are to be expected. Optimum operation would include continuous scanning of the terrain in the general direction of motion in order to select a "best" path and initiate avoidance maneuvers early. Systems

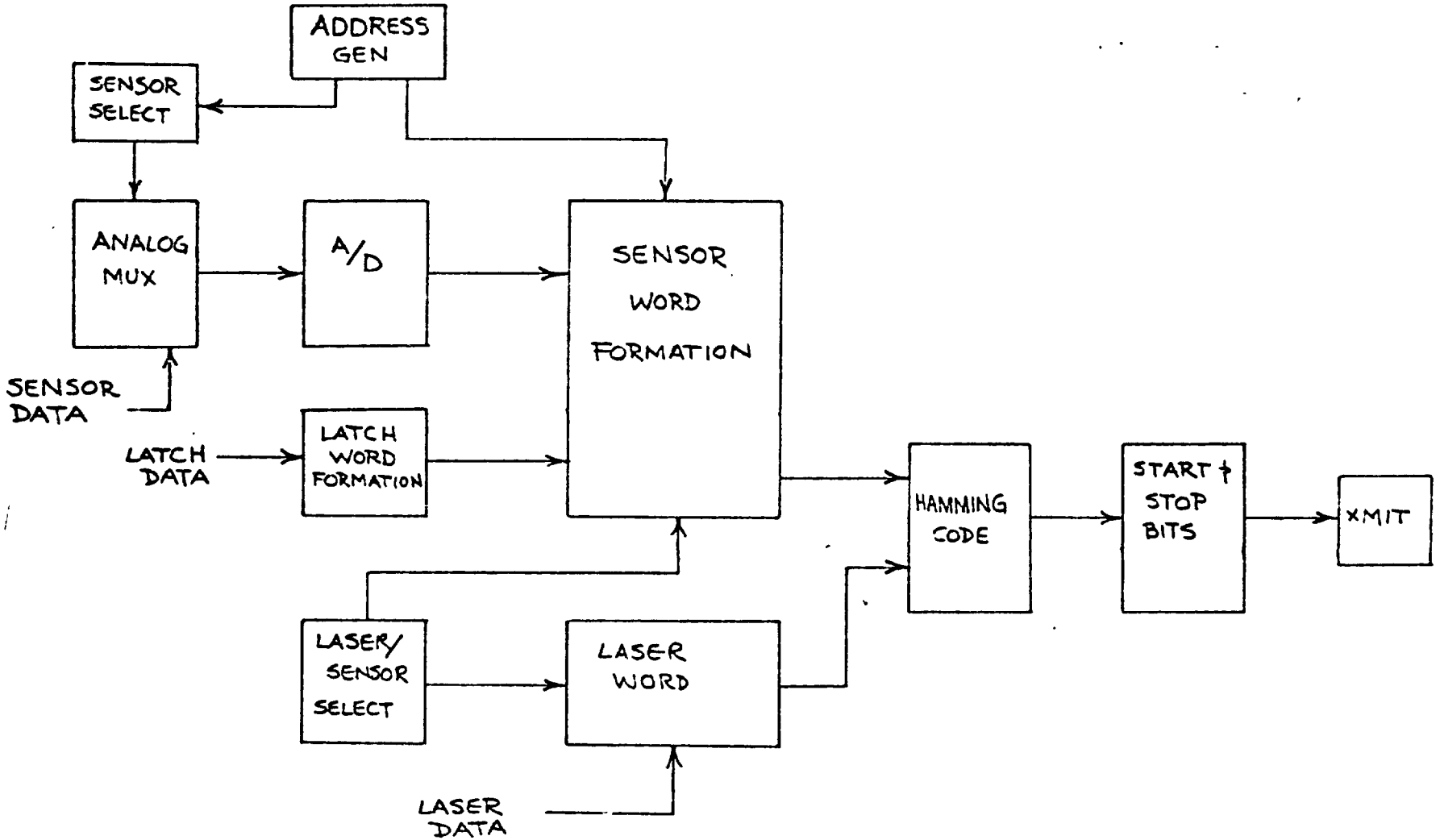

Fig. 13. Transmitter Encode Logic

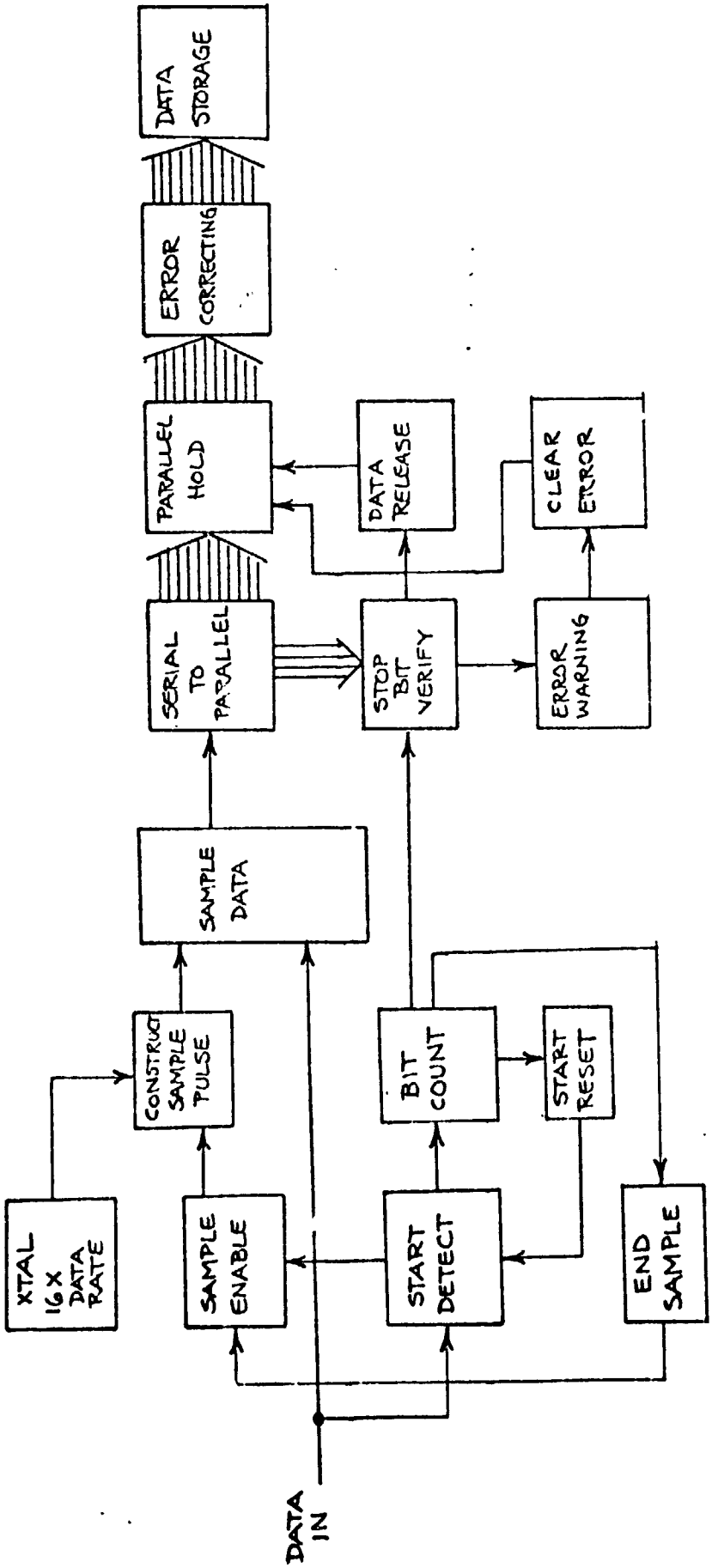

Fig. 14. Receiver Decode Logic

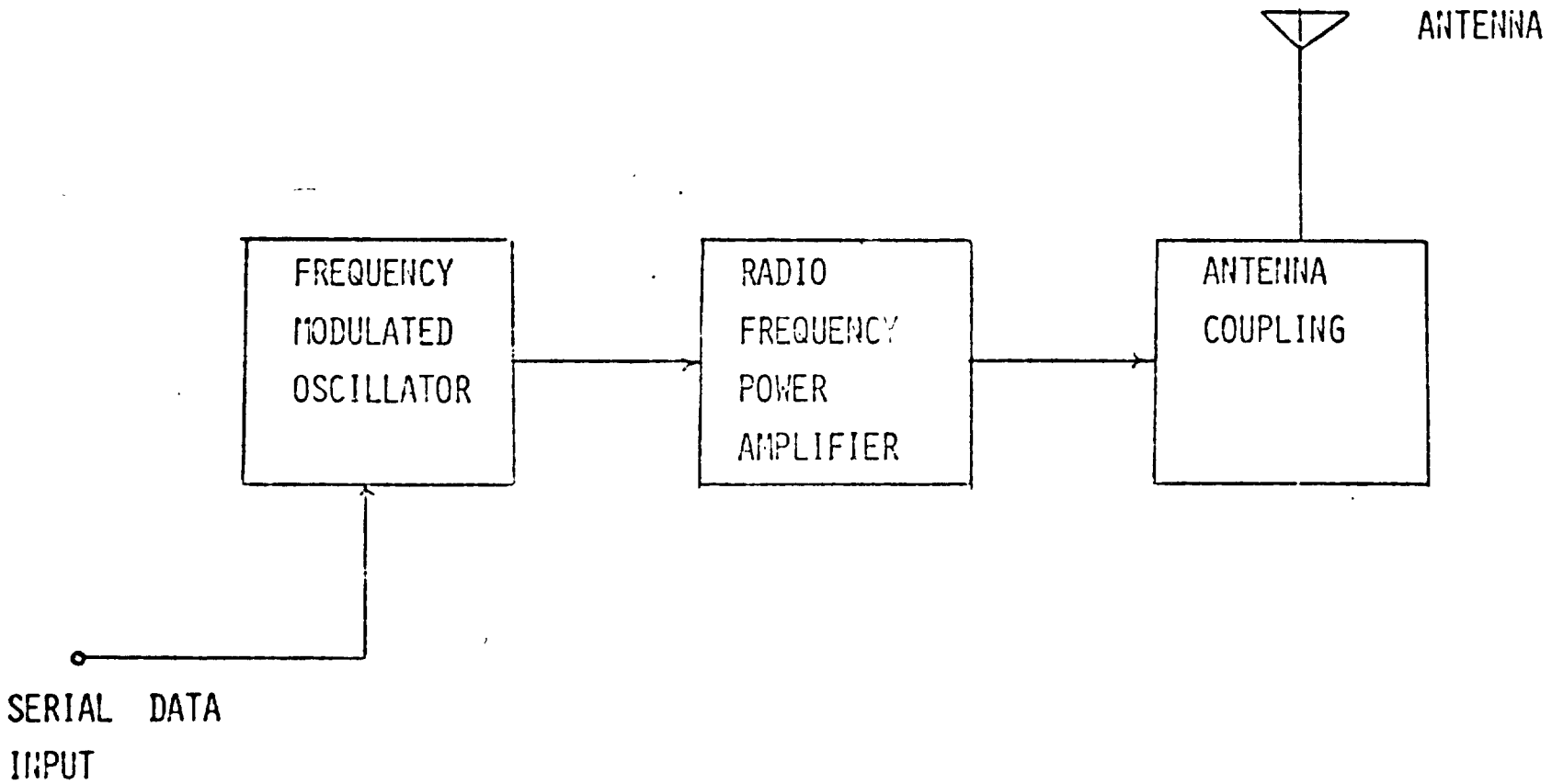

Fig. 15. RPI MRV Telemetry Transmitter

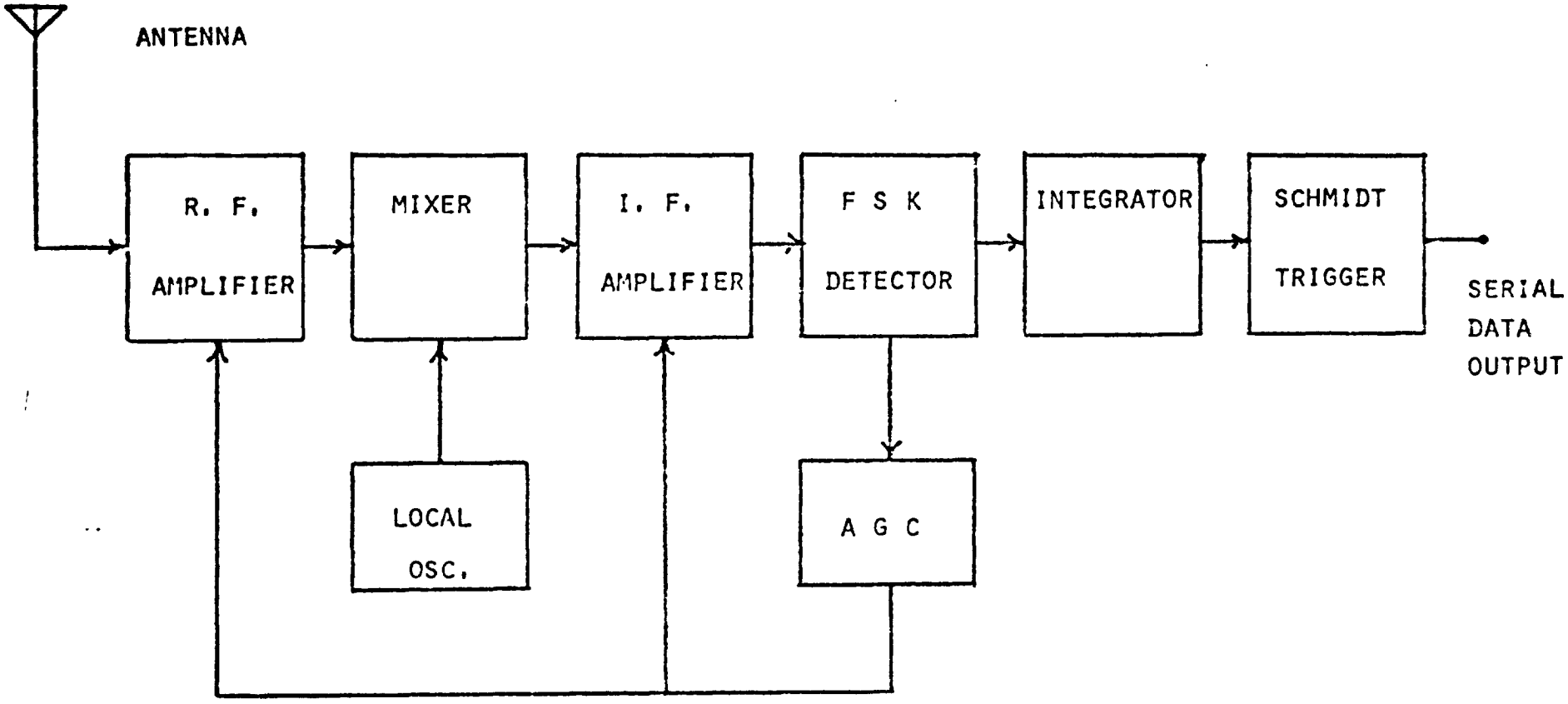

Fig. 16. RPI MRV Telemetry Receiver

TOP VIEW

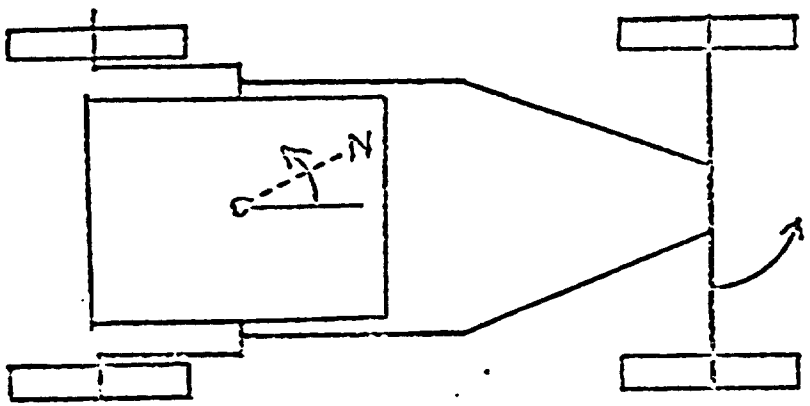

VERBAL INFORMATION

IN THIS AREA, VERBAL INFORMATION SUCH AS SPEED OR THE ACTUAL ANGLES WILL BE DISPLAYED ALONG WITH SWITCH POSITIONS AND LIGHT PEN SENSITIVE COMMANDS AVAILABLE.

SIDE VIEW

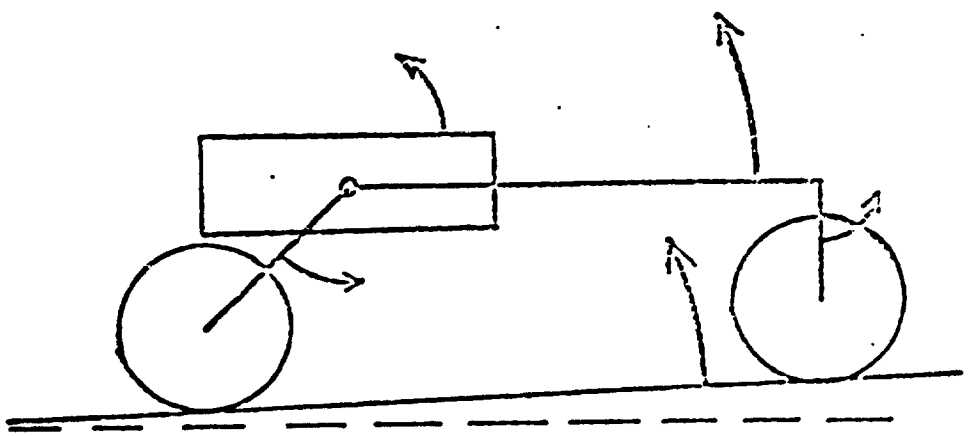

FRONT VIEW

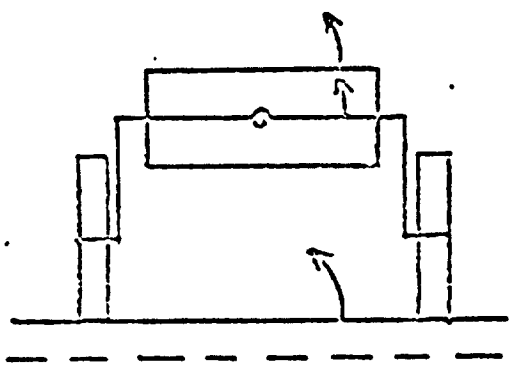

(Arro indicate changes in vehicle position revealed in that particular view)

Fig. 17. Typical IDIIOM CRT Display

of this sort were planned during the past several years, and they require a range finding sensor with a range resolution of a few centimers (~ 5 cm) at ranges to 30 meters, appropriate angular resolution, and scanning capability. Such range-finders can be built using pulsed laser sources, multiplier phototube detectors, and optical systems with an aperture of 5 to 10 cm. Implementation of such rangers with solid state detectors is just about possible theoretically and should become feasible in practice with advances in both laser and detector technology. The wide aperture required, and the necessity for a mechanical scanning arrangement makes the outlook for a system with the relatively short scan time required, somewhat dubious. Such a system, however, is still considered a long term possibility (Task D) and improvements in electro-optical materials may make a solid state scanning system feasible.

The short term objective has changed. Instead of a precise ± 5 cm, long range 3-30 meters, time-of-flight system, whose basic purpose is to supply detailed terrain data in quantity, the current objective is to impelement a short range, (0.5 - 2.5 meters) low resolution, triangulation system whose basic purpose is to supply the vehicle with information of the go-no-go variety. As a minimum, it is expected that both boulders and holes larger than some preset threshold can be detected with this arrangement. It is also possible that laser scanning and multiple detectors may provide rather detailed information regarding the terrain in the immediate vicinity of the vehicle.

Principles of Operation

The system is basically a reflected light detection arrangement, consisting of a light source with a relatively narrow beam angle directed at the terrain at a point of interest about one meter in front of a wheel. A light detector with a somewhat larger beam angle is located at a point as far as is practicable from the source, as shown in Figure 18. Reflections from the ground, with or without small variations in level, are received continually and are considered normal. Any very sudden drop off or barrier, however, will result in no reflections within the acceptance angle of the detector, as shown in Figure 18. This system for the detection of obstacles and drop offs is not new, but in actual use for a similar purpose as a mobility aid for the blind.

Implementation

A continuous source of light with high enough efficiency for high output with low power requirements is not available, but the injection laser can be pulsed to a very high output for a short time, making its average power drain quite low. It has the additional advantage of producing its light output from a very small area and over a small bandwidth, permitting a simple optical system to produce a narrow beam. The emission is around 9000 A, in the near infra red, a wavelength where semi-conductor detectors are quite sensitive and most minerals have reasonably nigh reflectivities. The transmitter circuit is shown in Figure 19. Operating from a supply source of 15 volts, it uses a total of 150 milliwatts to produce about five hundred 150 nano-second light pulses per second. It is packaged in a box approximately 14 x 10 x 9 cm, supported by an adjustable ball

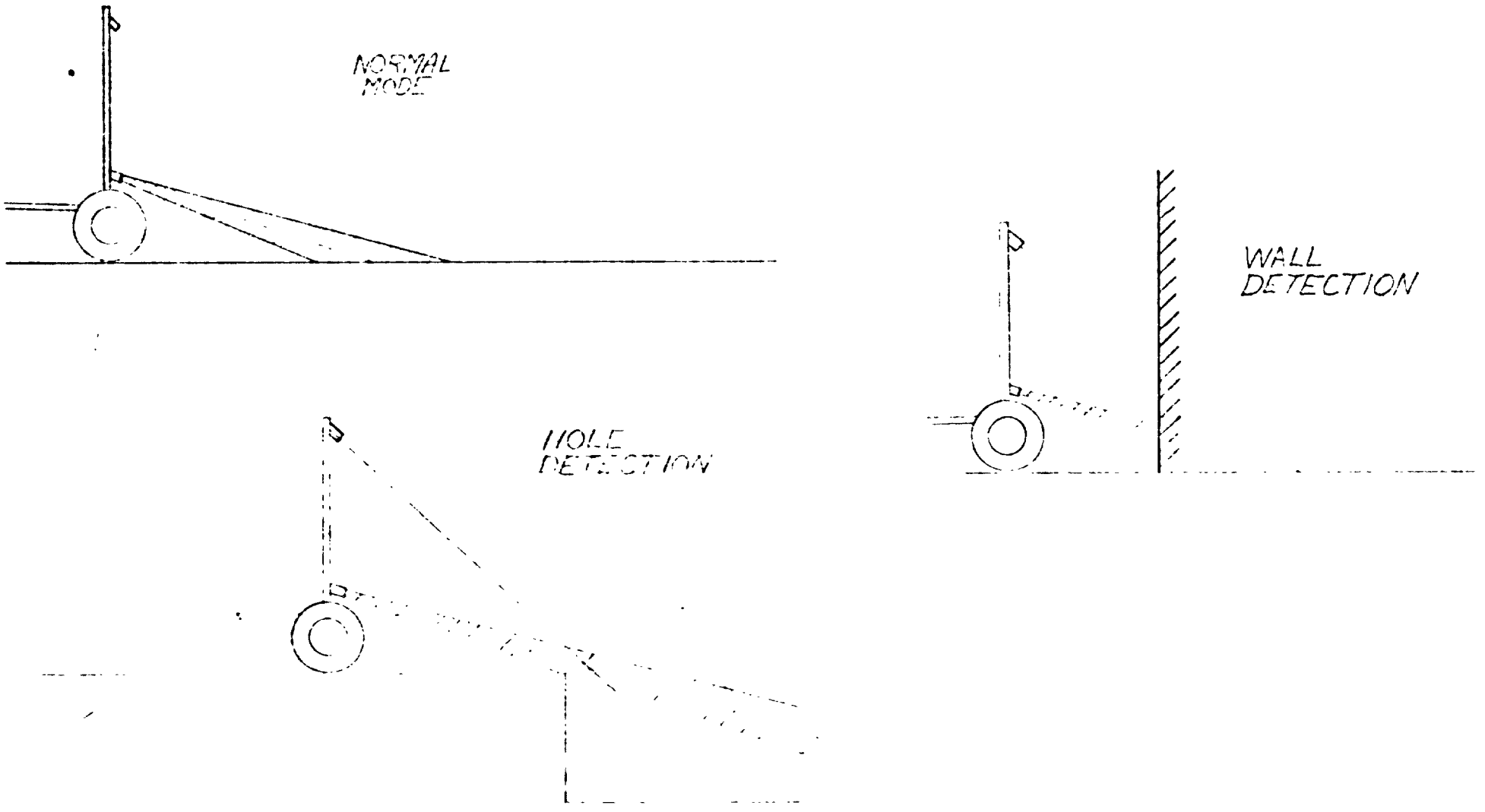

Fig. 18. Hazard Detection System Concept

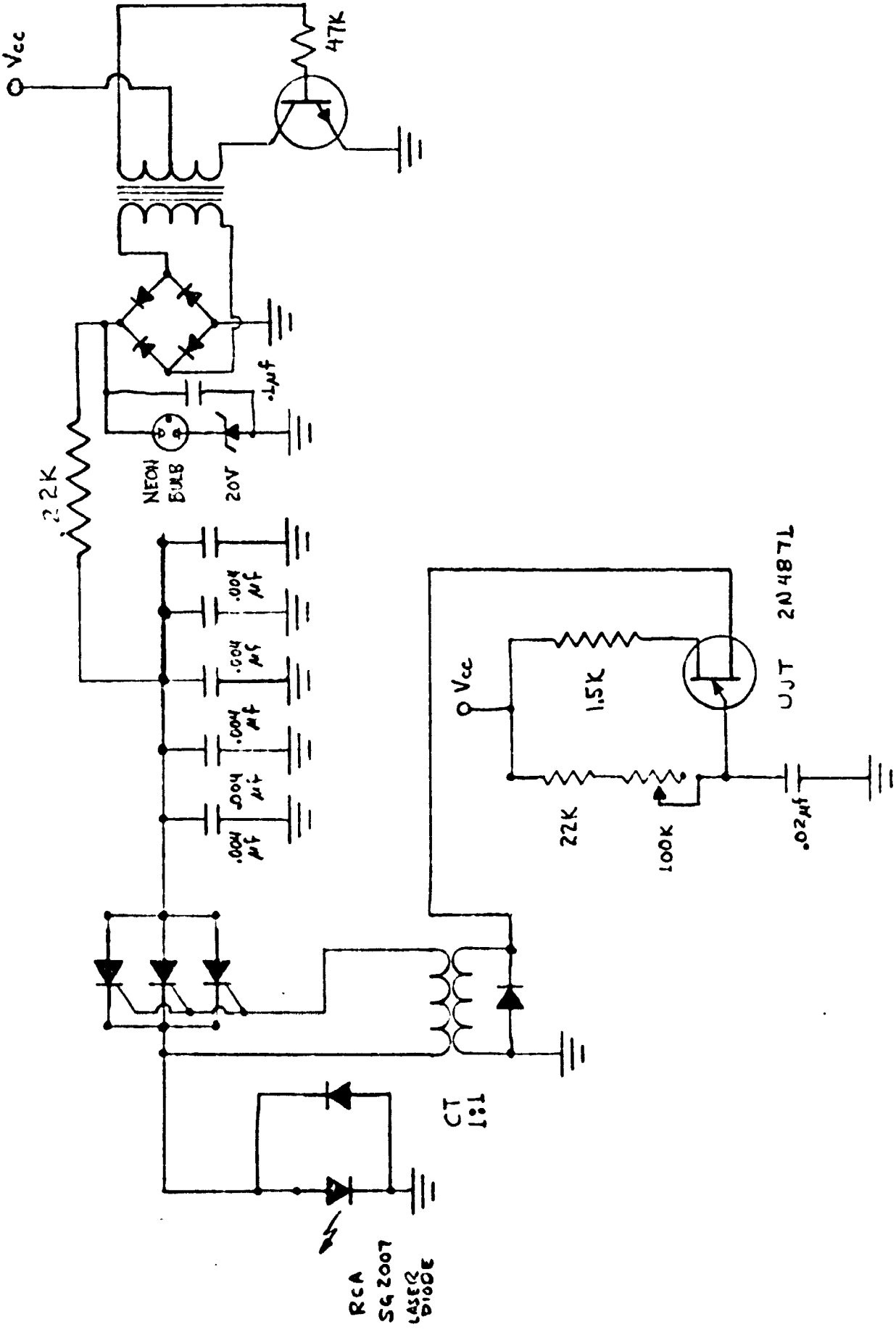

Fig. 19. Transmitter Electronics

and socket mount. The lens is 8.75 mm in diamter and has a focal length of 35 mm. Notice that there is an internal dc to dc converter to charge the storage capacitors to about 80 volts.

The receiver circuit is shown in Figure 20. It consists of a 25 mm diameter lens with 21 mm focal length focusing light on a 5D PIN photodiode, followed by a two stage low noise wide band preamplifier operating from a nine volt battery. The total power drain is 32.5 mw. The receiver box is about 10 x 7 x 5 cm. which is also ball and socket mounted for easy adjustment. The output feeds an amplifier and pulse stretcher, shown in Figure 21. Its output will be eventually rectified, and the absence of a signal used to indicate the presence of an obstacle or hole. For experimental work, however, it is very convenient to have an audible indication of reflections so the circuit shown in Figure 22 is used. Strong reflections produce a continuous audio tone. Marginally weak reflections produce an intermittent, raspy tone, and no reflections, no tone.

Discussion

The system has been shown to detect obstacles easily and drop-offs of about one third meter at about a two meter range with a one meter baseline, although echoes are weak from some very dark materials. Work is progressing on more carefully defining the receiver beamwidth needed and in considering the relative advantages of several configurations of several detectors and sources in order to better protect the vehicle.

Task C. Path Selection System Simulation, Development and Evaluation -
D. Matthews, D. Sharp, D. Campbell, J. Krajeweski
Faculty Advisor: Prof. D. K. Frederick

An autonomous Mars Roving Vehicle must detect and avoid obstacles on its way to some predetermined target. This task is aimed at the development and evaluation of sensing and avoidance schemes using a digital computer simulation. In the past year, progress has been made in the development and evaluation of both mid-range and short-range path selection systems. Improvements have also been made on the computer simulation package; improvements which will make the package a more effective design tool for the new project goals.

A mid-range path selection system with two and three beams fixed on the vehicle has been developed and tested. Uniform and non-uniform aximuth scans have been employed and encouraging results with positive obstacles have been obtained. In addition, a short-range system has evolved from a basic terrain modeling system with simple go/no-go conditions into a more sophisticated path evaluation scheme with memory capability. Further, the short range system has demonstrated its ability to avoid craters. Improvements have been made in the group's digital simulation, including modifications in the display of output so that results are more easily read and interpreted. The terrain generation and vehicle dynamics simulation are being improved so that the evaluation of the newly proposed triangulation hazard detection system will be easier and more realistic. Work is also underway to

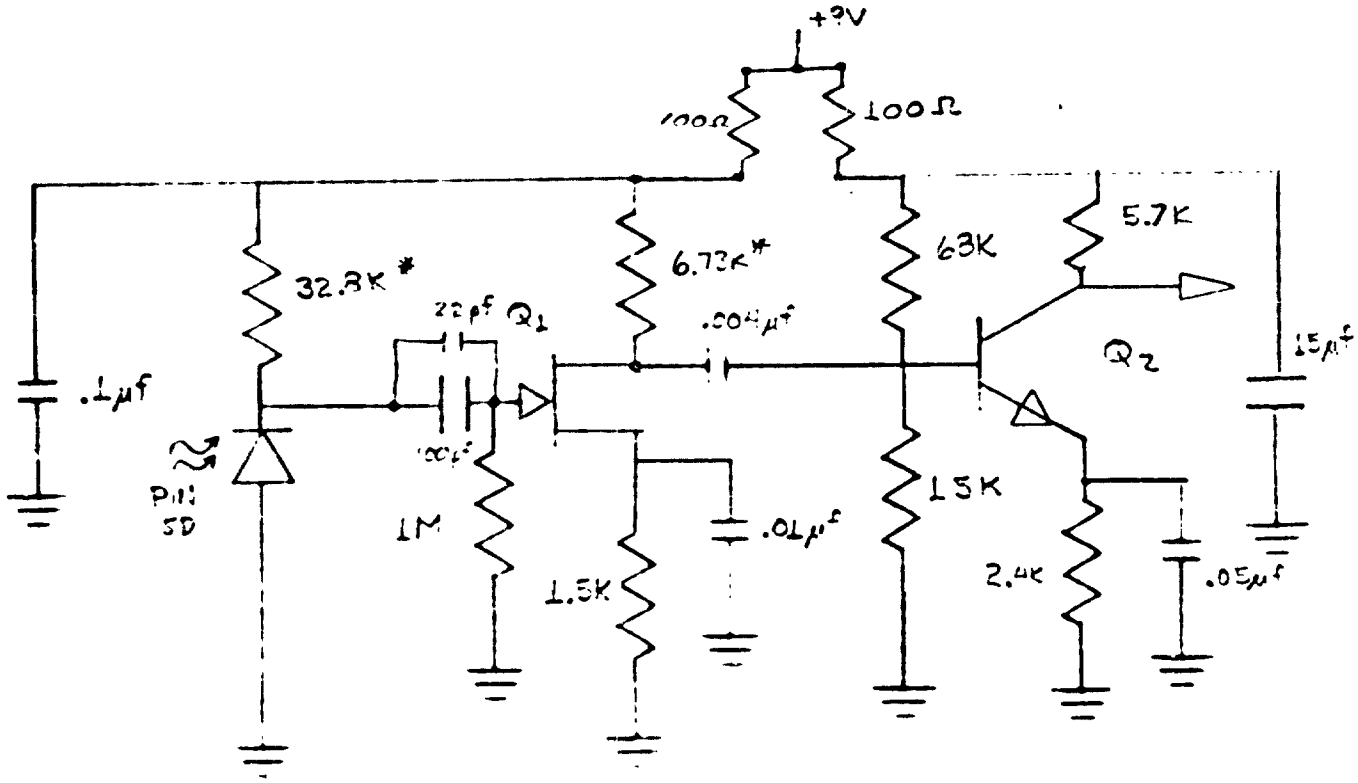

Q_1 2N4221A

Q_2 2N3563

* [illegible]

Fig. 20. Receiver Electronics

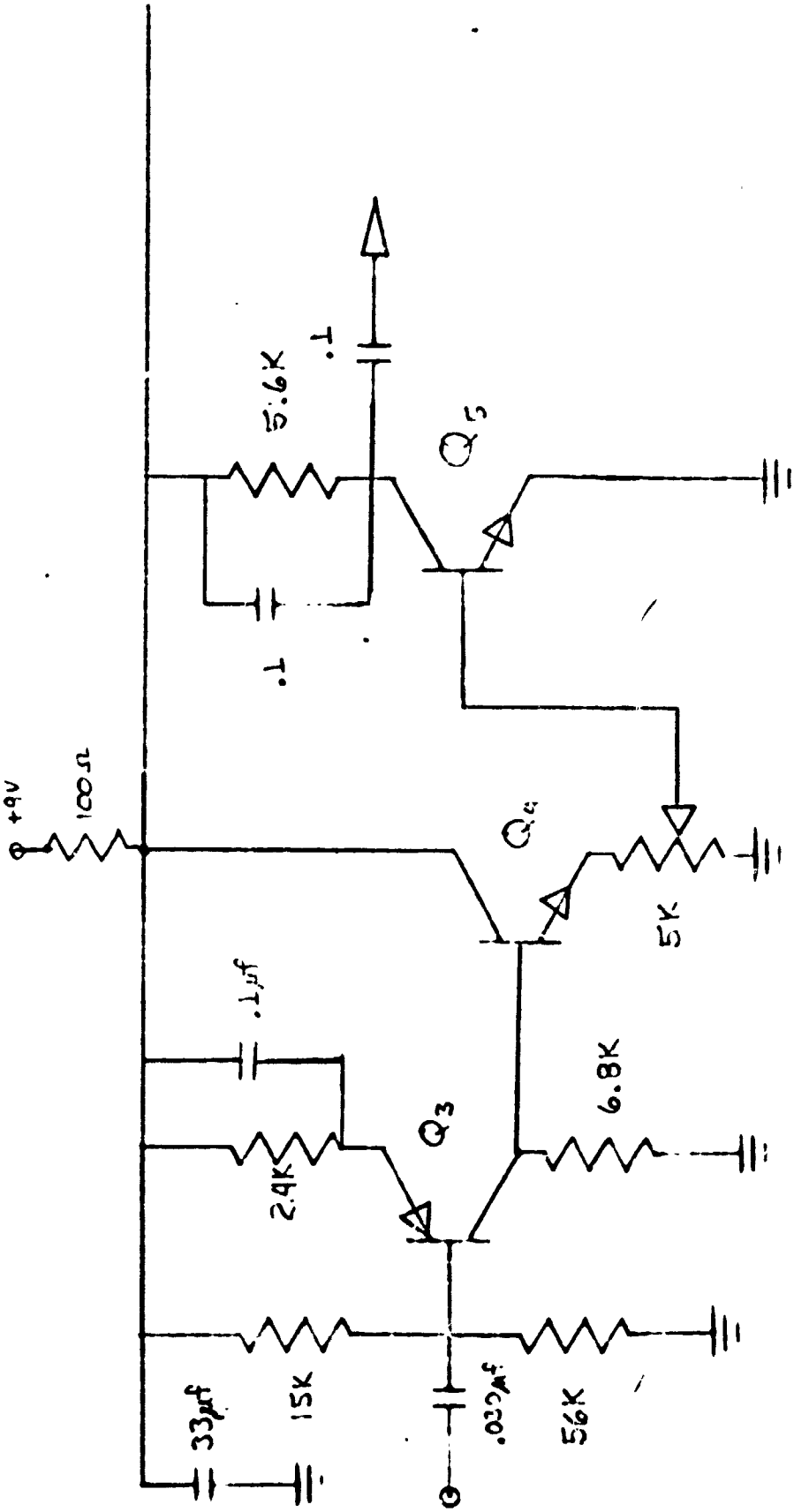

Fig. 21. Amplifier and Audio Converter Electronics

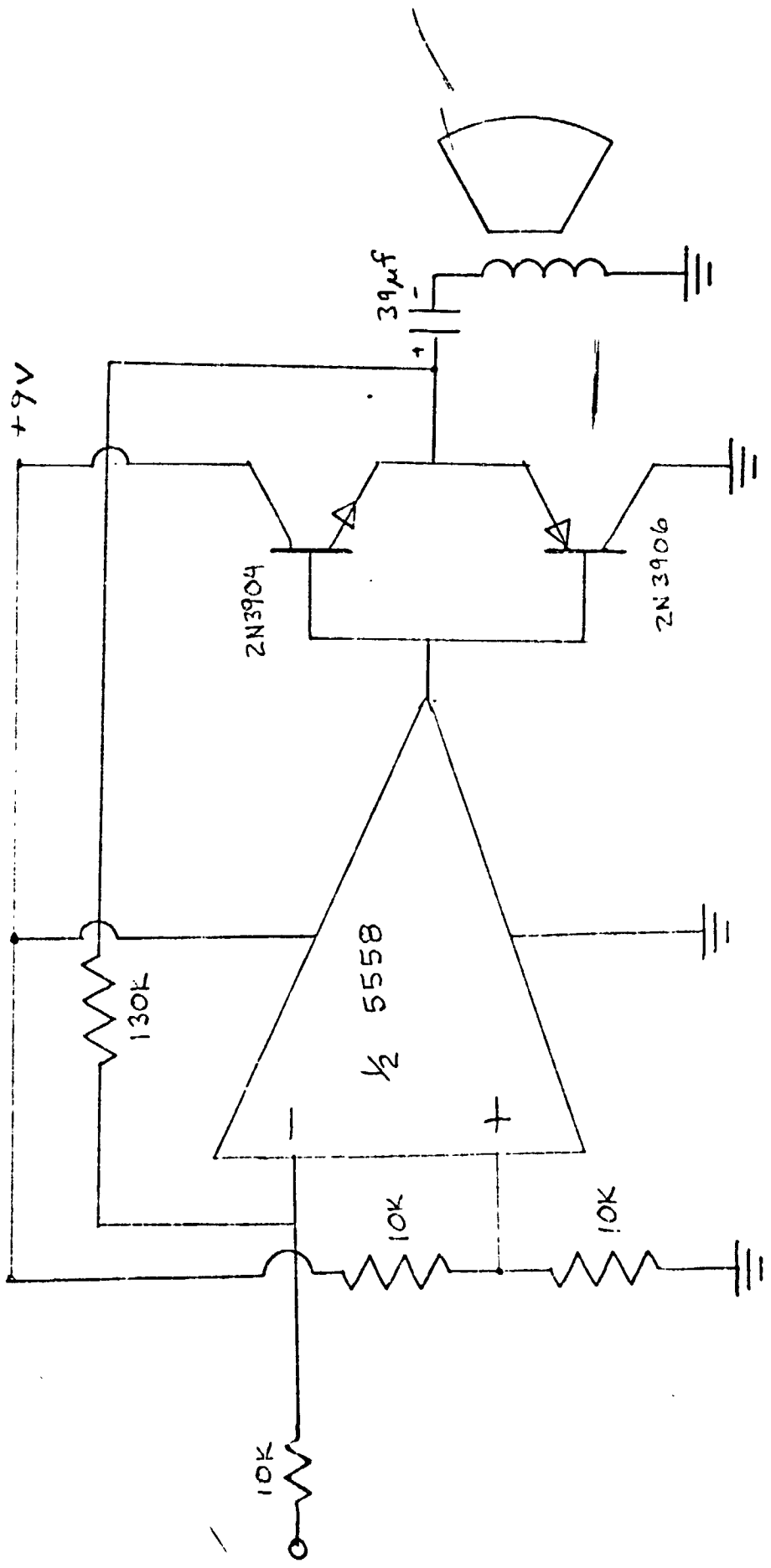

Fig. 22. Audio Amplifier Electronics

simulate the new sensor so that the triangulation scheme can be included in the digital simulation and an appropriate path evaluation algorithm can be developed for the vehicle.

C.3.a. Development of a Mid-Range Path Selection System

The objective of this subtask is to investigate the feasibility of a vehicle-fixed terrain scanning concept for mid-range path selection purposes. An optimal sensor configuration and path selection method may then be determined for this type of sensing system.

Analysis of a single beam sensing system, Ref. 1, has suggested refinements which have been incorporated in succeeding multi-beam systems. Both double and triple beam systems have been proposed and evaluated. The most recently evaluated system is an advanced, three beam system which employs nonuniformly spaced azimuth scans.

The general multi-beam system is described below and the results of the evaluation of the double beam version are briefly discussed. The advanced three beam system is then described and discussed in detail.

Multi-beam System Description

In general, a path selection system must sense the terrain, model the terrain using data from the sensor, and using the terrain model, select a path. Described below are the three distinct subsystems that perform these functions: the sensor, the terrain modeller, and the path selection algorithm.

Sensor Systems - The computer will simulate up to four sensors, mounted on a vertical mast which is fixed to the front of the vehicle. One can specify the number of sensors to be used and their heights on the mast. Each sensor scans in a plane perpendicular to the mast, making twenty-nine range measurements. The azimuths at which measurements are made are also specified by the user and can be uniformly or nonuniformly spaced. Note that this sensing scheme works for positive obstacles only (i.e. those obstacles which protrude above the ground). For a negative obstacle, an ideal sensor is simulated which senses the obstacle after the vehicle bumps into it.

Terrain Modeller - Taking the twenty-nine range measurements from the sensor, the terrain modeller generates a go/no-go map for fifteen possible forward paths. This is done by comparing the range measurements with a computed set of thresholds, which take into account the vehicle width and a specified buffer zone.

Path Selection Algorithm - There are two modes of operation for the algorithm. In normal operation, the algorithm sets the vehicle on the most direct, acceptable path to target. When all possible fifteen forward paths are blocked, the emergency mode is implemented. First, the vehicle is backed

up in a straight line. Then a new sensor scan is made and the most direct, acceptable path to target is again taken, excluding the seven forward paths which would again lead the vehicle across unsafe terrain. The emergency mode can also employ a memory capability at the user's option. If memory is used, a preferred side is chosen after taking a new sensor scan. This choice is made by summing the ranges on each side of the vehicle and selecting the side whose sum is largest. For a specified number of subsequent scans, the terrain modeller blocks paths on the unpreferred side.

Double Beam System Evaluation

The multi-beam mid-range system was first investigated using two sensors mounted on the mast at heights of 0.5 meters and 1.5 meters above the ground. This system was evaluated using the standard testing procedures described in Ref. 2, namely,

Case I	2x2 meter boulder encounters on flat base terrain
Case II	2/3 x 2/3 meter boulder encounters on flat base terrain
Case III	Gently rolling terrain
Case IV	Rolling incline
Case V	Boulder-crater field of moderate complexity

Each case was simulated in the absence of noise and with the addition of attitude and range noise. Combinations of range and attitude noise were also simulated.

During the simulation, the obstacle avoidance buffers were kept at 0.5 meters for the lower sensor and 1.0 meters for the upper sensor. A smaller buffer on the lower sensor resulted in a lower sensitivity to attitude noise and prevented the vehicle from overreacting to small boulders. By giving the higher sensor a larger buffer, the vehicle had enough time to initiate avoidance maneuvers around larger obstacles, avoiding unnecessary backups.

As indicated in Fig. 23, the system was capable of avoiding obstacles of a size comparable to the size of the vehicle. But as the size of the boulder decreased, the system had difficulty detecting them in time for avoidance maneuvers to be conveniently employed. Eventually, the system lost sight of the obstacle between successive beam shots indicating a need for decreased azimuth differences. This decreased azimuth difference was included in the three beam system, which is described later

As a result of wandering noted on rolling and inclined terrain, the threshold on the lower sensor was reduced, and a nonuniformly spaced azimuth differ-

Figure of Merit=0.978
No Noise was Used

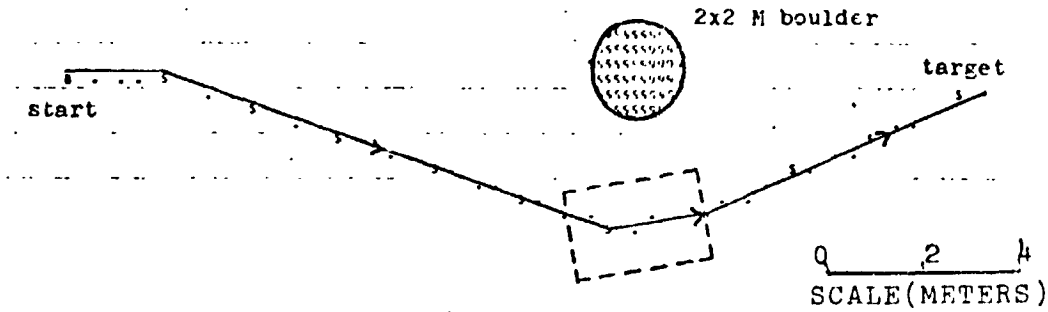

Figure of Merit=0.759
No Noise was Used

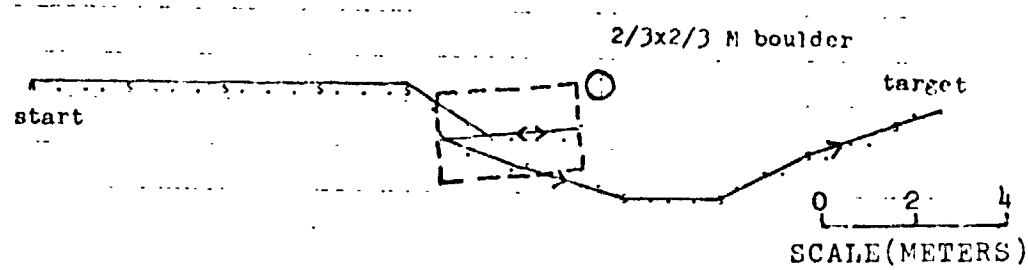

Fig. 23

PERFORMANCE OF THE DOUBLE BEAM SYSTEM
IN SINGLE BOULDER ENCOUNTERS
ON FLAT TERRAIN

was used. The configuration which was implemented is shown in Fig. 24. Since the azimuth differences decrease towards the front of the vehicle, the vehicle was not able to turn as sharply as before. But with decreased azimuth differences at the front of the vehicle, it was thought that the vehicle might not have to turn sharply since the vehicle could start avoidance maneuvers well in advance of any obstacles. Two possible alternative approaches were proposed for better vehicle performance on turns. One possible approach would be to slow the vehicle down when a sharp turn is required. Alternatively, one could increase the number of beam shots per scan and the number of possible paths. To avoid undue complication in the path selection algorithm, the former proposal was implemented.

Three-beam Mid-range System

As recommended by the two-beam study, another sensor was added at 1.0 meter, allowing for a lower threshold on the lower sensor, Ref. 3 and 4. Also, the nonuniform scanning scheme was carried over from the two beam system to increase the information known about the terrain in front of the vehicle. As indicated in Fig. 24, azimuth spacings were decreased towards the front of the vehicle.

It was noted that the three beam sensor system, with decreased thresholds on the lowest sensor and nonuniform scanning, wandered less than its simple two beam predecessor, as evidenced by comparing Fig. 25 with Fig. 26. It was found that on hilly and inclined terrain, the target was reached with a minimum of wandering about, but that there were a number of unnecessary backups required for small boulders on flat terrain. There appears to be a trade-off between performance with single boulder encounters and performance on an incline. Decreasing the thresholds for reduced wandering on inclines led to unnecessary backups with single boulder encounters. It is recommended that the thresholds be determined by vehicle attitude. Increasing the thresholds with a smaller in-path slope could lead to fewer backups on small boulders in flat terrain. As vehicle attitude increases, thresholds can be decreased so that the vehicle will not wander and will head directly for the target.

Simulation results on complicated boulder-crater fields, Fig. 27 and Fig. 28, show the trade-off that was made. Note that improved performance on the sloping terrain has resulted in numerous backups and a path whose figure of merit is low due to the lower thresholds necessary to prevent wandering on an incline. Further, the low figure of merit resulted from the mid-range system's inability to detect negative obstacles.

C.3.b. Short Range System

The objective of this subtask is to simulate a path selection system having sensing capabilities limited to a range of three meters, Ref. 5. It is hoped that the simulations run in this investigation will be sufficient to decide if the short range system can be used as:

1) a primary guidance system,

2) a guidance subsystem used with a midrange subsystem to detect small positive obstacles and craters, and/or

3) a backup guidance system.

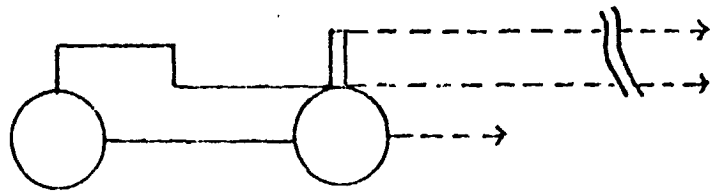

SIDE VIEW

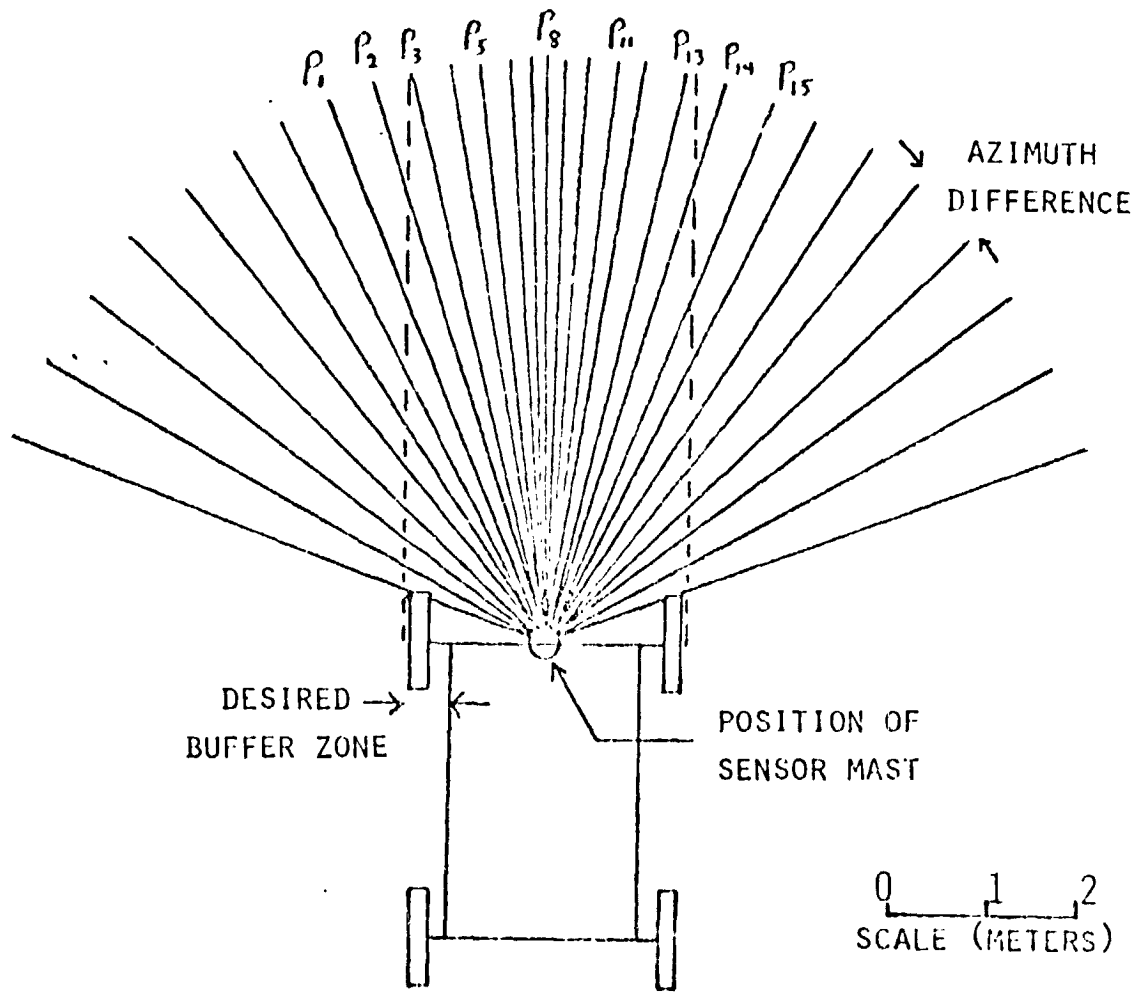

TOP VIEW

Fig. 24. Three Beam Mid-Range Sensor Configuration

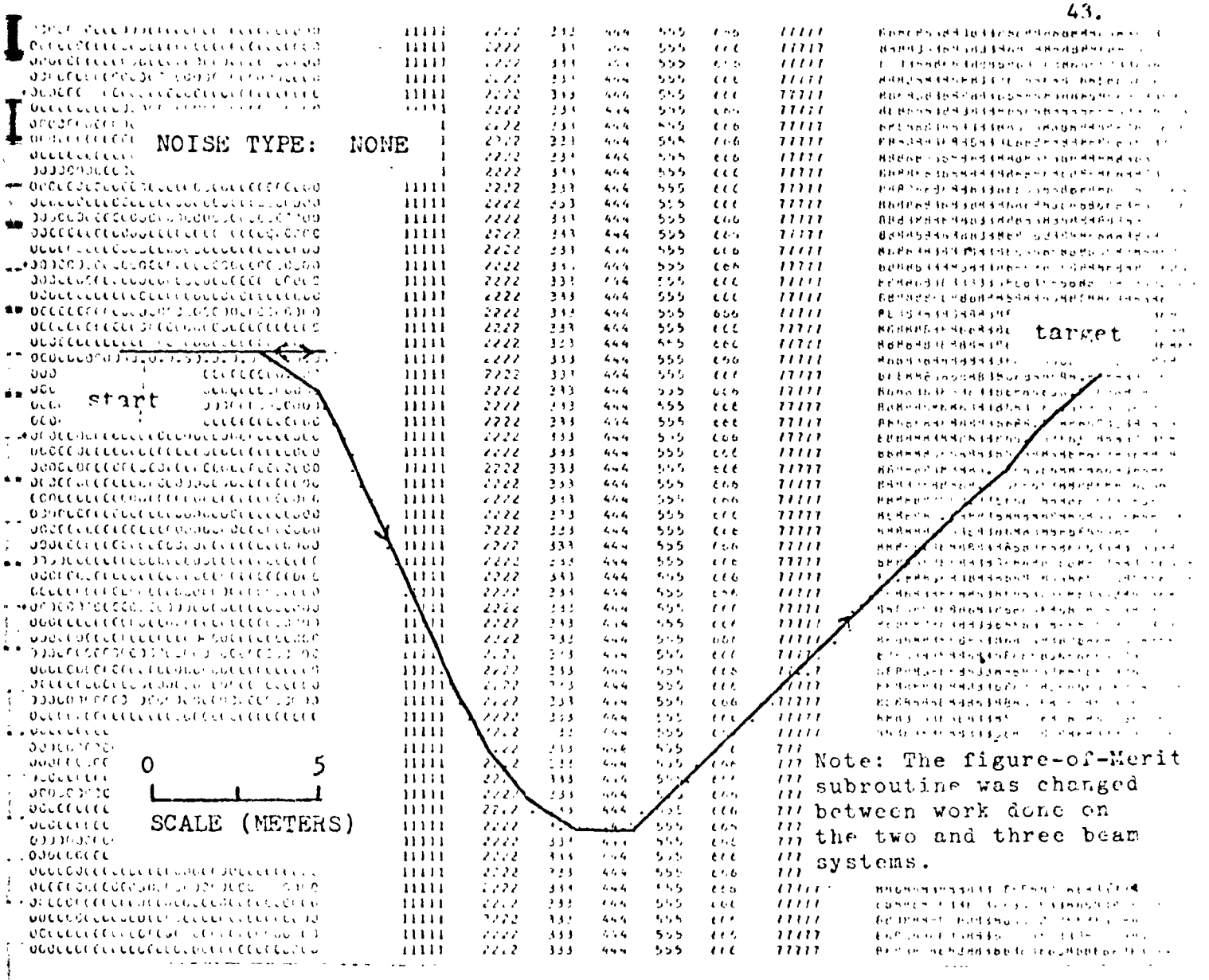

	0	1	2	3	4
SYMBOL	-0.10 10 0.07	0.35 10 0.47	0.97 10 1.31	1.63 10 1.96	2.28 10 2.60
RANGE IN ATTENUATORS (METERS)	5	6	7	8	9
	2.93 10 2.25	3.57 10 3.09	4.22 10 4.54	4.86 10 5.18	5.51 10 5.83

Fig. 25. Double Beam Mid-Range System with Uniform Scanning on a Rolling Incline.

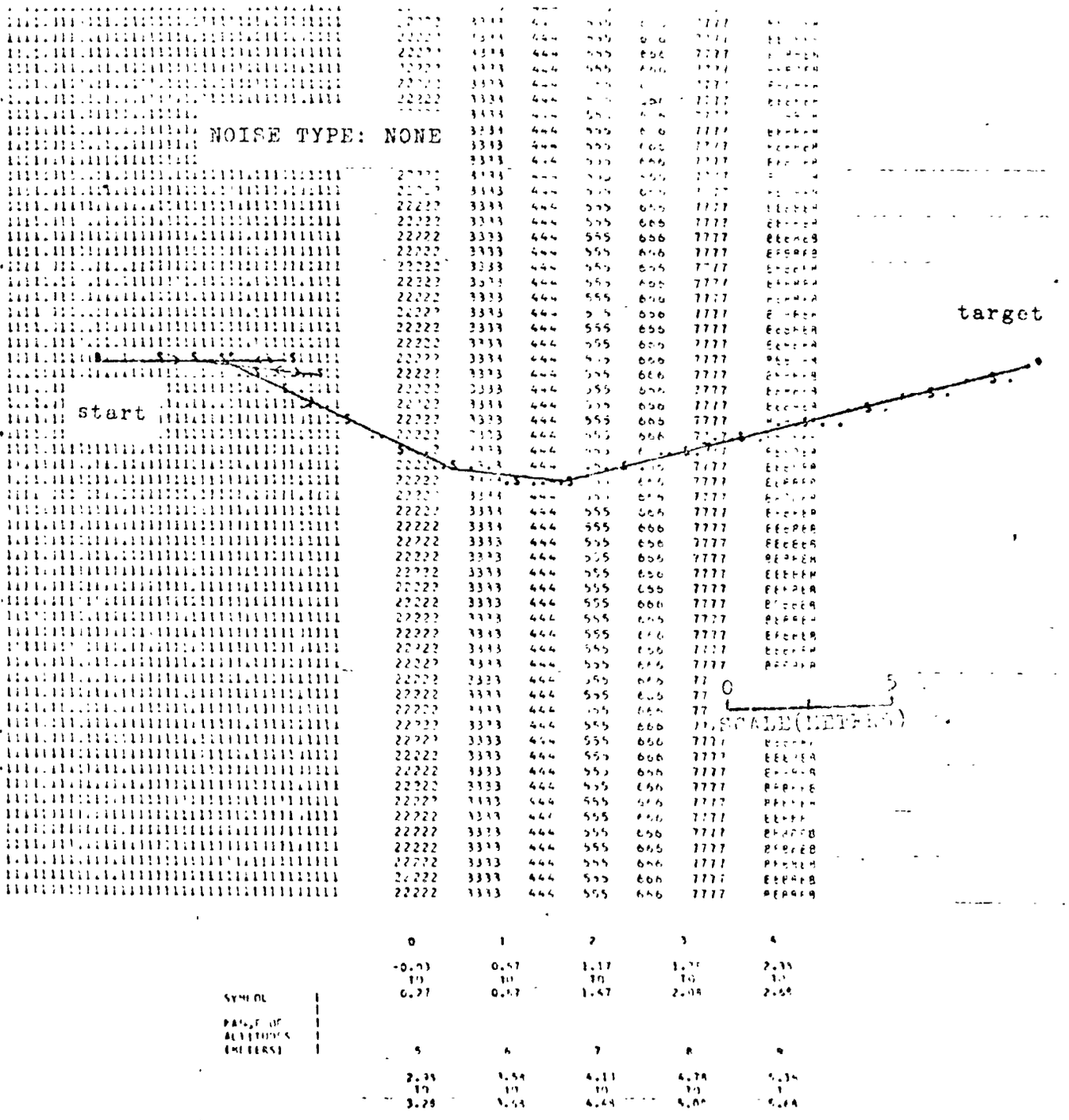

	0	1	2	3	4
	-0.03 to 0.27	0.27 to 0.57	1.17 to 1.47	1.77 to 2.08	2.38 to 2.68
SYMBOL					
PERCENT OF ALLOTTED TRIALS (METERS)					
	5	6	7	8	9
	2.38 to 2.98	2.98 to 3.28	4.11 to 4.41	4.71 to 5.01	5.31 to 5.61

Fig. 26. Triple Beam System with Reduced Thresholds on the Lower Sensor and Non-Uniform Scanning

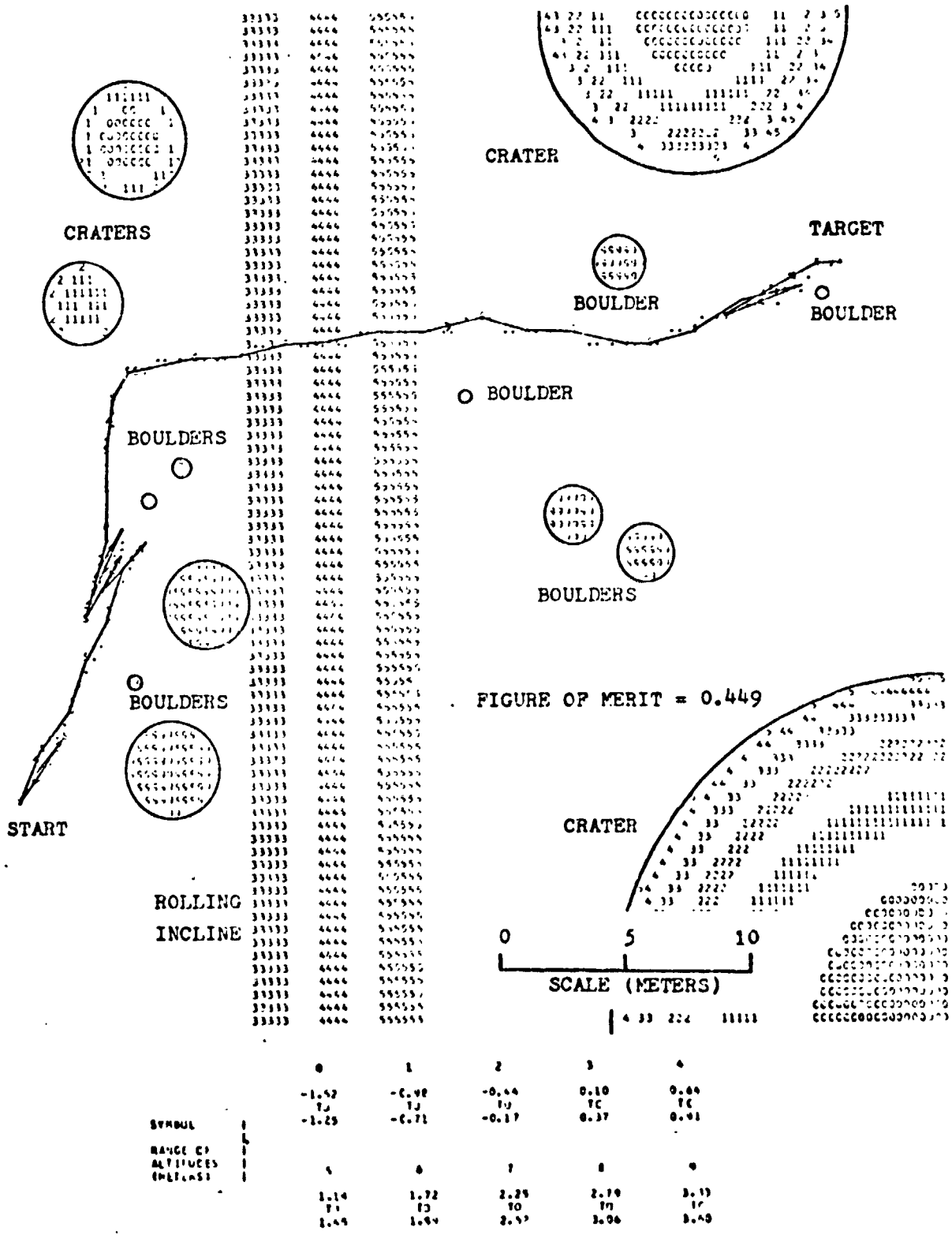

Fig. 27. Advanced, Three Beam System on a Complex Boulder-Crater Field

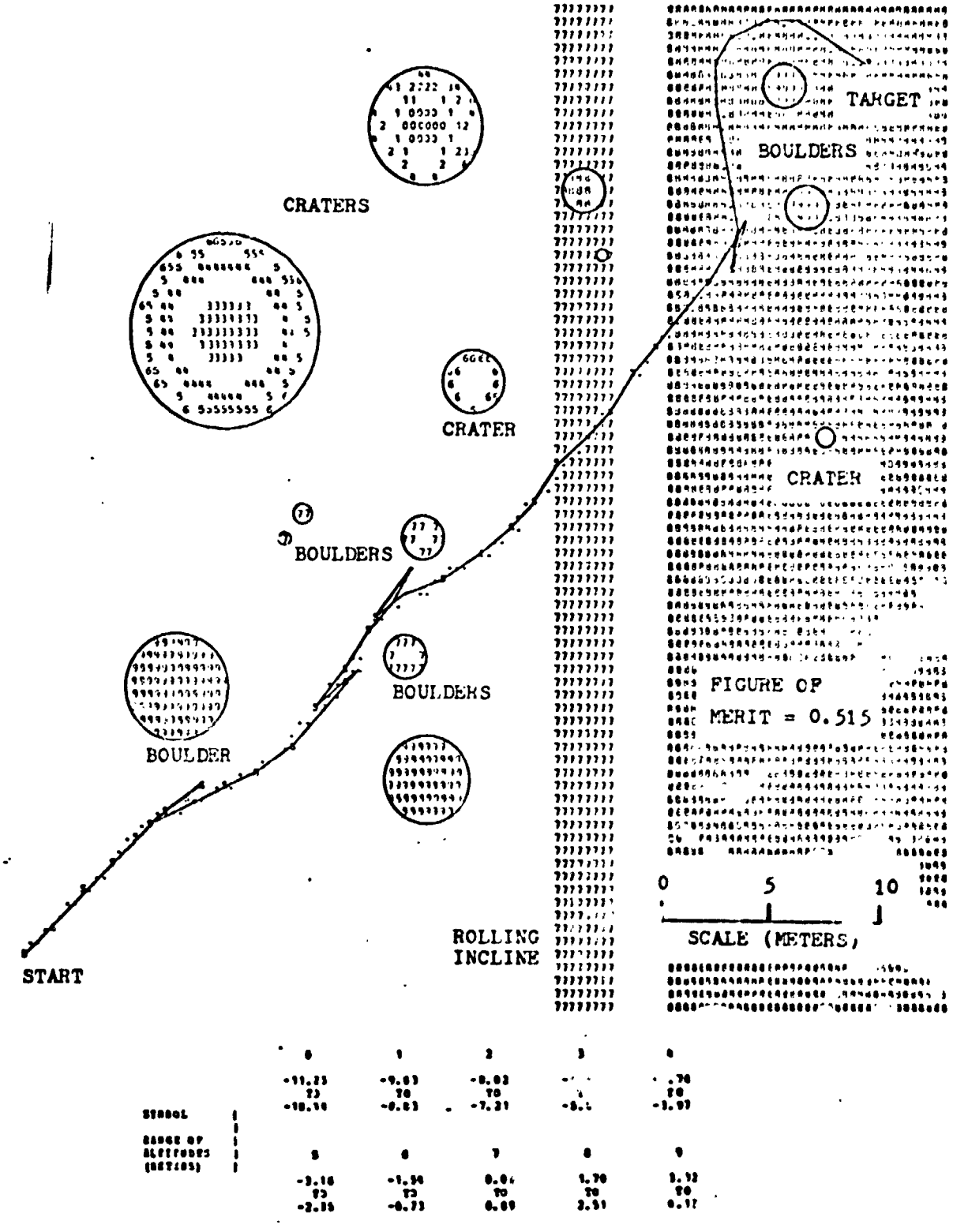

Fig. 28 Advanced, Three Beam System on a mpl ler-Crater Field

Note that the sensor described below is a conceptual configuration only and is not intended to indicate the need for a specific hardware design.

As in the mid-range case, the path selection system consists of a sensor, a terrain modeller, and a path selection algorithm. Each is described below.

Sensor - The sensor, analogous to a blind man with a cane, consists of two proximity detectors mounted at the end of an arm attached to the vehicle. A picture of the system is shown in Fig. 29. The arm sweeps from side to side and takes measurements in the forward and downward directions. Forward measurements were used to protect the arm by retracting it. Under normal operating conditions, the arm is two meters long, but it can be retracted to one meter if necessary. The downbeam measurements provide readings of the height of the terrain at the end of the arm relative to the height of the vehicle. This information is used in the terrain modeller.

Terrain Modeller - The terrain modeller makes use of three successive sweeps of the vehicle's arm to fit the terrain in each of the possible vehicle paths to a height function which is quadratic in the horizontal and vertical distances from the vehicle. Each path, illustrated in Fig. 30, is then evaluated by a path selection algorithm.

Path Selection Algorithm - The short range system takes the direct path to the target which meets all of the following criteria:

1) the in-path slope does not exceed the vehicle's ability to traverse it.

2) the cross-path slope does not exceed the maximum angle at which slippage is bound to occur.

3) the change in both cross-path and in-path slope is such that the vehicle will not be hung up or will not "bottom out".

4) there are no positive obstacles in the way, as found from the forward proximity sensor.

Simulation Results

Preliminary testing was run on the algorithm, following the standard testing procedure that was previously mentioned. Single boulder and single crater runs were made, with encouraging results. In Fig. 31, we see that the proximity sensor successfully avoided a positive obstacle using the forward proximity sensor and the arm's capability to retract. Although there was some wandering, obstacle avoidance proceeded nicely and the target was reached

a) Top View

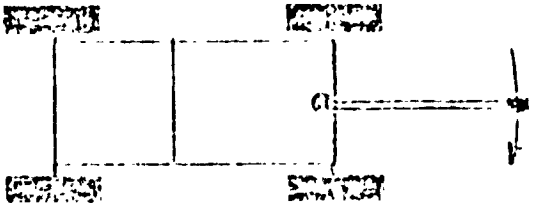

b) Side View

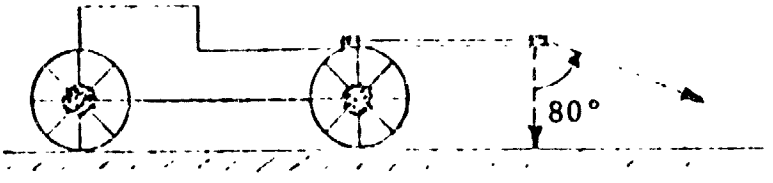

Fig. 29 - Short-Range System Sensor Configuration

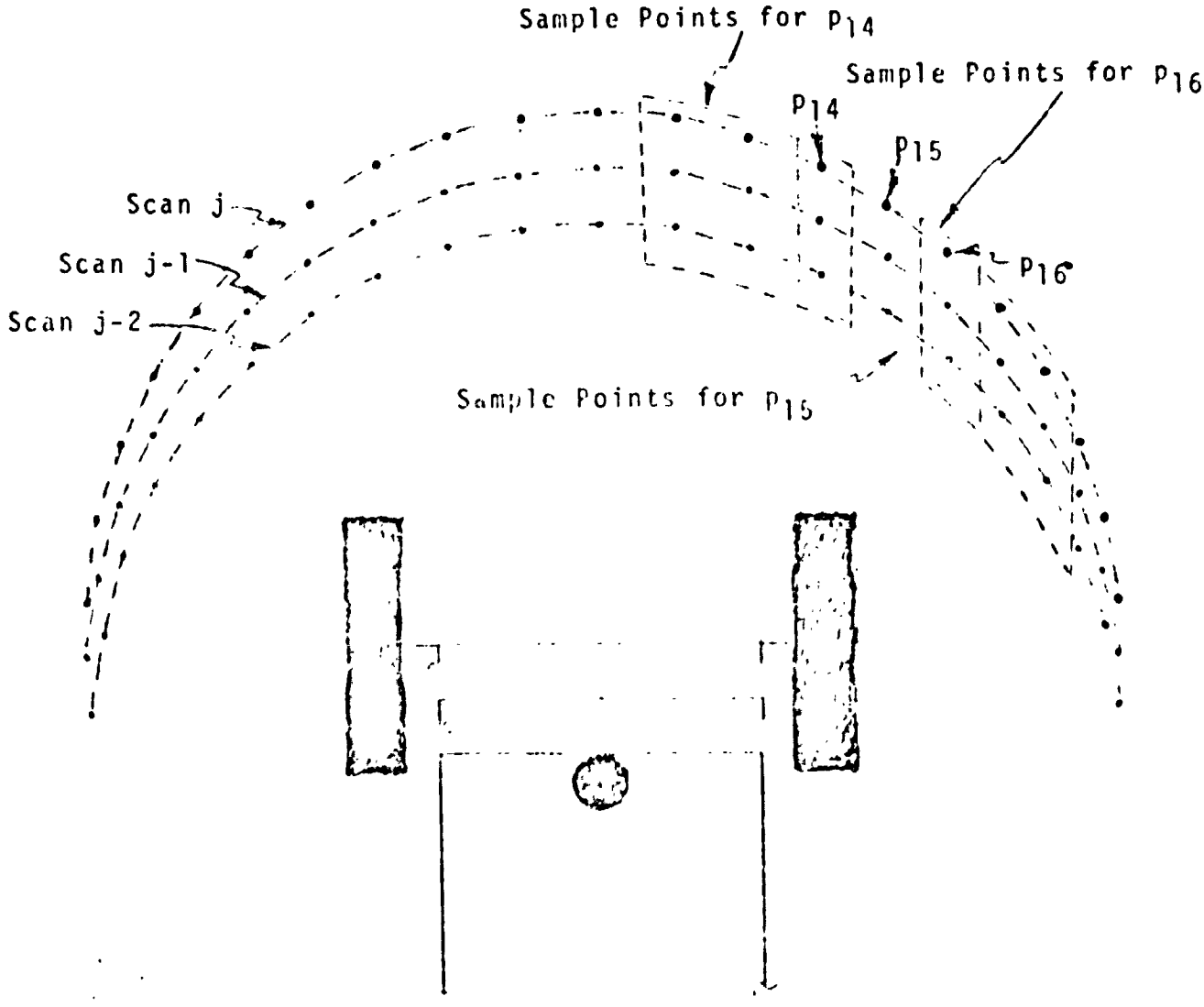

Fig.30. Sample Points for Terrain Modelling and Path Selection in the Short-Range System

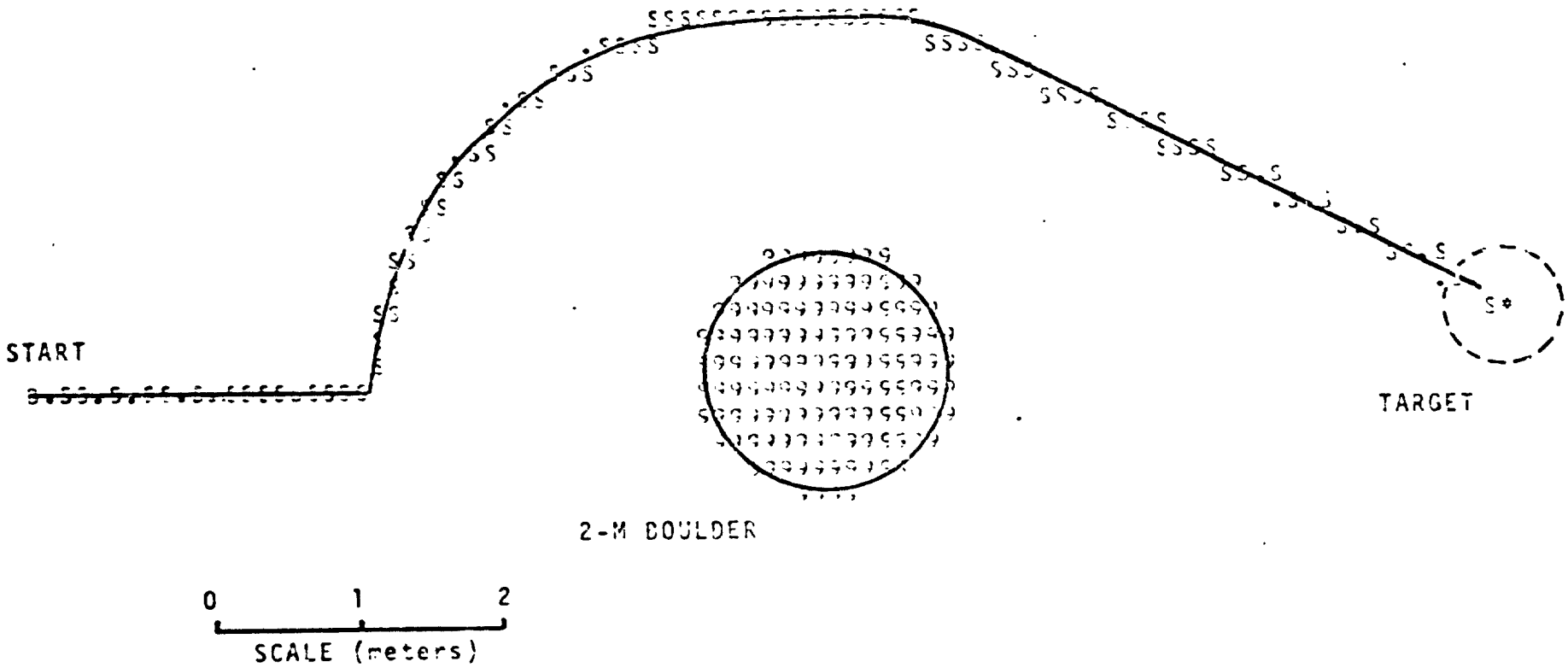

Fig. 31. Performance of the Short-Range System in an Encounter with a Boulder on Flat Terrain

A single crater encounter was simulated which resulted in this group's first success ul negative obstacle avoidance maneuver. The simulation is shown in Fig. 32.

One further feature of the system's path selection algorithm is the memory capability. Conceptually, information from the successive scans is stored so that when all paths are blocked, the vehicle can return to a previous decision point and find a new path to target. This concept is illustrated in Fig. 33. On scan 3, the vehicle decided to take a path around the boulder but later on scan 6 found itself in impassable terrain. The vehicle can then return to the decision point and circumvent the boulder by going around the opposite side. An actual simulation of this capability occurs in an early run of the algorithm, in Fig. 34. The vehicle found itself proceeding into the crater, having erroneously selected a path towards the crater from a previous scan. At the position marked X, the vehicle models the terrain and discovers that this path would not be passable. Finally, the vehicle uses its memory capability, returns to the decision point and moves around to the target. While the capabilities of the algorithm have not been fully tested, these initial results demonstrate that the short range concept warrants further study, refinement, and simplification.

General Conclusions

In viewing the work done to date, certain conclusions of a general nature can be made which should be applicable to sensing schemes other than the particular ones studied. Work done on the mid-range path selection system has led to studies of sensor placement, threshold distances, nonuniform scanning, and the effect of vehicle speed on the vehicle's turning ability. Vehicle memory has proven to be helpful when the vehicle is confronted with an emergency situation. Some general conclusions may also be drawn concerning the terrain modelling schemes that the Path Selection Systems Group has employed to date.

In the mid-range system (a system which detects positive obstacles on the order of ten meters away), one, two and three beam systems have been studied. On multiple beam sensing systems, the lower beams employ a lower threshold than the upper beams since small rolls and pitches can cause the lower beam to sense an obstacle when there are none. Also, the upper beams require longer thresholds so that obstacle avoidance of larger obstacles can begin with enough time for the obstacle to be successfully avoided without necessitating emergency backup maneuvers.

While the two beam system was being tested, it was found to have difficulty avoiding boulders which were smaller than the vehicle, but big enough to block vehicle passage. These boulders tended to be missed by the sensors because it was between the aximuth scans. Hence the scans were concentrated towards a more limited field of view, but most of the obstacles with which the vehicle must concern itself tend to be in front of the vehicle. Improved path selection performance resulted from these nonuniformly spaced azimuth scans.

After centering the scans twoard the front of the vehicle, the vehicle was found to be unable to turn as sharply as was previously the case. The reason for this was that the paths to be selected were also centered towards the front of the vehicle. Two possible solutions were proposed for increasing the vehicle's ability to turn. First, the beam shots per scan could be

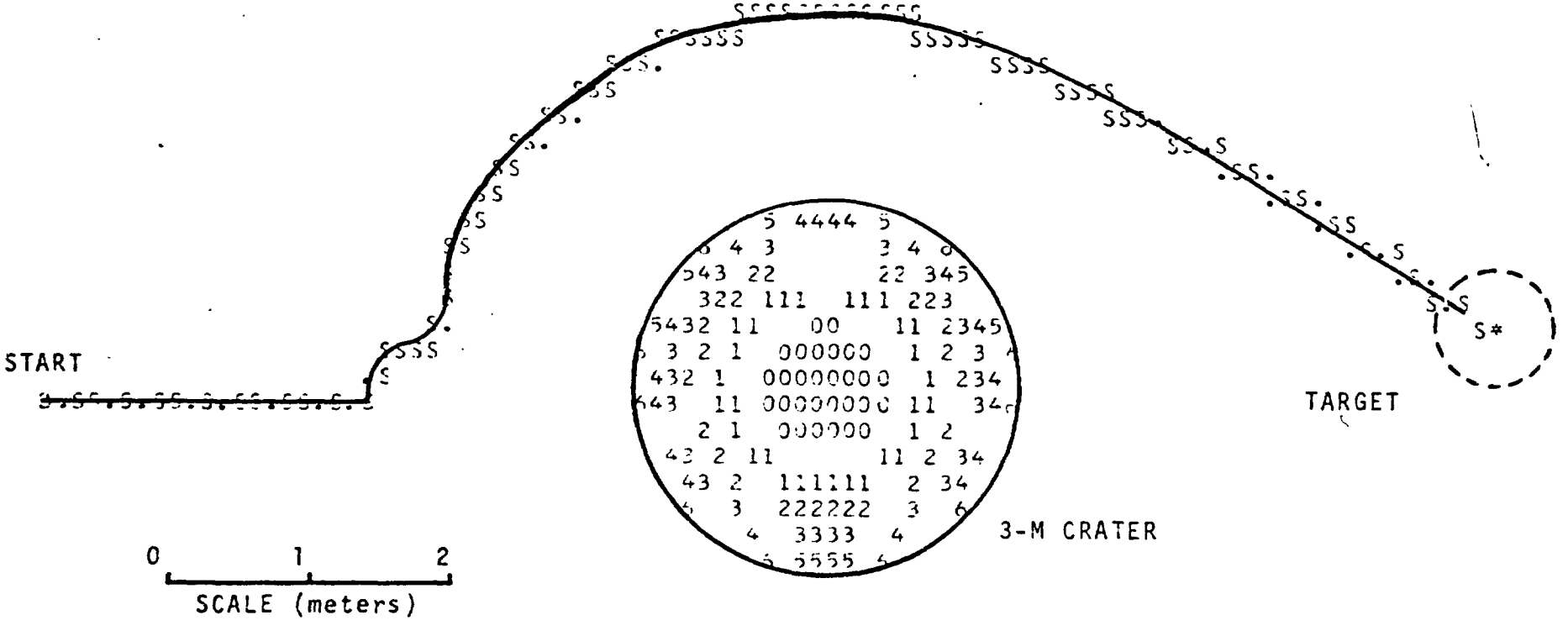

Fig. 32. A Successful Avoidance of a Crater on Flat Surroundings with the Short-Range System

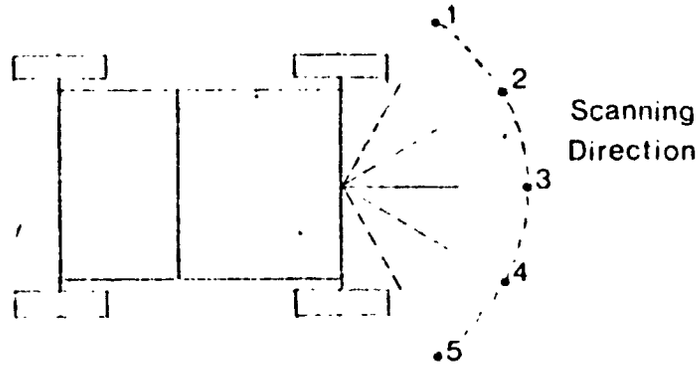

a) Sensor Configuration and Sensor Thresholds

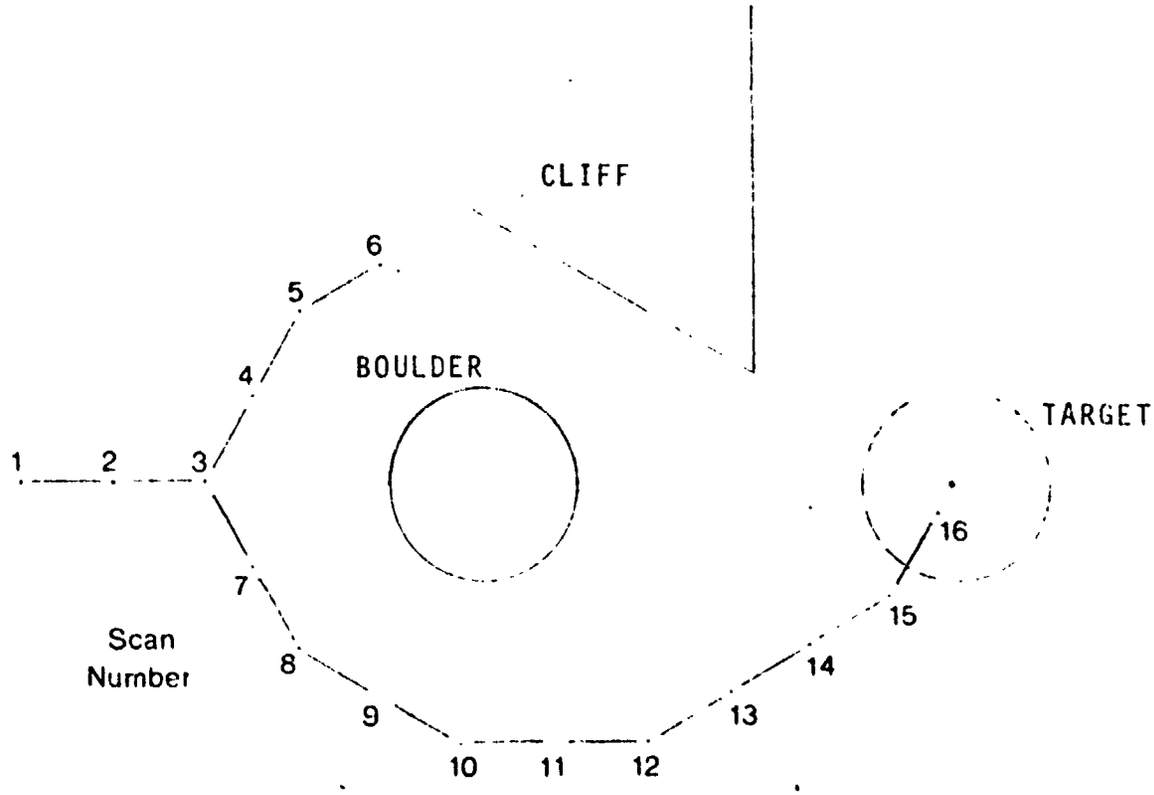

b) Vehicle Path

Fig. 33. Effects of Vehicle Memory for the Short-Range System

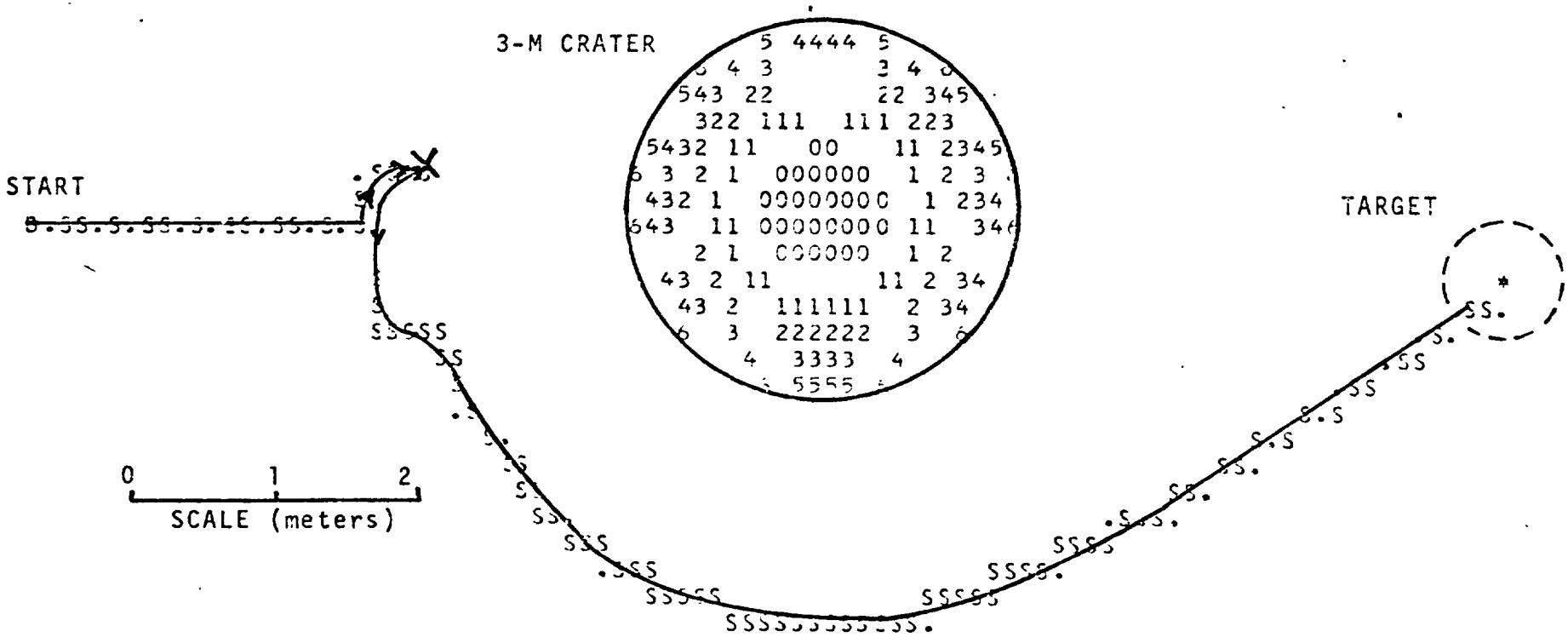

Fig. 34. The Short-Range System's Use of Memory to Redirect Vehicle Path

increased, thus increasing the number of paths available to the vehicle. Alternatively, vehicle speed could be reduced in the turn, making a wider range of paths available to the vehicle. The latter proposal was implemented since it did not complicate the path selection algorithm.

When all paths to the vehicle are blocked, the emergency mode of the path selection algorithm is activated. The vehicle must remember where the obstacle is or it may tend to bump into the obstacle repeatedly. Hangups of this sort were avoided using vehicle memory to block off paths which would again lead the vehicle towards the obstacle. This kind of algorithm is necessary in virtually any emergency mode operation of the path selection algorithm. Another possibility, especially with a short-range type of system, is to return to a previous decision point, a point where one path was chosen over another due to better target proximity. The alternative path can then be explored, decreasing the chances that the vehicle will be boxed in.

In modelling the terrain in front of the vehicle, computing the in-path slope from the height of the vehicle and the height of the short range sensor leads to an erroneous model of the actual terrain. That is, it assumes that the terrain is uniformly sloped between the sensor at a known arm length away, and the vehicle. Algorithms which employed this type of modelling performed poorly. An approach which led to the detection of a negative obstacle was to model the terrain using three previous sensor scans. A quadratic fitting algorithm was then used, and the cross-path and in-path slopes were then approximated. Although this algorithm has not been completely tested, preliminary testing indicates that negative obstacle avoidance is possible.

In light of the slower speeds and reduced terrain size of the new mini-rover concept, more realistic terrain representations and vehicle dynamics simulations have been formulated. These improvements are being incorporated in the simulation package.

The triangulation sensor proposed under Task B is being modelled and will be simulated so that appropriate path selection systems based upon this concept can be simulated and design alternatives studied. This work will provide direct support for the ongoing vehicle and sensor hardware work during the coming academic year.

Documentation of the simulation program will continue to receive a considerable amount of effort in order to improve its effectiveness.

Task D. Obstacle Detection and Terrain Modeling

Investigations continued in the areas of obstacle detection by edge perception, computer graphic evaluation of edge detection procedures, terrain modeling, range measurement scanning concepts, laser range finder errors and obstacle classification. Summary progress reports covering each of these topics follow below.

Task D.1.a. Obstacle Detection - Ranjan Sonalkar
Faculty Advisor: Prof. C. N. Shen

The objective of this task is to develop a practical and reliable obstacle detection scheme which will make use of the range matrix obtained by a laser rangefinder. The range measurements may contain errors of anywhere between $\pm$ 5 cm to $\pm$ 10 cm. The Four Directional Ratio (FDR) algorithm developed last year has been documented in Ref. 6. The algorithm takes advantage of the fact that a significant change in the range readings occurs as the laser crosses the obstacle edges. For example, as the laser crosses the top edge of a boulder (positive obstacle) or the near edge of a crater (negative obstacle), the measured range increases suddenly and the FDR identifies these edges by detecting the corresponding range changes. However, the bottom edge of a boulder and the far edge of a crater, constitute changes in slopes and not ranges. The change in range caused by the change in slope, is then too small to be detected by the FDR algorithm. However, complete characterization of the obstacle is necessary for the rover to successfully negotiate the path towards its destination. Therefore, it was deemed necessary that the FDR algorithm be improved or a new one designed, which will fulfill the requirements.

The new algorithm that is proposed and is an adaptation of the Rapid Estimation Scheme (RES) described in Refs. 9 and 10 is documented in Refs. 7 and 8.

Outline of the Scheme

The range measurements contain errors, presumably of known statistics. Therefore, the measurements are not exact and cannot be fully relied upon. Also, the slope changes at the edges of obstacles have small effects on the range measurements and the effects are of the order of magnitude of the errors. These difficulties suggest the use of some kind of a reliable probabilistic mechanism to detect the edges, which will also be able to distinuish between the measurement errors and the changes of slopes at obstacle edges.

The scheme processes each column of the range matrix to determine whether an edge intersects it, Fig. 35. Each column is processed upwards, element by element and three consecutive elements are considered simultaneously. Three hypotheses are defined as follows:

H_1: Edge exists between stage i and i+1

H_2: Edge exists between stage i+1 and i+2

H_3: Edge, if any, exists after stage i+2

The three hypotheses are represented by the 3 branches of a decision tree, Fig. 36. Decision theory is employed to determine the correct hypothesis, which is equivalent to determining the position of an edge in a column.

Three different range estimates are obtained according to the three hypotheses. The estimate which matches the measured range best and is within the specified

CULLEN RANGE DATA FOR ONE METER HEMISPHERICAL BOULDER AT A DISTANCE OF 20.00 METERS WITH MARK SILVER

BETA MAX = 9.8 DEGREES BETA MIN = 5.0 DEGREES BETA INCREMENT = .20 DEGREES
THETA MAX = 4.0 DEGREES THETA MIN = -4.0 DEGREES THETA INCREMENT = .40 DEGREES

R(1,1)-----(BETA MIN, THETA MIN)
R(25,1)-----(BETA MAX, THETA MIN)

R(1,21)-----(BETA MIN, THETA MAX)
R(25,21)-----(BETA MAX, THETA MAX)

UNDISTORTED BY NOISE

34.38	34.38	34.38	34.38	34.38	34.38	34.38	34.38	34.38	34.38	34.38	34.38	34.38	34.38	34.38	34.38	34.38	34.38	34.38	34.38	34.38	34.38	34.38	34.38	34.38
33.13	33.13	33.13	33.13	33.13	33.13	33.13	33.13	33.13	33.13	33.13	33.13	33.13	33.13	33.13	33.13	33.13	33.13	33.13	33.13	33.13	33.13	33.13	33.13	33.13
31.88	31.88	31.88	31.88	31.88	31.88	31.88	31.88	31.88	31.88	31.88	31.88	31.88	31.88	31.88	31.88	31.88	31.88	31.88	31.88	31.88	31.88	31.88	31.88	31.88
30.75	30.75	30.75	30.75	30.75	30.75	30.75	30.75	30.75	30.75	30.75	30.75	30.75	30.75	30.75	30.75	30.75	30.75	30.75	30.75	30.75	30.75	30.75	30.75	30.75
29.69	29.69	29.69	29.69	29.69	29.69	29.69	29.69	29.69	29.69	29.69	29.69	29.69	29.69	29.69	29.69	29.69	29.69	29.69	29.69	29.69	29.69	29.69	29.69	29.69
28.69	28.69	28.69	28.69	28.69	28.69	28.69	28.69	29.69	29.69	29.69	29.69	29.69	29.69	29.69	29.69	29.69	29.69	29.69	29.69	29.69	29.69	29.69	29.69	29.69
27.75	27.75	27.75	27.75	27.75	27.75	27.75	27.75	29.69	29.69	29.69	29.69	29.69	29.69	29.69	29.69	29.69	29.69	29.69	29.69	29.69	29.69	29.69	29.69	29.69
26.88	26.88	26.88	26.88	26.88	26.88	26.88	27.75	29.69	29.69	29.69	29.69	29.69	29.69	29.69	29.69	29.69	29.69	29.69	29.69	29.69	29.69	29.69	29.69	29.69
26.13	26.13	26.13	26.13	26.13	26.88	27.75	29.69	29.69	29.69	29.69	29.69	29.69	29.69	29.69	29.69	29.69	29.69	29.69	29.69	29.69	29.69	29.69	29.69	29.69
25.38	25.38	25.38	25.38	25.38	26.13	27.75	29.69	29.69	29.69	29.69	29.69	29.69	29.69	29.69	29.69	29.69	29.69	29.69	29.69	29.69	29.69	29.69	29.69	29.69
24.63	24.63	24.63	24.63	25.38	26.13	27.75	29.69	29.69	29.69	29.69	29.69	29.69	29.69	29.69	29.69	29.69	29.69	29.69	29.69	29.69	29.69	29.69	29.69	29.69
23.94	23.94	23.94	23.94	24.63	26.13	27.75	29.69	29.69	29.69	29.69	29.69	29.69	29.69	29.69	29.69	29.69	29.69	29.69	29.69	29.69	29.69	29.69	29.69	29.69
23.31	23.31	23.31	23.31	24.63	26.13	27.75	29.69	29.69	29.69	29.69	29.69	29.69	29.69	29.69	29.69	29.69	29.69	29.69	29.69	29.69	29.69	29.69	29.69	29.69
22.69	22.69	22.69	22.69	24.63	26.13	27.75	29.69	29.69	29.69	29.69	29.69	29.69	29.69	29.69	29.69	29.69	29.69	29.69	29.69	29.69	29.69	29.69	29.69	29.69
22.13	22.13	22.13	22.13	24.63	26.13	27.75	29.69	29.69	29.69	29.69	29.69	29.69	29.69	29.69	29.69	29.69	29.69	29.69	29.69	29.69	29.69	29.69	29.69	29.69
21.56	21.56	21.56	21.56	24.63	26.13	27.75	29.69	29.69	29.69	29.69	29.69	29.69	29.69	29.69	29.69	29.69	29.69	29.69	29.69	29.69	29.69	29.69	29.69	29.69
21.06	21.06	21.06	21.06	24.63	26.13	27.75	29.69	29.69	29.69	29.69	29.69	29.69	29.69	29.69	29.69	29.69	29.69	29.69	29.69	29.69	29.69	29.69	29.69	29.69
20.56	20.56	20.56	20.56	24.63	26.13	27.75	29.69	29.69	29.69	29.69	29.69	29.69	29.69	29.69	29.69	29.69	29.69	29.69	29.69	29.69	29.69	29.69	29.69	29.69
20.06	20.06	20.06	20.06	24.63	26.13	27.75	29.69	29.69	29.69	29.69	29.69	29.69	29.69	29.69	29.69	29.69	29.69	29.69	29.69	29.69	29.69	29.69	29.69	29.69
19.63	19.63	19.63	19.63	19.63	19.63	19.63	19.63	19.63	19.63	19.63	19.63	19.63	19.63	19.63	19.63	19.63	19.63	19.63	19.63	19.63	19.63	19.63	19.63	19.63
19.19	19.19	19.19	19.19	19.19	19.19	19.19	19.19	19.19	19.19	19.19	19.19	19.19	19.19	19.19	19.19	19.19	19.19	19.19	19.19	19.19	19.19	19.19	19.19	19.19
18.75	18.75	18.75	18.75	18.75	18.75	18.75	18.75	18.75	18.75	18.75	18.75	18.75	18.75	18.75	18.75	18.75	18.75	18.75	18.75	18.75	18.75	18.75	18.75	18.75
18.38	18.38	18.38	18.38	18.38	18.38	18.38	18.38	18.38	18.38	18.38	18.38	18.38	18.38	18.38	18.38	18.38	18.38	18.38	18.38	18.38	18.38	18.38	18.38	18.38
17.97	17.97	17.97	17.97	17.97	17.97	17.97	17.97	17.97	17.97	17.97	17.97	17.97	17.97	17.97	17.97	17.97	17.97	17.97	17.97	17.97	17.97	17.97	17.97	17.97
17.63	17.63	17.63	17.63	17.63	17.63	17.63	17.63	17.63	17.63	17.63	17.63	17.63	17.63	17.63	17.63	17.63	17.63	17.63	17.63	17.63	17.63	17.63	17.63	17.63

CONTAMINATED BY ZERO MEAN, .05 METER STANDARD DEVIATION, GAUSSIAN NOISE

34.34	34.37	34.38	34.33	34.37	34.27	34.34	34.41	34.34	34.33	34.36	34.37	34.27	34.38	34.46	34.38	34.30	34.35	34.44	34.33	34.29
33.11	33.17	33.12	33.15	33.17	33.09	33.12	33.12	33.09	33.05	33.16	33.03	33.09	33.24	33.09	33.13	33.12	33.11	33.07	33.07	33.09
31.84	31.89	31.86	31.92	31.89	31.89	31.91	31.87	31.84	31.84	31.85	31.92	31.89	31.80	32.02	31.91	31.91	31.87	31.89	31.82	31.91
30.83	30.85	30.79	30.83	30.87	30.74	30.82	30.82	30.84	30.73	30.90	30.79	30.70	30.82	30.79	30.67	30.72	30.68	30.84	30.78	30.74
29.73	29.76	29.76	29.69	29.72	29.62	29.66	29.62	29.62	29.89	29.93	29.98	29.75	29.73	29.69	29.69	29.72	29.70	29.61	29.62	29.71
28.76	28.73	28.75	28.69	28.81	28.80	28.64	28.67	19.91	19.79	19.76	19.82	19.99	28.69	28.72	28.68	28.69	28.74	28.64	28.61	28.76
27.74	27.81	27.72	27.65	27.87	27.77	27.78	19.86	19.73	19.62	19.62	19.63	19.75	19.83	27.71	27.70	27.78	27.73	27.72	27.77	27.75
26.42	26.61	26.77	26.79	26.63	26.64	19.89	19.72	19.49	19.50	19.50	19.61	19.69	19.72	19.82	26.81	26.83	26.98	26.91	26.90	26.82
26.15	26.07	26.09	26.16	26.13	26.03	19.67	19.63	19.56	19.59	19.60	19.47	19.62	19.71	19.67	19.93	26.09	26.14	26.15	26.10	26.21
25.34	25.38	25.35	25.43	25.39	19.61	19.63	19.31	19.49	19.49	19.42	19.39	19.40	19.55	19.62	19.78	25.51	25.39	25.34	25.34	25.43
24.52	24.65	24.58	24.60	24.63	19.74	19.60	19.43	19.42	19.45	19.39	19.34	19.40	19.58	19.56	19.21	24.53	24.67	24.53	24.58	24.65
23.45	23.40	23.38	23.47	19.97	19.75	19.51	19.33	19.27	19.32	19.27	19.34	19.43	19.46	19.48	19.71	19.92	23.94	23.94	23.97	23.88
23.37	23.19	23.31	23.29	19.81	19.60	19.69	19.39	19.37	19.45	19.26	19.32	19.34	19.42	19.52	19.66	19.84	23.35	23.30	23.32	23.28
22.64	22.74	22.63	22.64	19.81	19.58	19.66	19.37	19.39	19.27	19.20	19.33	19.32	19.51	19.45	19.59	19.74	22.73	22.64	22.69	22.71
22.13	22.12	22.04	22.17	19.74	19.56	19.45	19.31	19.23	19.31	19.27	19.20	19.39	19.35	19.37	19.44	19.76	22.13	22.20	22.20	22.11
21.54	21.60	21.62	21.51	19.72	19.47	19.47	19.33	19.24	19.26	19.24	19.22	19.25	19.24	19.45	19.53	19.65	21.55	21.62	21.45	21.59
21.02	21.07	21.10	21.05	19.72	19.47	19.45	19.35	19.23	19.28	19.19	19.31	19.35	19.35	19.37	19.45	19.64	21.10	21.06	21.06	21.09
20.54	20.63	20.56	20.54	19.65	19.47	19.42	19.29	19.14	19.18	19.21	19.20	19.30	19.27	19.37	19.44	19.64	20.04	20.59	20.68	20.55
20.07	20.05	20.00	20.01	19.69	19.46	19.42	19.32	19.37	19.25	19.16	19.28	19.27	19.31	19.44	19.50	19.63	20.01	19.98	20.06	20.03
19.57	19.63	19.64	19.65	19.68	19.53	19.32	19.38	19.27	19.32	19.22	19.16	19.34	19.30	19.44	19.40	19.66	19.54	19.53	19.64	19.59
19.19	19.18	19.17	19.10	19.19	19.15	19.27	19.19	19.18	19.19	19.13	19.21	19.14	19.25	19.28	19.18	19.23	19.21	19.14	19.21	19.17
18.77	19.77	18.67	18.80	19.80	18.74	18.69	18.70	18.91	18.79	18.80	18.65	18.71	18.75	18.75	18.77	18.80	18.78	18.75	18.81	18.72
18.36	18.37	18.37	18.36	18.28	18.43	18.36	18.31	18.36	18.32	18.42	18.25	18.36	18.30	18.38	18.26	18.42	18.41	18.29	18.41	18.28
17.93	18.02	17.91	17.95	17.95	18.00	17.95	18.00	17.95	17.98	17.97	17.94	17.91	17.97	18.00	17.91	17.96	17.99	17.92	18.04	17.94
17.65	17.67	17.63	17.73	17.65	17.72	17.61	17.63	17.55	17.64	17.61	17.64	17.57	17.63	17.63	17.59	17.59	17.60	17.60	17.65	17.64

Fig. 35. Range Matrix for a One Meter Hemispherical Boulder at a Distance of Thirty Meters

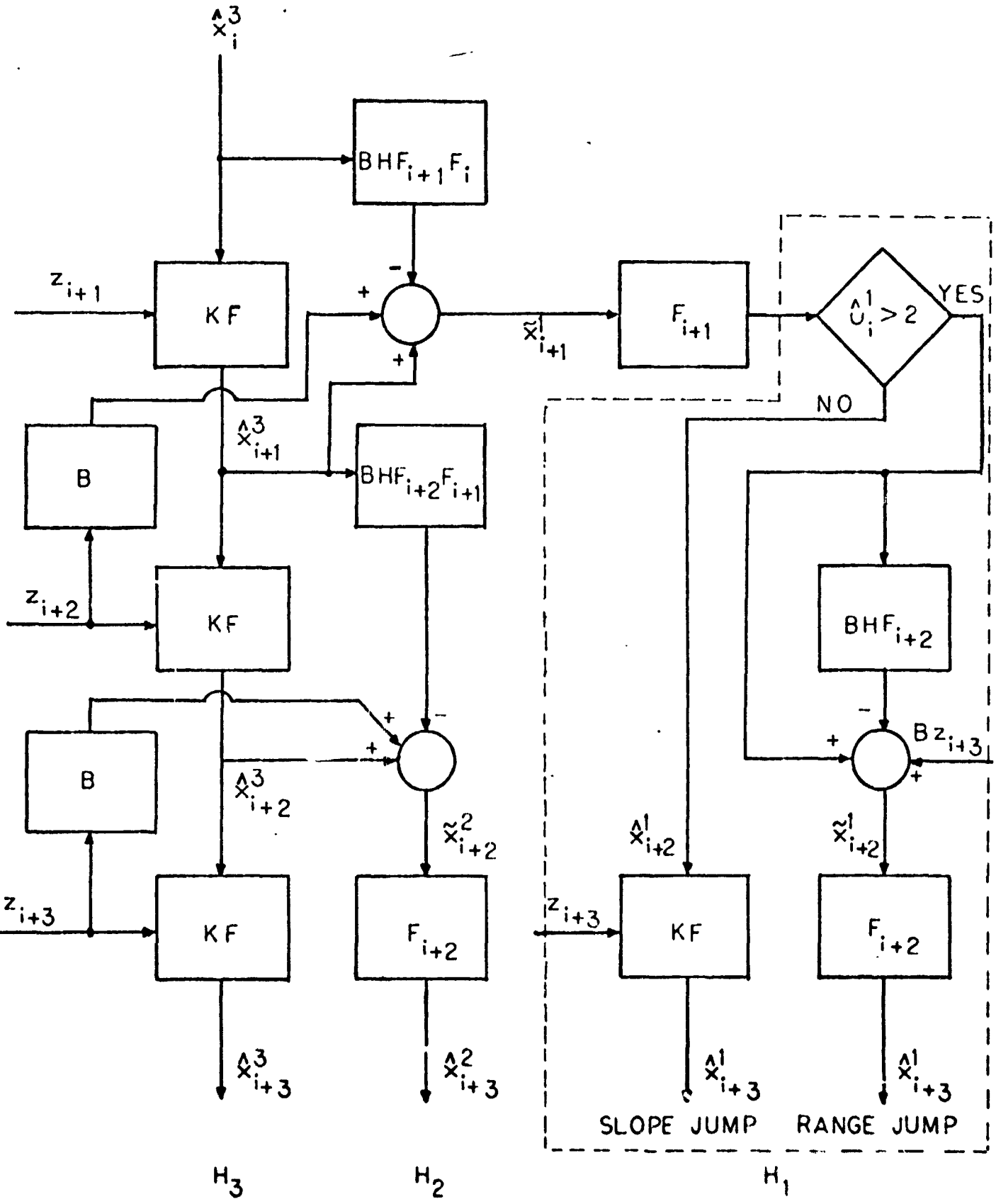

Fig. 36. DECISION TREE FOR PROCESSING COLUMNS

error statistics should belong to the correct hypothesis.

Decision Rule Mechanics

If branch 1, Fig. 36, is found to give the best fit to the data, then it is chosen which implies that the edge occurs between stages i and i+1 in the column under consideration. Another decision tree is then initiated at stage i+3 to start reaching for the next edge, if any. If branch 1 cannot be chosen, then it is rejected and the next observation is processed. At this next stage, previous hypothesis 2 (branch 2) becomes the new hypothesis 1 (branch 1) and a new hypothesis 2 (branch 2) is generated at stage i+3. This process is repeated till the end of the column is reached.

To work out the details of the scheme, the following two things are necessary.

1) Estimates of ranges and slopes conditioned on the three hypotheses at each stage of observation.

2) A decision rule which will determine the correct hypothesis after having obtained the estimates.

Examining Fig. 37 it is obvious that the horizontal components of the edges (top and front edges of boulders) will be detected while processing columns. However, the vertical components of the edges (side edges of boulders) can be determined only if we process rows also, in the same way as columns. Therefore, a similar analysis is performed on the rows, Fig. 38.

Model Definition

The rangefinder scans an area in front of it by varying azimuth and the elevation angles to obtain an (m x n) range matrix which has the same noise in it due to the errors in measurement, Eq. (1), Fig. 35. The noise is assumed to be zero mean, Gaussian with a standard deviation σ. In Eq. (1) Z_{ij} is the noise contaminated measurement.

$$Z = \begin{vmatrix} z_{m1} & z_{m2} & \cdots & z_{mj} & \cdots & z_{mn} \\ \vdots & \vdots & & \vdots & & \vdots \\ & & & z_{(i+1)j} & & \\ z_{i1} & \cdots & z_{i,j-1} & z_{ij} & z_{i,j+1} & \cdots \\ & & & z_{(i-1)j} & & \\ \vdots & \vdots & & \vdots & & \vdots \\ z_{11} & \cdots & & & & z_{1n} \end{vmatrix} \qquad (1)$$

$$z_{ij} = d_{ij} + v_{ij} \qquad (2)$$

Model Along a Column

Even though the adjacent rows and columns are related due to their proximity,

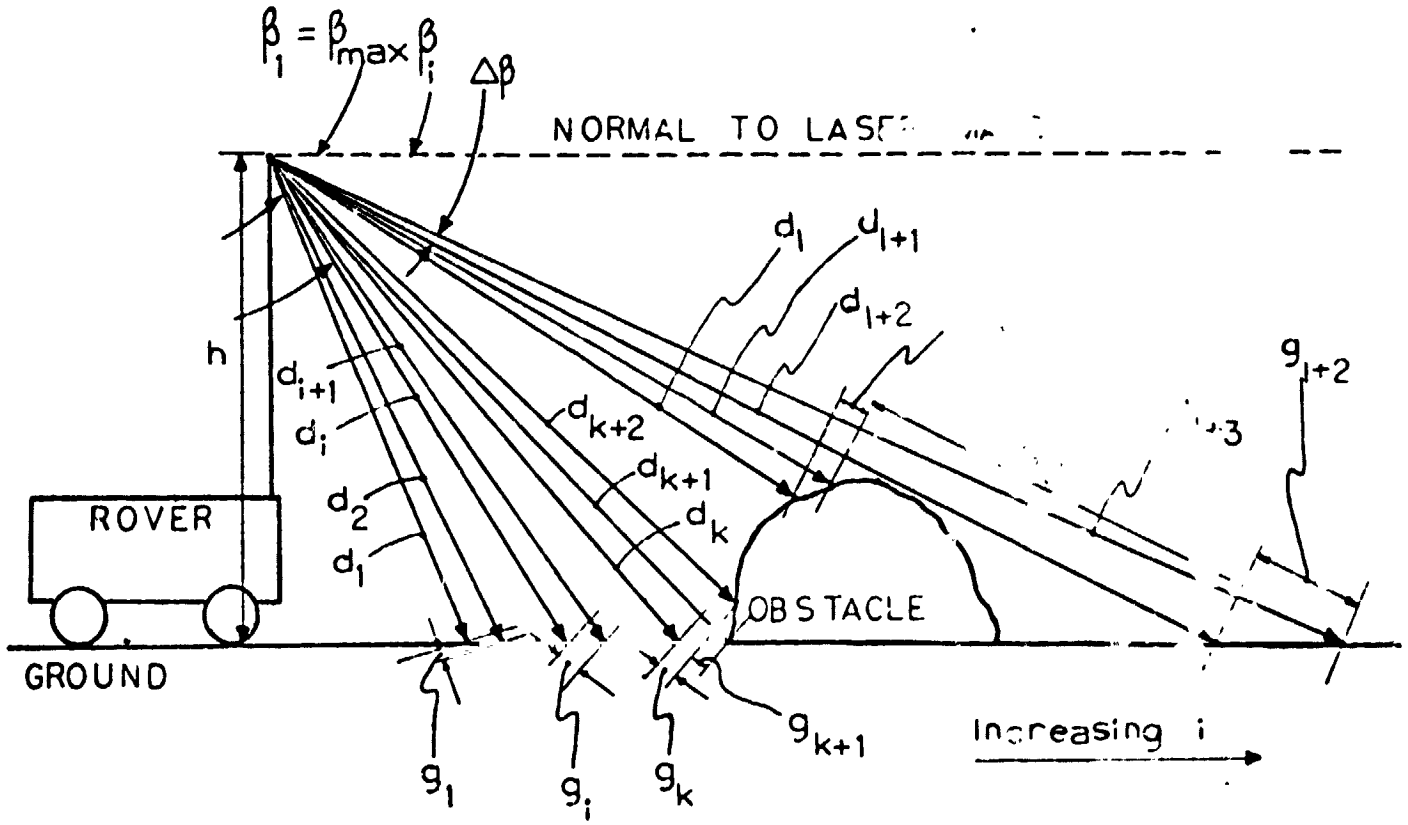

(a) Side View

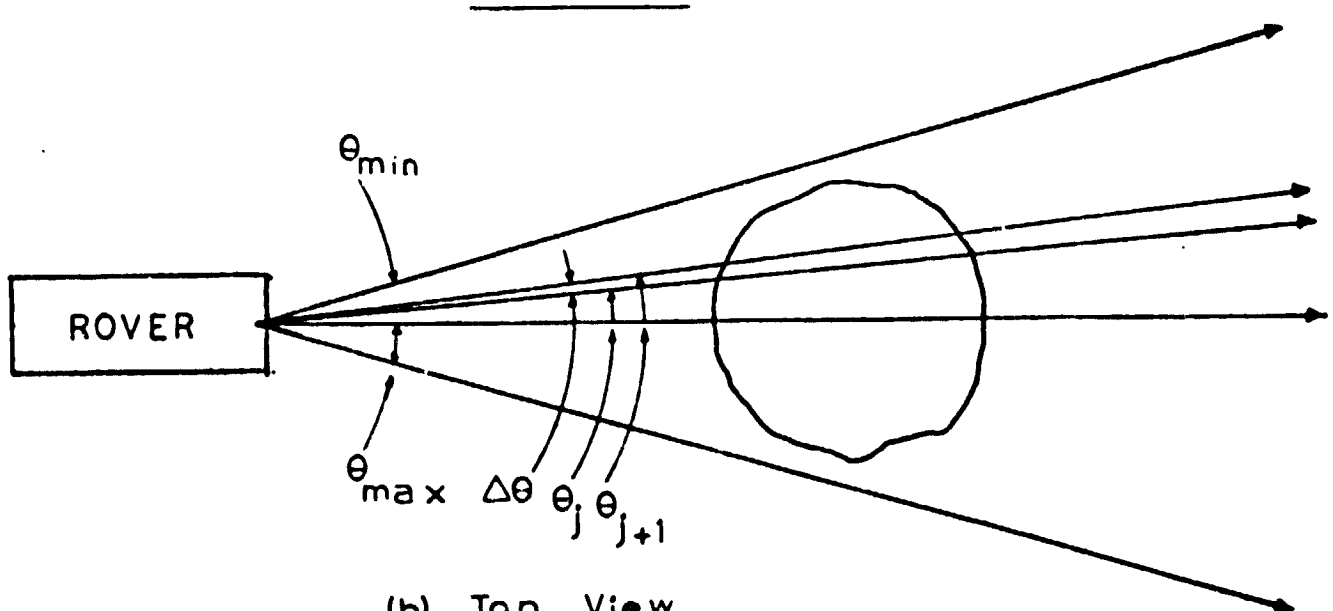

(b) Top View

Fig. 37. SCANNING NOTATION

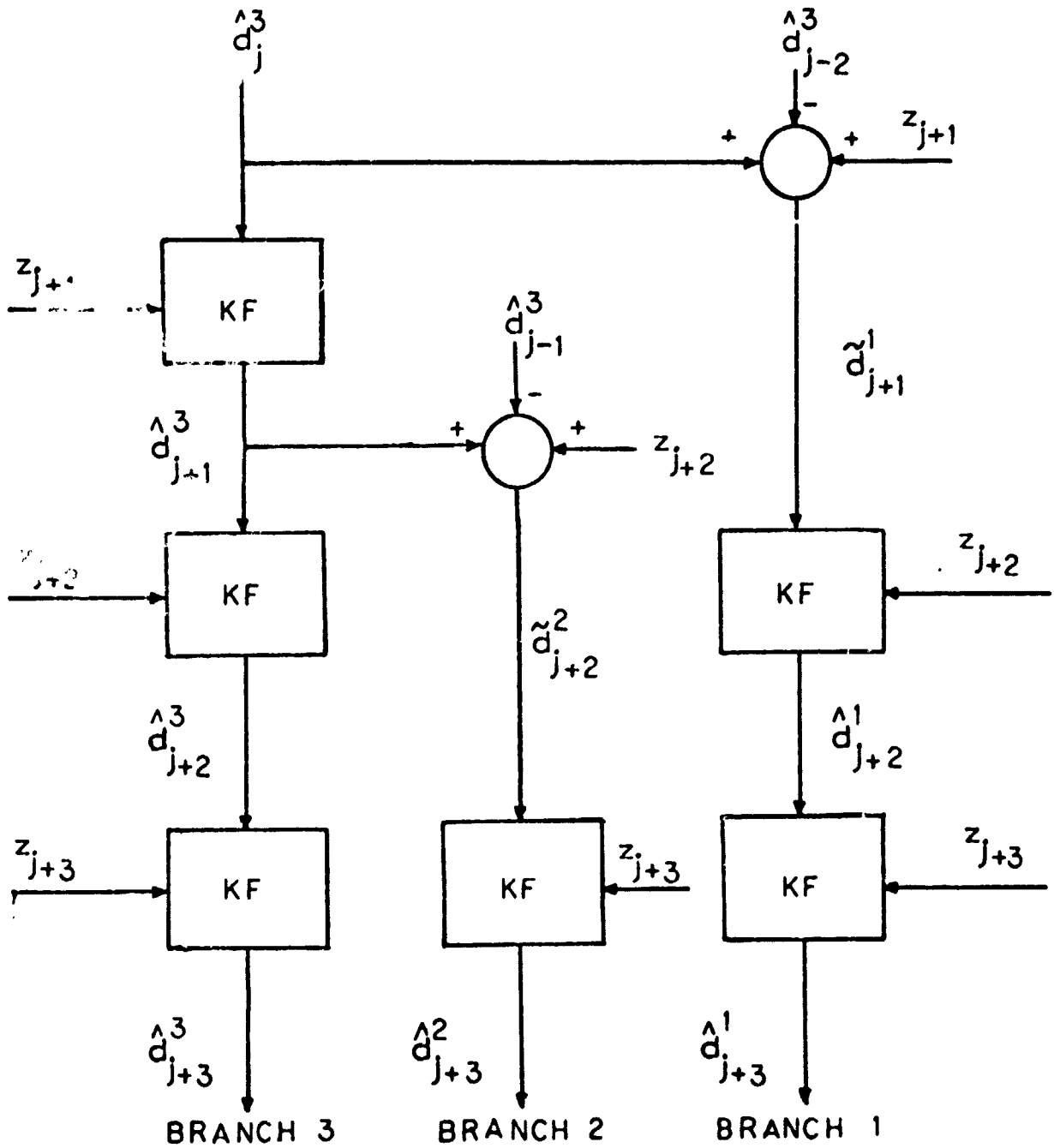

KF ≡ KALMAN FILTER, Eq. (6.3-5)

Fig. 38. DECISION TREE FOR PROCESSING ROWS

they may be considered independent of each other. The range (d_i) and the changes in the ranges (g_i) are defined to be the states of the system for each element of a single column. For a fairly gradual terrain g_i will be slowly varying, if not constant. With "i" the variable index along the length of any column, the system equation can be written as follows:

$$X_{i+1} = F_i X_i + W_i + B u_K \delta_{iK} \qquad i = 1, m \qquad (3)$$

where $X_i = \begin{vmatrix} d_i \\ g_i \end{vmatrix}$, $F_i = \begin{vmatrix} 1 & 1 \\ 0 & f_i \end{vmatrix}$; $B = \begin{vmatrix} 0 \\ 1 \end{vmatrix}$, the quantity u_K is

the change in g_K which will occur at the bottom edge of a boulder or the far edge of a crater. The Kronecker delta δ_{iK} emphasizes the fact that the change occurs at the edge at stage K. The quantity f_i which is the ratio of g_{i+1} to g_i depends on the variation of g_i along the terrain and $f_i > 1$ if the column is processed upward, i.e. with increasing range on a flat terrain. It may be set equal to unity as an approximation. W_i is a noise vector representing the roughness of the terrain and the inexactness of the model.

On a flat terrain, the range, d_i , will steadily increase, Fig. 36 and g_i is almost constant. As the range readings cross the bottom edge, d_i will not increase as much so that there will be a sudden decrease in g_i. This is the abrupt change, i.e. jump in g_i to be detected. The sudden increase in d_i which occurs at the top edge of a boulder or the near edge of a crater can be modelled as two consecutive jumps of opposite signs in g_i and g_{i+1} Fig. 37. Eq. (2) along a column reduces to the following

$$z_{i+1} = H x_{i+1} + v_{i+1} \qquad (4)$$

where the error v_{i+1} has the statistics, $E(v_{i+1}) = 0$ and $E(v_i v_j) = \sigma^2 \delta_{ij}$. The matrix $H = |1 \quad 0|$ since only range measurements are obtained.

Model Along a Row

Only the horizontal components of the obstacle edge shown in Fig. 35 will be detected when columns are processed separately. The vertical components will be detected only if the rows are processed too. The vertical components in a row cause changes only in the ranges, hence it is unnecessary to estimate the range differences, and only a one-dimensional state is defined.

$$d_{j+1} = d_j + W_j = u_K \delta_{jK} \qquad j = 1,n \qquad (5)$$

u_K is the change that occurs at the vertical component of an edge in any row. The covariance q is given some value after experimentation.

Estimation of d_i and g_i in a Column

If there are no obstacles in the path, the term u_K in Eqs. (3) and (5) is

is zero and Kalman Filter will give good estimates of the states.

Occurrence of an edge will change d_K or g_K suddenly and KF will not then be optimal. In such case, an estimate of the change conditioned on the three hypotheses defined earlier will have to be calculated.

Input Estimates

For the two dimensional case, Eqs. (3) and (4) show that u_i will appear in z_{i+2} but not in z_i or z_{i+1}. Therefore, a second residue is defined as follows:

$$r_{i+2} = z_{i+2} - HF_{i+1}F_i\hat{x}_i \tag{6}$$

and a suitable performance index may be defined and minimized to show that r_{i+2} is the best estimate of u_i.

$$\hat{u}_i = r_{i+2} = E(x_i/H_1) \tag{7}$$

Similarly, $\hat{u}_{i+1} = E(u_{i+1}/Z) = r_{i+3}$ (8)

New state estimates are obtained by augmenting the KF estimates, by the input estimates obtained above

$$\tilde{X}1_{i+1} = E(X_{i+1}/H_1) = \hat{X}_{i+1} + B\hat{u}_i$$

$$\tilde{X}2_{i+2} = E(X_{i+2}/H_2) = \hat{X}_{i+2} + B\hat{u}_{i+1} \tag{9}$$

where $\hat{x}_{i+1}$ and $\hat{x}_{i+2}$ are KF estimates.

Top Edges of Boulders and Front Edges of Craters

The parameters B and u_i in Eq. (3) are defined to model the changes in g_i directly, which occur due to slope changes in the terrain. However, the top edges of boulders and front edges of craters cause large changes in the ranges "d_i" themselves. A jump of d_{i+1} to d_{i+2} in Fig. 37 can be equivalently modelled as two consecutive changes of opposite polarity, i.e. g_i to g_{i+1} and g_{i+1} to g_{i+2}. These jumps are always large as compared to the small jumps caused by the slope variations. Therefore, $\hat{u}_{i+1}$ is also calculated if u_i is found to be large. The program uses 2 meters as the threshold value, which, if exceeded by u_i, indicates the occurence of a range jump.

The Decision Algorithm

Bayes decision rule, Ref. 11, is used to determine which of the three hypotheses is most likely to be correct. The complete details are described in Refs. 7 and 8.

The horizontal component of the edge detected in a column is denoted by the symbol "x", the vertical component of the edge detected while moving along a row is denoted by "0" and their overlaps by "x" as in Figs. 39-44.

Results

Figs. 39-44 give the outlines of boulders and craters at different distances, with the scan concentrated around the obstacles. Most of the bottom edges of the boulders and some of the far edges of the craters are obtained. The vertical components of the edges denoted by zeros in the figures for the craters give an idea of the extent of the craters, as opposed to only the front edge obtained by the FDR.

Larger increments in the distances, at greater ranges, cause the bottom edge to be detected more clearly for the boulder at 30m than at 10 m.

Conclusions

By this method of added complexity, more information has been extracted from the range matrix. The FDR computer program required 3 seconds to process the range matrix and obtain the incomplete edge while the proposed RES method requires 6 seconds to obtain a more complete outline, on the IBM 360/67 computer. A choice or a compromise will have to be made depending on (a) time between scans, (b) available computational capacity on the rover, (3) satisfaction of requirements, etc.

Task D.1.b. Minicomputer Simulation of Obstacle Edge Detection Systems -
J. Sher and D. Jacobs
Faculty Advisor: Prof. C. N. Shen

The objective of this task was to develop a simulation of the laser range finder data of multiple obstacles on a minicomputer and to display visually the application of the methods of perceiving the hazard by the edge detection methods. This extends prior work which was directed to detection of a single hemispherical boulder, Ref. 12.

Range Calculation

Figure 45 shows the parameters of the laser scanning range. The laser range finder is mounted on a mast, d meters above the ground. An on-board computer will control the direction of the beam, varying the elevation angle, β, and the azimuth angle, δ, in order to form a searching area on the ground in front of the Rover. The total azimuth and elevation angle ranges are each divided into 25 equal increments. Starting at the minimum azimuth angle and at the minimum elevation angle, the range data is determined for that set of angular coordinates. The elevation angle is now increased by one increment, and the range data is determined again. When the range data has been determined for all of the elevation angles at the minimum azimuth angle, the azimuth angle is increased by one increment and the above procedure is repeated. The range data is stored in matrix form, where each element of the matrix represents the spherical coordinates of that point.

The value of the range data for each pair of coordinates is equal to the distance along the laser beam to where the laser beam impinges on the obstacle.

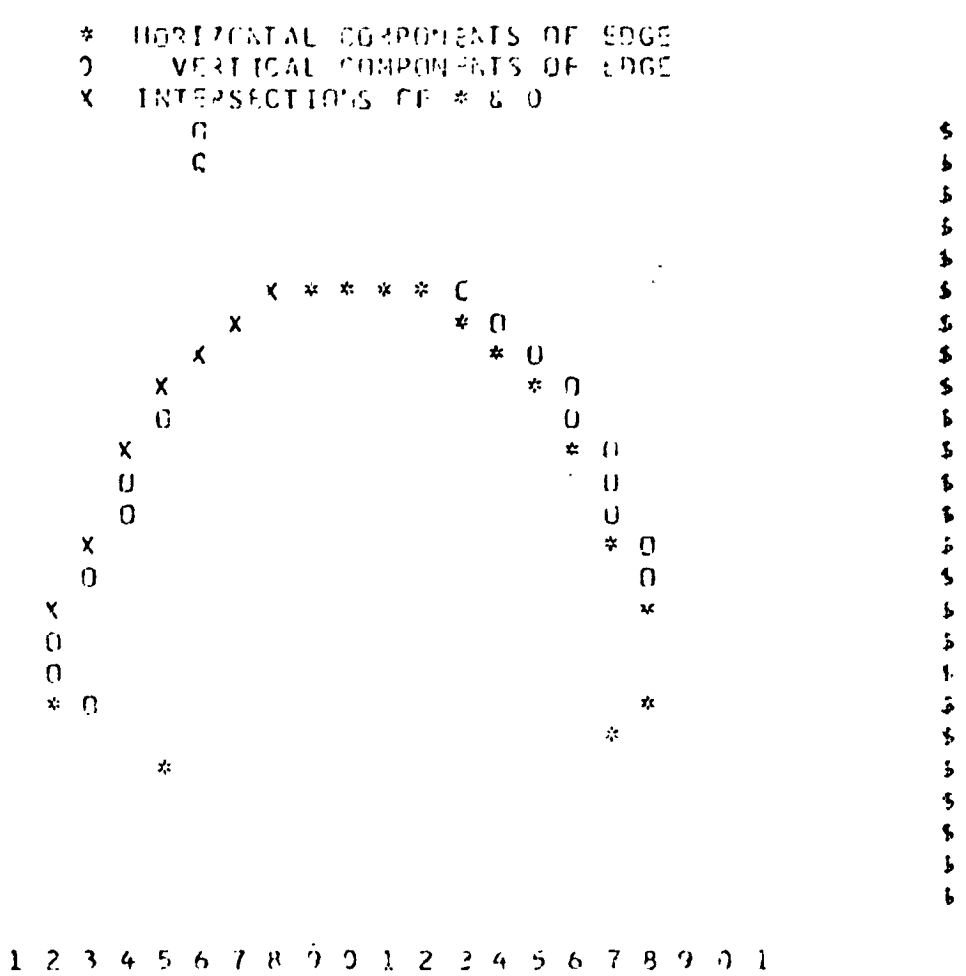

Fig. 39. Outline of a Hemispherical Boulder of One Meter at a Range of Ten Meters

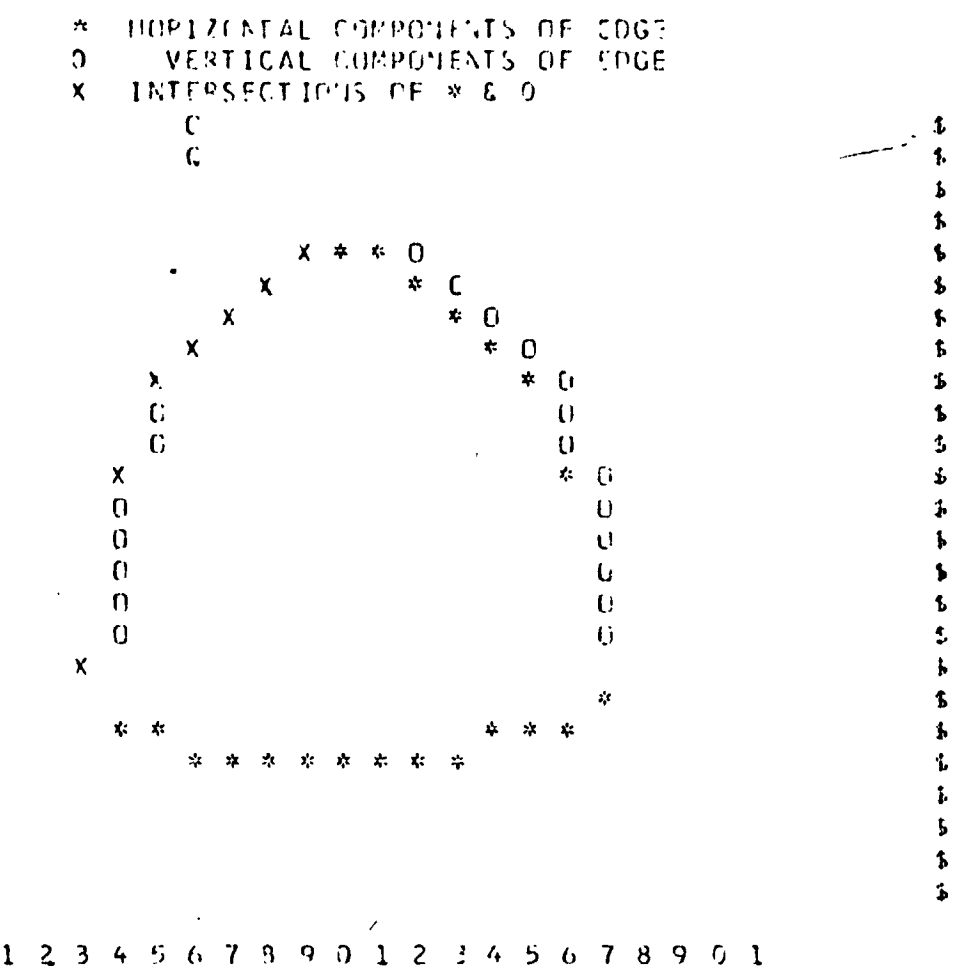

Fig. 40. Outline of a Hemispherical Boulder of One Meter Radius at a Distance of Twenty Meters.

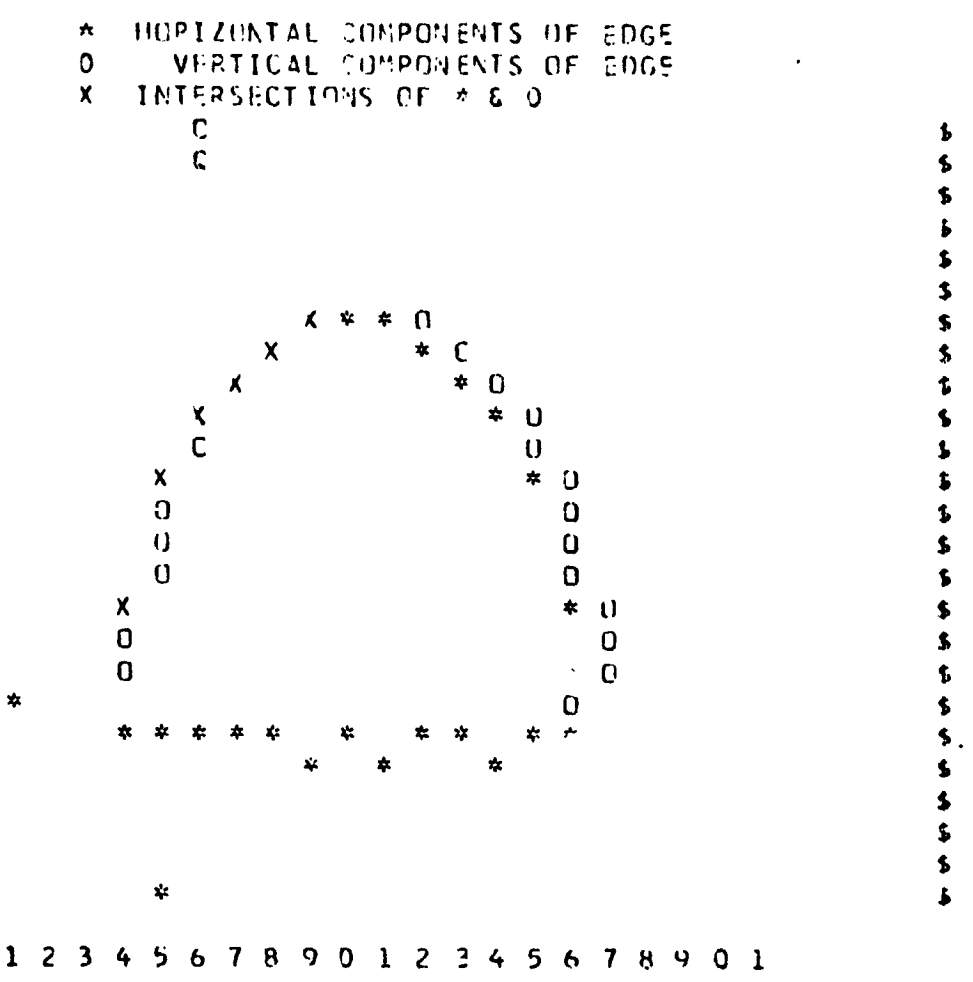

Fig. 41. Outline of a Hemispherical Boulder of One Meter Radius at a Distance of Thirty Meters

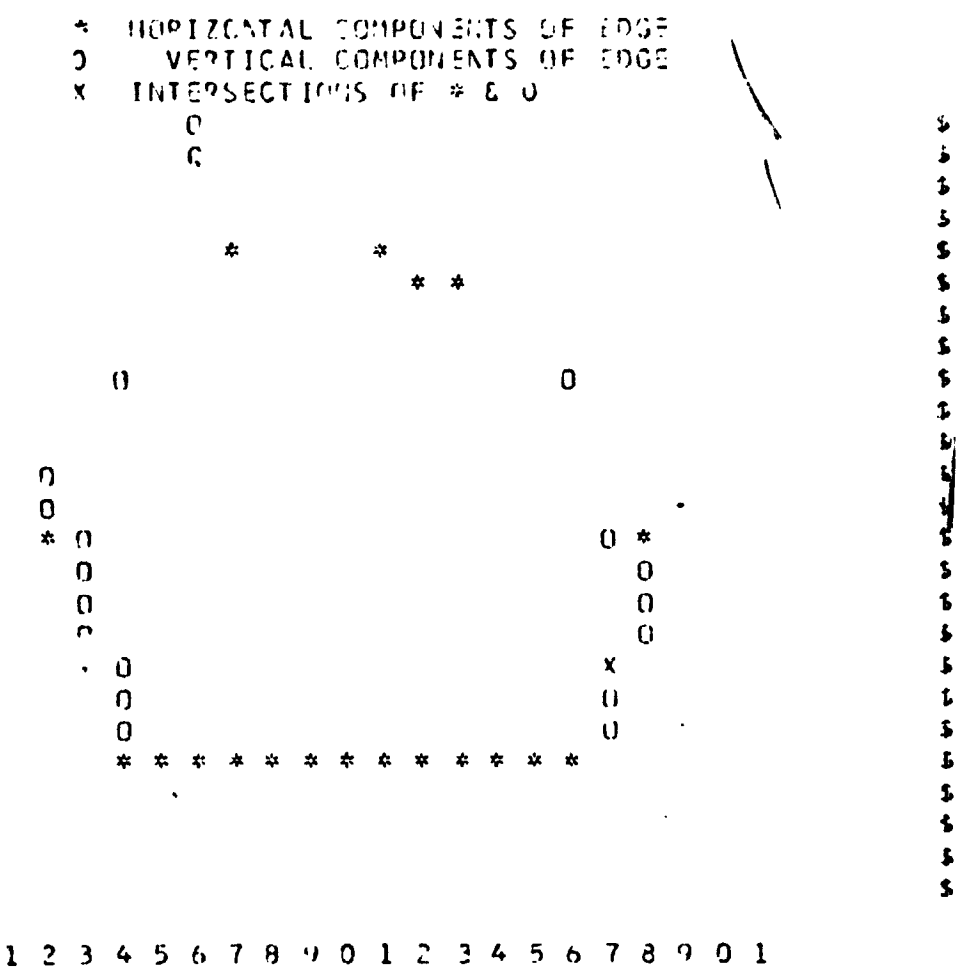

Fig. 42. Outline of a Hemispherical Crater of One Meter Radius at a Distance of Ten Meters

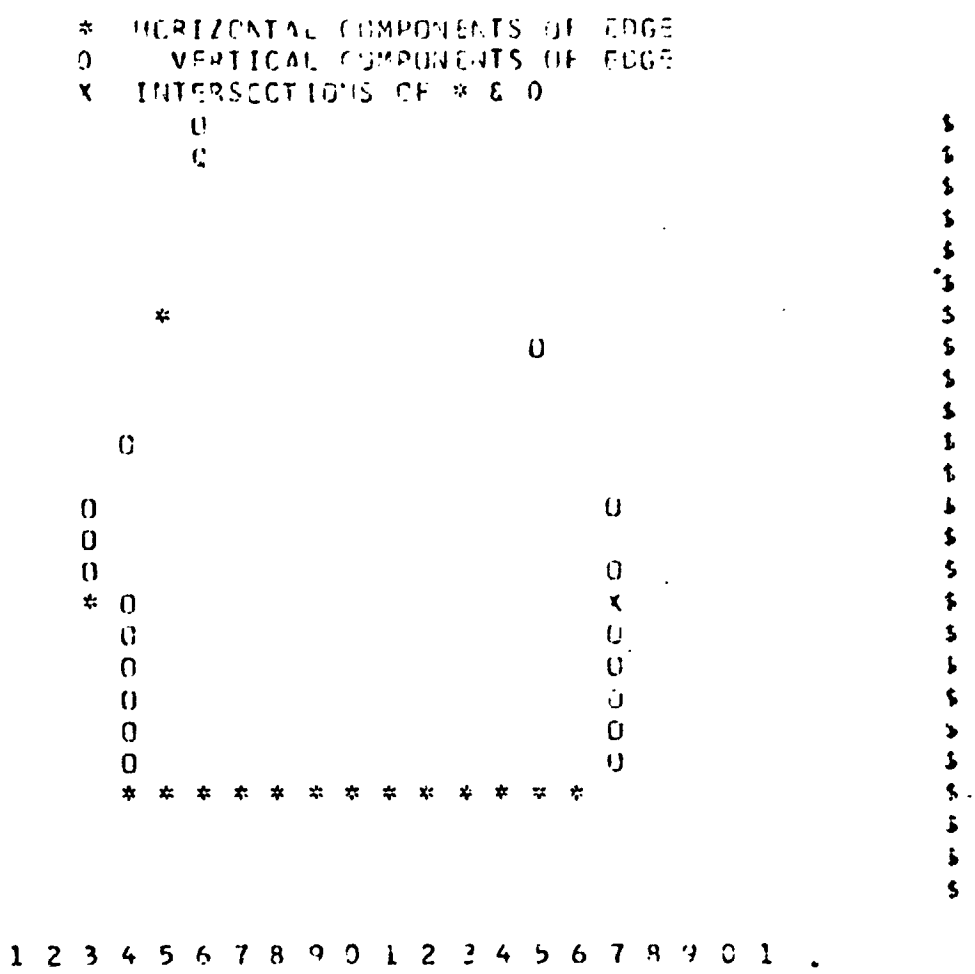

Fig. 43. Outline of a Hemispherical Crater of One Meter Radius at a Distance of Twenty Meters

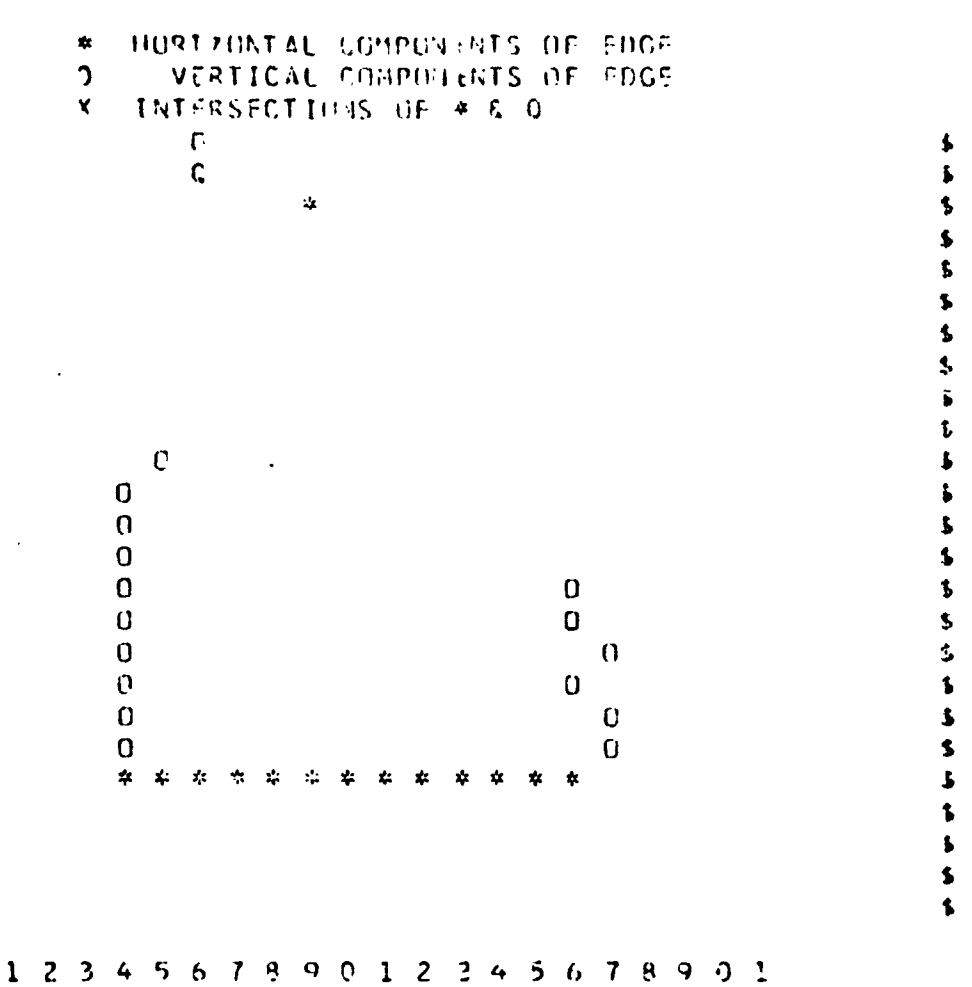

Fig. 44. Outline of a Hemispherical Crater of One Meter Radius at a Distance of Thirty Meters

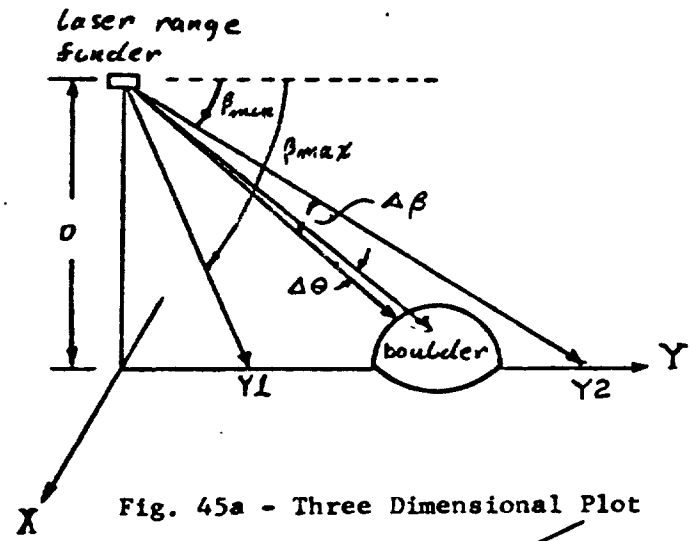

Fig. 45a - Three Dimensional Plot

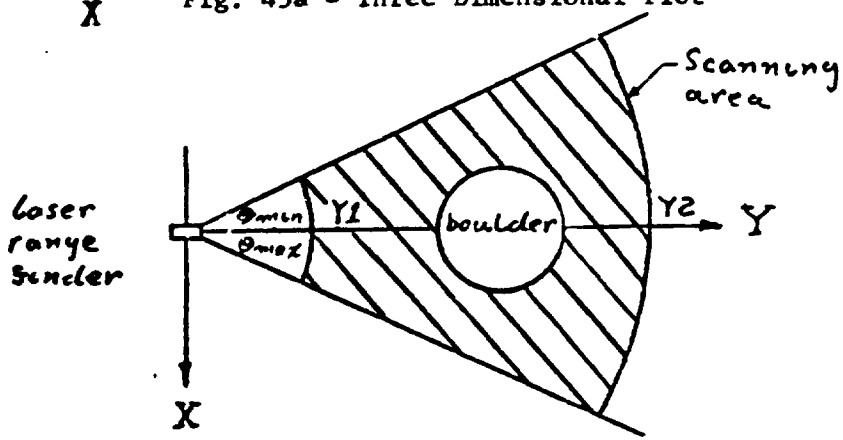

Fig. 45b - Top View

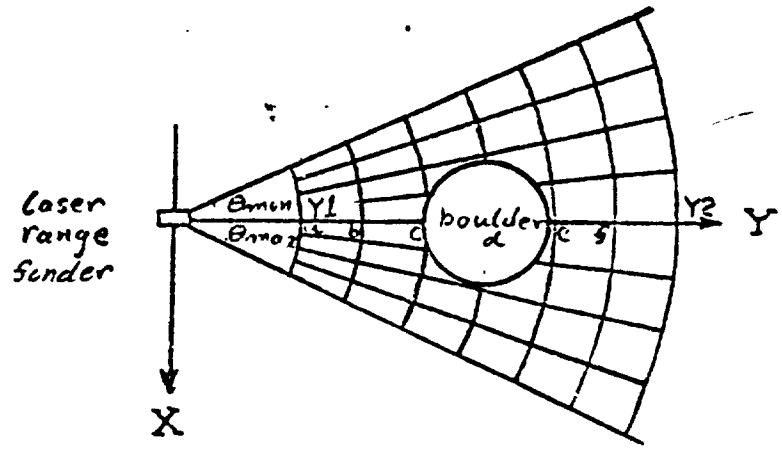

Fig. 46. Grid Division of the Scanned Area

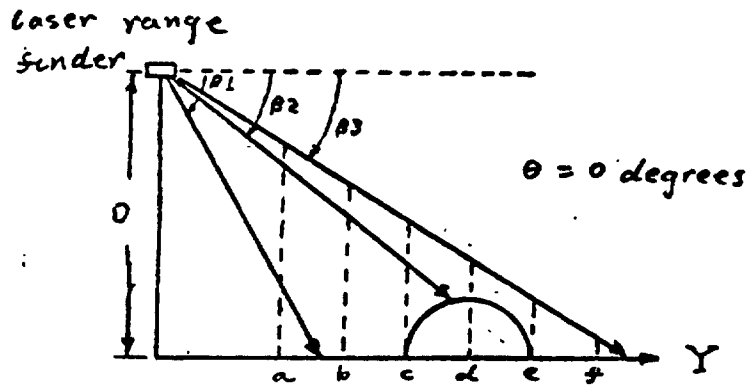

Fig. 47. Searching Scheme to Determine Impingement Point of Beam

To find this distance, the height of the laser beam, starting at a minimum distance along the laser beam, is compared to the height of the obstacle at this point. If the difference between these heights is less than a given tolerance value, the length of the laser beam is calculated. If the difference is greater than the tolerance, the distance along the laser beam is increased by a given increment value. The above procedure is repeated until the difference is within the tolerance value, or until the sign of the difference changes. A sign change indicates that the obstacle is between the present coordinates and the one previous to the increment. A bisection search is now used to converge in on the obstacle - laser beam intersection point.

Figures 46 and 47 show this searching scheme. Points a, b, c, etc. show the projection of the laser beam as it increments out toward the obstacle. Due to the long execution time of the minicomputer, the searching range was shortened from the minimum and maximum Y values of the laser to the minimum and maximum Y values around the obstacle, as shown in Figure 48.

To simulate the occurence of noise, as would be found in the actual system, a range data matrix corrupted by noise is calculated. An algorithm described by Ref. 13 has been applied to generate a gaussian distribution of random numbers, which is then added to the range data matrix.

Edge Enhancement

In order to determine the coordinates of an obstacle from the range data that has been corrupted with noise, the edge of the obstacle is calculated using the normalized Laplacian algorithm, Ref. 14. This consists of comparing an element in the corrupted range data matrix with the surrounding elements. The obstacle edge will be located at the coordinates where there is a large change in the value of an element in the rage data matrix. This sharp change of values is shown up using the following equation:

$$n_{i,j} = \frac{a_{i-1,j} + a_{i+1,j} + a_{i,j-1} + a_{i,j+1} - 4a_{i,j}}{a_{i-1,j} + a_{i+1,j} + a_{i,j-1} + a_{i,j+1}}$$

where $a_{i,j}$ is an element of the range data. When the value of the magnitude of the Laplacian is greater than a given threshold value, the obstacle edge is located at those coordinates. A matrix is now formed that indicates at what location the edge is at.

Graphic Display

The IDIIOM (Information Displays, Incorporated, Input-Out Machine) provides an interactive graphic display system. The parameters are displayed and the top view of the rover, obstacles, and searching area are displayed showing the relationships at these parameters. The program can be interrupted by pointing the light pen at an area of the screen designated for the specific action to be taken. For example, a parameter can be changed by pointing the light pen at the area of the screen that has the value of the parameter displayed. This will cause a message to be printed on the typewriter terminal telling how to enter the new value for the parameter.

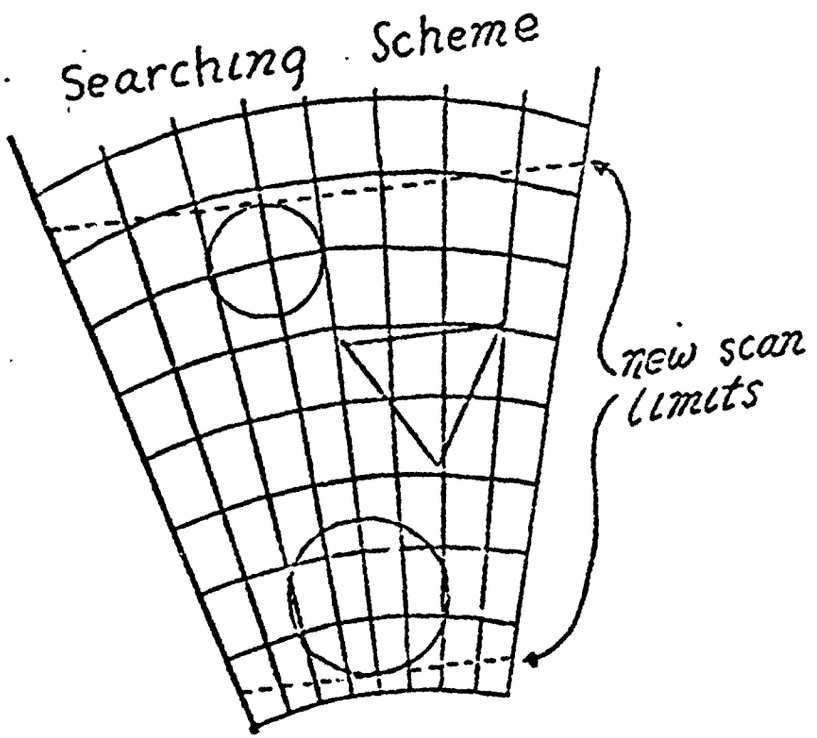

Fig. 48. Scan Area is Limited to Zone in which Obstacles are Located

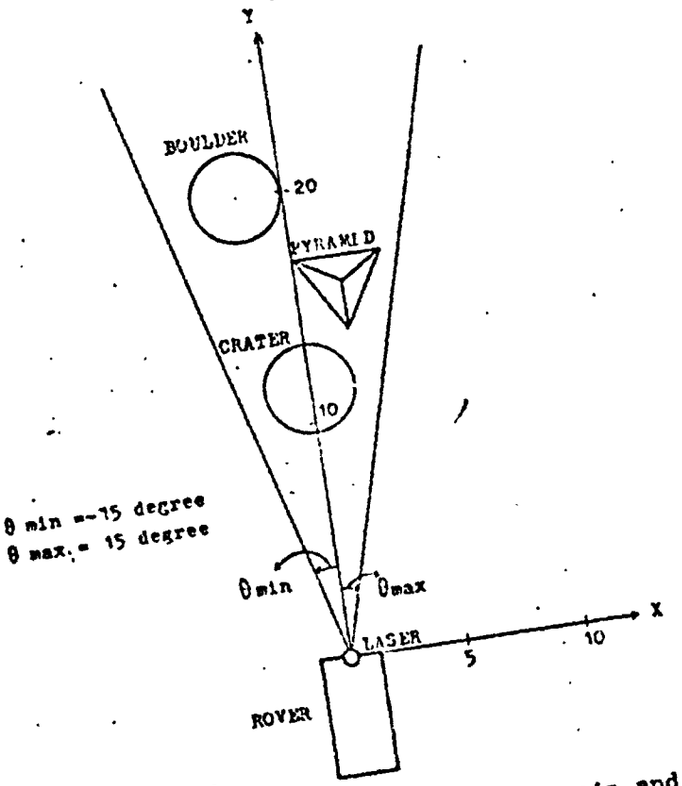

Fig. 49. Top View of Model of Terrain and Obstacles

Results of the Simulation

Figure 49 illustrates the layout of the obstacles used in the simulation. The obstacles include a pyramid, a boulder, and a crater.

The first simulation places the pyramid at (1.2, 17), according to the coordinate system in Figure 49. The boulder is at (-1, 20), and the crater at (0, 13). The height of the pyramid and the radius of the boulder are all 1 meter, the radius of the crater is 1.5 meters. The laser is placed at the origin with a height of d = 2 meters. The total azimuth angle is 15 degrees, assuming that (θ_{min}) and (θ_{max}) have the same magnitudes. The vertical scan covers the region between 10 meters and 50 meters from the rover, corresponding to (B_{min}) = 2.3 degrees and (B_{max}) = 11.3 degrees.

Simulation results from the IBM 360/67 are shown in Figures 50 and 51. Figure 50 includes the undistorted range data matrix and the one corrupted by noise. Figure 51 shows the normalized Laplacian matrix and the edge enhancement results. The threshold values used in this case are .03 for the inner edge and -.04 for the outer edge. In Figure 51, the inner edge is represented by "X", and the outer edge by "."

In the second simulation, the pyramid is placed at (1,20) with a height of 1 meter, the boulder at (0,11) with a radius of 1 meter, and the crater at (0,15) with a radius of 2 meters. All other parameters are the same as those used in the first simulation. Figure 52 shows the undistorted and the noise corrupted range data matrices. The normalized Laplacian matrix and the edge enhancement results are included in Figure 53.

The simulation on the IDIIOM has the advantage of a direct access to change the parameters. Three pictures can be displayed on the screen, as shown in Figures 54 through 56. Figure 54 lists the specifications for all the parameters used. All the parameters in this figure can be changed by using the light pen for interrupting and the typewriter terminal for inputting the new values.

Figure 55 displays the layout of the obstacles and the terrain, corresponding to the specifications in Figure 54. Figure 55 shows the edge enhancement results. The second line includes the inner and the outer threshold values, which can be changed by using the light pen and the typewriter terminal. The bottom line is used to transfer pictures, e.g., by pointing the light pen at "top view", the top view in figure will replace the existing picture.

By using the graphic display, the simulation becomes interactive with the operator. The parameters are displayed on the screen, and their values can be changed by interrupting the display with the light pen and typing in the new values on the typewriter terminal. Light pen interrupts can also be used to display the top view, display the range data, display the edge enhancement, display the parameters, or reset the parameters back to their initial values.

This simulation provides investigators with a flexible tool which can be used to evaluate alternative schemes for detecting obstacles and the effect of data density and accuracy.

UNDERSTATED BY NOISE

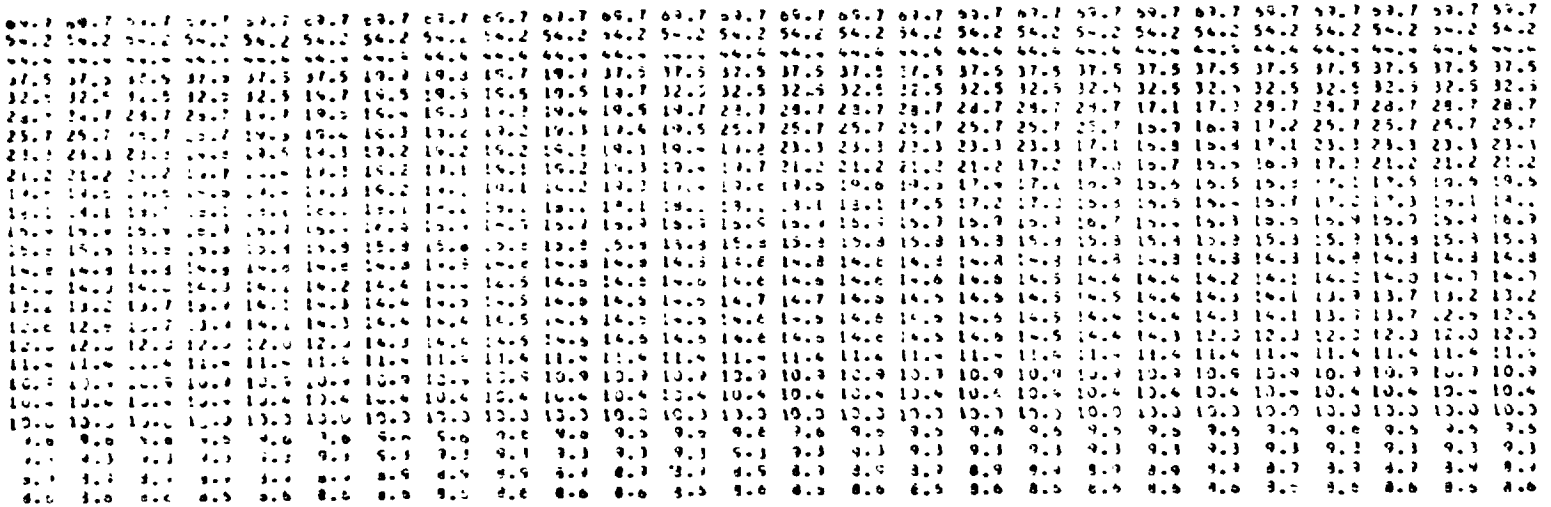

CONTAMINATED BY ZERO MEAN, 0.05 METER STANDARD DEVIATION, GAUSSIAN NOISE

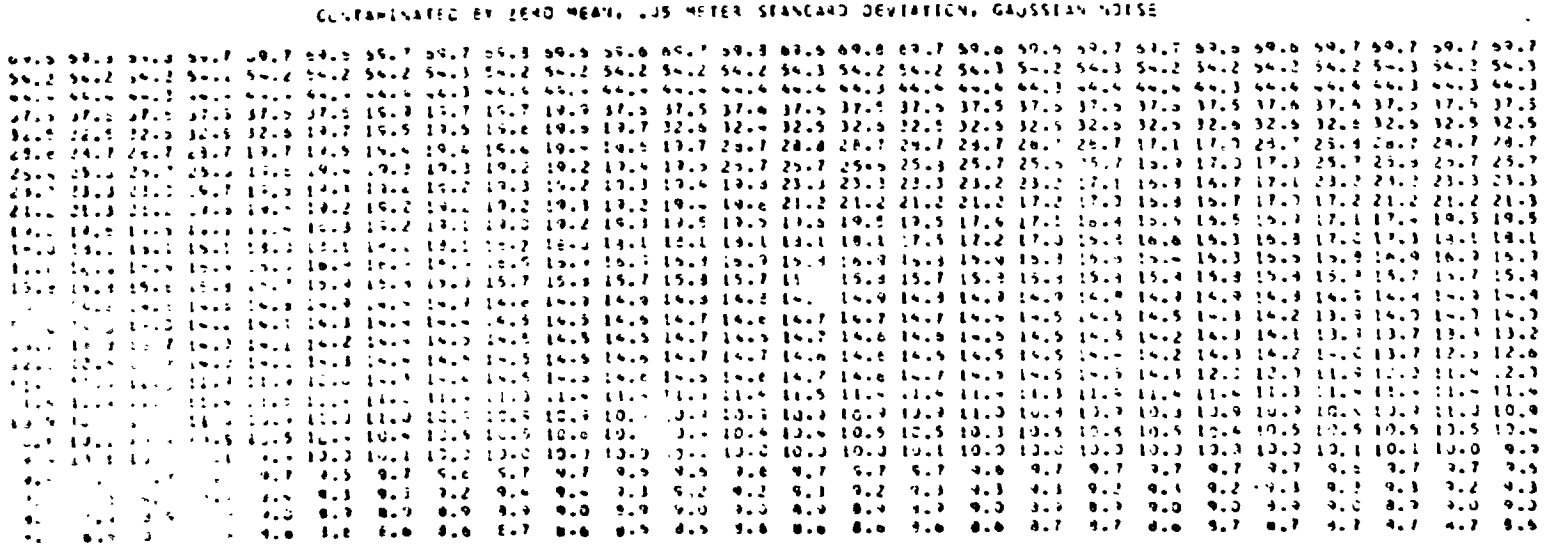

Range Matrices R and R' of the First Simulation

NORMALIZED LAPLACIAN EDGE DETECTION SCHEME

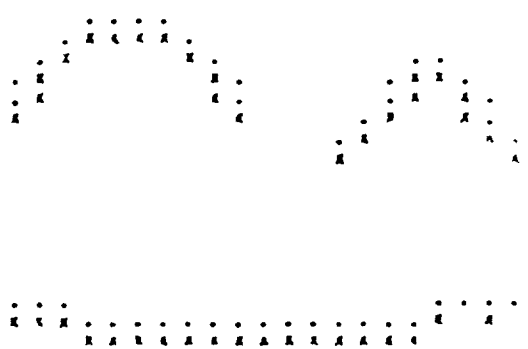

Fig. 51. Matrix N and Edge Enhancement of the First Simulation

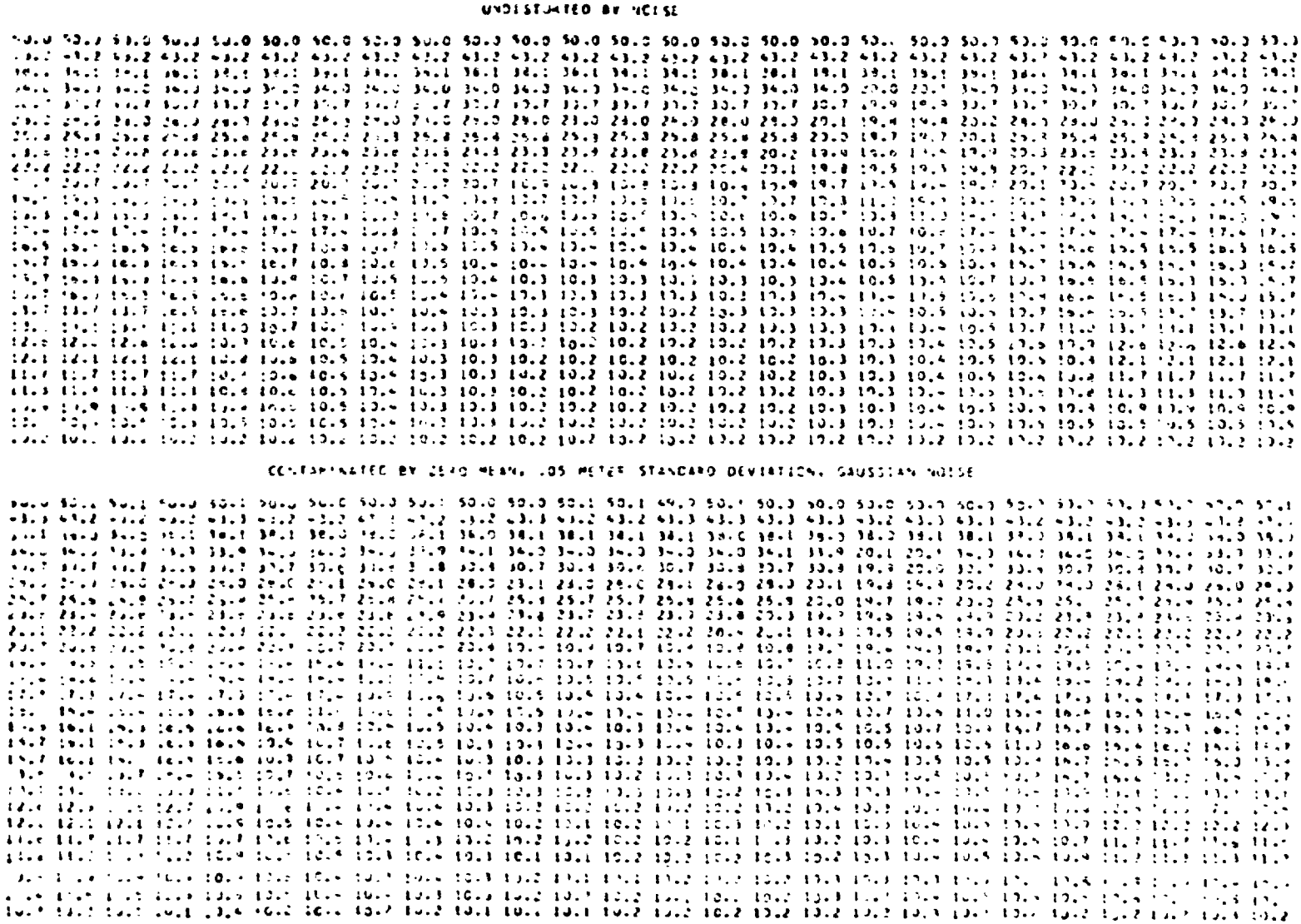

Fig. 52. Measurement Matrics R and R' of the Second Simulation

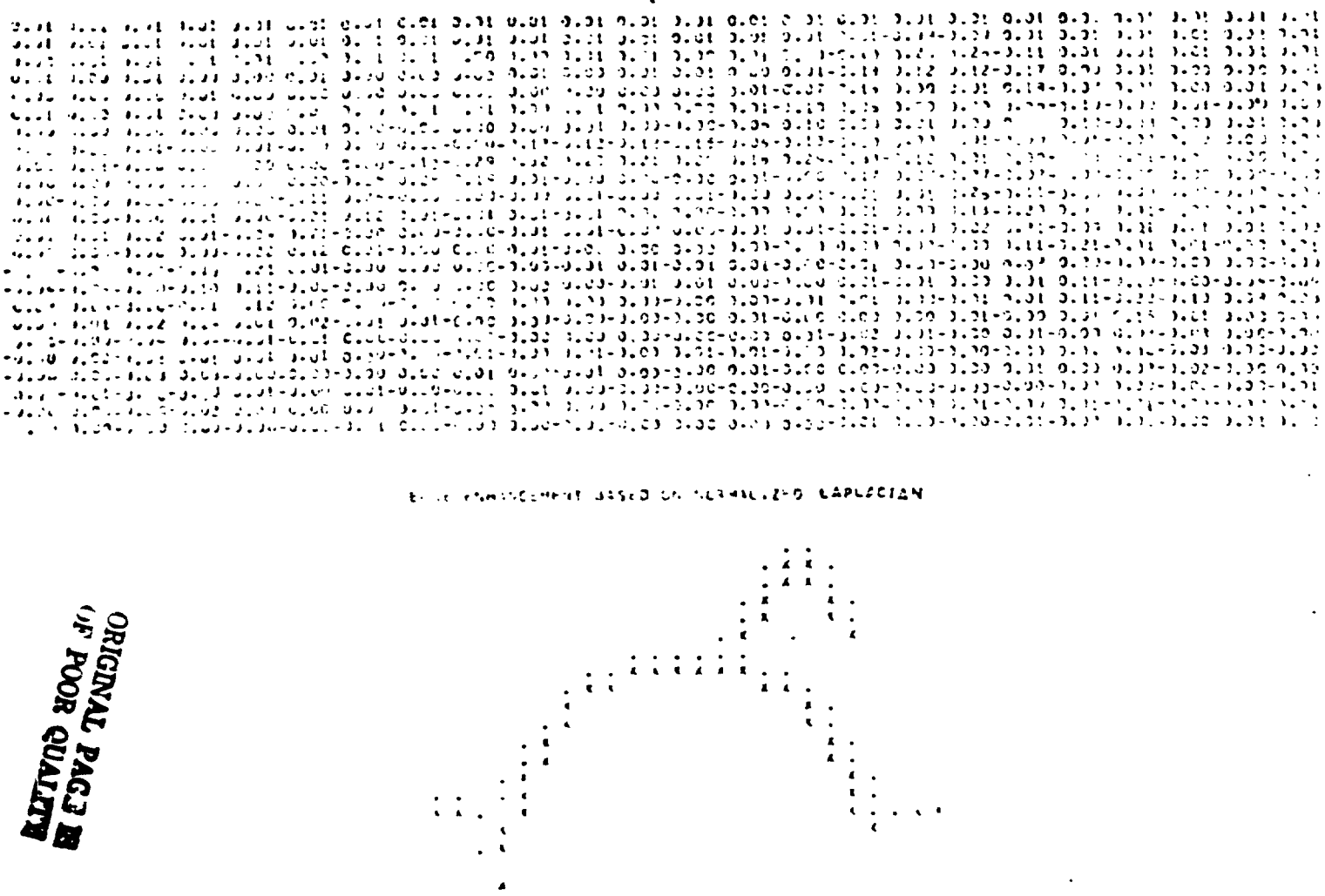

Fig. 53. Matrix N and Edge Enhancement of the Second Simulation

RECOGNITION OF 3-D OBSTACLES
*** A SIMULATION

STUDENT: JONE-SHIAN SHER
ADVISOR: PROF. C. N. SHEN

THIS PROGRAM SIMULATES THE EDGE DETECTION SCHEME
USED BY THE RANGE FINDER OF THE MARC ROVER

A PYRAMID, A BOULDER AND A CRATER ARE USED AS OBSTACLES

OBSTACLE SPECIFICATIONS

1. LOCATION (X,Y) IN METERS

   ROVER IS AT (0.0, 0.0)
   PYRAMID IS AT (1.0, 16.0)
   BOULDER IS AT (-1.0, 18.0)
   CRATER IS AT (0.0, 12.0)

2. SIZE IN METERS

   HEIGHT OF THE RANGE FINDER IS 2.0 M
   HEIGHT OF THE PYRAMID IS 1.0 M
   RADIUS OF THE BOULDER IS 1.0 M
   RADIUS OF THE CRATER IS 1.5 M

SCANNING RANGE AND NOISE:

1. HORIZONTAL SCAN COVERS 15.0 DEGREE
   MAX. THETA = 15.0 DEGREE MIN. THETA = -15.0 DEGREE

2. VERTICAL SCAN COVERS 10.0 M TO 50.0 M FROM ROVER
   MAX. BETA = 11.3 DEGREE MIN. BETA = 2.3 DEGREE

3. GAUSSIAN NOISE: MEAN VALUE 0.0 CM
   STANDARD DEVIATION 5.0 CM

RESET TOPVIEW RANGE DATA EDGE DETECTION

Fig. 54. Specification Display

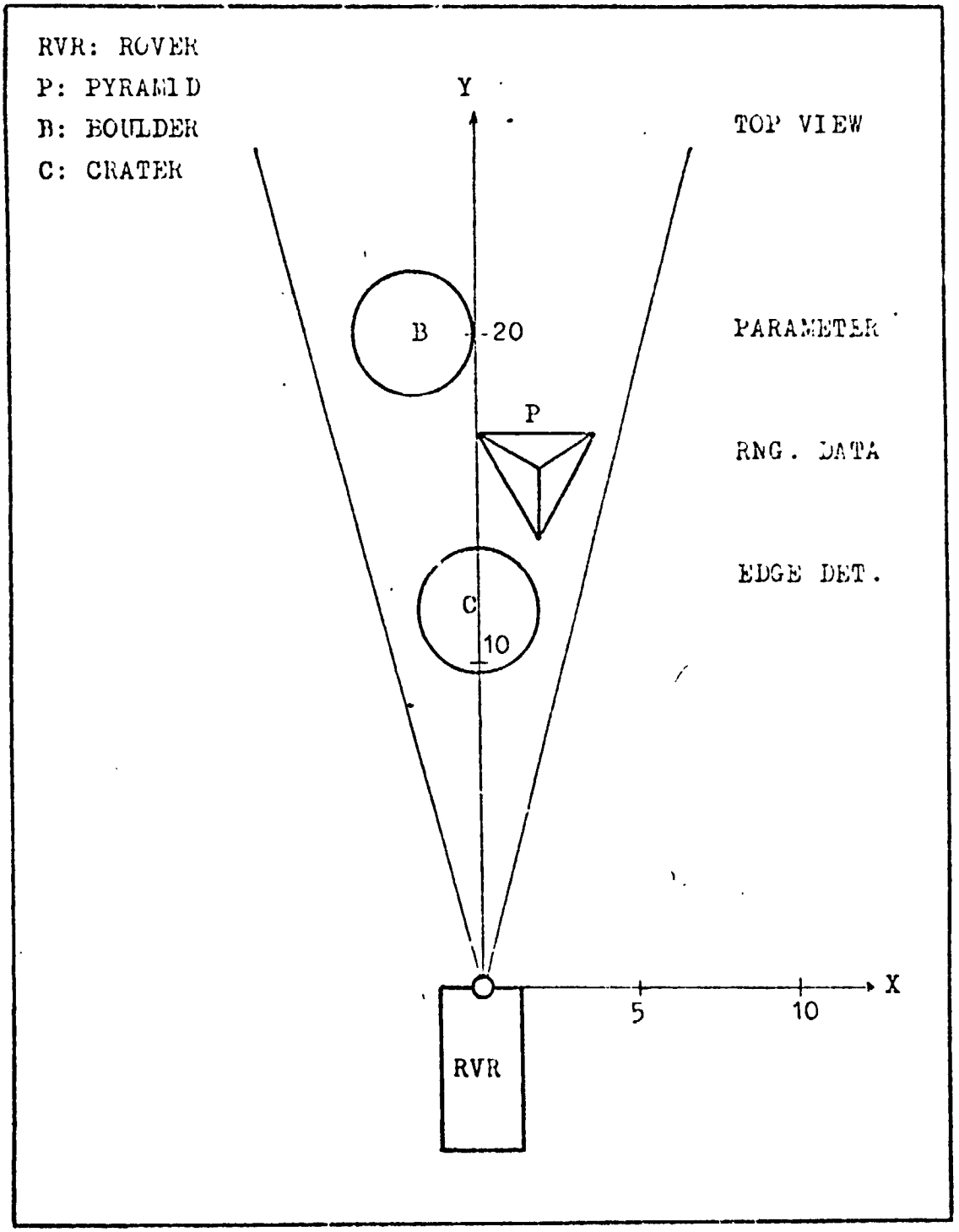

Fig. 55. Top View Display

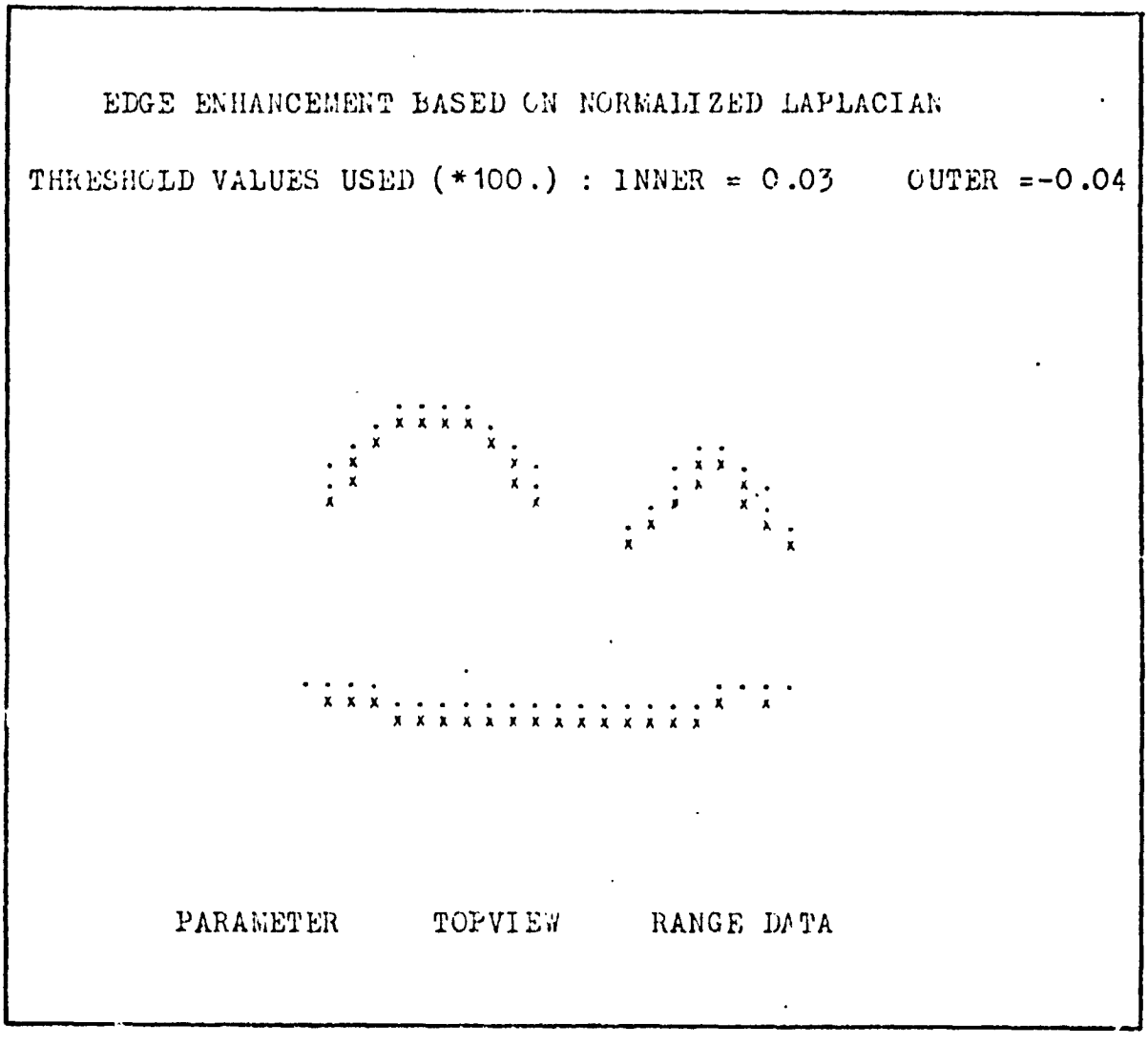

Fig. 56. Edge Enhancement Display

Task D.2. Obstacle Classification - K. Leung
Faculty Adviser: Prof. C. N. Shen

The objective of this task is to develop the minimum set of parameters and the conditions required to determine the passability or impassability of terrain. The ability to classify local terrain features by a minimum number of parameters is of critical importance to those groups concerned with the development of path selection algorithms, Task C, and of hazard detection hardware, Tasks A and B.

It has been determined that a minimum of four parameters as related by three inequality conditions which must be satisfied simultaneously will be necessary. Further analysis may reveal that additional information may be required to achieve path selection systems of high reliability while at the same time minimizing built-in safety margins, i.e. as through unnecessarily large threshold values.

The analysis was approached by considering a number of fundamental questions. Is the object under consideration positive (boulder) or negative (crater)? Is the object of a size relative to the vehicle so that it deserves consideration, Figure 57? Are the heights and gradients of the object either too large or of the wrong shape, Figure 58? Is the object in a surrounding as to make it an obstacle, Figure 59? Does the combination of objects represent a hazard, even though the objects taken separately are not a hazard, Figure 60?

From these and other related questions were deduced a set of Conditions of Impassability.

1. Instability - This is the situation where each wheel of the rover is subjected to terrain of different height such that the rover might be overturned.

   Shown in Figure 61 is a parameter α, which is defined as the angle made by the rover's direction of forward movement with the horizontal plane. For a vehicle, there is a threshold value of α, denoted as α^*, such that the vehicle is stable when α is less than this value. The value of α^* depends on the position of the vehicle's center of gravity and the distance between the front and rear wheel axles, which can be predetermined experimentally. Hence, a prospective passable path must produce an α less than α^* along the path. Similarly, an angle β, can be defined as the angle made by the wheel axle with the horizontal plane and β^* its maximum value for which the vehicle is stable, as shown in Figure 61.

2. Steepness - The vehicle's limited traction will not permit it to climb a slope of more than α_2^*. The threshold angle α_1^* is due to stability consideration only. Since α_2^* is smaller than α_1^*, stability can be insured if α_2^* is used as the threshold value of α for passability. Hereafter, α_2^* will be referred to as α^*.

3. Abrupt Changes in Height - Because of the structure of the vehicle it cannot climb a vertical height of more than H^*.

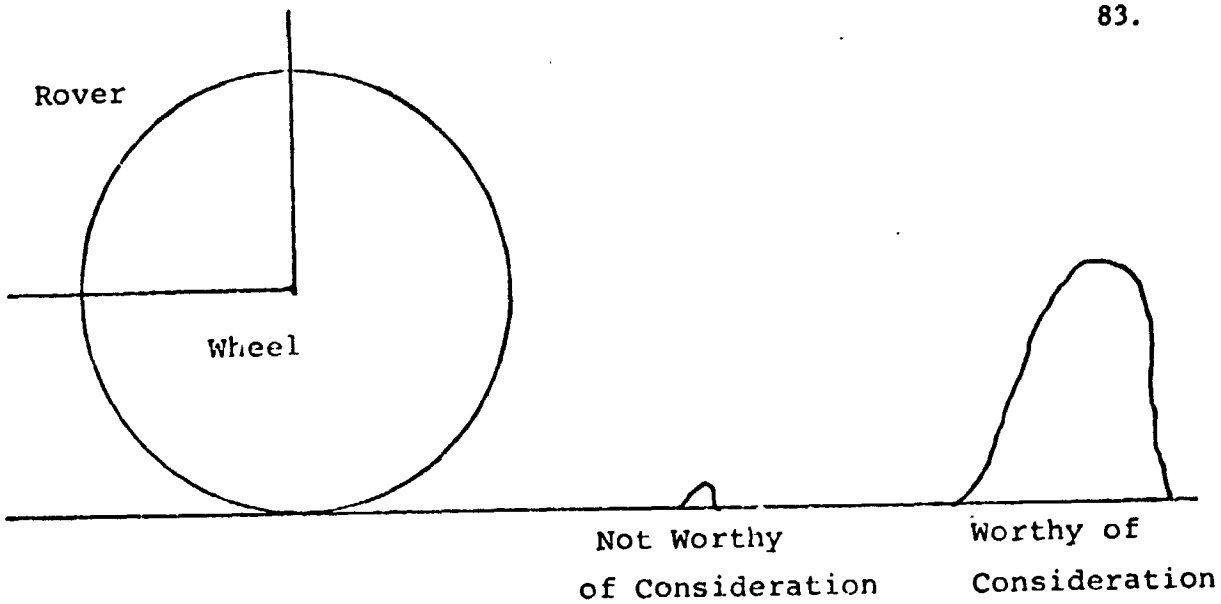

Fig. 57. Different Object Sizes Deserve Different Consideration

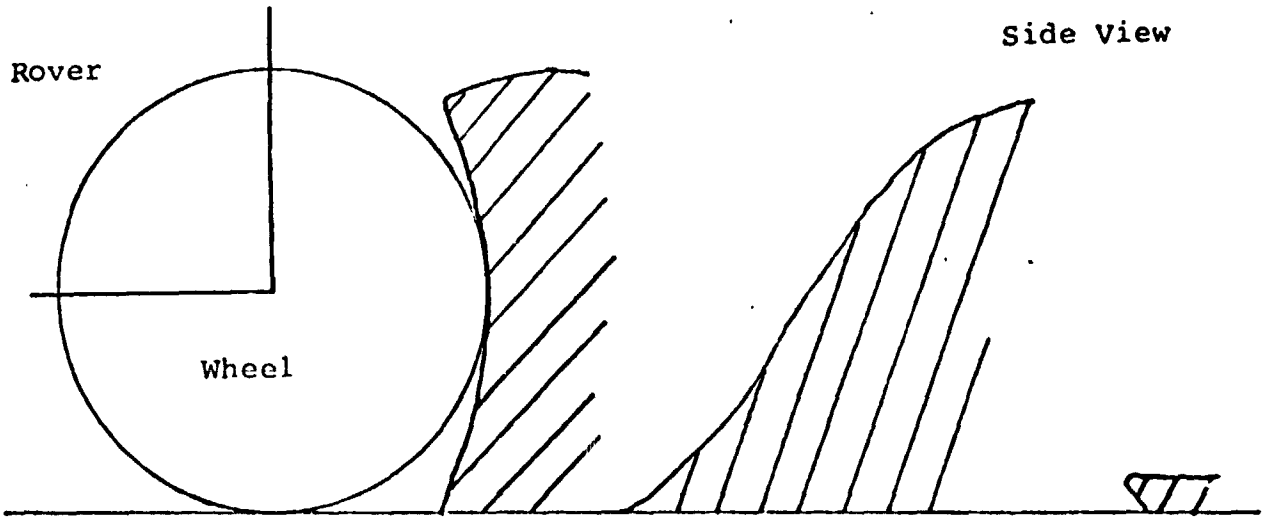

Fig. 58. Some Combinations of Height, Shape and Slope Are Passable, Others Are Not

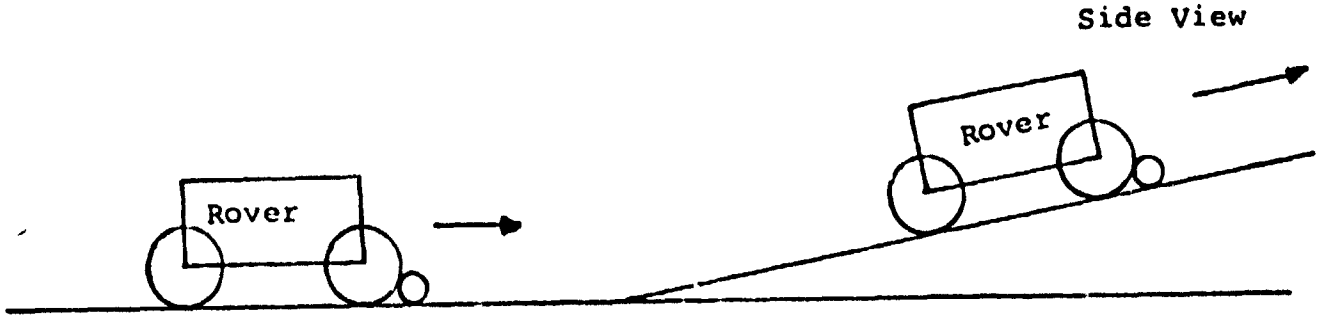

Fig. 59. The Same Object in Two Different Surroundings

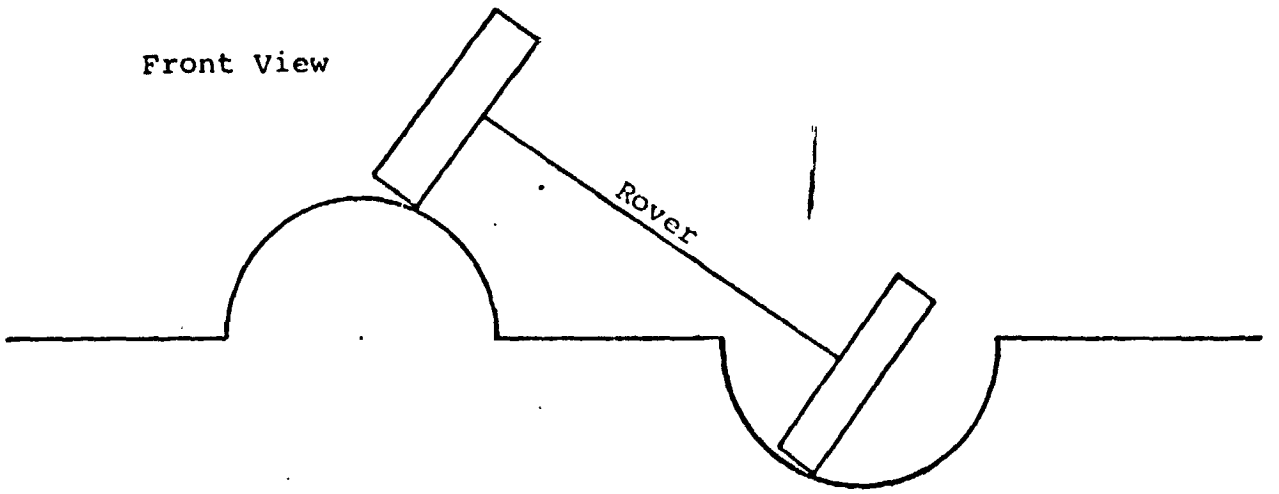

Fig. 60. This Combination of Boulder and Crater May Cause Instability

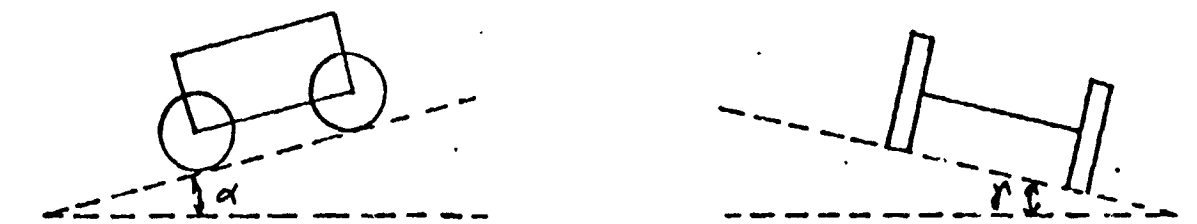

(i) SIDE VIEW

(ii) FRONT VIEW

Fig. 61. Illustration of the Quantities α and γ

Hence a parameter H is defined as the vertical height of a step. Therefore if a prospective path is passable, the H along the path must be less than H^*.

4. Clearance - This is the problem that the underside of the rover may contact the terrain, either damaging or immobolizing the rover.

Consider first a two-dimensional case. Assume that the dimensions of the wheels and their positions relative to the rover body are as shown in Figure 62. The distance between the wheel axles is denoted by L. Let S be the one-dimensional terrain, given by

$$z = f_1(X) \qquad (1)$$

Let the line segment L representing the wheel contact points be moved such that its end points coincide with the surface of the terrain. For points on S between P and Q, the distance between terrain surface and the segment L can be calculated. Depending on the design of the rover. it is necessary that adequate clearance be provided. if D is defined as the available clearance, then $g < D$ for all points on the path trajectory.

In the more general two-dimensional terrain problem, assuring that adequate ground clearance will be available is more difficult. It is necessary to fit a plane to the four wheel contact points and compare the terrain coordinates for all points within the space to this plane. The maximum value of the difference, g, so calculated is to be compared with the clearance, D, determined from the vehicle design.

Lists of Situations, Parameters and Passability Requirements

Below is a list of situations the rover will encounter as possible obstacles. For each situation there is a set of parameters in terms of which the passability requirements will be written.

S_1: Vehicle is roving on flat inclined plane as shown in Figure 61.

Parameters: α and γ

Passable if: $$\left(\frac{\tan\alpha}{\tan\alpha^*}\right)^2 + \left(\frac{\tan\gamma}{\tan\gamma^*}\right)^2 < 1$$

The sum of squares $(\tan\alpha)^2 + (\tan\gamma)^2$ is the square of the gradient of the terrain the vehicle is on, which leads us to the above expression.

S_2: Vehicle is roving on boulders (craters) on a horizontal plane, as shown in Figure 63.

Parameters: $\gamma = \arcsin \dfrac{(h_1 - h_2)}{w}$

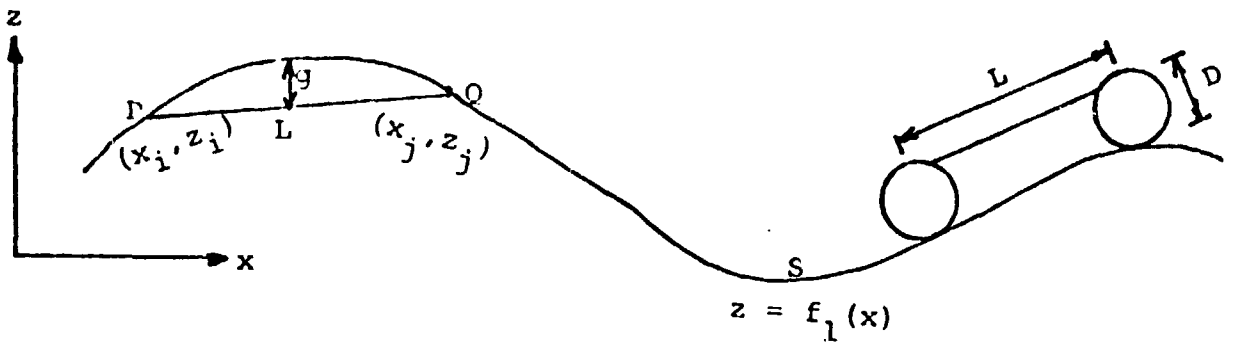

Fig. 62. Determination of Clearance in a Two-Dimensional Case

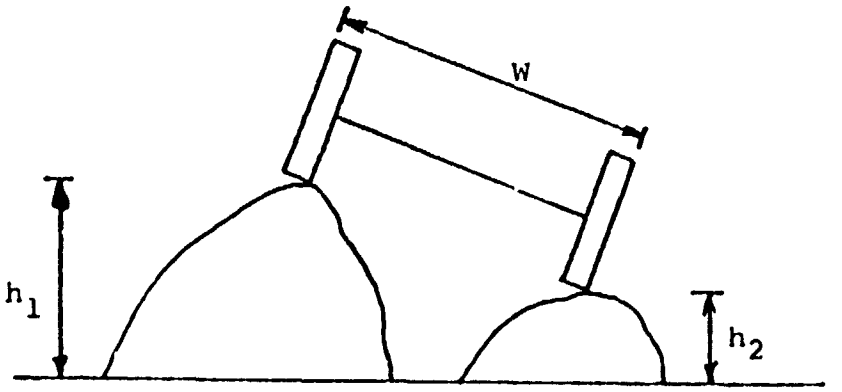

Fig. 63. Boulder (Crater) Combinations

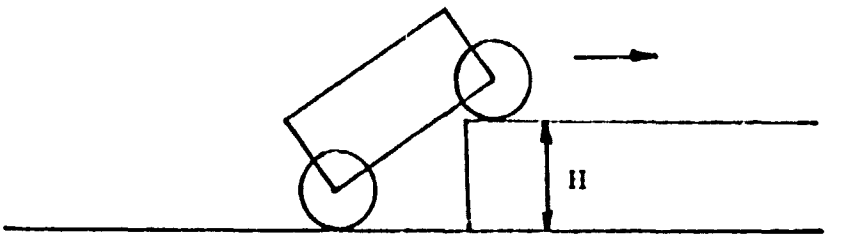

Fig. 64. Vehicle is ascending a step

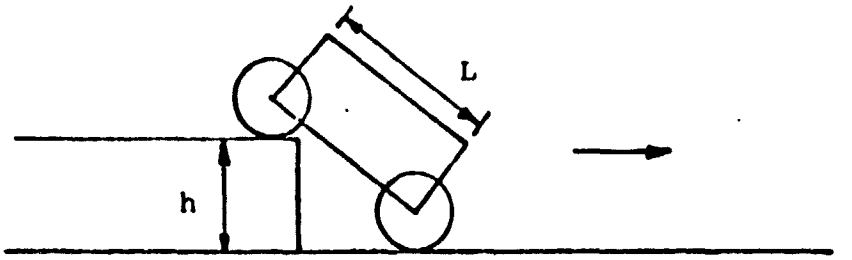

Fig. 65. Vehicle is descending a step

Passable if: $(\frac{\tan \alpha}{\tan \alpha_*})^2 + (\frac{\tan \gamma}{\tan \gamma_*})^2 < 1$

where α is the pitch angle of the vehicle.

S_3: Vehicle is descending a step, as shown in Figure 65.

Parameters: $\alpha = -\arcsin \frac{h}{L}$

Passable if: $(\frac{\tan \alpha}{\tan \alpha_*})^2 + (\frac{\tan \gamma}{\tan \gamma_*})^2 < 1$

where γ is the roll angle of the vehicle.

S_4: Vehicle is ascending a step, as shown in Figure 64.

Parameter: H

Passable if: $(\frac{H}{H_*})^2 < 1$

S_5: Clearance as shown in Figure 62

Parameter g

Passable if: $(\frac{g}{g_*})^2 < 1$, $g^* = D$

Now, let us define a situation S to encompass S_1, S_2,..., and S_5, with

parameters: α, γ, H and g and

passable if: $(\frac{\tan \alpha}{\tan \alpha_*})^2 + (\frac{\tan \gamma}{\tan \gamma_*})^2 < 1$ (1)

and $(\frac{H}{H_*})^2 < 1$ (2)

and $(\frac{g}{g_*})^2 < 1$ (3)

The reason for having three inequalities is that α and γ are dependent on each other, H is independent of α, γ and g, and g is independent of the other three parameters. The angle α^* is the maximum value of α only when $\gamma = 0$, and γ^* is the maximum of γ when $\alpha = 0$. Hence the use of inequality (1) eliminates the case when both α and γ are close to but less than α^* and γ^* respectively.

Also, coupling inequality (2) with inequality (3) using a logical AND means that it is acceptable to have both H and g close to but less than H^* and g^* respectively. Therefore, situation S is not an obstacle only when inequalities (1), (2) and (3) are all satisfied.

As a next step, it remains to demonstrate that the inequalities which are proposed and the parameters required therein will provide the essential terrain information required for an efficient yet reliable hazard detection and path selection system. It may prove necessary to increase the number of descriptive parameters and conditions if reduced safety margins are found to be necessary.

Task D.3. Terrain Modeling - Audbur Thompson
Faculty Advisor: Prof. C. N. Shen

In order for a Mars Roving Vehicle to navigate autonomously, it must possess the capability of recognizing passable terrain, which in turn requires the ability to mathematically model that terrain. This task involves the development of a method which will supply such a capability to the rover. The major task is to develop a scheme which can model small sections of the Martian terrain using laser range finder data. The scheme must also be able to limit discontinuities present at common boundaries of modeled sections. The purpose of such a procedure is to determine gross slopes and gradients of the nearby terrain. With this information, it will be possible to define lines of constant gradient, which will identify forbidden zones where the gradient is too large for the rover to negotiate.

Note that obstacle detection is not an objective of this task. The objective is to find general gradients. In fact, one aim is to find the gradient of terrain upon which small objects about the size of the rover are located. The detection of these objects if left to Tasks D.1.a and D.1.b.

Concept of the Two-Dimensional Spline Function

From a single scan a laser range finder will provide a large number of data points to the rover. These points must somehow be fitted to a two-dimensional polynomial which models the terrain. One possible approach is to fit a high order polynomial expanded about one point to a large number of data points. But high order polynomials involve large numbers of cross product terms, and expansion about one point leads to less local accuracy. Thus the approach chosen for this task is the two-dimensional spline function. Sections of the terrain are fitted piecewise to low order two dimensional polynomials, each expanded about a different point. The terrain is then represented by a large number of such sectional polynomials.

Initial Modeling Scheme

In the initial analysis, two sections which share a common vertical boundary are modeled. To formulate the spline functions, six data points arranged as in Figure 66 are used. Each data point is given a cross-path coordinate, an in-pathcoordinate, and a height, denoted by a, b, and h, respectively. The dashed vertical line represents the common boundary.

Consider the four leftmost points. The height of any point within the area they enclose may be represented by the two-dimensional polynomial

$$h = C_{00} + C_{10}(a-a\ ) + C_{01}(b-b\ ) + C_{11}(a-a\ )(b-b\ )$$

In finding the C's, which are unknown coefficients, the given heights of

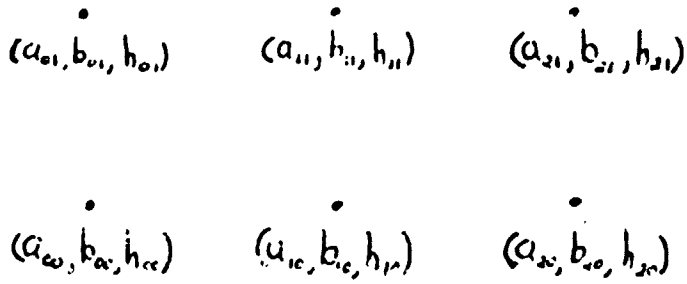

Fig. 66. Data Point Arrangement for Initial Modeling Method

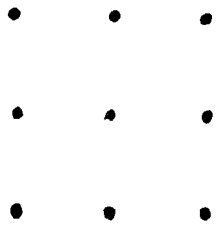

Fig. 67a. One Section

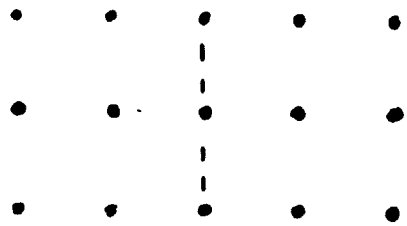

Fig. 67b. Two Sections with One Common Boundary

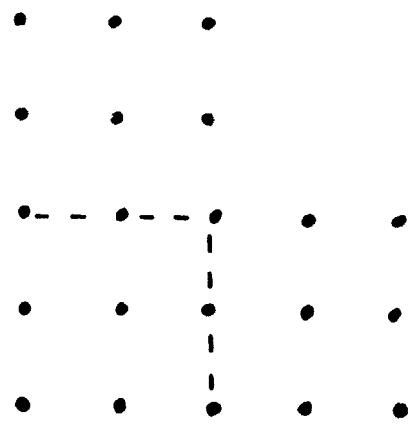

Fig. 67c. Addition of a Third Section having one common horizontal boundary

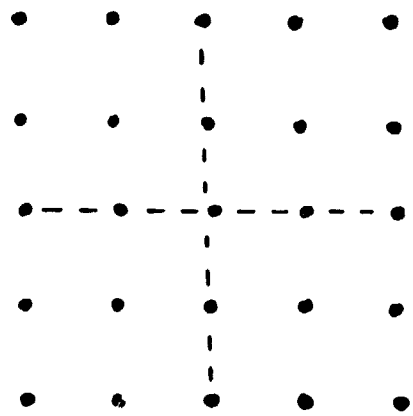

Fig. 67d. Addition of a Fourth Section Having Two Common Boundaries

the four data points may be expressed in matrix form as

$$\begin{vmatrix} h_{00} \\ h_{10} \\ h_{01} \\ h_{11} \end{vmatrix} = \begin{vmatrix} 1 & 0 & 0 & 0 \\ 1 & a_{10}-a_{00} & b_{10}-b_{00} & (a_{10}-a_{00})(b_{10}-b_{00}) \\ 1 & a_{01}-a_{00} & b_{01}-b_{00} & (a_{01}-a_{00})(b_{01}-b_{00}) \\ 1 & a_{11}-a_{00} & b_{11}-b_{00} & (a_{11}-a_{00})(b_{11}-b_{00}) \end{vmatrix} \cdot \begin{vmatrix} C \\ C_{10} \\ C_{01} \\ C_{11} \end{vmatrix} \quad \text{or } h' = A'X'$$

Next consider the rightmost four points in Figure 66. Since it is desired to expand about (a_{10},b_{10}), the matrix equation for these point heights is

$$\begin{vmatrix} h_{10} \\ h_{20} \\ h_{11} \\ h_{21} \end{vmatrix} = \begin{vmatrix} 1 & 0 & 0 & 0 \\ 1 & a_{20}-a_{10} & b_{20}-b_{10} & (a_{20}-a_{10})(b_{20}-b_{10}) \\ 1 & a_{11}-a_{10} & b_{11}-b_{10} & (a_{11}-a_{10})(b_{11}-b_{10}) \\ 1 & a_{21}-a_{10} & b_{21}-b_{10} & (a_{21}-a_{10})(b_{21}-b_{10}) \end{vmatrix} \cdot \begin{vmatrix} C \\ C_{10} \\ C_{01} \\ C_{11} \end{vmatrix} \quad \text{or} \quad h = A X$$

In order to proceed later with the optimization step, both systems must be expressed in one matrix equation. Consequently,

$$h\# = Ax \text{ where } h\# = \begin{vmatrix} h' \\ h* \end{vmatrix} \quad A = \begin{vmatrix} A' & 0 \\ 0 & A* \end{vmatrix} \quad X = \begin{vmatrix} X' \\ X* \end{vmatrix}$$

The height of the terrain anywhere within these six data points is represented by the pair of two dimensional polynomials. Along the common boundary, the height, cross-path slope, or in-path slope of any point may be determined using either section model. It is thus possible that discontinuities exist at such points for these terrain parameters.

Method of Optimization

Discontinuities in slope values will make it difficult to obtain reasonably accurate iso-gradient lines, and necessitates the development of some method which will limit these discontinuities. The approach chosen is the minimization of a performance function comprised of three terms. The first term indicates the square of the difference between the measured height of the data points, and the height at the same points of any optimized model. The second and third terms are, respectively, a measure of the discontinuity occurring in cross-path and in-path slope along the boundary. Including scalar weighting ξ and ρ, the performance function becomes

$$J = \left|Ax-h\right|^T \left|Ax-h\right| + \xi/b_{11}-b_{10} \int_{b_{10}}^{b_{11}} \left[\frac{\partial h_R}{\partial a} - \frac{\partial h_L}{\partial a}\right]^2 db +$$

$$\rho/b_{11}-b_{10} \int_{b_{10}}^{b_{11}} \left[\frac{\partial h_R}{\partial b} - \frac{\partial h_L}{\partial b}\right]^2 db$$

where R and L refer to right and left. The last two terms can be expanded and expressed in matrix form so that

$$J = \left|Ax-h\right|^T \left|Ax-h\right| + \xi x^T F x + \rho x^T G x$$

If J is minimized with respect to X, the new estimate of the coefficients, now optimized, is

$$X = \left| A^T A + \varsigma F + \rho G \right|^{-1} A^T h$$

Stochastic Problem

If range measurement noise is considered, a minimum variance calculation should be performed in conjunction with the preceding operation. This involves the inversion of an 8x8 matrix expressing the covariance of the heights of the data points used. But since both sections are dealt with simultaneously, and two points are in common to the sections, two rows of the covariance matrix are identical. Thus the matrix cannot be inverted. This stochastic analysis fails because eight unknowns are being determined simultaneously from six pieces of data. Due to this impasse, it was decided to modify the scheme.

The Revised, Extendable Model

The revised modeling scheme and optimization procedure are simply modifications of those described previously. The aim of the modeling scheme to maintain the total number of unknowns found to be less than or equal to the number of additional data points used. For the four term polynomial used previously, a square array of nine points arranged as in Figure 67a is used. As noted in Figure 67d, the minimum number of data points added in expanding to an adjacent section is four. For a given section, the four unknowns can be found from the nine data points by using the least squares method. The appropriate matrix equation for the heights is

$$\begin{vmatrix} h_{00} \\ h_{10} \\ h_{20} \\ h_{01} \\ h_{11} \\ h_{21} \\ h_{02} \\ h_{12} \\ h_{22} \end{vmatrix} = \begin{vmatrix} 1 & 0 & 0 & 0 \\ 1 & a_{10}-a_{00} & b_{10}-b_{00} & (a_{10}-a_{00})(b_{10}-b_{00}) \\ 1 & a_{20}-a_{00} & b_{20}-b_{00} & (a_{20}-a_{00})(b_{20}-b_{00}) \\ 1 & a_{01}-a_{00} & b_{01}-b_{00} & (a_{01}-a_{00})(b_{01}-b_{00}) \\ 1 & a_{11}-a_{00} & b_{11}-b_{00} & (a_{11}-a_{00})(b_{11}-b_{00}) \\ 1 & a_{21}-a_{00} & b_{21}-b_{00} & (a_{21}-a_{00})(b_{21}-b_{00}) \\ 1 & a_{02}-a_{00} & b_{02}-b_{00} & (a_{02}-a_{00})(b_{02}-b_{00}) \\ 1 & a_{12}-a_{00} & b_{12}-b_{00} & (a_{12}-a_{00})(b_{12}-b_{00}) \\ 1 & a_{22}-a_{00} & b_{22}-b_{00} & (a_{22}-a_{00})(b_{22}-b_{00}) \end{vmatrix} \begin{vmatrix} D_{00} \\ A_{00} \\ B_{00} \\ C_{00} \end{vmatrix} \quad \text{or} \quad h = T X$$

By least squares fit

$$X = \left| T_{00}{}^T \; T_{00} \right|^{-1} T_{00}{}^T \; h_{00}$$

The revised optimization procedure works with only one set of coefficients at a time. To do this, assume that the elements of vector X have been found, and are fixed. Consider a data section to the immediate right, as shown in Figure 67b. In a manner analagous to the one above, a matrix T_{20}

and a vector h_{20} may be formed. The resulting performance function, which deals only with the elements of X_{20} is similar to the one used initially, except a term has been added to penalize boundary height discontinuities.

$$J' = \left|T_{20}x_{20}-h_{20}\right|^T \left|T_{20}x_{20}-h_{20}\right| + \frac{\alpha}{b_{22}-b_{20}} \int_{b_{20}}^{b_{22}} \left|h_R-h_L\right|^2 \, db$$

$$+ \frac{\beta}{b_{22}-b_{20}} \int_{b_{20}}^{b_{22}} \left|\frac{\partial h_R}{\partial a} - \frac{\partial h_L}{\partial a}\right|^2 \, db + \frac{\gamma}{b_{22}-b_{20}} \int_{b_{20}}^{b_{22}} \left|\frac{\partial h_R}{\partial b} - \frac{\partial h_L}{\partial b}\right|^2 \, db$$

Remembering that the elements of X_{20} are fixed, this expression may be written in matrix form, minimized with respect to X_{20}, an optimized set of coefficients.

If a section directly above the first is considered, as in Figure 67a, a set of new, but similar boundary conditions may be derived.

Further to find X_{22} for the additional section depicted in Figure 67d, it is only necessary to derive a similar performance function consisting of six boundary terms. Six terms are needed since two common boundaries exist. Note that for the resulting optimization, X_{02} and X_{20} are assumed to be fixed.

If it is assumed then that once found, the parameters of a section expressed in a vector X are fixed, a recursive scheme exists which will add any number of additional sections to the model. Section polynomials can be found individually, without altering those of previously modeled sections.

Numerical Example

To demonstrate the modeling procedure, a numerical example which modeled six terrain sections was run on the computer. The data points are spaced one meter apart. The situation represents a planar slope on which is located a one meter radius boulder. The data point heights are as follows, where the dashed lines indicate common boundaries.

1.	1.	1.	1.	1.	1.75	1.
.75	.75	.75	.75	.75	.75	.75
.5 ---	.5 ---	.5 ---	.5 ---	.5 ---	.5 ---	.5
.25	.25	.25	.25	.25	.25	.25
0	0	0	0	0	0	0

The best way to display the results is by the iso-gradient maps of Figure 68. For Figure 68a, the slope discontinuity penalty was given a zero weighting. The line made up of "2's" represents the gradient line whose value is 25°. The area inside the two lines thus has a gradient greater than 25°, indicating the presence of the boulder.

C-12

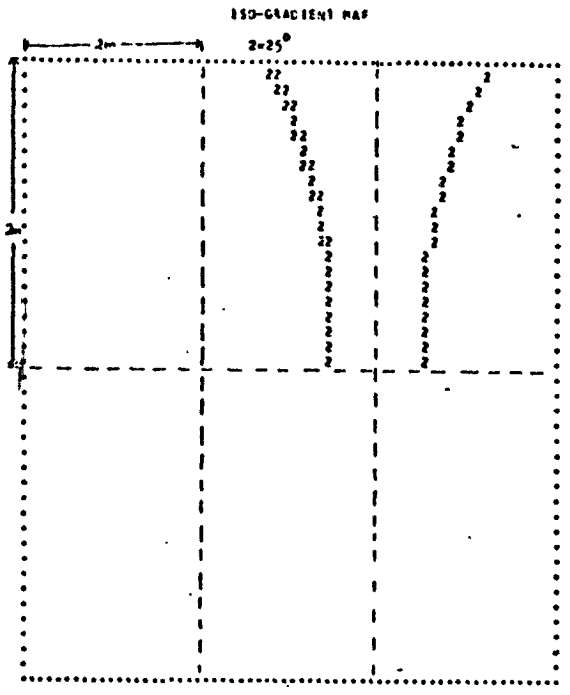

Fig. 68a. Slope Penalty = 0

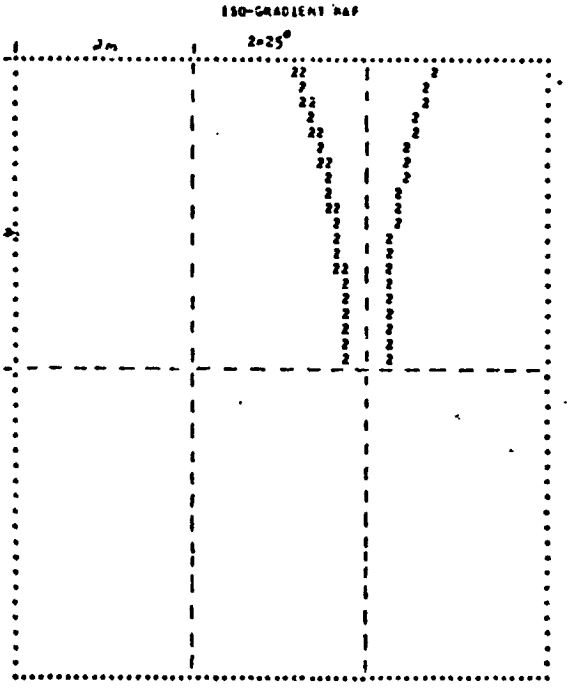

Fig. 68b. Slope Penalty = 1.0

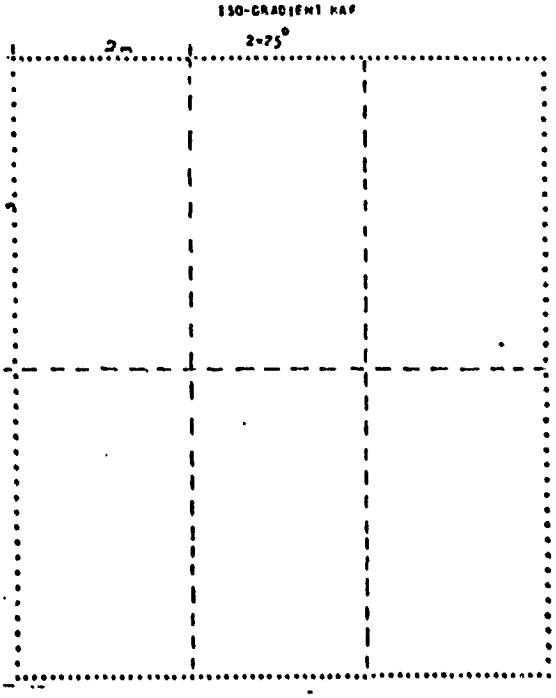

Fig. 68c. Slope Penalty = 10

Fig. 68. Ingradient Maps Showing 250 Gradient Lines

But it is desired to find the gradient in the vicinity of the boulder. For Figures 68b and 68c the slope discontinuity penalty weighting is raised to unity, and then ten. For these higher weightings the 25^{o} line disappears. Thus the model is producing a terrain representation whose gradients are those in the vicinity of the boulder, which in reality is about 14^{o}.

Conclusions

The proposed terrain modeling procedure can find general slopes and gradients of terrain, and subsequently define lines of constant gradient. The method is recursive, and any number of sections can be easily modeled. Each section requires only about .15 seconds of computer time on the IBM 360/67. With further development it appears that the two dimensional spline function modeling technique can be used to formulate iso-gradient maps of the general terrain features. Beyond this point, the following extensions should be considered:

a) A full stochastic study should be undertaken to determine the exact effects of range measurement noise.

b) The present scheme requires rectangular arrangement of data points. Since this will seldom be the case for real terrain, the boundary conditions must be generalized.

c) From other examples, it was found that higher slope penalties are needed in some situations than in others to attain adequate results. Thus it might be appropriate to study the possibility of variable penalty weightings.

D.4.a. Measurement Scanning Concepts - Mark Friedman
Faculty Advisor: Prof. C. N. Shen

The objective of this subtask is to develop scanning concepts for laser rangefinder hazard detection system. This involves determining the minimum field of view and data density. This is required to ensure that the measured range data will provide accurate and reliable results when used by obstacle detection and the terrain modeling techniques described under Tasks D.1.a and D.3.

The basic scanning parameters are shown in Figure 69. The field of view is defined by β, the rangefinder elevation angle measured down from the horizontal, and θ, the rangefinder azimuth angle. The rangefinder will scan the field at constant increments of β and θ denoted by $\Delta\beta$ and $\Delta\theta$ respectively. The inpath point spacing is Δb and the cross-path spacing is Δa. The quantity $\Delta b'$ is the vertical data point spacing as shown in Figure 69.

The safety requirements and capabilities of the rover provided the criteria for defining the field of view parameters given in Table 1. The requirements of the terrain modeling and obstacle detection procedures made it necessary to divide the scan into a near scan (3-16m) and a far scan (16-30m). Each was treated as a separate field of view and using the same criteria as above, the parameters of Table 2 were derived.

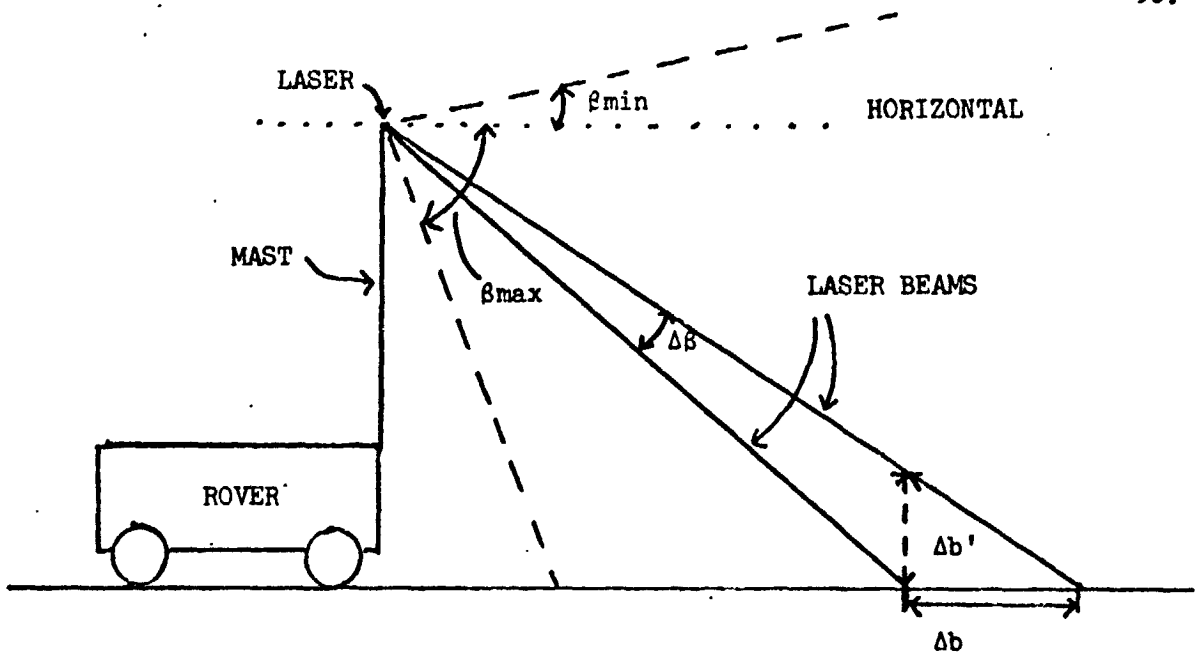

(a) Side View

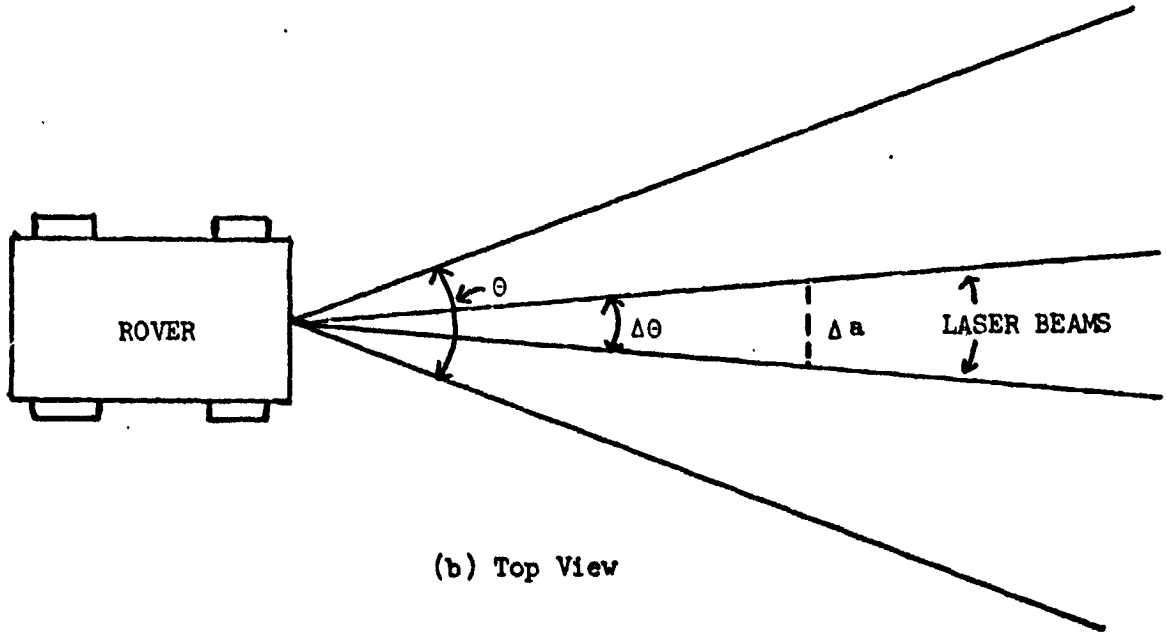

(b) Top View

Fig. 69. Scanning Parameters

Table 1

Single Terrain Scan

β_{max}	57.5°
β_{min}	-19.6°
β_{tot}	77.1°
Θ_{tot}	53.0°
$\Delta\beta$	.76°
$\Delta\Theta$	1.91°

Table 2

Divided Terrain Scan

	Near Scan	Far Scan
β_{max}	57.5°	10.6°
β_{min}	-14.6°	-19.6°
β_{tot}	72.1°	30.2°
Θ_{tot}	53.0°	53.0°
$\Delta\beta$	1.4°	.76°
$\Delta\Theta$	3.6°	1.91°
N_Θ	15	28
N_β	52	40
N	780	1120

N_{tot} = 1900 data points

The data point spacing parameters were determined from the requirements of the modeling procedures. However the obstacle detection routines call for a significantly smaller data point spacing than the terrain modeling procedure. This problem was approached in two ways.

The first procedure referred to as the Terrain and Zoom Scan Procedure is to scan the field with a data point spacing appropriate for the terrain modeling technique. This spacing would not give a well defined outline of an obstacle but would at least give an indication of its presence. The second scan would be a "zoom" scan with reduced spacing aimed at the obstacle location indicated in the previous terrain scan. The total number of points in the terrain scan would be about 1900 (Table 2). Using an expected scanning rate of 1 msec/data point, this would give a scan time of 1.9 sec. The time of the zoom scan would probably be from 2 to 5 sec depending upon the size of the obstacle. The disadvantages of this method are considerable. The hardware modifications for the zoom scan are likely to be quite complicated and the presence of more than one obstacle in the field would require multiple zoom scans between each terrain scan.

These disadvantages may be easily avoided by again using near and far scans with data point spacing set for obstacle detection. Software techniques may then be used to systematically skip over some points to achieve the spacing required for terrain modeling.

In an effort to reduce the total scan time, three sets of far scan parameters have been derived for this obstacle scan procedure and are given in Table 3. Each saving in scan time was made by reducing the field of view of the far scan.

The scan time and total number of data points taken can be reduced by a third procedure namely the Corridor Scan dividing the field into M corridors as shown in Figure 73. This procedure is to be applied to the full width for ranges from 3 to 30 meters with M = 5. The scan will again be divided into two subscan types. First, an initial scan with low data point spacing will be taken of the whole field to merely indicate the presence of obstacles. Then a corridor scan with higher data point density will be taken for only those corridors which show promise of passability.

The Corridor Scan method is expected to result in reduced necessary on-board computer core and reduced calculation time of the range data processing techniques, Tables 4a and 4b.

By examining the avoidance time and the number of scans per field for the Corridor Scan Procedure, it is seen that the maximum scanning range can be reduced from 30 meters with little added danger to the vehicle if the vehicle's average speed is less than about 0.2 meters per second.

Terrain and Zoom Scan Method

The rover is expected to be able to traverse a positive or negative slope up to 25°. This is used to calculate β. The quantity β_{max} is derived for the situation of the rover approaching a negative slope change of 25° and scanning at 3 m for the near scan and 15 meters for the far scan as shown in Figure 70. Figure 71 shows the situation used for the calculation

Table 3 Divided Obstacle Scan

	Near Scan 3-15m	Far Scan A. Full width, 15-30m	B. Reduced width, 15-30m	C. Reduced width, 15-25m
β_{max}	57.5°	11.3°	11.3°	11.3°
β_{min}	-13.8°	-19.6°	-19.6°	-18.4°
β_{tot}	71.3°	30.9°	30.9°	29.7°
θ_{tot}	53.0°	53.0°	36.9°	36.9°
$\Delta\beta$	.77°	.38°	.38°	.46°
$\Delta\theta$	.77°	.38°	.38°	.46°
N_θ	69	114	97	80
N_β	92	81	81	64
N	6348	9234	7857	5120

Table 4a

Initial Scan Parameters

β_{tot}	77°
θ_{tot}	53°
$\Delta\beta$	1°
$\Delta\theta$	1°
N_I	4081
T_I	4.1 seconds

Table 4b

Corridor Scan Parameters

β_{tot}	34.3°
θ_{tot}	10.6°
$\Delta\beta$	.38°
$\Delta\theta$	.38°
N_C	2520
T_C	2.5 second

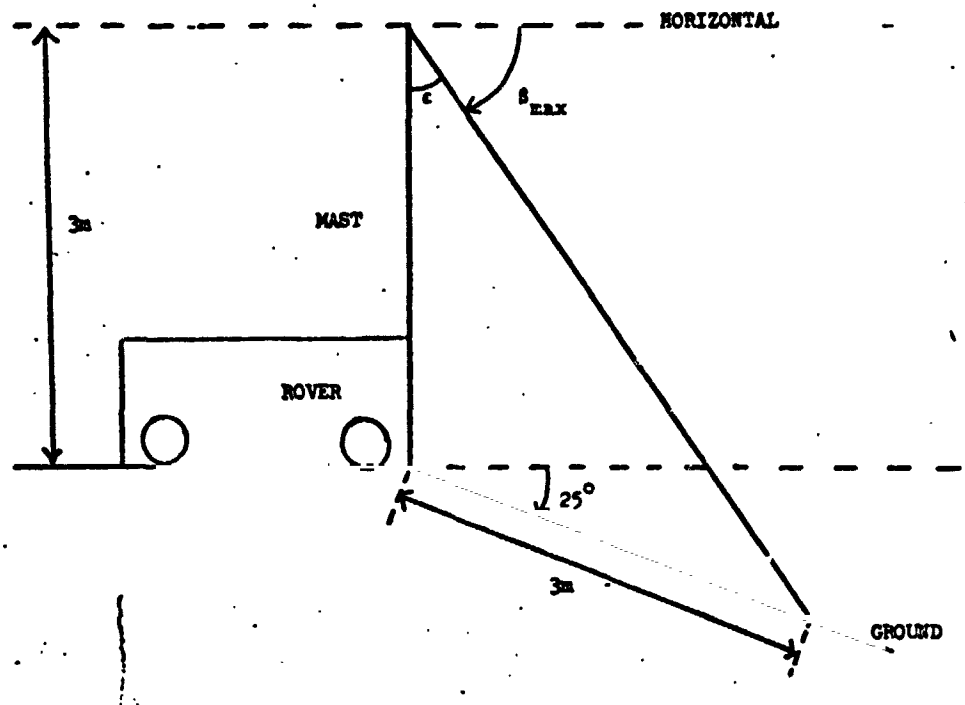

Fig. 70. Situation for Beta Max.

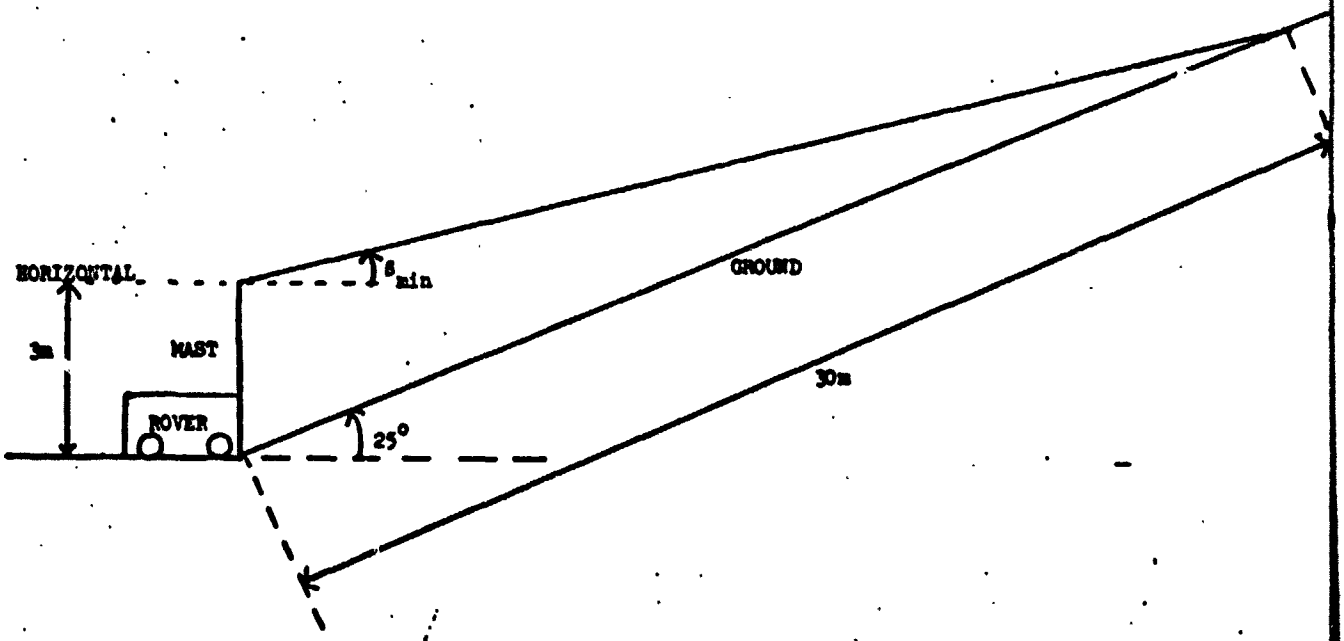

Fig. 71. Situation for Beta Min.

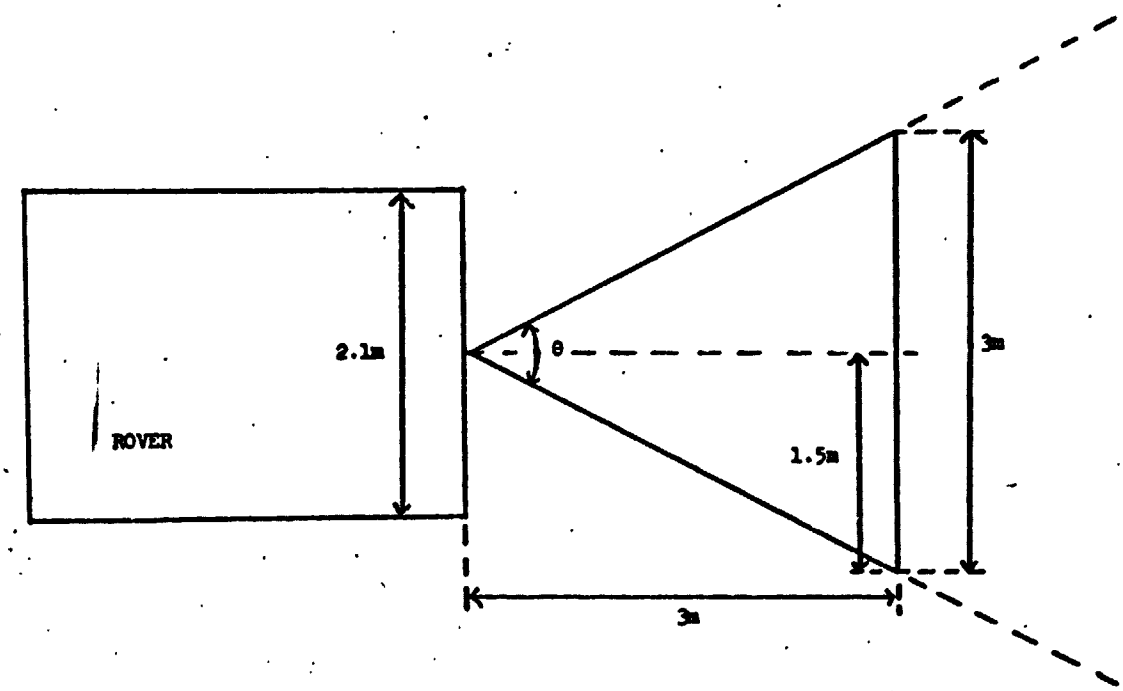

Fig. 72. Situation for Theta

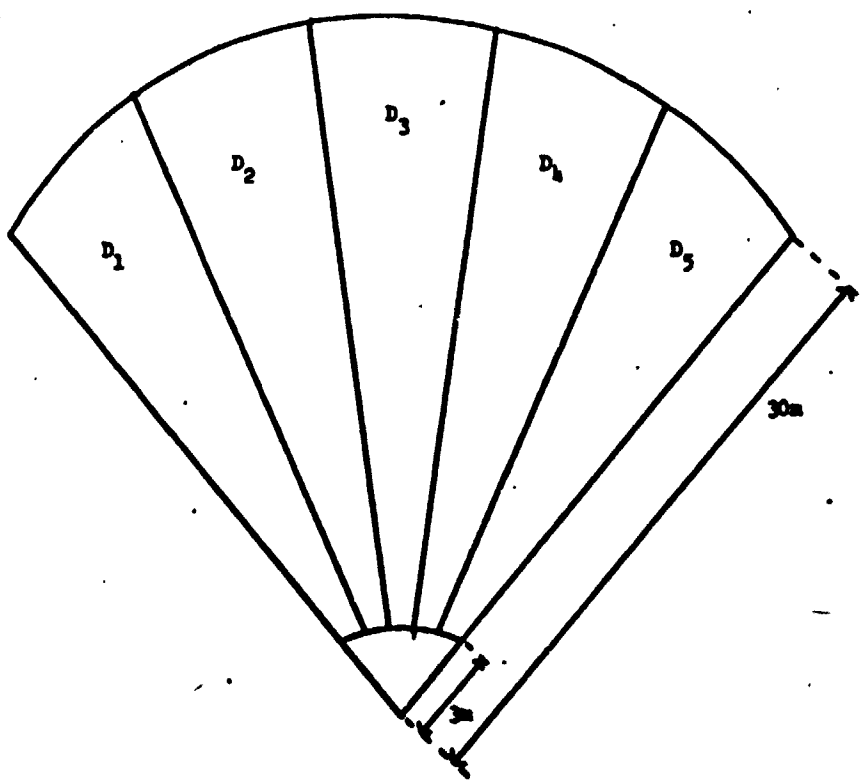

Fig. 73. Scanned Field Divided into M Corridors

of β_{min}. The rover is approaching a positive slope change of 25° and scanning at 15 meters for the ner scan and 30 meters for the far scan.

The quantity Θ is calculated so that the rangefinder can scan the width of the vehicle, expected to be about 2.1 meters plus an allowance on each side or 3 meters total at a distance of 3 meters as shown in Figure 72. Table 2 gives the values derived above. The values for the field of view parameters in Table 1 and Table 3 are similarly derived.

In Table 1, $\Delta\Theta$ was set so that the rangefinder would sense an object of one meter width with at least one data point at the farthest range. The quantity $\Delta\beta$ was set so that an object at least 0.4 meter high could be detected with one data point at the farthest range. The height 0.4 meter was chosen because the vehicle is expected to be able to roll over an object of lesser height.

With the scanning increments calculated above the data point spacing becomes very small at close ranges. This would give rise to large error in the terrain modeling procedure, Ref. 15. Even when the field of view was divided as in Table 2 the error was unacceptable for ranges closer than about 8 meters.

The number of data points per scan is denoted in Table 2 as N. The total number of scanning points per field divided by the expected scanning rate of 1 msec/data point gives the total scan time of 1.9 seconds.

If a terrain scan with parameters similar to Table 2 were used, a terrain modeling procedure, Ref. 16 would of course be used but an obstacle detection routine would also be applied to the range data. Although the data point spacing would be too large to give a well defined outline of an obstacle, the routine would give an indication of either the top edge of a boulder or the near edge of a crater, Ref. 17. A zoom scan would then be utilized with reduced data point spacing aimed at the obstacle location given by the terrain scan. The extent of the "zoom" would depend on the size and range of the obstacle. The number and range of the obstacle's warning points could be used to determine the proper amount of data point reduction.

Obstacle Scan Method

Table 3 gives the scanning parameters of the Obstacle Scanning Procedure. The scanning increments $\Delta\beta$ and $\Delta\Theta$ are calculated by setting Δa and $\Delta b'$ (see Figure 69) both equal to .2 meters at the farthest range for the near and for the far scan. This gives a minimum data point density on the face of an obstacle of 5 points per meter which is assumed to be sufficient for a well defined outline of the obstacle.

Three sets of far scan parameters have been derived and given in Table 3 in an effort to minimize the total scan time by reducing the field of view of the far scan. Far scan A extends from 15 to 30 meters with a full angular width of 53°. Far scan B also extends from 15 to 30 meters but the angular width has been reduced to about 37° giving a minimum linear width of 10 meters. The angular width of far scan C is reduced as in far scan B but extends from 15 meters to only 25 meters. From the values given

for the number of scanning points it is seen that the total scan time for this method will be from about 11 to 16 seconds.

Corridor Scan Concept

In the corridor scan concept the initial scan will have a low density spacing. Its purpose is merely to indicate which corridors contain obstacles but not to show their outlines. It will do this by comparing the range of each data point to range values of clear level terrain which will be stored in the on-board computer. Each point which differs significantly from its "clear" value will be assigned a danger value d_{ij} where i indicates the i^{th} corridor and j runs from one to N, the number of points in the corridor. Then each corridor may be assigned a danger value D_i:

$$D_i = \sum_{j=1}^{N} d_{ij} \qquad i = 1, M$$

The d values should be dependent on λ, the level of the obstacle point height and R the obstacle point range, with a closer and taller obstacle point being assigned a larger danger value.

As an example of how λ may be determined, consider Figure 74. Range values for three levels are stored and compared to the data. If the obstacle point falls between -0.2m and +0.2m it is given λ =0 and does not contribute to d. If it falls between 0.2m and 0.4m it is assigned λ = 1 and if it is above 0.4m or below -0.2m it is given λ=2. A higher danger value is given to negative obstacles since their actual depth is usually difficult to sense.

The next step in the procedure is to make a scan decision based on the corridors' danger values. One possible method is as follows:

(1) If there is one or more corridors with $D \leq D_s$ travel in the direction of the safe corridor nearest the center of the field with no detail corridor scan.

(2) If $D_i > D_u$; i=1,M, the vehicle may have to stop and do a complete detail scan.

(3) Otherwise choose smallest D, and do a detail corridor scan.

(4) If detail corridor scan shows an obstacle, try next larger D.

In step 1, D_s is a low danger value such that a corridor with a D less than D_s would be almost completely clear and level. A corridor near the center of the field is preferred since more is known about the terrain surrounding this corridor than an outside corridor such as corridor 1 or 5 (Figure 73). An exception to this rule would be if three corridors together each had D less than D_s such as corridor 1, 2 and 3. In this

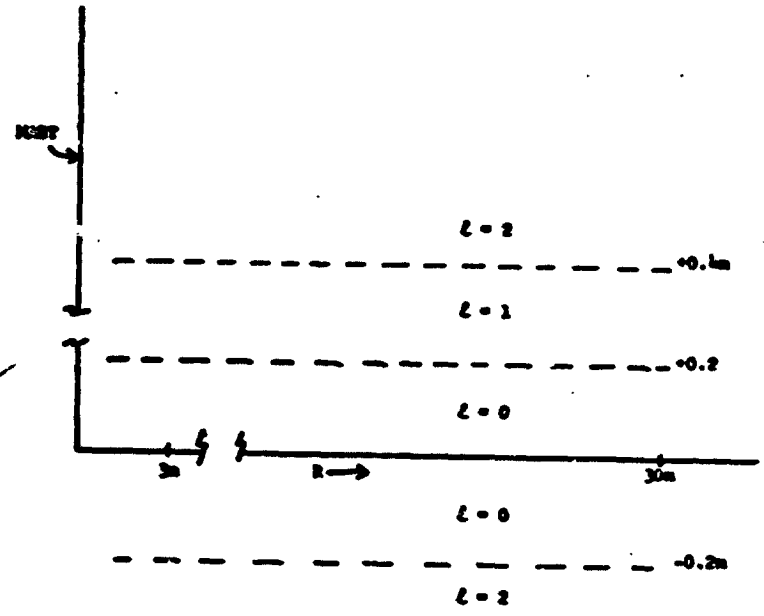

Fig. 74. Determination of " "

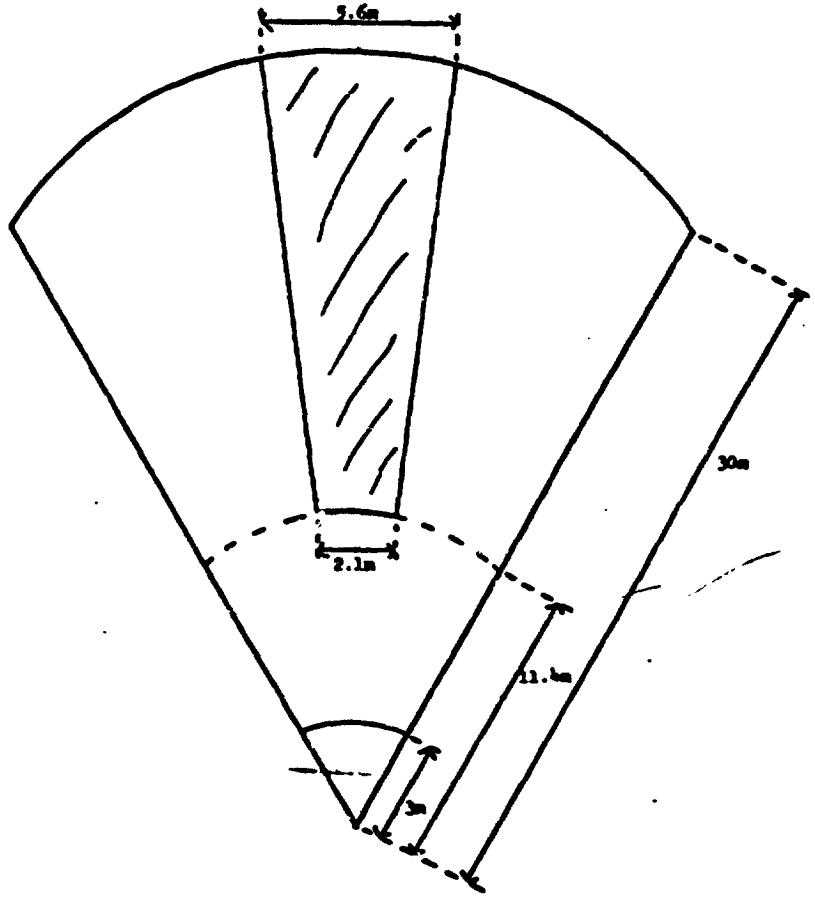

Fig. 75. Corridor Scan

case corridor 2 would be the safest.

In step 2, D_u is a greater danger value such that there is a high probability that there exists an obstacle which could not be avoided. Two or possibly three corridor scans may be necessary (step 4); however, if the terrain is so rough that three corridor scans show unavoidable obstacles, step 2 would probably have been satisfied and this field would have be completely avoided before any detail scans were made.

As shown in Figure 75, each corridor is narrower than the vehicle's width of 2.1 meters at ranges closer than 11.4 meters, so that there will be some ground over which the vehicle will travel which cannot be completely modeled with the corridor scan alone. This gives a criterion for determining the proper density of the initial scan. The density should be set at 5 points per meter at the range of 11.4 meters so both terrain modeling and obstacle detection techniques may be performed on this near sector. This gives the initial scan parameters shown in Table 4a.

The parameters of the corridor scan as shown in Table 4b were derived by setting the density at 5 points per meter at the 30 meter range. Each corridor scan need only extend from 30 meters down to 11.4 meters since for closer ranges the initial scan density is proper for the terrain modeling techniques. As before, it is assumed that software pre-processing will be used to systematically skip data points to achieve the proper lower spacing required by the terrain modeling procedures.

Scan Time Performance

The maximum scanning range should be chosen so that, once the vehicle gets within this range of an obstacle, it should have enough time to detect it reliably and avoid it safely. This analysis so far has assumed a maximum scan range R_{max} of 30 meters. This is somewhat arbitrary since the vehicle's average speed has not been specified.

To ensure accurate detection of an obstacle, it is desired to have the number of scans denoted as $\mathcal{A}$ which can be made as the vehicle travels the length of its field of view as large as possible. This number can be simply calculated from the following relation:

$$\mathcal{A} = \frac{\text{(maximum scan range)}}{\text{(scan time)}\quad\text{(vehicle speed)}}$$

This calculation has been performed for the Corridor Scan Procedure. Table 5 shows the results of this calculation for a vehicle speed of 1 meter per second. The maximum range is R_{max}. T is the total scan time, and Z is the distance traveled by the vehicle during one total scan. The total scan time is equal to the constant initial scan time of 4.1 seconds plus the time of the corridor scan which is dependent on the maximum scanning range. Figure 76 shows a graph of $\mathcal{A}$ versus R_{max} for various vehicle speeds.

For safe obstacle avoidance, the time from the end of the total scan which covers the obstacle to the time at which the vehicle reaches the obstacle should be as great as possible. Assuming the scan begins just when the obstacle is at R_{max}, this time, called T_a, is just equal to:

TABLE 5

Scan Time Performance

R_{max} (meters)	T (sec)	Z (meters)	Q	T_A (sec)
15	4.7	4.7	3.19	10.3
20	5.1	5.1	3.93	14.9
25	5.7	5.7	4.38	19.3
30	6.6	6.6	4.54	23.4
35	7.8	7.8	4.48	27.2
40	9.0	9.0	4.44	31.0

For Corridor Scan Procedure. Vehicle speed equals 1 meter per sec.

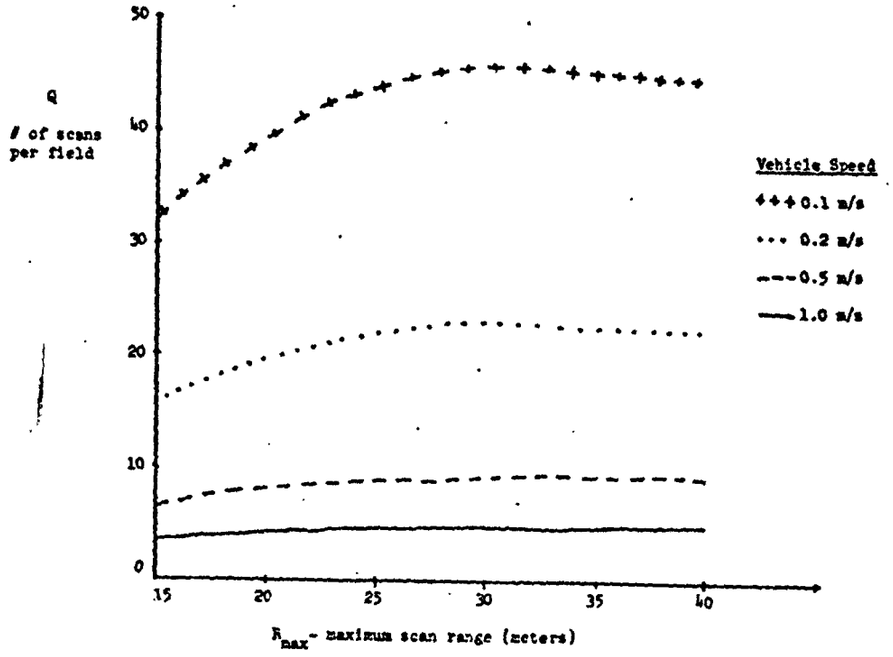

Fig. 76. Number of Scans Per Field as a Function of Maximum Scan Range

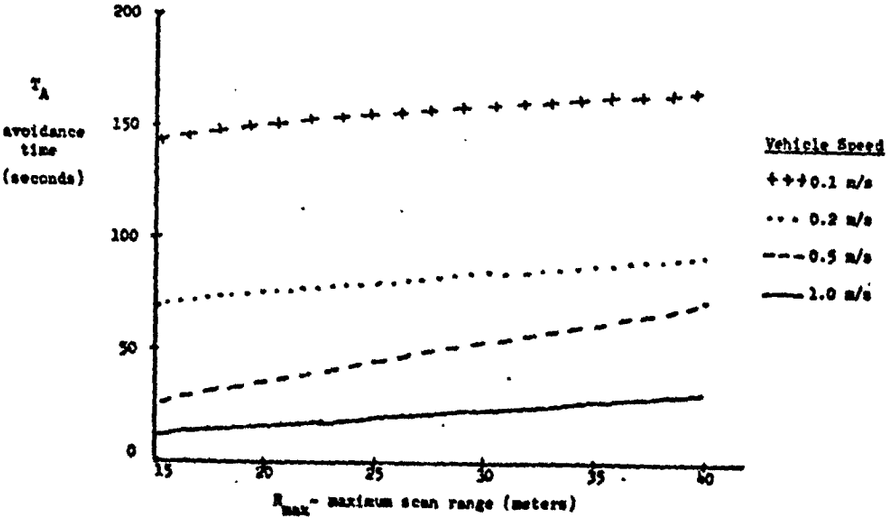

Fig. 77. Avoidance Time as a Function of Maximum Scan Range

$$T_A = \frac{(\text{maximum scan range})}{\text{vehicle speed}} - (\text{total scan time})$$

Table 5 also shows the avoidance times T_A for each R_{max} for a vehicle traveling at 1 meter per second. Figure 77 is a graph of T_A versus R_{max} for various vehicle speeds for the corridor scan procedure.

In Figure 76, it is seen that $\mathcal{Q}$, the number of scans per field is indeed a maximum for a maximum scan range of 30 meters. However, for vehicle speeds of 0.2 to 1 meter per second, this performance is not greatly reduced by reducing the maximum scanning range to 20 meters. But at these speeds, Figure 77 shows that the avoidance time would be cut down by about 35%. For slower speeds on the order of 0.1 meters per second, the avoidance time is not significant in this consideration. The number of scans per field and the avoidance time is so great for a vehicle speed as low as 0.1 meters per second that the maximum scanning range could probably be cut all the way down to 15 meters or below with little danger to the vehicle.

Conclusion

The total scan time for the terrain and zoom method will depend on the number and size of the obstacles in the field of view of the rangefinder. For three obstacles and assuming the scan time of the zoom scan to be the same as the terrain scan, the total scan time would be about 8 seconds which is substantially less than the scan time of the obstacle scan approach. However, the hardware and software problems involved in the variable spacing reduction of the zoom scan and the aiming of the zoom scan are expected to be quite great. It is felt that the obstacle scan method, where the field is scanned with small data point spacing for obstacles and data points are systematically skipped over prior to terrain modeling, will be much simpler and more desirable.

The corridor scan method is a combination of the terrain and zoom scan method and the obstacle scan method and avoids some of the disadvantages of each. For the obstacle scan about 15,500 points are taken in a scan time of 15.5 seconds, but an initial scan and one corridor scan takes only 6.6 seconds for the necessary 6600 points. The scan time is reduced to 4.1 seconds if the terrain is completely clear and a corridor scan is not needed. Besides the reduction in scan time, the Corridor Scan procedure reduces the necessary core required in the on-board computer and the complicated data processing techniques are used less often and with less data point. The hardware changes are expected to be small since the parameters of the corridor scan are fixed and a continuously variable data point spacing is not necessary.

Once a vehicle speed is specified, the maximum scan range may be chosen to best reflect safety considerations using the curves of Figures 76 and 77. Perhaps the maximum scan range can be reduced from 30 meters so that less data points will be acquired. If the vehicle's average speed is only 0.1 meter per second, the maximum scan range can probably be safely cut in half. Then less computer core will be required and the range data processing techniques will be applied to less points, further simplifying the terrain sensing system.

Task D.4.b. Laser Rangefinder Error - M. Friedman
Faculty Advisor: Prof. C. N. Shen

It is the objective of this subtask to investigate the range error due to the finite width and spread of the rangefinder laser beam. This is necessary in order to ensure applicability and reliability of the terrain modeling and obstacle detection procedures which use the range data.

The beam, originating from a height of 3 meters, will strike the surface of the ground at a fairly acute angle at the farther scanning ranges, causing the projection to be spread along the surface of the terrain. Parts of the beam will return to the rangefinder receiver at slightly different times since they were reflected at slightly different ranges. Hence, even if a very sharp pulse was transmitted, the received pulse will be spread out significantly in time giving an ambiguous range measurement.

It was found that the spread at the projection increases as the target range increases. The spread for a particular range may be minimized by proper choice of the transmitter aperture diameter. For the greatest range of interest, 30 meters, the optimum aperture diameter was found to be .78 centimeter. Table 6 gives the spread for various ranges between 3 and 30 meters. The aperture diameter used was 0.78 centimeter which is optimum only at 30 meters.

The measured range value will always be less than the true value by an amount dependent on the range. However, this analysis was performed with the assumption at level ground, i.e., the target is assumed to be oriented horizontally with respect to the rover. Therefore, the error cannot simply be added to the measured value to get the true value since the rover will encounter targets at various orientations at all ranges.

If a constant discriminator set at a level of 50% is used as the return pulse time detector, the range error at 30 meters due to the beam spread will be about 6.27 cm. This accuracy is expected to be acceptable for reliable use of the image enhancing procedures.

The Spread Equation

Figure 78 shows the laser rangefinder geometry with the rover on level ground. The beam, transmitted from the top of the rover mast, may be pictured as originating from a point source located behind the rover. The beam is assumed to be a right circular cone of solid angle $2\,\theta_d$ where θ_d is the angle of dispersion of the beam. The beam diameter at the transmission point at the tope of the mast is equal to the diameter, D, of the final aperture of the transmitter optical system whether it is a lens, a stop, or the laser element itself. The intersection of the beam cone with the plane of the ground defines the projection as an ellipse whose length in the major axis is taken to be, S, the spread of the beam projection.

From this geometry it is seen that S is a function of the mast height H, the range of the target R_o, the aperture diameter D and the angle of dispersion θ_d. The spread equation is:

$$S = \left[\sqrt{R_o^{2+H^2}}\sin\theta_d + \frac{D\cos\theta_d}{2}\right]\left[\frac{\sqrt{R_o^{2+H^2}}}{H\cos\theta_d + R_o\sin\theta_d} + \frac{\sqrt{R_o^{2+H^2}}}{H\cos\theta_{\,} - R_{\,}\sin\theta_d}\right.$$

Table 6

Spread S vs. Range R_o for the case where D=.78 cm, H=3m, and $1.22\lambda = 10{,}000$ Å

Range (m)	Spread (cm)
3.0	1.26
10.0	3.64
15.0	5.97
20.0	8.75
30.0	15.61

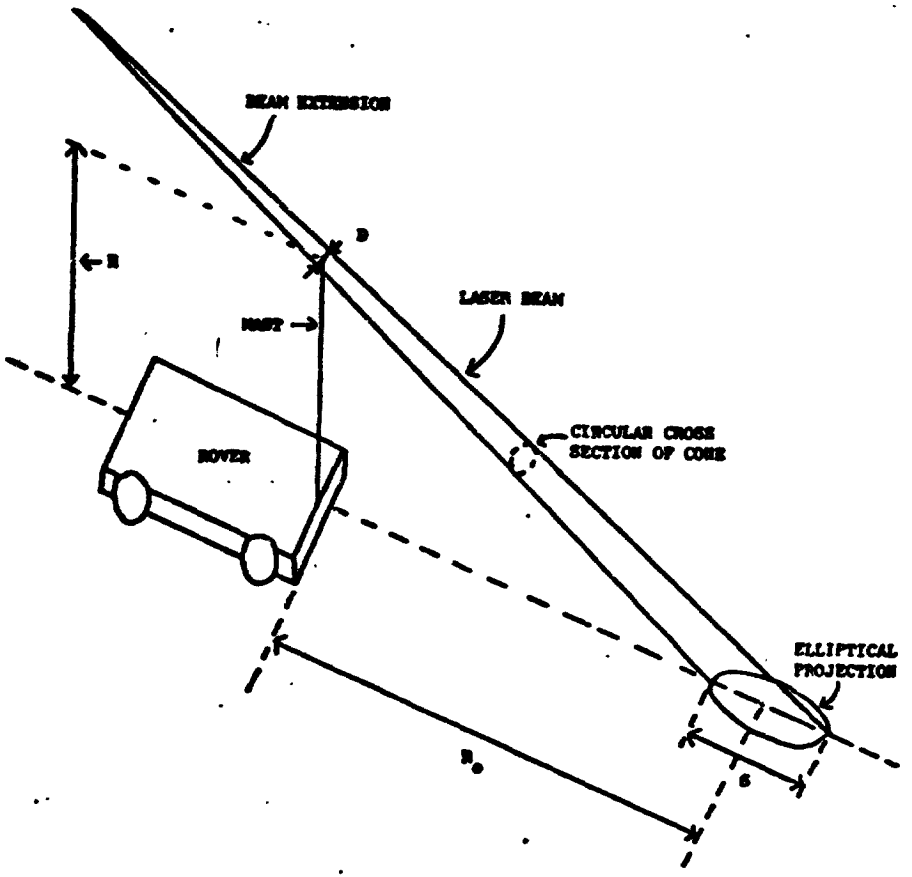

Fig. 78. Rover Range Finder Geometry

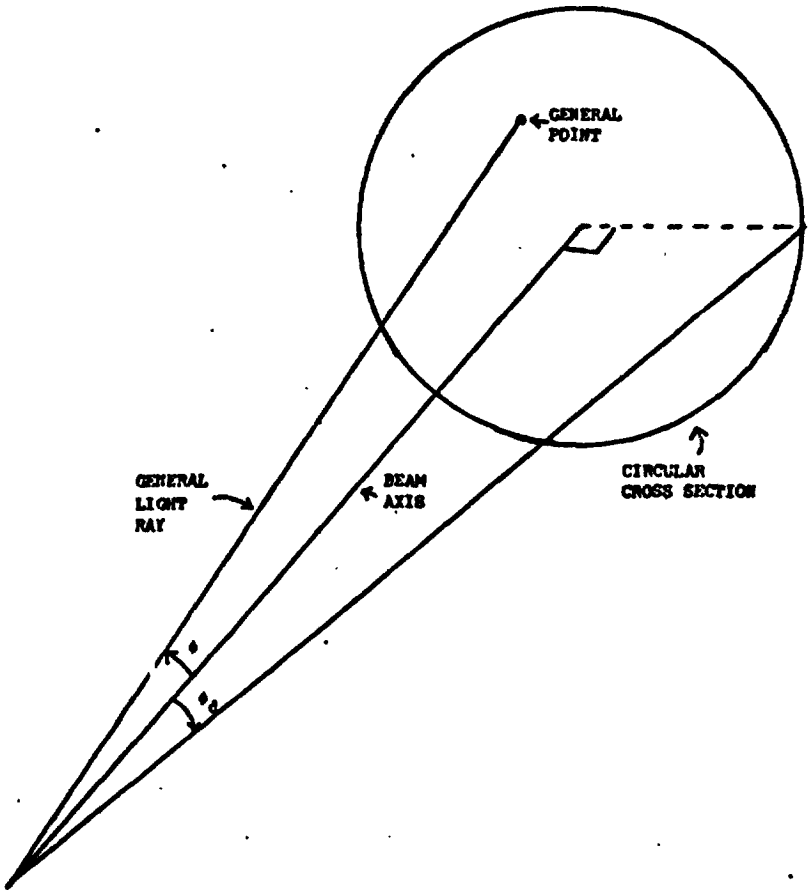

Fig. 79. The Laser Beam - A Right Circular Cone

and making small angle approximations for Θ_d:

$$\frac{\partial S}{\partial R_o} = \frac{4\,\Theta_d\,R_o}{H} + \frac{D\,R_o}{H\sqrt{R_o^2 + H^2}} \qquad (2)$$

Intensity Pattern

If the angle of dispersion can be given in terms of basis rangefinder system parameters such as the aperture diameter and beam wavelength, the spread and therefore the range error may be minimized by proper choice of these parameters. This necessary relation is dictated by the beam intensity pattern.

The intensity at a general point in the pattern is a function of Θ, the angle from the beam axis to this general point, Ref. 18 and 19, as shown in Figure 79. Specifically:

$$I(\Theta) \propto \left[\frac{2\,J_1 \left(\frac{\pi D \sin\Theta}{\lambda}\right)}{\frac{\pi D \sin\Theta}{\lambda}} \right]^2 \qquad (3)$$

where J_1 is the first order Bessel function

D is the aperture diameter

and λ is the beam wavelength

Figure 80 shows a graph of this relation.

The first minimum occurs when the argument of the Bessel function is equal to 1.22π. If the beam is approximated by a cone extending only to this first minimum, the angle of dispersion may be determined by setting the argument of the Bessel function equal to 1.22π. The angle will be on the order of milliradians; thus, $\sin\Theta_d$ may be approximated by Θ_d. Solving for Θ_d:

$$\Theta_d = \frac{1.22\lambda}{D} \qquad (4)$$

Diameter Optimization

Substituting equation (4) into equation (1) gives:

$$S = \left[\sqrt{R_o^2 + H^2} \sin\frac{1.22\lambda}{D} + \frac{D}{2}\cos\left(\frac{1.22\lambda}{D}\right) \right] \cdot \left[\frac{\sqrt{R_o^2 + H^2}}{H\cos\left(\frac{1.22\lambda}{D}\right) + R_o \sin\left(\frac{1.22\lambda}{D}\right)} + \frac{\sqrt{R_o^2 + H^2}}{H\cos\left(\frac{1.22\lambda}{D}\right) - R_o \sin\left(\frac{1.22\lambda}{D}\right)} \right] \qquad (5)$$

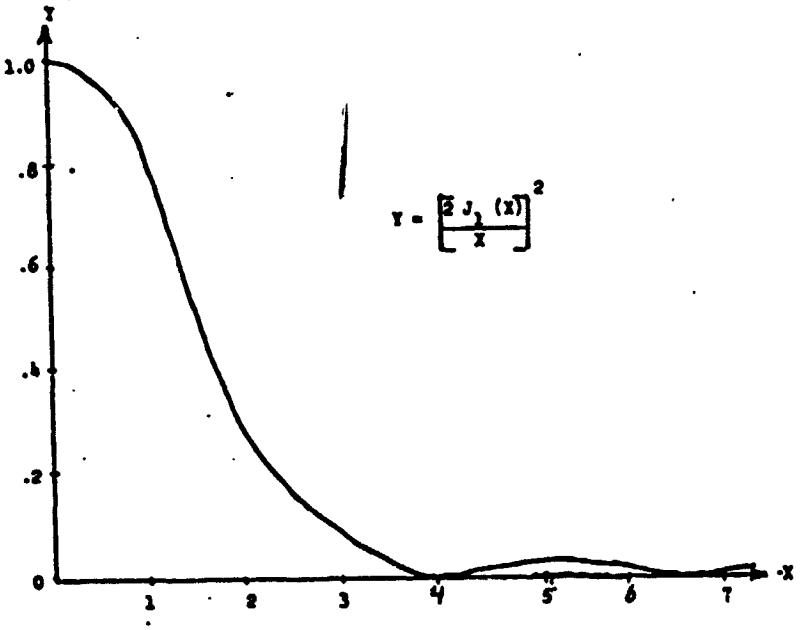

Fig. 80. Intensity Pattern Relation

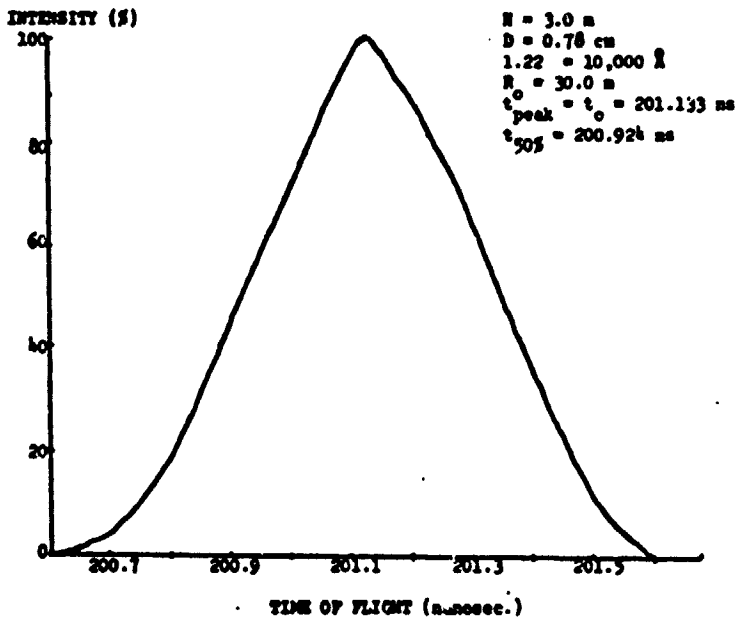

Fig. 82. Return Pulse Shape

The mast height has been set at 3 meters, the range is to vary from 3 to 30 meters, and the wavelength will presumably be set according to the actual laser used and will probably be in the infrared region. This leaves only D, the aperture diameter, to be adjusted so as to minimize the spread. The optimum diameter can be found by setting the partial derivatives of S with respect to D equal to zero. The second derivative is positive indicating that the spread will be a minimum for this optimum D.

Pulse Shape

As stated previously, the projection will be an ellipse. Figure 81 shows the ellipse and defines the coordinate system to be used in the pulse shape determination. The equation of such an ellipse is:

$$\frac{(x-h)^2}{a^2} + \frac{y^2}{b^2} = 1 \qquad (6)$$

where h, a, and b are shown in the fiture.

These elliptical parameters can be related directly to the system parameters.

If this ellipse is divided into rectangular sections as shown in Figure 81, all the energy returned from a particular rectangle will arrive at the range-finder receiver at approximately the same time. Therefore, each rectangle of width Δx is related to a unique time at the receiver. The intensity of the light at the receiver at each t is proportional to the power density of the light leaving each rectangle. The constant of proportionality is assumed to include the path length even though each rectangle is at a slightly different distance. At distances on the order of tens of meters these small path-length differences have a negligible effect on the light intensity. The major effect of these slight distance variations is the varying time of flight of the energy reflected by each rectangle.

The power density leaving each rectangle is equal to the product of the intensity of the light incident to the rectangle and the area of the rectangle. However the intensity is not constant on any particular rectangle. Thus, an integral of the following form will have to be calculated for each rectangle:

$$\Delta I_R = K \cdot P_t = K \int_{-\frac{\Delta x}{2}}^{\frac{\Delta x}{2}} \int_{-l/2}^{l/2} I_t(x,y)\, dy dx \qquad (7)$$

where I_R - intensity at receiver

P_t - power density leaving target

K - constant of proportionality

x - width of rectangle

and the length of each rectangle, l , is taken to be equal to the width of the ellipse at the value of x corresponding to the center of that rectangle.

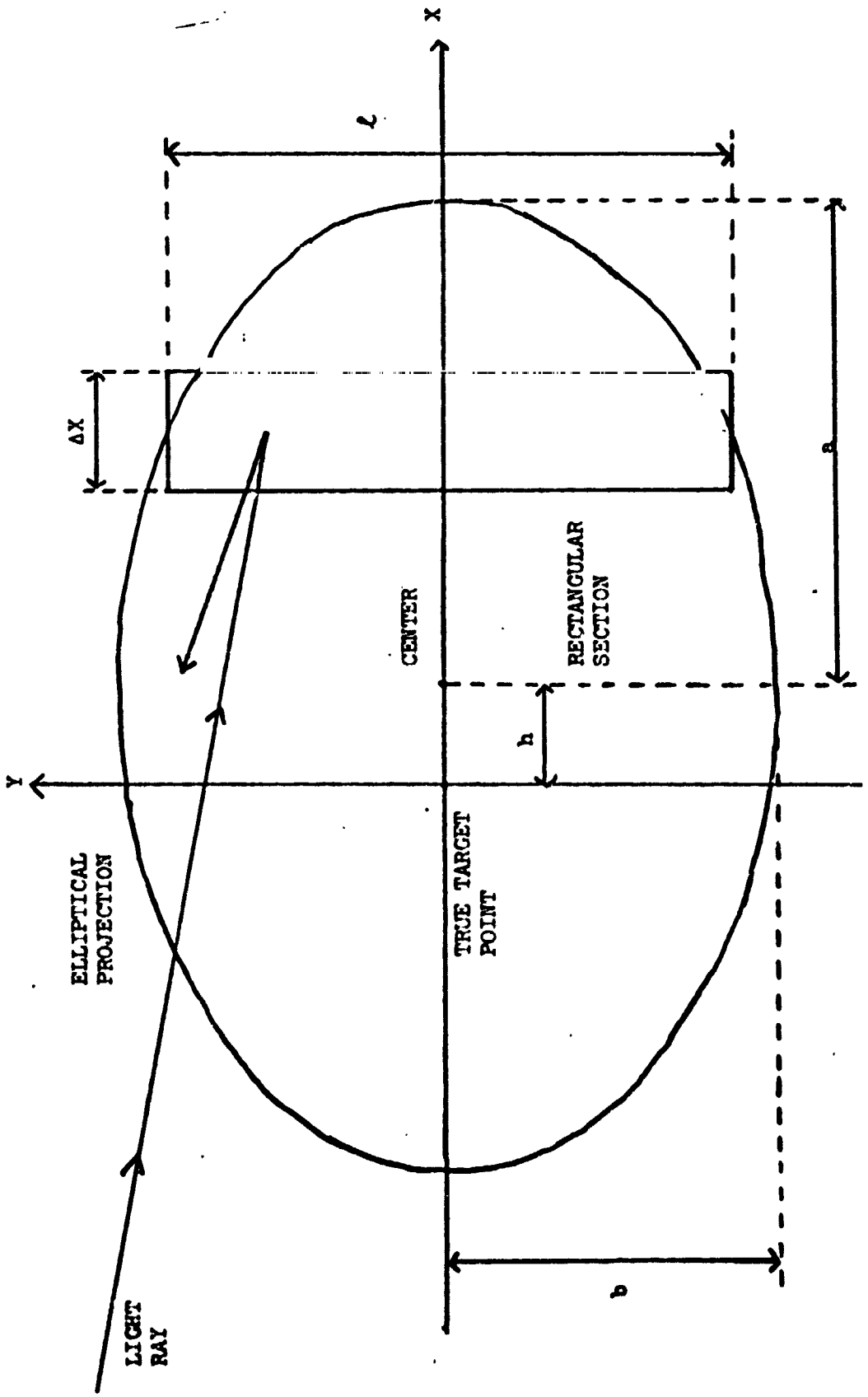

Fig. 81. Elliptical Projection

From equation 6:

$$\ell = 2y = 2b \left[1 - \frac{(x-h)^2}{a^2} \right]^{\frac{1}{2}} \qquad (8)$$

If Δx is made the same for every rectangle the integration over x can be included in the proportionality constant.

$I_t(x,y)$ is indirectly given by equation (3). $I(\theta)$ can easily be transformed from the polar system based on the circular beam to the rectangular system based on the elliptical spot.

The intensity of each rectangle can now be related to a distinct time of flight Δt. If each ΔI_R is evaluated and plotted against its respective Δt, the resulting curve will approximate the shape of the return pulse.

Figure 82 shows the return pulse shape for a range 30 meters and optimum aperture diameter of .78 cm. Equation 7 was used with Δx set at 1.5 mm giving about 100 rectangles.

Subtracting the time at which the leading edge of the pulse reaches 50% of the maximum from the peak time gives a time error of .209 nanosecond or an equivalent range error of 6.27 cm.

The optimal laser rangefinder parameters have been determined for the 30 meter range. As the studies under Tasks C and D proceed, alternative maximum ranges of interest may be identified and a re-optimization of parameters will be in order.

Task E. Chemical Analysis of Specimens

One important phase of the initial missions to Mars is the search for organic matter and living organisms on the martian surface. The present concept for attaining this objective consists of subjecting samples of the atmosphere and surface material to certain chemical and biochemical reactions and thereafter analyzing the products produced, probably in a combination gas chromatograph/mass spectrometer (GC/MS). The gas chromatograph is proposed for separating complex mixtures evolved from the experiments into small groups of similar chemical species. Chemical analysis of these groups would be accomplished in the mass spectrometer. It is the objective of this task to provide engineering techniques and design criteria for creating and improving such a system.

Most of the previous effort has involved the systems analysis of the gas chromatograph using simulation, Ref. 20, 21, and 22. This technique uses mathematical models, which incorporate fundamental parameters evaluated from reported experiments, to explore various concepts and to direct further experimental research. Application of prior work to characterize chromatograph performance and improve the mathematical model was considered during the past year. Task problems were attacked by a two-member team, each of whom pursued a specific assignment:

1. Chromatograph system characteristics
2. Chromatograph simulation development

Task E.1. Chromatograph System Characteristics - C. J. Rose
Faculty Advisor: Prof. P. K. Lashmet

It was the objective of this task to develop techniques for designing chromatograph systems using simulation models and concepts briefly considered previously, Ref. 23. As the purpose of the chromatograph is to separate chemical species, this initial effort involved a quantitative definition of the degree of separation attained in a chromatographic column of particular design, operating under specific conditions. A large value for this degree of separation implies a chromatogram having distinct peaks, whereas a low value suggests poor separation or overlapping peaks. The degree of separation is a function of the physical parameters of the chromatograph and the chemical characteristics of the materials being separated. On this basis, this task considered the following: developing a generalized simulation procedure; determining the effect of design parameters upon the degree of separation through simulation; and obtaining realistic characteristics of the sample injection pulse. Progress, detailed in a recent report, Ref. 24, is summarized below.

To evaluate the concept of separation, a computer procedure was developed to simulate the chromatograph. Simulation was accomplished by numerically convolving a previously developed model, Ref. 20 and 25, with typical sample injection pulses represented by data. The generalized simulation procedure treated a maximum of five components so practical mixtures could be considered, especially in the region of overlapping peaks. The simulation used actual sample sizes, carrier gas compositions, and real and dimensionless time so the results could be directly related to actually observed system operation.

In a chromatogram, the output signal is the sum of composition contributions of all components. Based on this concept, chromatograph performance, was defined as

$$S_i = A_i/A \qquad (1)$$

where

S_i = separation of component i for the peak where the component predominates.

A_i = contribution of component i to the area under the peak where the component predominates

A = total area under the peak of interest.

In these studies, the areas were computed from simulations over a finite peak width of four standard deviations ($4\sqrt{\mu_2}$ (2) where μ_2(2) was the second time moment about the mean) centered about the peak mean. Prior studies have shown that at least 94% of the chromatogram area lay within this region. S_i was the effective composition of component i in the peak where component i should appear. It ranged from unity for complete separation to zero for essentially no separation; i.e., the sample was small compared to amounts of other interfering chemicals. Thus each component was assigned a value of S indicative of its separation from the other components.

For excellent separation, a high value of S, perhaps 0.85 or higher, would be expected.

This index of performance required analysis of system simulations. To develop preliminary estimates of S prior to such simulations, the approximation of the output pulses by Gaussian curves was investigated. Since Gaussian-type curves are defined by the first and second time moments which are known from the characteristics of the input pulse and the chromatograph differential equations, Ref. 25 and 26, the separation S can be rapidly estimated from design parameters without a simulation.

For a binary system, assuming superposition of the individual chromatograms, the separation of component I became

$$S_I = \frac{A_I}{A_I + A_{II}}$$

where the chromatogram areas A_I and A_{II} were obtained by simulation. The time interval for determining the areas was

$$\theta_I \pm 2\sqrt{\mu_I(2)}$$

where θ_I was the mean or first time-moment about the origin for the chromatogram of component I and $\mu_I(2)$ was the variance or second time-moment about the mean θ_I. Rearrangement of the separation equation gave

$$A_I/A_{II} = S_I/(1 - S_I)$$

or as an approximation

$$A_I/A_{II} \quad (\text{Gaussian Area}_I/\text{Gaussian Area}_{II})(N_I/N_{II}) \qquad (2)$$

where N_I and N_{II} were the total amounts of components I and II respectively.

For a given binary system under consideration, the first and second moments for the chromatograms for both components were determined as a function of the physical parameters from the system equations, Ref. 25. As shown in Figure 83, the Gaussian area for component I became

$$\int_{\bar{\theta}_I - \lambda_I\sqrt{\mu_I(2)}}^{\bar{\theta}_I + \lambda_I\sqrt{\mu_I(2)}} \bar{y}(\theta)\, d\theta$$

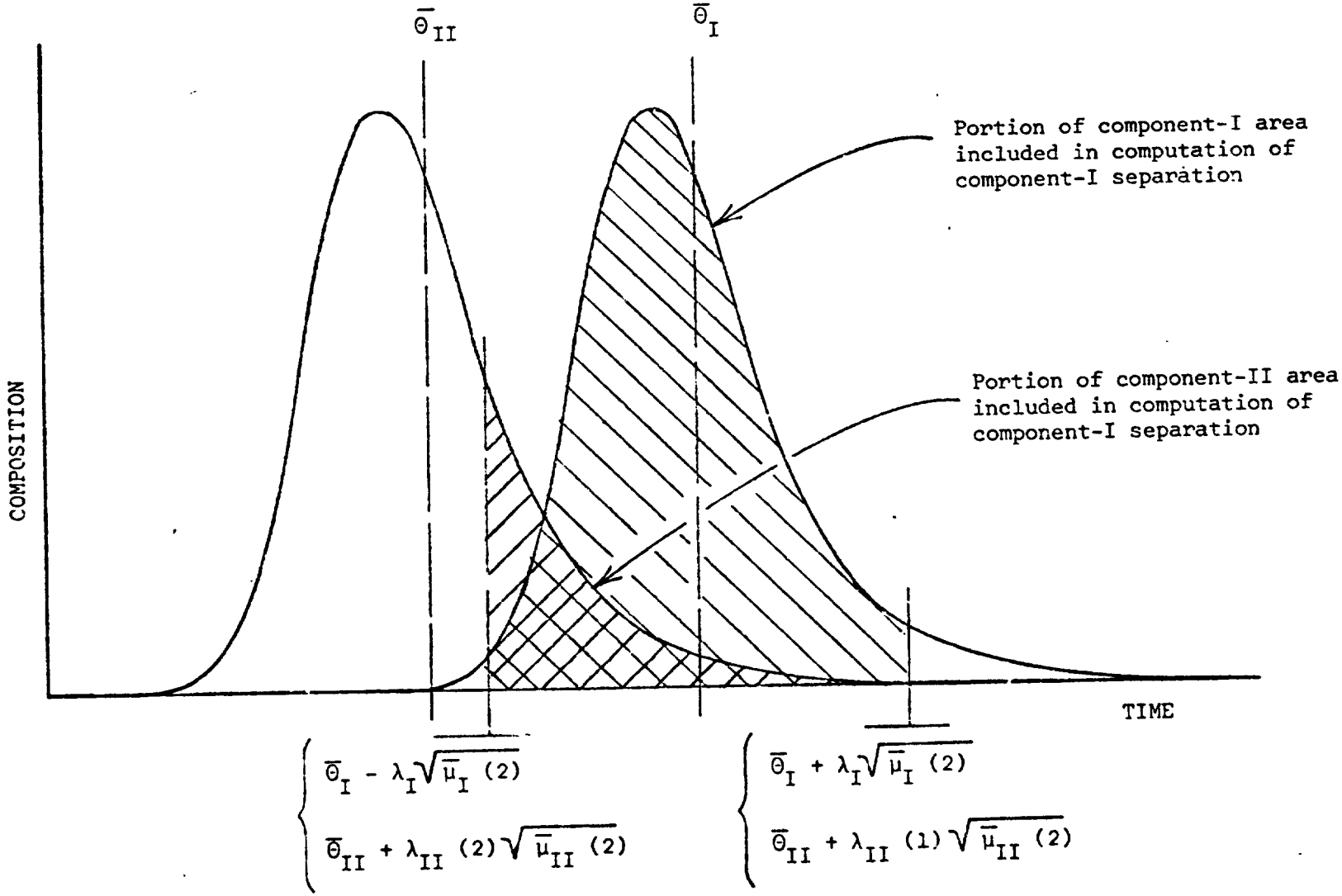

Fig. 83. Concept of separation for component I in bi... system.

where

θ = dimensionless time = vt/L

L = column length

t = time

v = interstitial gas velocity

and $\bar{y}_I(\theta)$ was a normal distribution function having mean $\bar{\theta}_I$ and variance $\bar{u}_I(2)$. For $\lambda_I = 2$, the area was 0.9545. As shown in Fig. 83, the Gaussian area for component II included within the above integration interval was

$$\text{Gaussian Area}_{II} = \int_{\theta_I - \lambda_I \sqrt{\bar{\mu}_I(2)}}^{\bar{\theta}_I + \lambda_I \sqrt{\bar{\mu}_I(2)}} \bar{y}_{II}(\theta)\, d\,\theta$$

$$= \int_{\bar{\theta}_{II} + \lambda_{II}(2)\sqrt{\bar{\mu}_{II}(2)}}^{\bar{\theta}_{II} + \lambda_{II}(1)\sqrt{\bar{\mu}_{II}(2)}} \bar{y}_{II}(\theta)\, d\,\theta$$

where $\bar{y}_{II}(\theta)$ was a normal distribution function having mean $\bar{\theta}_{II}$ and variance $\bar{\mu}_{II}(2)$. The time corresponding to λ_I of component I was associated with a $\lambda_{II}(1)$ of component II. Similarly $-\lambda_I$ was associated with a $\lambda_{II}(2)$. For the situation of Fig.83, the governing relations were

$$\lambda_{II}(1) = \left[\bar{\theta}_I - \bar{\theta}_{II} + \lambda_I \sqrt{\bar{\mu}_I(2)} \right] / \sqrt{\bar{\mu}_{II}(2)}$$

$$\lambda_{II}(2) = \left[\bar{\theta}_I - \bar{\theta}_{II} - \lambda_I \sqrt{\bar{\mu}_I(2)} \right] / \sqrt{\bar{\mu}_{II}(2)}$$

Figure 84 has compared the approximate method of computing separation, Eq. 2, with the exact method, Eqn. 1. Simulations reported earlier, Ref. 23, were the basis of this comparison. Use of Gaussian-type outputs yielded a first-order approximation to the separation, although on the average the predictions were optimistic. However, it is a valuable preliminary design tool.

To relate more clearly this research to the Mars mission, information was compiled on physical characteristics of proposed systems and possible

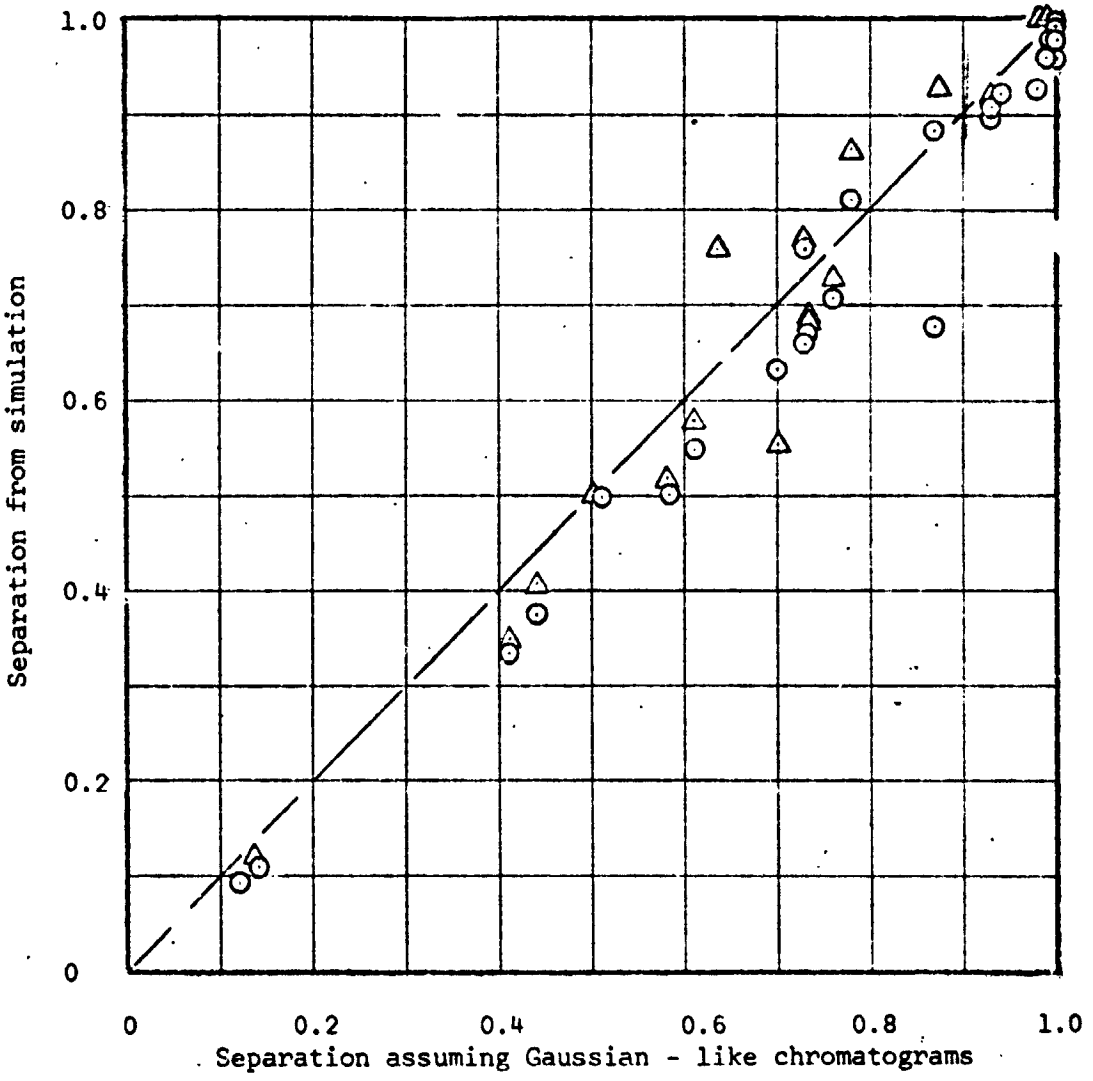

Fig. 84. Comparison of separation functions for binary system derived from simulation and Gaussian - like chromatograms.

O - separation for first - appearing component
Δ - separation for second - appearing component

chemicals postulated for separation. Research performed at Jet Propulsion Laboratory provided a guide on chemicals which might be expected. The chromatogram for a 24-component test mixture using a Chromosorb-W column coated with 5% Dexsil, Ref. 27, has been reproduced in Fig. 85. Estimates of the thermodynamic parameter mR_0 for the components have been summarized in Table 7. These provide a practical range of values of the parameter for future system studies.

Descriptions of physical systems have appeared in several reports, Ref. 28, 29, 30, 31. For these representative systems, the Peclet numbers, or dispersion parameters, were estimated using a parameter estimating program developed earlier, Ref. 21. As summarized in Table 7, Peclet numbers encountered in practical chromatographs range from several hundred for minicolumns to 30,000 for very long columns.

Previous studies, Ref. 23, have shown that the sharpness of the sample input pulse often determines whether or not separation between two similar substances will occur. To determine realistic characteristics of input pulses, experiments were conducted on the test facility, Ref. 32, to obtain the effect of sample size, carrier gas flow rate, and other parameters upon the input pulses. Samples of gaseous ethylene were injected into a composition detector using a minivalve, shown schematically in Fig. 86. Typical ethylene pulses obtained for three helium carrier gas flowrates are shown in Fig. 87. Moment analysis of pulses from sixteen experiments have been summarized in Figures 88 and 89. The peak mean and standard deviation have been reported as dimensionless ordinates through use of τ, the time ethylene remained in the sample loop during the injection process. The abscissa is the ratio of sample size to carrier gas flow rate. The ratio of carrier gas pressure to sample loop pressure has been shown parametrically. These curves summarize approximate effects of design parameters on the input pulse characteristics and provide a means of assessing the effect of a design upon the separation occurring within the chromatograph.

Task E.2. Chromatograph Simulation Development - M.P. Feinberg
Faculty Advisor: Prof. P. K. Lashmet

It was the objective of this task to develop and evaluate a practical, nonlinear adsorption model to account for composition-dependent effects observed in previous research, Ref. 33 and 34. A system of three coupled partial differential equations was derived earlier to describe these effects, Ref. 35. Excessive computation time due to the complexity of the system of equations, Ref. 35 and 36, indicated a simplification of the model was required. Voytus, Ref.25, derived a simplified model which considered axial interparticle diffusion, convection, and equilibrium adsorption/desorption using a linear isotherm. Assumptions for this model, designated as the equilibrium adsorption model, included negligible mass transport effects between the carrier gas and the adsorbent and no intraparticle diffusion effects. The resulting partial differential equation was solved analytically using a convolution integral, Ref. 20. Although the model simulated many systems well, in a few instances model predictions deviated consistently from actual data. The variation of the thermodynamic parameter mR_0 in such systems with composition supported the idea that a nonlinear, composition-dependent isotherm should be considered. Preliminary work on solving the resulting nonlinear equations begun earlier, Ref. 37, was continued. Activities,

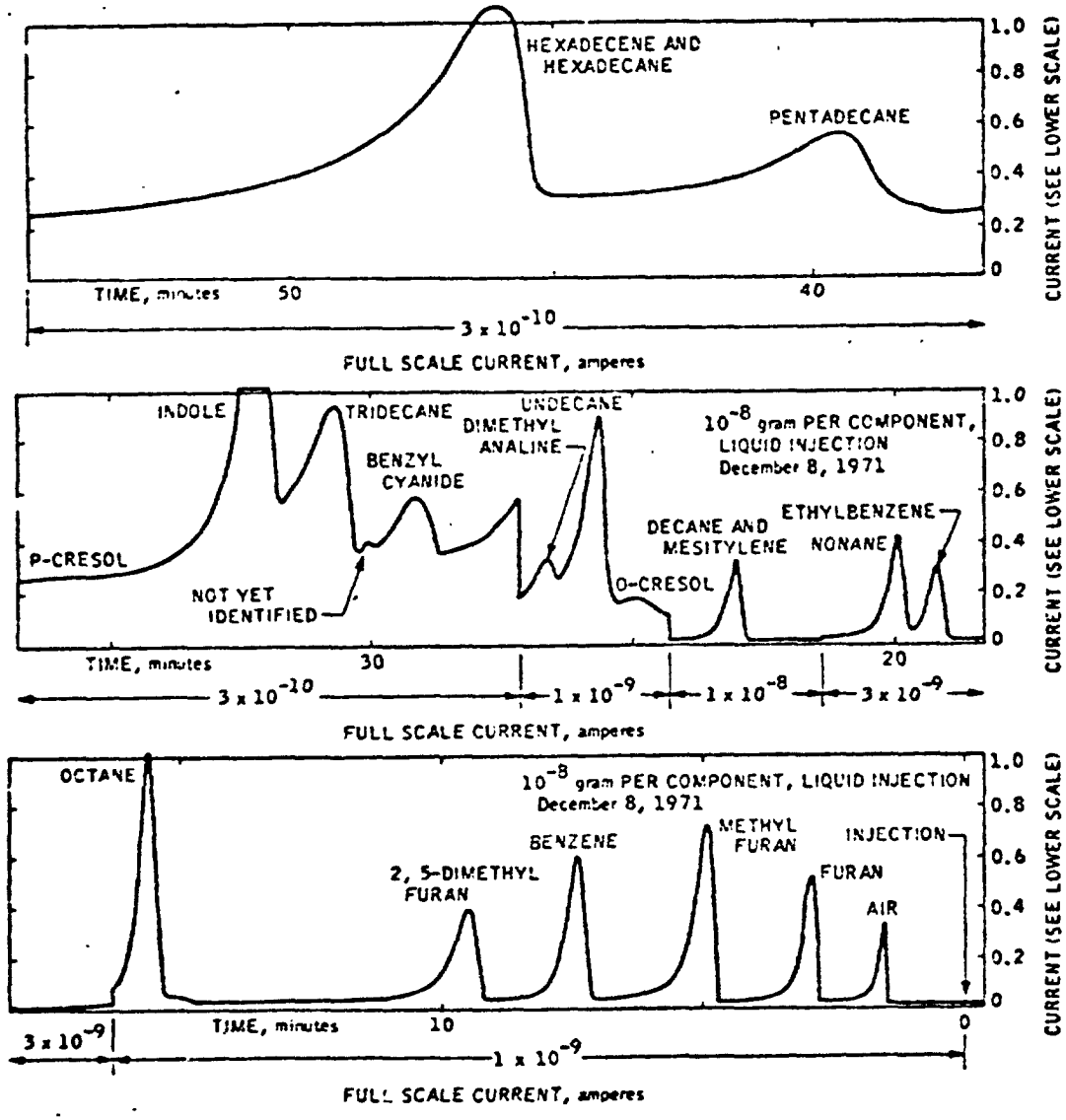

Fig. 85. Chromatogram for 24-component test mixture.

Table 7. Range of Parameters for Typical Chromatographic Systems

RANGE OF THE THERMODYNAMIC PARAMETER mRo
(JPL Multicomponent Test Mixture)

Compound	Breadboard Time (min)	Dimensionless Time	mRo
Air	1.45	2.58	0.632
Furan	2.92	5.19	0.238
Methyl Furan	4.93	8.77	0.1286
Benzene	7.41	13.19	0.0820
2,5-Dimethyl Furan	9.53	16.96	0.0626
Octane	15.67	27.90	0.0372
Ethylbenzene	19.25	34.27	0.0301
Nonane	19.98	35.57	0.0289
Decane & Mesitylene	23.40	41.66	0.0246
o-Cresol	25.00	44.51	0.0230
Undecane	25.68	45.72	0.0224
Dimethylanaline	26.70	47.54	0.0215
Benzyl Cyanide	29.17	51.93	0.0196
Tridecane	30.7	54 66	0.0186
Indole	32.30	57.51	0.0177
p-Cresol	35.00	62.32	0.0163
Pentadecane	39.50	70.33	0.0144
Hexadecene	46.00	81.90	0.0124

RANGE OF THE DISPERSION PARAMETER Pe

Column Dimensions	Carrier Gas	Peclet Number Range
0.25mm dia. x 0.025m long	helium, 0.5ml/min	146 - 164
6.3mm dia. x 2.0m long	helium, 60ml/min	3560 - 4910
0.76mm dia. x 6.1m long	helium, 2ml/min	16000 - 30000
2.5mm dia. x 4.9m long	helium, 40ml/min	6400 - 15000

CARLE MINI-VALVE OPERATION

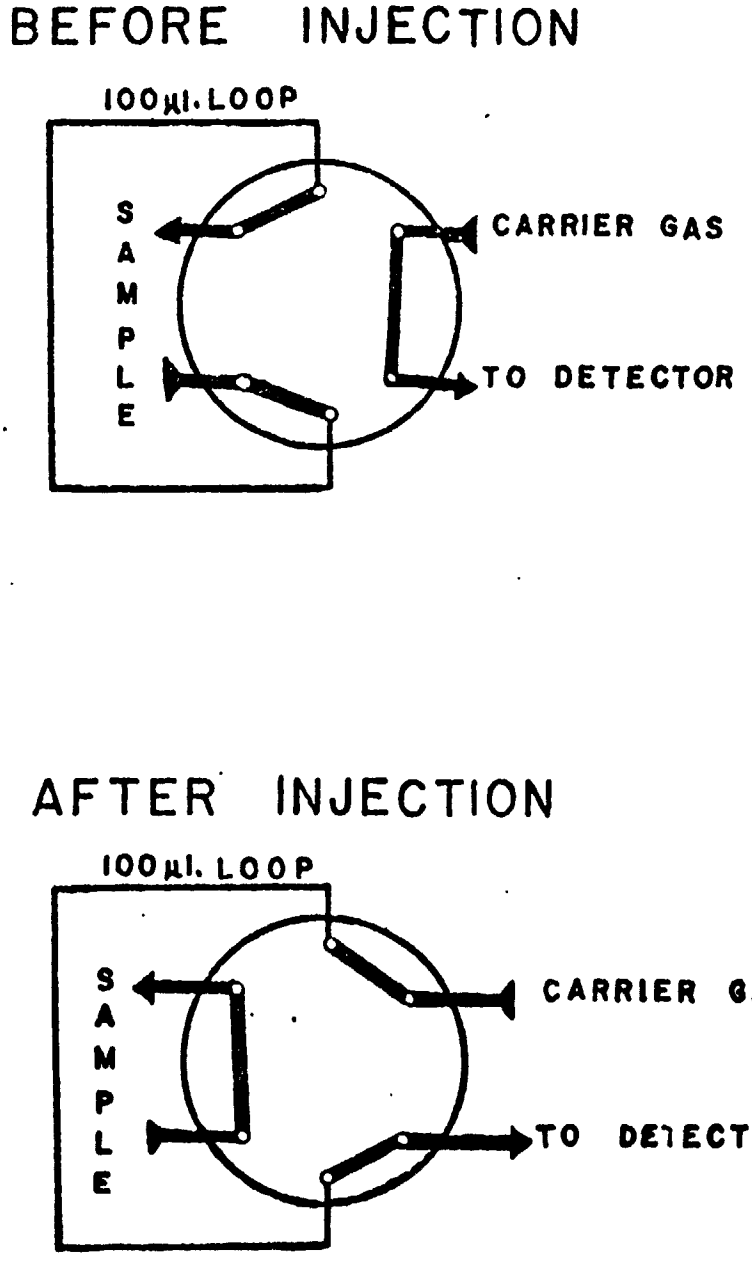

Fig. 86. Concept of minivalve for injecting gas samples,

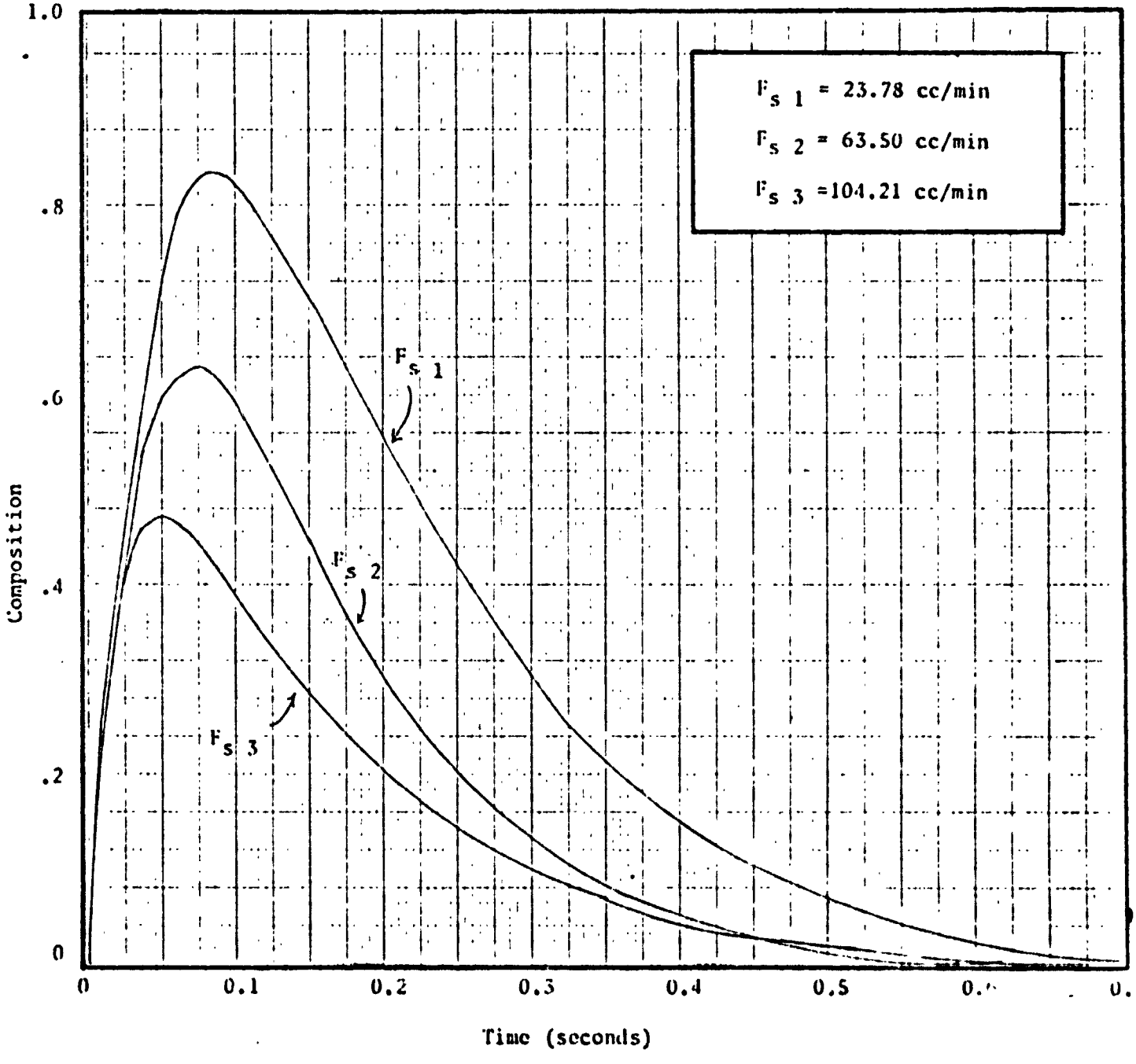

Figure 87. Input Pulses of Ethylene Gas for Various Flowrates

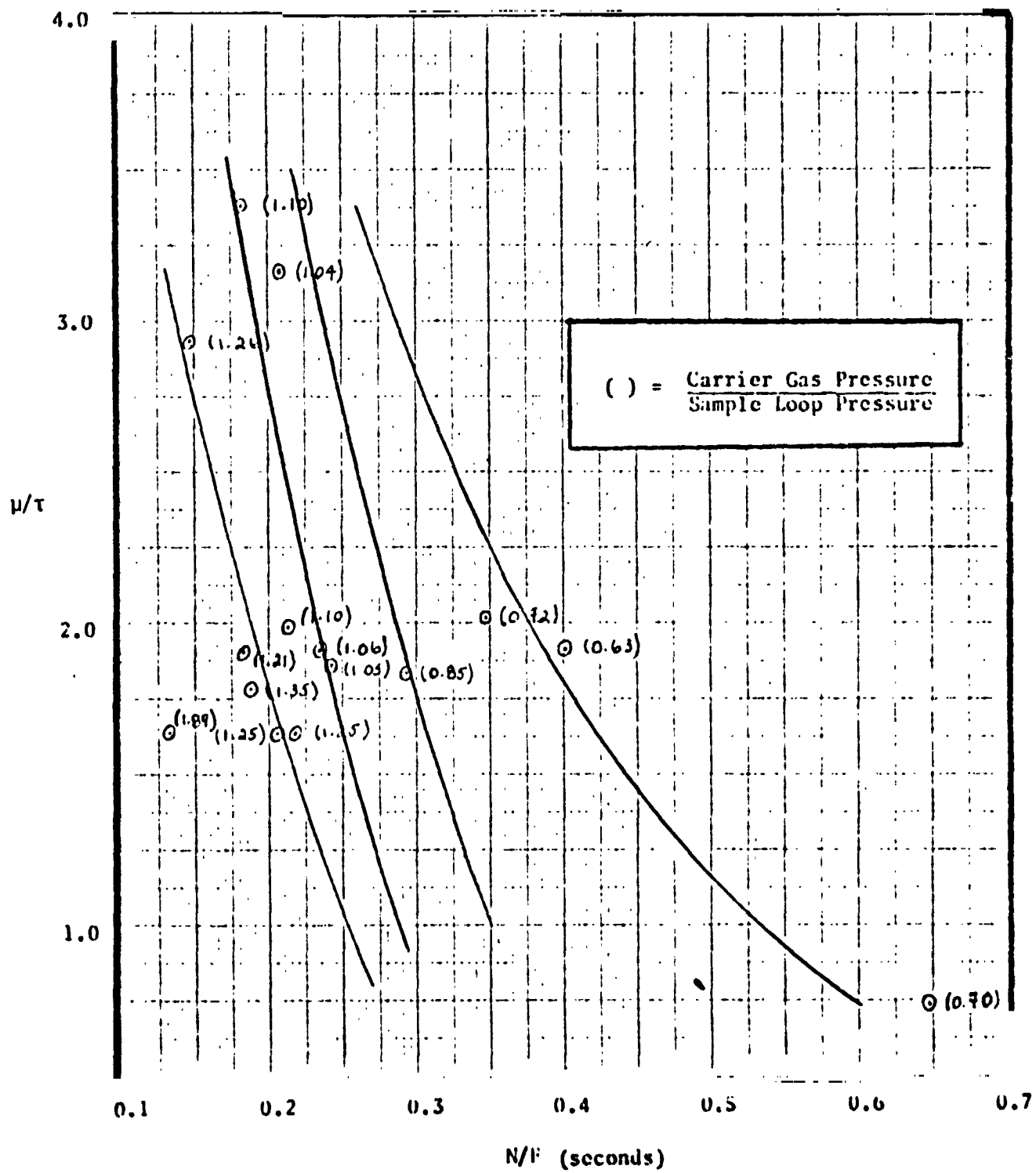

Figure 88. Effect of Sample Size and Carrier Gas Flowrate on the Mean of the Input Pulse for Ethylene Gas

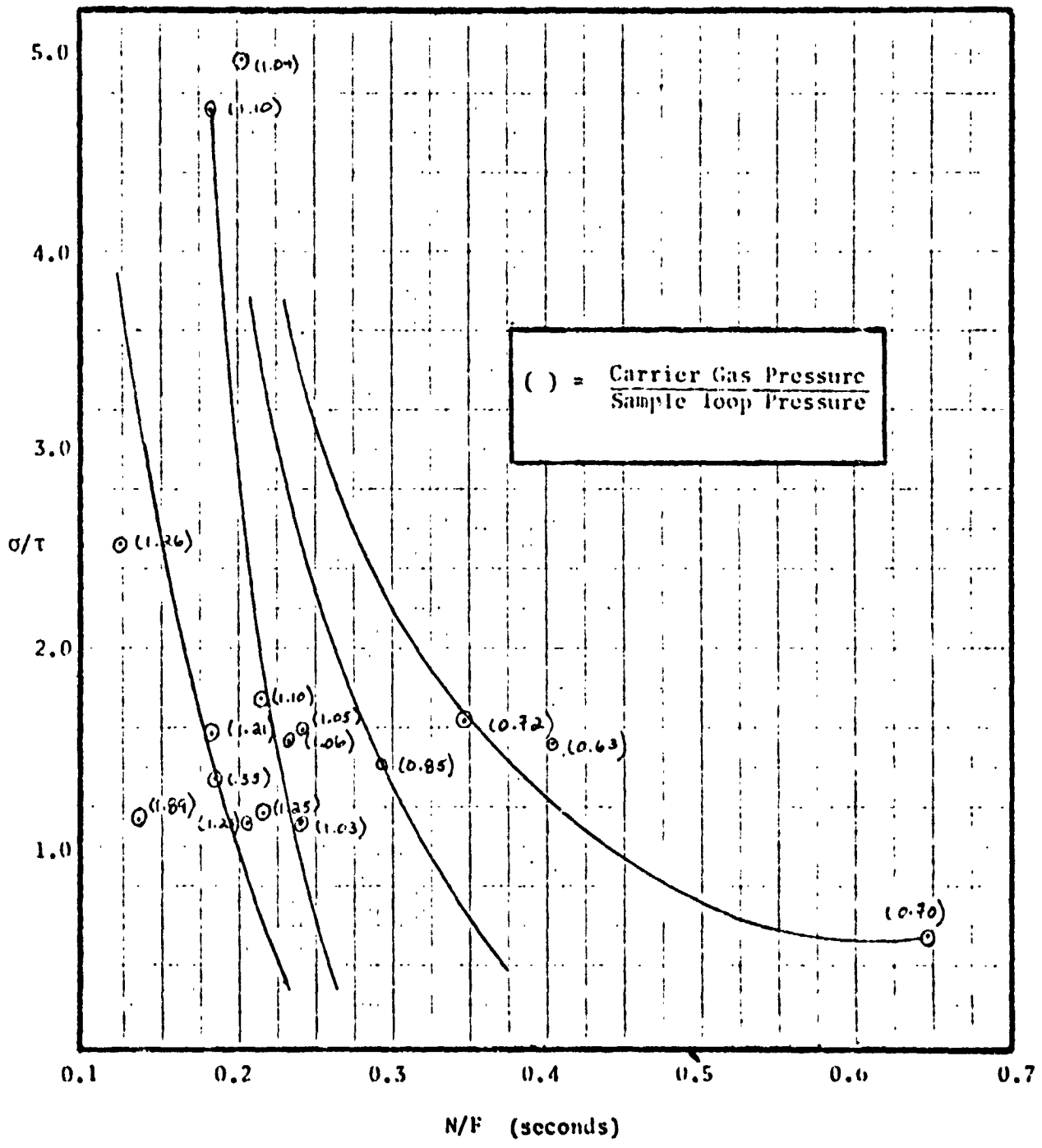

Figure 89. Effect of Sample Size and Carrier Gas Flowrate on the Standard Deviation of the Input Pulse for Ethylene Gas

detailed in a recent report, Ref. 37, have been summarized below.

Two versions of the equilibrium adsorption model were investigated. The first version, Eqn. 1 of Fig. 90 incorporating a linear isotherm, has been solved analytically, Ref. 20, 21. The second version, Eqn. 2 of Fig. 90, incorporated the Langmuir isotherm into the model as a means for accounting for the observed composition-dependent effects. Analytical techniques were not available for solving the resulting nonlinear equation, so numerical methods were used. Because of instability problems with an orthogonal collocation procedure used previously, Ref. 34, the simple, finite difference scheme of Crank-Nicolsen was used. To obtain experience with the method, it was first applied to the linear version, Eqn. (1), since an analytical solution was available for comparison. The Crank-Nicolsen method replaced partial derivatives by finite differences, Fig. 91, which can be viewed as double averages of the compositions about the point of interest: position, (i); time, (N + 1/2). These finite difference expressions were substituted into the partial differential equation, giving a system of algebraic equations having a tridiagonal system matrix which was solved by the Thomas algorithm, Ref. 28. Considerable effort was made in the coding to eliminate calculations involving multiplication by zero in order to reduce computation time. This additional coding reduced the computing effort by about 35%. Good comparison between the numerical and analytical results gave confidence in the method.

To apply the method to the nonlinear version, Eqn. (2), a modification was required because of the nonlinear coefficient of the time derivative. A predictor-corrector technique was used. Initially the partial derivatives were replaced by finite differences as in the linear version. The composition-dependent coefficient of the time derivative was treated by a method developed by Douglas, Ref. 29. As shown in Fig. 92, $y_{i,n+1/2}$ is approximated by its value at the previous time step, $y_{i,n}$ and a correction factor $(T/2)(\partial y/\partial T)_{i,n}$ where T is time. This derivative was approximated by its value from the partial differential equation in which the derivatives and compositions were evaluated at the previous time step. This approximation for the nonlinear term was substituted into the differential equation, Eqn. 2, and the resulting system of algebraic equations was solved by the Thomas algorithm. A new estimate for the nonlinear term was then made by averaging the compositions

$$y_{i,n+1/2} = (y_{i,n} + y_{i,n+1})/2$$

This result was substituted into the partial differential equations, and the procedure was continued until convergence was obtained. The technique provided a workable means for numerically solving Eqn. 2 and evaluating it as a chromatograph model.

The effect of changing adsorption parameters in this simulation model have been shown in Fig. 93 for three cases, each having the same peak time. The chromatogram for the simple, linear adsorption model ($K = 0$) was sharp and exhibited little spreading. As K increased, the leading edge remained sharp while the trailing edge tailed. This type of spreading was typical of data not represented well by simple linear model. It was noted that the Langmuir constant K affected the peak time, so the thermodynamic parameter mR_0 was reduced as K was increased to maintain a constant peak time.

I. Material balance for equilibrium adsorption model

$$\frac{\partial y}{\partial \theta} + \left(\frac{1}{R_o}\right)\frac{\partial x}{\partial \theta} = \left(\frac{1}{Pe}\right)\frac{\partial^2 y}{\partial z^2} - \frac{\partial y}{\partial z}$$

- $\frac{\partial y}{\partial \theta}$ — fluid-phase accumulation
- $\left(\frac{1}{R_o}\right)\frac{\partial x}{\partial \theta}$ — adsorbent accumulation
- $\left(\frac{1}{Pe}\right)\frac{\partial^2 y}{\partial z^2}$ — axial dispersion
- $\frac{\partial y}{\partial z}$ — bulk flow

II. Adsorption isotherm

a. Linear: $x = y/m$

b. $x = \dfrac{(y/m)}{1 + (y/m)}$

III. System equation

a. Linear:
$$\frac{\partial y}{\partial \theta}\left[1 + (1/mR_o)\right] = \left(\frac{1}{Pe}\right)\frac{\partial^2 y}{\partial z^2} - \frac{\partial y}{\partial z} \qquad (1)$$

b. Langmuir:
$$\frac{\partial y}{\partial \theta}\left[1 + \frac{(1/mR_o)}{\left[1 + (y/m)\right]^2}\right] = \left(\frac{1}{Pe}\right)\frac{\partial^2 y}{\partial z^2} - \frac{\partial y}{\partial z} \qquad (2)$$

IV. Nomenclature

- L = column length
- m = adsorption constant = $1/K$
- Pe = Peclet numbers
- R_o = Adsorbent capacity - related constant
- t = time
- v = interstitial gas velocity
- x = concentration on adsorbent
- y = concentration in gas phase
- z = fraction of distance down column
- θ = dimensionless time = $v\,t/L$

Fig. 90. Equations for equilibrium adsorption model

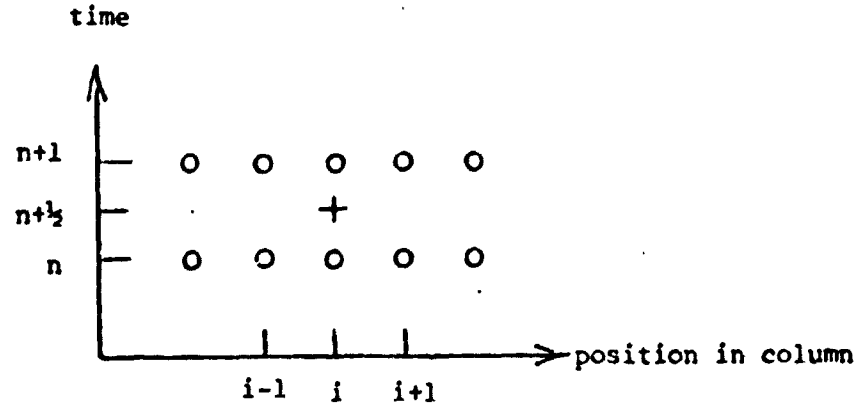

$$\left(\frac{\partial Y}{\partial Z}\right)_{i,n+\frac{1}{2}} \approx \frac{1}{2}\left[\frac{Y_{i+1,n+1} - Y_{i-1,n+1}}{2(\Delta Z)} + \frac{Y_{i+1,n} - Y_{i-1,n}}{2(\Delta Z)}\right]$$

$$\left(\frac{\partial^2 Y}{\partial Z^2}\right)_{i,n+\frac{1}{2}} \approx \frac{1}{2}\left[\frac{Y_{i+1,n+1} - 2Y_{i,n+1} + Y_{i-1,n+1}}{(\Delta Z)^2} + \frac{Y_{i+1,n} - 2Y_{i,n} + Y_{i-1,n}}{(\Delta Z)^2}\right]$$

$$\left(\frac{\partial Y}{\partial Y}\right)_{i,n+\frac{1}{2}} \approx \frac{Y_{i,n+1} - Y_{i,n}}{(\Delta T)}$$

Fig. 91. Crank-Nicolsen algorithm for linear version of model.

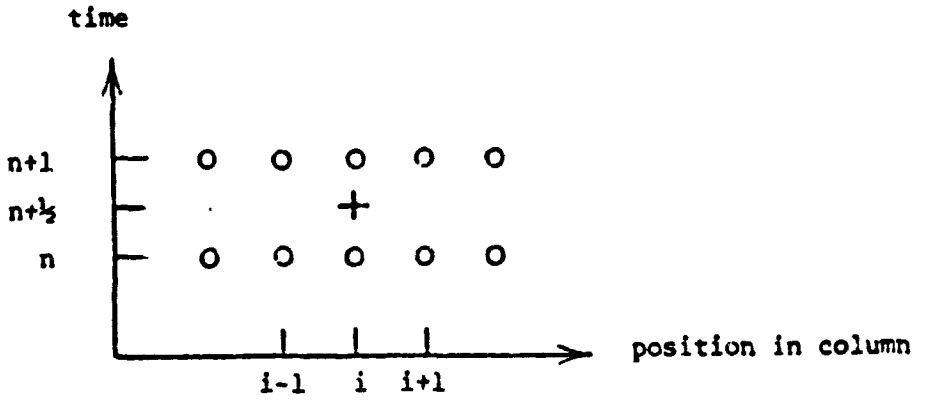

$$\left(\frac{\partial Y}{\partial Z}\right)_{i,n+\frac{1}{2}} \approx \frac{1}{2}\left[\frac{Y_{i+1,n+1}-Y_{i-1,n+1}}{2(\Delta Z)} + \frac{Y_{i+1,n}-Y_{i-1,n}}{2(\Delta Z)}\right]$$

$$\left(\frac{\partial^2 Y}{\partial Z^2}\right)_{i,n+\frac{1}{2}} \approx \frac{1}{2}\left[\frac{Y_{i+1,n+1}-2Y_{i,n+1}+Y_{i-1,n+1}}{(\Delta Z)^2} + \frac{Y_{i+1,n}-2Y_{i,n}+Y_{i-1,n}}{(\Delta Z)^2}\right]$$

$$\left(\frac{\partial Y}{\partial T}\right)_{i,n+\frac{1}{2}} \approx \frac{Y_{i,n+1}-Y_{i,n}}{(\Delta T)}$$

$$Y_{i,n+\frac{1}{2}} = Y_{i,n} + \frac{\Delta T}{2}\left(\frac{\partial Y}{\partial T}\right)_{i,n} \quad \text{for evaluating nonlinear function}$$

where

$$\left(\frac{\partial Y}{\partial T}\right)_{i,n} = \frac{1}{1+\dfrac{1}{mR_0(1+KY_{i,n})^2}}\left[\frac{1}{Pe}\left(\frac{\partial^2 Y}{\partial Z^2}\right)_{i,n} - \left(\frac{\partial Y}{\partial Z}\right)_{i,n}\right]$$

$$\left(\frac{\partial^2 Y}{\partial Z^2}\right)_{i,n} = \frac{Y_{i+1,n}-2Y_{i,}+Y_{i-1}}{(\Delta Z)^2} \quad ; \quad \left(\frac{\partial Y}{\partial Z}\right)_{i,n} = \frac{Y_{i+1,n}-Y_{i-1,n}}{2(\Delta Z)}$$

Fig. 92. Crank-Nicolsen algorithm for nonlinear version of the model.

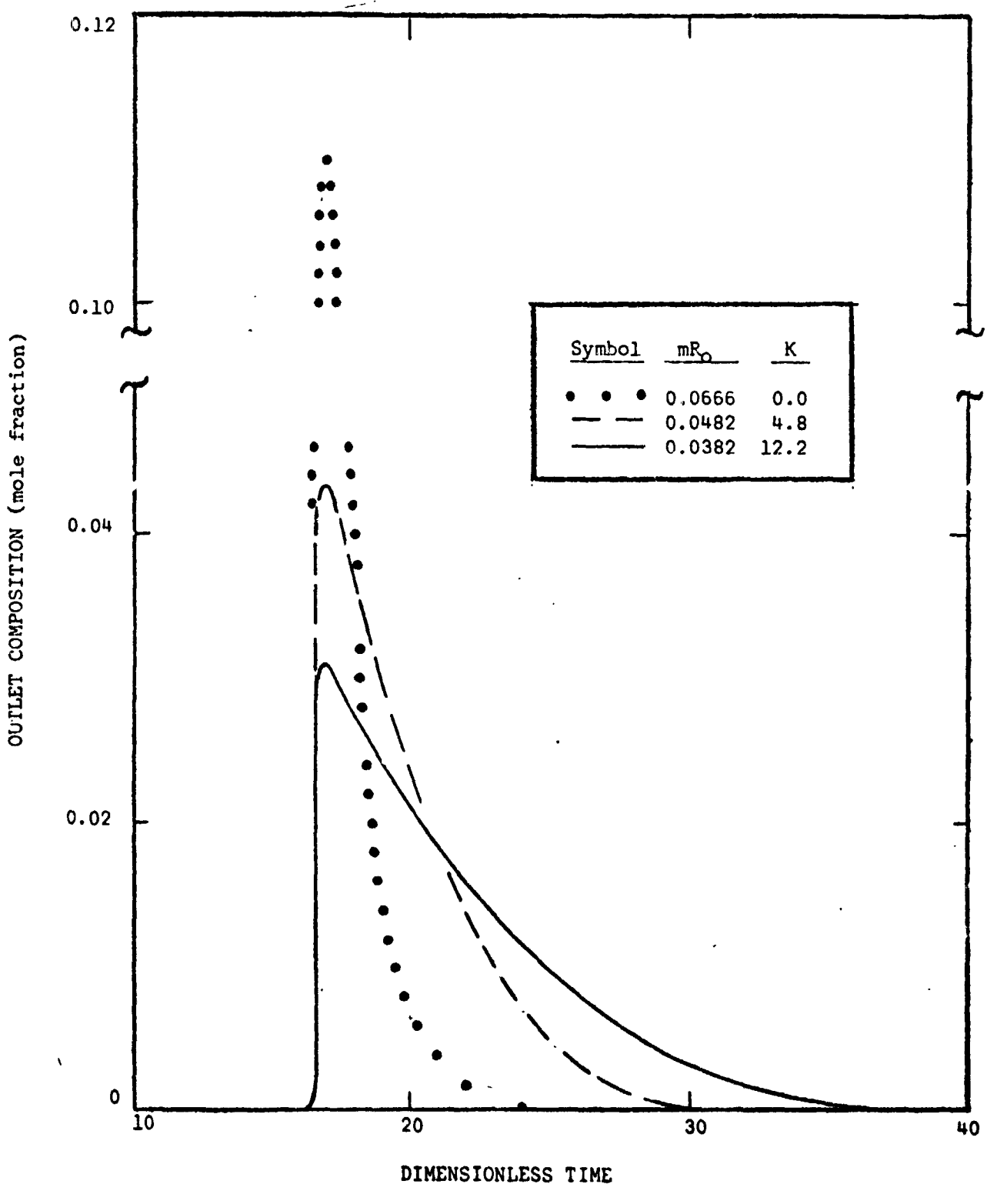

Figure 93. Effect of Adsorption Parameters Upon Chromatogram

The chromatograms of Fig. 93 were prepared to simulate data for n-heptane on Chromosorb C-102 obtained earlier, Ref. 34. To fit these data, a secant procedure adjusted the values of K to provide the observed peak time for an assumed mR_0. If predicted and observed gas compositions at the peak time differed, a new value of mR_0 was selected, and the procedure was repeated. Table 8 has summarized results for several simulations of the n-heptane data. Good representation of the data was obtained for valuesof 0.0426 and 8.6 for mR_0 and K respectively. Since the nonlinear model also reduced to the linear model for dilute solutions, it was concluded that it offered promise as a general simulation tool for the chemical systems encountered in this study.

The Crank-Nicolsen procedure, while providing good numerical solutions to the nonlinear model, was computationally inefficient. Depending upon the chromatographic system studies, between 25 and 60 minutes of IBM 360/67 computer time were required to fit a set of experimental data. Such computational efforts were excessive for practical application of the model, so future work will concern the development of a more efficient numerical procedure.

TABLE 8

COMPARISON OF THE SIMULATION PEAK HEIGHTS FOR VARIOUS MRO'S WITH THE ACTUAL PEAK HEIGHT (N-HEPTANE ON CHROMOSORB-102 AT 200°C)

Thermodynamic Parameter, mRo	Langmuir Constant, K	Peak Height (mole fraction)
0.0382	12.2	0.0308
0.0426	8.6	0.0333
0.0482	4.8	0.0430
ACTUAL DATA	—	0.0353

REFERENCES

1. Boheim, S.L. and Purdon, W.C., "Path Selection System Simulation and Evaluation for a Martian Roving Vehicle," RPI Technical Report MP-29, Rensselaer Polytechnic Institute, Troy, New York, December 1972.

2. Campbell, R.S. and Simonds, R.R., "Path Selection System Development and Evaluation for a Martian Roving Vehicle," RPI Technical Report MP-42, Rensselaer Polytechnic Institute, Troy, New York, May 1974.

3. Sharp, D.S. and Campbell, R.S., "Path Selection System Simulation and Evaluation for a Martian Roving Vehicle," to be issued as a RPI Technical Report, Rensselaer Polytechnic Institute, Troy, New York, June, 1975.

4. Sharp, D.S., "Development and Evaluation of a Three-Beam Mid-Range Path Selection System," RPI Master's Project Report, Rensselaer Polytechnic Institute, Troy, New York, May, 1975.

5. Matthews, D.W., "Development and Evaluation of a Short-Range Path Selection System with Forward and Back-Up Mode Memory," RPI Master's Project Report, Rensselaer Polytechnic Institute, Troy, New York, June 1975.

6. Analysis of Design of a Capsule Landing System and Surface Vehicle Control System for Mars Exploration, RPI Technical Report MP-36, Rensselaer Polytechnic Institute, Troy, New York, 1973-1974.

7. Sonalkar, R.V., "Rapid Estimation of States Subject to Unknown Inputs," Ph.D. Thesis, Rensselaer Polytechnic Institute, June 1975.

8. Sonalkar, R.V. and Shen, C.N.,"Mars Obstacle Detection by Rapid Estimation Scheme from Noisy Laser Rangefinder Reading," Milwaukee Symposium on Automatic Computation and Control, Milwaukee, Wisc., April 1975.

9. Sanyal, P., and Shen, C.N., "Bayes Decision Rule for Rapid Detection and Adaptive Estimation Scheme with Space Applications," IEEE Transaction on Automatic Control, Vol. AC-19, No. 3, June 1974, pp 228-231. Short version of the paper presented at JACC, 1973, Columbus, Ohio.

10. Sonalkar, R.V., and Shen, C.N., "Rapid Estimation and Detection Scheme for Unknown Descretized Rectangular Inputs," Proceedings of JACC, June 1974, Austin, Texas. To be published in IEEE Transactions on Automatic Control, Vol. 20, No. 1, Feb. 1975.

11. Sage, A.P. and Melsa, J., "Estimation Theory with Applications to Communication and Control," McGraw Hill, New York, 1971.

12. Reed, M., Sanyal, P. and Shen, C.N., "A Practical Obstacle Detection System for the Mars Rover," Proceedings of Milwaukee, Wisconsin, March 1974, pp. 317-322.

13. Papoulis, A., Probability, Random Variables, and Stochastic Processes, McGraw-Hill Book Co., Inc., 1965.

14. Neuberger, A., "Characterization of Pictures by Essential Contours," M.S. Thesis, M.I.T., 1966.

15. Shen, C.N. and Burger, P., "Stochastic Estimates of Gradient from Laser Measurements for an Autonomous Martian Roving Vehicle," Proceedings of the Third IFAC Symposium, The Hague/Delft The Netherlands, June 1973.

16. D'Angelo, K.R. and Shen, C.N., "Parameter Estimation for Terrain Modeling from Gradient Data," Proceedings of the Seventh Hawaii International Conference on System Sciences, Honolulu, Hawaii, January 1974.

17. Reed, M., Sanyal, P., and Shen, C.N., "A Practical Obstacle Detection System for the Mars Rover," Proceedings of the Milwaukee Symposium on Automatic Control, March 1974, pp. 317-322.

18. Morgan, J., Introduction to Geometrical and Physical Optics, New York: McGraw-Hill, 1953, pp. 251-55.

19. Beiser, L., "Laser Scanning Systems," in LASER APPLICATIONS, (M. Ross ed.), New York: Academic Press, 1974, Vol. II, pp. 56.

20. Benoit, G.L., "Reduction of Chromatographic Data and Evaluation of a G.C. Model," RPI Technical Report MP-22, Rensselaer Polytechnic Institute, Troy, New York, June 1971.

21. Keba, P.S., and Woodrow, P.T., "A Comparison of Two Gas Chromatograph Models and Analysis of Binary Data," RPI Technical Report MP-27. Rensselaer Polytechnic Institute, Troy, New York, July 1972.

22. Benoit, G.L., Lashmet, P.K., and Woodrow, P.T., "Evaluation of a Gas Chromatograph Model," 168th National Meeting, American Chemical Society, Atlantic City, New Jersey, September 1974.

23. Stovall, A.N., "Chromatographic Systems Analysis: Design Parameter Evaluation," M. Eng. Project Report, Rensselaer Polytechnic Institute, Troy, New York, May 1974.

24. Rose, C.J., "Chromatograph System Characteristics," M. Eng. Project Report, Rensselaer Polytechnic Institute, Troy, New York,May 1975.

25. Voytus, W.A., "Chromatographic Systems Analysis: Moment Analysis of the Equilibrium Adsorption Model," RPI Technical Report MP-9, Rensselaer Polytechnic Institute, Troy, New York, August 1969.

26. Woodrow, P.T., "Preliminary Numerical Analysis of Improved Gas Chromatograph Model," RPI Technical Report MP-36, Rensselaer Polytechnic Institute, Troy, New York, September 1973.

27. Conley, J.M., "Breadboard Test Report: 24 Component Liquid Injections of 7 and 8 December 1971," Interoffice Memorandum 8227-JC-71-081, Jet Propulsion Lab., Calif. Inst. Tech., Pasadena, December 20, 1971.

28. Silva, T.F., "Chromatographic Systems Analysis: First-Order Model Evaluation," RPI Technical Report MP-1, Rensselaer Polytechnic Institute, Troy, New York, September 1968.

29. Wilhite, W.F., "A Micro Gas Chromatograph for Descent Analysis of the Martian Atmosphere," JPL Space Programs Summary No. 37-35, v. IV, pp. 228-234, Jet Propulsion Lab., Calif. Inst. Tech., Pasadena, October 1965.

30. Wilhite, W.F., "Developments in Micro Gas Chromatography," Tech. Rept. 32-805, Jet Propulsion Lab., Calif. Inst. Tech., Pasadena, March 1966.

31. Wilhite, W.F., "Gas Chromatography Column Development for Analysis of the Martian Atmosphere," JPL Space Programs Summary No. 37-40, v. IV, pp. 119-123, Jet Propulsion Lab., Calif. Inst. Tech., Pasadena, August 1966.

32. Baer, S.R., and Benoit, G.L., "Chromatograph Test Facility," RPI Technical Report MP-19, Rensselaer Polytechnic Institute, Troy, New York, March 1971.

33. Meisch, A.J., "Binary Chromatographic Data and Estimation of Adsorbent Porosities," RPI Technical Report MP-31, Rensselaer Polytechnic Institute, Troy, New York, July 1973.

34. Lavoie, R.C., "Composition Dependent Effects in Gas Chromatography," RPI Technical Report MP-41, Rensselaer Polytechnic Institute, Troy, New York, May 1974.

35. Woodrow, P.T., "Analysis of Chromatographic Systems Using Orthogonal Collocation," RPI Technical Report MP-40, Rensselaer Polytechnic Institute, Troy, New York, May 1974.

36. Lashmet, P.K., and Woodrow, P.T., "Simulation of Pulsed, Distributed Systems Using Orthogonal Collocation," 78th National Meeting, American Institute of Chemical Engineers, Salt Lake City, Utah, August 1974.

37. Feinberg, M.P., "A Nonlinear Model for Gas Chromatograph Systems," M. Eng. Project Report, Rensselaer Polytechnic Institute, Troy, New York, May 1975.

38. Von Rosenberg, D.U., "Methods for the Numerical Solution of Partial Differential Equations," American Elsevier, New York, 1969.

39. Douglas, J., Jr., "The Application of Stability Analysis in the Numerical Solution of Quasi-Linear Parabolic Differential Equations," Trans. Am. Math. Soc., 89, 484-518 (1958).

A P P E N D I X A

AN ANALYSIS OF THE EDUCATIONAL IMPACT OF NASA GRANT NGL 33-018-091 OVER THE PAST EIGHT YEARS AT RENSSELAER POLYTECHNIC INSTITUTE

THE EDUCATIONAL IMPACT OF NASA GRANT NGL 33-018-091 AT RENSSELAER POLYTECHNIC INSTITUTE

I. INTRODUCTION

The project supported by NASA Grant NGL 33-018-091 was initiated in the Fall of 1967 and has continued to the present time. During this period of time the project goals have been modified to reflect technical progress at Rensselaer and elsewhere and in reaction to long-range NASA planetary goals. During the past four years, the project goals have been consolidated and focussed on problems related to the "housing, protecting, servicing and transporting" of scientific instrumentation by an unmanned roving vehicle for the exploration of the planet Mars.

As of this time, an imaginative vehicle concept has been conceived, designed, constructed and tested. In depth studies of terrain sensing concepts and devices, of obstacle (hazard) detection systems and of path selection systems simulation, development and appraisal, have been conducted and are continuing. All of these tasks focus on technical questions which NASA has judged to represent prime challenges to successful execution of an unmanned exploration of the planet Mars. These tasks and the additional program in optimal design of a gas chromatograph separation system were judged to be germane not only to NASA but also to the team of faculty members involved.

In appraising the value of this effort at Rensselaer over the past eight years two of NASA's original goals in establishing the program should be considered. One of these goals was to obtain technical support in developing a vehicle and related systems which would serve as a roving laboratory for unmanned exploration of Mars. The question of value with respect to this goal can be judged by individuals with technical competence and responsibilities. An indication of the productivity of the effort may be gained from the listing of reports and papers and presentations contained in Appendices A and B.

This summary report addresses the second of NASA's goals, namely, to provide meaningful educational experiences in design for engineering students at all educational levels. It is our conclusion that the program, which has involved some 188 student participants at all academic levels, has been an outstanding success in this regard. The basis for reaching this conclusion and a description of how the objectives of engineering design education are achieved are described below.

II. THE EDUCATIONAL PROCESS

In establishing the specific technical tasks, three criteria were employed:

1. The tasks must be relevant and critical to projected NASA missions,

2. The tasks must offer significant opportunity for the professional growth of the faculty involved and must be in areas where the faculty have special expertise,

3. The tasks must involve problems providing meaningful design experiences for participating students.

These criteria have guided the faculty team in proposing technical activities. During the past eight years some ten major tasks, Table I, have been explored and a very much larger number of sub-tasks have been pursued. Some 188 different students have participated in these various activities for periods of time ranging from one semester to three or more years. In appraising the value of the educational experience, the organization of the project, the student responsibilities, the reporting system, the role of the program monitors as well as the design process are worth reviewing.

II.A. Project Organization

The typical overall project organization is illustrated in Figure 1 which applied to the 1973-1974 academic year. The five major tasks are coordinated by a project director who does not have direct responsibility for the work of individual students. However, the project director working with the faculty responsible for each major task area, and at appropriate times with student participants, defines the major scopes, goals, targets and inter-relationships. The faculty responsible for the major tasks work with the student to define more detailed scopes, goals and targets consistent with the overall plan. Figure 2, which is typical, illustrates the organization of the vehicle tasks. Sub-tasks are themselves sub-divided and organized according to the needs of the sub-task.

One of the project director's major responsibilities is to identify "interface" activities between major tasks and to develop those inter-relationships between sub-task groups required to insure compatability of the technical effort. As noted in a later section, this aspect contributes in a very real way to the student's education in that the engineer is generally not free to optimize his solution to a particular problem without considering the impact of his proposal on other components of the system.

This organization also emphasizes the need for the two-way flow of information to assure that tasks are proceeding on schedule towards a consolidated goal.

II.B. Student Responsibilities

The student's responsibilities include: definition of his problem within the framework of the major goals which have been specified, specification of constraints and performance requirements, development of a schedule for achieving the defined goals, performance of the indicated task within the specified time and preparation of appropriate reports. These responsibilities represent a radical change in the student's academic experience. For the first time in his career, he is posed with defining his problem on the basis of reality and looking for imaginative and optimal solutions which are generally severely constrained. While it is true that he has the benefit of faculty review and guidance, he has to carry the main burden. Preparation of and adherence to a reasonable time schedule for a task which may last a full academic year or more is also a new and valuable experience as are the identification of key barriers to an acceptable solution and the perception of problem-solving as a planned and logical sequence. Not the least of his new experience is the need to convey through oral and written reports the consequences and worthiness of his investigations.

The student finds that his academic background rarely provides all the knowledge and tools that he will need to solve his problem. He must gain additional knowledge from textbooks, handbooks, vendor's materials, and technical journals. He may have to conduct special research to gain the necessary information. He will have to build or find alternatives to demonstrate the validity of his recommendations. This is sharp contrast to his regular course work where his assignments are inevitably tailored to the subject matter.

The student also finds that frequently the problem requirements extend beyond his nominal disciplinary interest. For example, many of the mechanical engineering students working on the vehicle frequently find that electrical and electronic considerations are of equal importance to the mechanical considerations in resolving the problem at hand.

II.C. The Reporting Responsibilities

The reporting responsibilities of the students are illustrated in Figure 3 which is a typical program schedule. The project work refers to the schedule developed by the student, his faculty advisor and the project director as discussed under Section II.B. The student is responsible for preparing brief written summary reports for the technical monitor prior to each of five or six progress review meetings. The student must also make an oral presentation using such audio-visual materials and demonstrations as appropriate at these review meetings. He is required to prepare material for the mid-year and end-of-year progress reports summarizing project progress for the interval. Finally, he is responsible for either as an individual or as a member of a team for writing detailed technical reports describing the investigations at key milestones. These technical reports receive wide distribution within NASA and other governmental agencies and interested industrial groups.

The educational benefit derived by these reporting experiences also contrasts sharply with normal academic programming. The student realizes for the first time that his documentation has the serious objective of conveying meaningful information to readers who are not necessarily familiar with the specific problem and who can be expected to be professionally critical. The faculty and the project director make it abundantly clear that the reporting is more than a nominal chore, and that quality reporting is vital not only for this project's purposes but also as a routine requirement of quality professional practice as an engineer.

II.D. The Role of the Program Monitors and Formal Presentations

During the past eight years, the students have benefited greatly from the involvement of program monitors representing the Jet Propulsion Laboratory. These monitors and other visitors selected on the basis of their particular expertise are present for the periodic progress review meetings at which the students make oral presentations of their work. The monitor has a multiple responsibility. He is a critic in the sense that he appraises the technical quality of the work. He also serves as a colleague in suggesting alternative approaches, methods, materials, etc. He provides valuable guidance in helping direct the work to useful purposes and is an important source of information.

From the student's view, the monitor is a client. The student's goal is to transmit clearly and concisely the state of his work to the monitor and to be able to respond effectively to questions, criticisms and suggestions.

The impact of the technical monitors, the selected guests, and the industrial and governmental visitors at the annual review is profound. The student realizes that he is facing a "hostile" audience and is no longer in the sheltered academic womb. The audience is not personally "hostile" but it is an audience of practicing professionals whose personal careers and challenges demand a certain level and quality of performance. The student realizes at an early point that his work is going to be judged on this more serious level. This realization has a substantial effect on how the student approaches his particular task and the intensity with which he applies himself as major milestones loom in the schedule.

II.E. The Design Process

Although there are many ways to describe the design process, the elements of the process inevitably include four major steps:

1. Problem definition, constraint identification and information gathering.
2. Development of alternative concepts.
3. Analysis of alternatives.
4. Decision making and implementation.

The process is inherently iterative since new information and knowledge may require a restatement of the problem, may offer new alternatives or may demand additional analysis. The objective is, of course, to try to minimize this activity but above all to move towards the strongest solution within the time constraints.

The student's experience implants firmly this type of a design procedure into his personality. He finds that these practical problems do not yield well to a haphazard attack; he finds by experience and example that they can be approached systematically and creatively. His faculty advisor's questions, the project director's inquiries and the monitor's comments reinforce dramatically the concepts of: Is this really the problem? Will your concept be compatible with the remaining system? Will it meet the established goal? Are there not better ways? etc. It is observed that the student's attitude and operational method have been strongly influenced by participation in this project.

III. STUDENT INVOLVEMENT AND PRODUCTIVITY

It was noted earlier that the participating faculty have concluded that the NASA's educational objectives in supporting these activities have been achieved to an exceptional degree. It is fair to inquire as to the basis of this conclusion since it is in the self-serving interest of the faculty involved to reach this favorable conclusion.

One measure of the quality of the educational experience in design lies in the solutions to the problems as proposed in the technical reports and/or represented by the hardware and software produced. On an overall basis, the faculty appraisal is very favorable. Although a minority of the students do not achieve the desired educational goals, the majority do demonstrate a substantial growth and maturation and some develop to an exceptional degree as evidenced by the technical reports listed in Appendix A. The faculty view appears to be supported by the favorable appraisals of the monitors and guests not only of the quality of the technical work but also of the presentations.

An alternative measure of the quality of the technical work is provided by the papers which have been published and the presentations which have been made at professional meetings. The diversity and extent of this activity is exhibited in Appendix B listing some 40 papers and presentations, the large majority of which are critically reviewed. This would suggest that the quality of the work is regarded as being professionally acceptable. It is worth noting that most of the papers are co-authored by faculty and students providing an additional enrichment of the students academic experience.

The quality of the student's work is also reflected by the fact that Rensselaer students received Second Prizes in the Graduate Division of contests sponsored by the Lincoln Arc Welding Foundation in both 1970 and 1971.

Perhaps the most compelling argument of all is the enthusiasm of students participating in the project over the years a evidenced by the number involved. Table II lists the number of participating students by their educational level for each of the eight years of the project. These data are also shown graphically in Figure 4. Some 188 students have had a significant involvement in the project including 8 doctoral degree, 110 master degree and 70 baccalaureate recipients. The involvement ranged from a minimum of one semester (relatively rare) to three years for most doctoral candidates. The average involvement of master's and bachelor's candidates is about one full academic year.

The strong student response, which has been growing as shown in Figure 4, is due primarily to the student's perception of project participation as a valuable as well as interesting educational experience. The very large majority of the students participate without receiving any financial support from project funds since the project can only provide such assistance for 5.5 to 6.0 full-time equivalent research assistants/yr or a maximum of 48 such assistantships over the years. Since the doctoral candidates probably represent some 20 F.T.E. assistantships during their residence, it is clear that the attractiveness of the project is due more to the student's perception of the worthiness of the experience and training and less to the prospects of financial support.

IV. DISCUSSION

In appraising the value of the project several questions deserve consideration:

1. Has the attitude and ability of the participating students to address and resolve engineering design problems been developed to the desired level?

2. Would these students have achieved these qualities in the absence of the project?

3. What have been the professional careers of these students following graduation?

4. What are the technological implications of this type of a NASA program?

Faculty related to the project and other faculty aware of the activity are convinced that the attitudes and abilities of the students towards engineering design have been strengthened substantially and that the majority of students take with them on graduation a unique perspective towards professional practice. This conviction, which is based on our intimate interactions with the students, is supported by the contents of the technical reports, publications and presentations listed in Appendices A and B. It is also supported by the reactions of our program monitors, guests and visitors and by the awards our students have received.

This experience in design provided to Rensselaer students is particularly germane since design education at engineering schools across the nation continues to represent a low priority to the academic faculties on average. Despite the pressures of the accreditation societies to restore vigorous, imaginative and in-depth education in design to its rightful place over the past fifteen years, strong programs in design remain relatively few in number and most design education is severely lacking in reality and relevance. This is not to infer that engineering students are not exposed to a reasonable number of courses that relate to design but rather that the emphasis is on standard approaches to well-defined areas within the disciplines involved. The students rarely have an opportunity to address open-ended problems with relevance and real need. It is our conviction that the large majority of the 188 students involved in this project would not have achieved these educational benefits in the absence of the NASA project.

The dilemma of providing meaningful experiences in design has been proclaimed in numerous publications over the past decade. The dilemma appears to be the result of two factors: (a) the real or imagined reward systems in engineering schools which emphasize scholarship in fundamental research areas and (b) the lack of real problems which are in fact relevant to some element of our society. These two factors are not unrelated. The first factor can be made less significant or be eliminated depending on the extent that industry and governmental agencies see fit to recognize and support relevant problem areas. Truly significant problems inevitably require faculty involvement of quality and this involvement will lead to new concepts and methods worthy of academic recognition.

It is in this respect that NASA's generous support over the years has had a profound impact on education at Rensselaer. Faculty participants do not have to be coerced to become involved. Their labors are rewarded not only by the satisfaction of helping these young people mature but also more tangibly by the respect shown by colleagues and supervisors. The project has not only produced good problem solutions for NASA but has also led to papers and presentations enhancing the faculty member's image at Rensselaer and elsewhere. The enthusiastic participation of faculty carries over to the students who

become attracted to the project. In turn, this reaction has led to widespread recognition of the project by the student body on the campus. During the past four years, th. "Mars Project" has been one of the highlight presentations to prospective students, at Parent's Weekends and at alumni affairs. The publicity the project received on campus has been instrumental in encouraging improvements in a number of design courses. Many students other than those participating on the project have gained in a more direct way because the participating faculty carry over these design concepts and experiences in courses which they are teaching. Thus there has been a direct impact on the teaching of design.

While these peripheral benefits are welcome, the long-lived impact has been on the students and faculty who have participated in project activities. Their attitudes, procedures and abilities have been molded in an irreversible manner. The key to these educational benefits has been NASA's willingness to provide: (1) problems of substance whose solutions are truly needed, and (2) the financial support to make the problem solving process possible. NASA's commitment to the project has had an unquestioned effect on faculty and student interests. The Jet Propulsion Laboratory's commitment in providing program monitors has had a similar effect. Without these commitments it is not believed that the in-depth involvement of Rensselaer faculty and students could have been maintained. Indeed, with NASA's moral and financial support, the project activity has intensified in time with the result that this year 37 students are participating in the program.

One of NASA's and other governmental agencies' major concerns with supporting educational activities at universities is that students may be encouraged to follow programs of study leading to specializations incompatible with national needs or interests. In some cases, these agencies have found it necessary to maintain research programs of basic long-term value but relatively low priority to provide reasonable employment for the resulting graduates. This has certainly not been the case of this project at Rensselaer. Summarized in Table III are the employment data of degree recipients over the three-year period, July 1, 1971 through June 30, 1974. Of the 41 graduates for whom we have data, all but three selected positions in the civilian economy. Only a small number of graduates were involved with aerospace concerns reflecting the reduction of emphasis on the space program in recent years. While we cannot document their activities with precision, the contacts we have had with a considerable number of these graduates indicate that the majority are using and benefiting from the skills they gained from the project. Samplings of the postgraduation activities of graduates of earlier years follow similar patterns. Thus, this project aimed at producing technology for NASA has had the by-product effect on contributing to the civilian economy.

Although the question of technological implications of this type of NASA program is not directly germane to the educational question, it is worthy of consideration. The vast majority of research projects at universities attract only those students for whom the projects provide stipends and tuition. As noted earlier, two-thirds and more of the effort has been provided by students who do not receive any direct financial support from the project. Their involvement is due to their interest in the individual problems and the project as a whole and to what, we believe, is their perception of the educational value of participation. Thus a project of this

type has the effect of "multiplying" NASA funds. A relatively modest level of support produces student and faculty efforts far greater than what can be expected on a direct quid pro quo basis. The technical productivity in terms of hardware and software far exceeds that which could reasonably be expected from a normal "business" relationship. Thus, over the years NASA has gained a substantial "leverage" on its funding in terms of the productivity.

The creativity inherent in young people and in faculty represents another aspect of the technological considerations. While it would be admitted that established aerospace vendors are without question far more qualified to design and produce the space-qualified hardware and software required for the missions, we would challenge with considerable vigor that such vendors can develop concepts more creatively. Indeed, we have some conviction that most industrial organizations cannot compete in this regard. As an example, the roving vehicle concept which has been developed over the past four years at Rensselaer is considered by many outsiders as a significant candidate for a planetary rover. It has some extraordinary features which are not possessed by any of the concepts proposed by industrial contributors. Neither the students nor the faculty are constrained by preconceptions as to what may be possible. The net effect is that the devices and systems which are proposed incorporate many novel features.

In summary, the project has provided an exceptional experience and opportunity for students and faculty. Both groups have been enriched significantly by the activity. A significant number of unusually qualified graduates have entered professional practice in the civilian sector and substantial technical contributions have been made to NASA and the public.

V. CONCLUSIONS

1. The objective of developing the ability of engineering students to resolve design problems of substance has been achieved without qualification. The students who have participated on the project have gained an experience which is rare at universities.

2. In the absence of the NASA support, these students would not have developed their ability in design to the levels which were achieved.

3. The eight faculty members who have been involved directly have gained valuable educational experiences which have carried over in their teaching and have impacted on the education of many more students.

4. The project activity attracted some 188 student participants including 8 doctoral, 110 masters and 70 bachelor degree recipients over the past 8 years. Less than one-third of the participating students received stipend and/or tuition support from the project.

5. The project's success in attracting such large number of students is due primarily to:

(a) NASA's commitment in providing "real" problem opportunities and the support for seeking further solutions, and

(b) JPL's commitment in providing interested and effective program monitors.

6. The very large majority of graduates entered the civilian economy and are contributing to the national interest in widely diverse fields.

7. The technological productivity of the project far exceeded expectations for the funding levels involved. This is due to the large number of students participating without compensation. Thus, a very substantial "leverage" of NASA funds was obtained.

8. The technical contributions to the NASA programs and to the nation at large were substantial and are reflected in hardware and software which was produced. These results have been disseminated to the public through almost 50 technical reports and some 40 papers and presentations at professional society meetings.

9. The inherent creativity of young people is amply demonstrated by the hardware and software which was developed in response to the problems which were addressed.

RENSSELAER MARS PROJECT ORGANIZATION

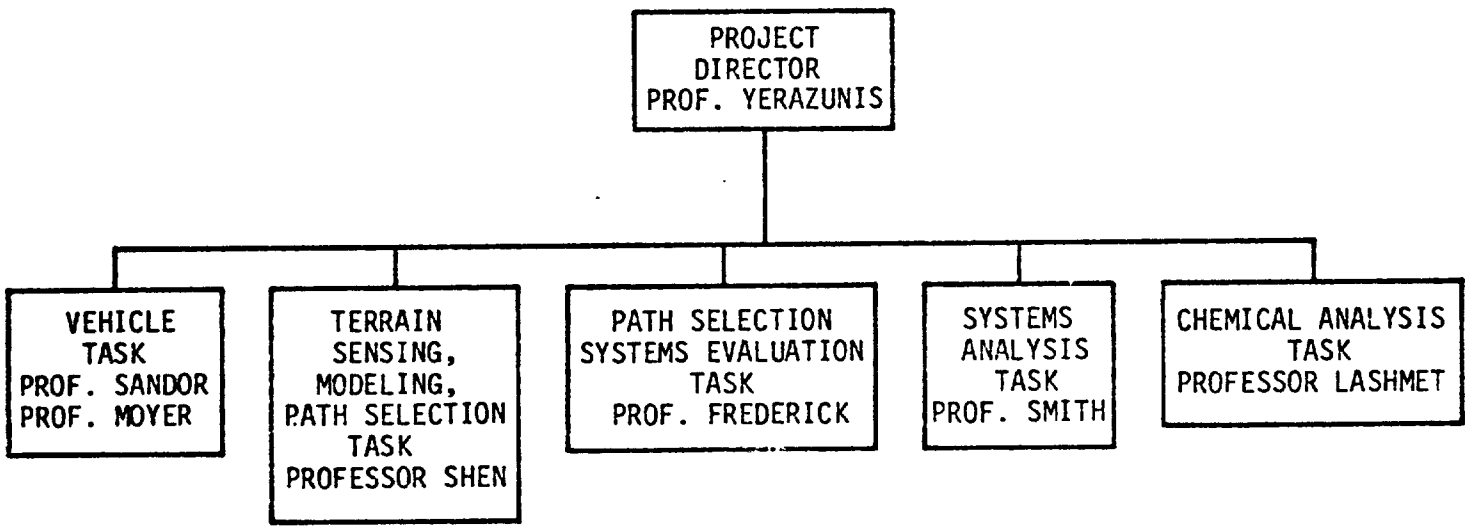

Figure 1. Typical Project Organization

VEHICLE TASK ORGANIZATION

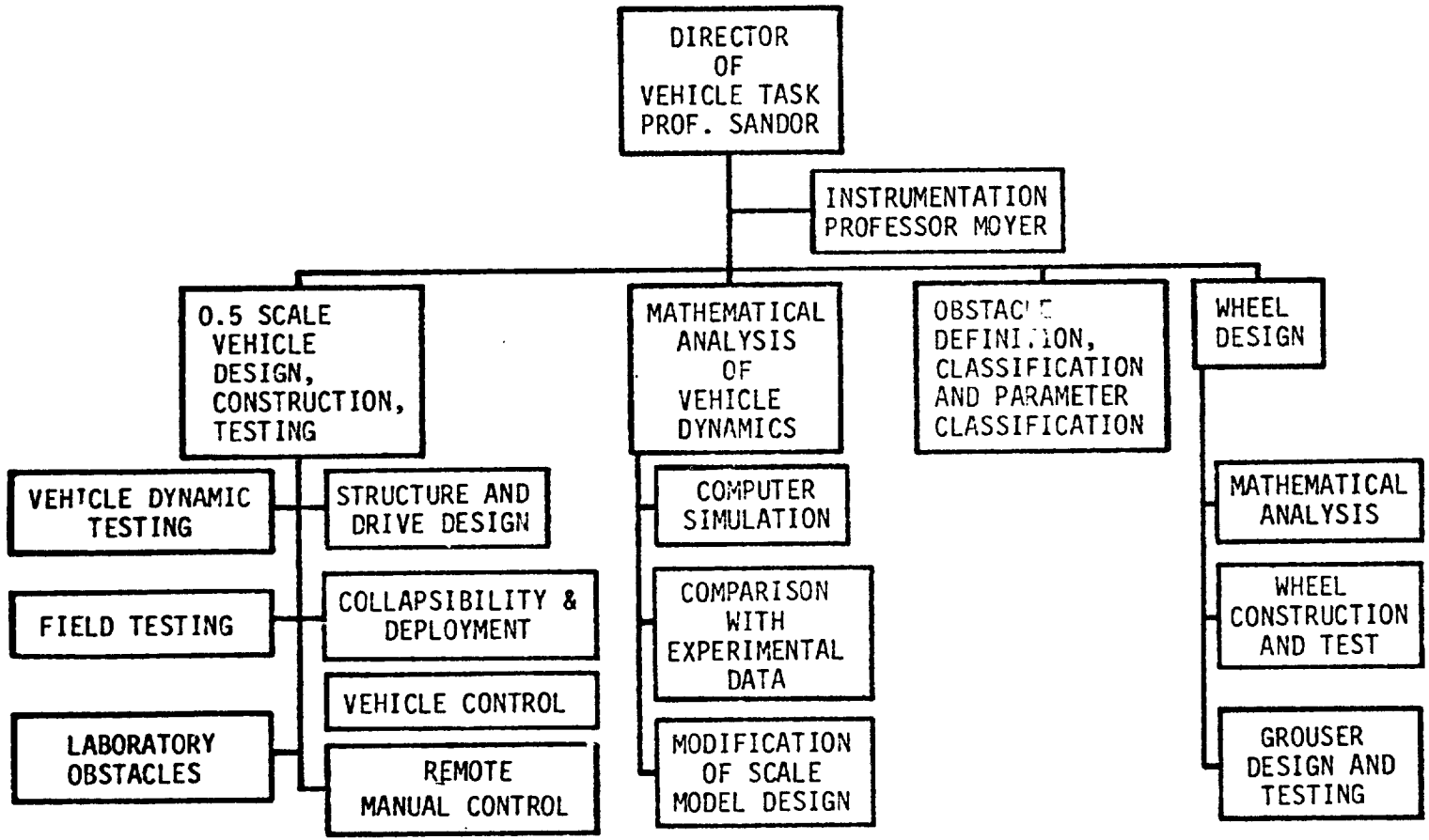

Figure 2. Vehicle Task Organization

TYPICAL PROGRAM SCHEDULE

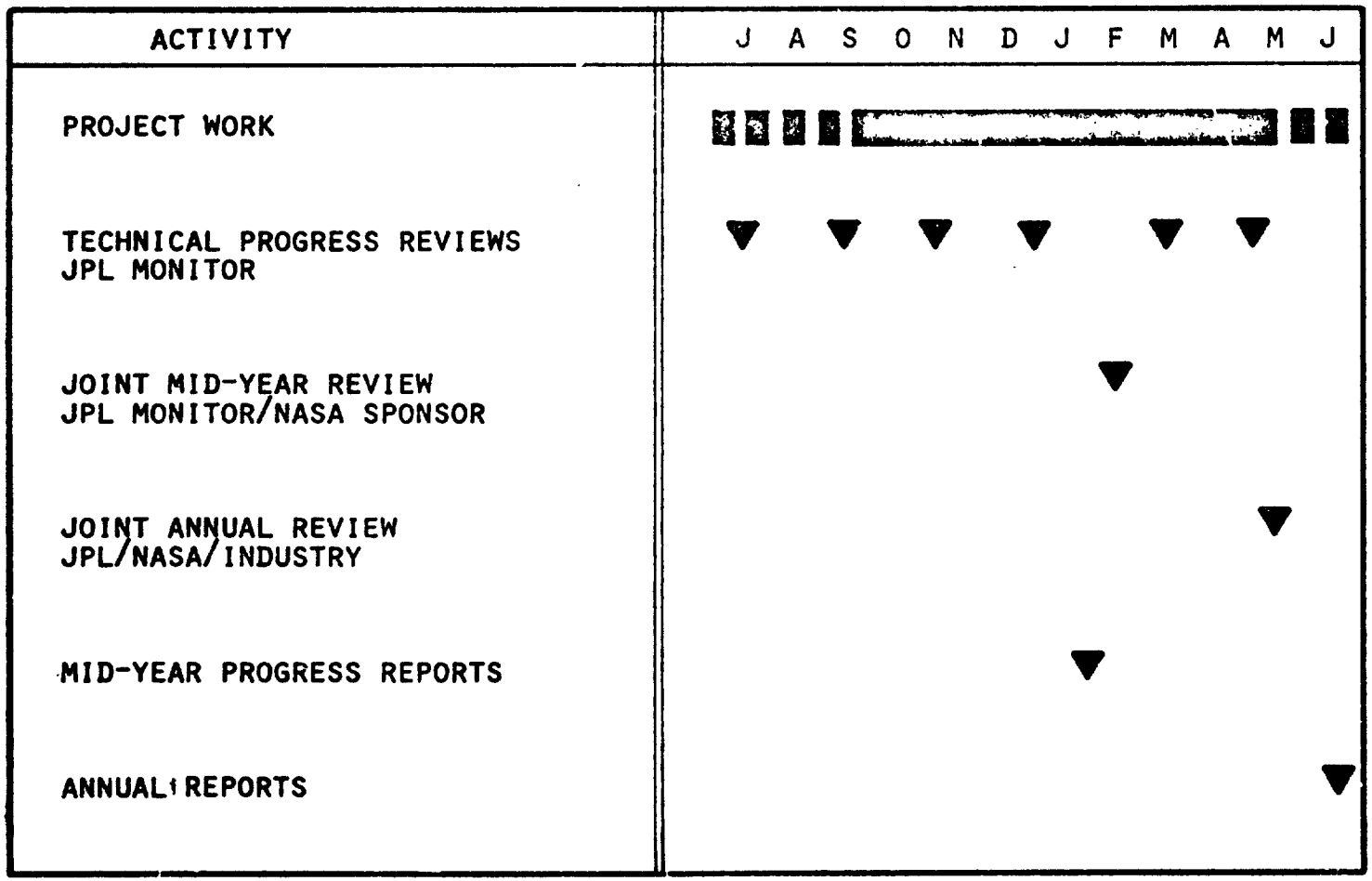

Figure 3. Typical Program Schedule

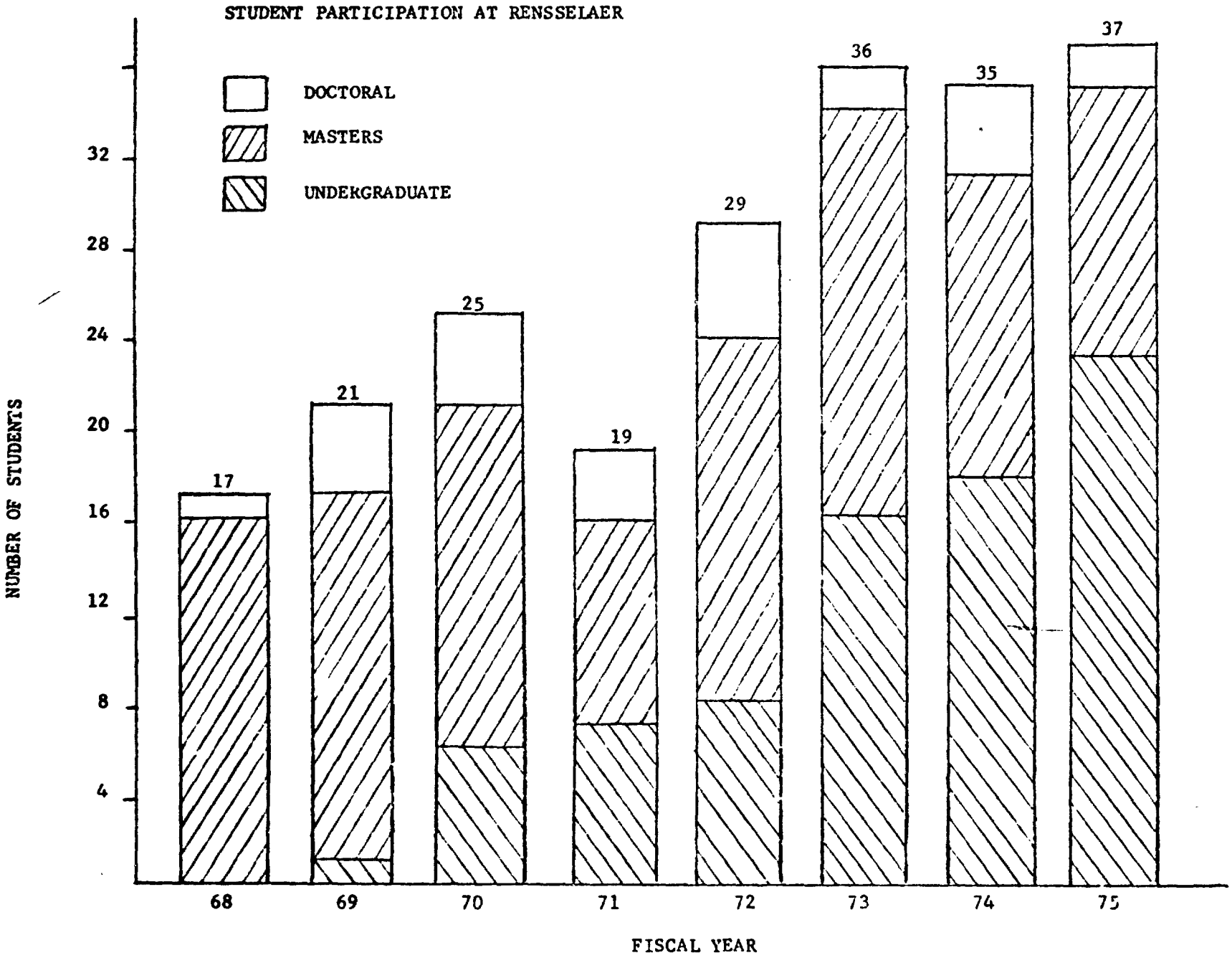

Figure 4. Student Participation at Rensselaer

TABLE I

SUMMARY OF MAJOR TASKS

On-Line Updating of Martian Atmosphere Parameters during Entry

Adaptive Trajectory Control

Feasibility of Autogyro Landing System

Global Navigation of a Mars Roving Vehicle

Optimization of an Unmanned Mars Surface Exploration Mission

Design, Construction and Evaluation of a Mars Roving Vehicle

Obstacle Detection and Terrain Modeling for an Autonomous Rover

Hazard Detection Systems

Path Selection Systems Simulation, Development and Evaluation

Chemical Analysis Systems Design

TABLE II

STUDENT PARTICIPATION IN THE NASA-SUPPORTED
MARS EXPLORATION PROJECT

	1968	1969	1970	1971	1972	1973	1974	1975
Doctoral Students	1	4	4	3	5	2	4	2
Masters Students	16	16	15	9	16	18	13	12
Bachelors Students	-	1	6	7	8	16	18	23
	17	21	25	19	29	36	35	37

	Total Participants[1]	Degrees Granted[2]
Doctoral Students	26	8
Masters Students	115	110
Bachelors Students	79	70
	220	188

(1) The number of participants exceeds the number of degrees granted because some students participate for more than one year.

(2) The number of degrees is estimated.

TABLE III

EMPLOYMENT OF PARTICIPANTS FOLLOWING GRADUATION, 1972-1974[1]

IBM	5
General Electric	5
Raytheon	4
Eastman Kodak	3
Rohm and Haas	2
Armed Forces	1
U.S. Air Force Academy	1
Construction Ind.	1
Belfates & Pavarini, Arch.	1
Turnkey Systems, Inc.	1
Proctor and Gamble	1
Burroughs	1
Rochester Telephone	1
Sanders Associates	1
Union Carbide	1
General Motors	1
Pratt and Whitney	1
Sikorsky	1
Babcock & Wilcox	1
Bell Laboratory	1
Naval Architecture Lab	1
Stone and Webster	1
Hewlitt Packard	1
Corning Glass	1
U.S.Government Lab	1
Western Electric	1
Returned to India	1
	41

(1) The total number of degrees earned by participants during the academic years, July 1, 1971 through June 30, 1974 is estimated at 57. Since alumni employment records are seldom complete, our knowledge of employment following graduation is limited to 41 of these students.

APPENDIX A

RPI TECHNICAL REPORTS

Sliva, Thomas F., "Chromatographic Systems Analysis: First-Order Model Evaluation," RPI Technical Report MP-1, Rensselaer Polytechnic Institute, Troy, N.Y., September 1968.

Janosko, R.E., "On-Line Parameter Updating of the Martian Atmosphere with Minimum Storage," RPI Technical Report MP-2, Rensselaer Polytechnic Institute, Troy, N.Y., January 1968.

Frederick, D.K., et al., "Analysis and Design of a Capsule Landing System and Surface Vehicle Control System for Mars Exploration," RPI Progress Report MP-3, Rensselaer Polytechnic Institute, Troy, N.Y., February 1969.

Frederick, D.K., et al., "Analysis and Design of a Capsule Landing System and Surface Vehicle Control System for Mars Exploration," RPI Progress Report MP-4, Rensselaer Polytechnic Institute, Troy, N.Y., July 1969.

Hedge, L.F., "Trajectory Control for Mars Entry by Discrete Changes of Drag Surface and Flight Path," RPI Technical Report MP-5, Rensselaer Polytechnic Institute, Troy, N.Y., August 1969.

LaBarbera, G., "Short Range Obstacle Detection Systems," RPI Progress Report MP-6, Rensselaer Polytechnic Institute, Troy, N.Y., September 1969.

Rayfield, W.P., "The Design Study of a Lightweight Rotor Hub for a Mars-Landing Autogyro," RPI Technical Report MP-7, Rensselaer Polytechnic Institute, Troy, N.Y., September 1969.

Voytus, W.A., "Chromatographic Systems Analysis: Moment Analysis of the Equilibrium Adsorption Model," RPI Progress Report MP-9, Rensselaer Polytechnic Institute, Troy, N.Y., August 1969.

Krum, R.C., "Chromatographic Systems Analysis: Sample Injection Problem," RPI Progress Report MP-10, Rensselaer Polytechnic Institute, Troy, N.Y., August 1969.

Mancini, R.J., "Terrain Modeling for Surface Vehicle Guidance," RPI Technical Report MP-11, Rensselaer Polytechnic Institute, Troy, N.Y., August 1969.

Frederick, D.K., et al., "Analysis and Design of a Capsule Landing System and Surface Vehicle Control System for Mars Exploration," RPI Technical Report MP-12, Rensselaer Polytechnic Institute, Troy, N.Y., March 1970.

Wilson, J.V., "Instrumentation Study of Primary Navigation System for a Mars Roving Vehicle," RPI Technical Report MP-13, Rensselaer Polytechnic Institute, Troy, N.Y., May 1970.

Pavarini, C., and Chrysler, Jr., J.H., "Terrain Modeling and Path Selection by an Autonomous Martian Exploratory Vehicle," RPI Technical Report MP-14, Rensselaer Polytechnic Institute, Troy, N.Y., June 1970.

Frederick, D.K., et al., "Analysis and Design or a Capsule Landing System and Surface Vehicle Control System for Mars Exploration," RPI Technical Report MP-15, Rensselaer Polytechnic Institute, Troy, N.Y., July 1970.

RPI TECHNICAL REPORTS (Continued)

Rayfield, W.P., "Mars Roving Vehicle Configuration," RPI Technical Report MP-16, Rensselaer Polytechnic Institute, Troy, N.Y., August 1970.

Goldberg, A.L., and Frankel, P.J., "A Body-Bound Navigation System," RPI Technical Report MP-17, Rensselaer Polytechnic Institute, Troy, N.Y., June 1970.

Frederick, D.K., et al., "Analysis and Design of a Capsule Landing System and Surface Vehicle Control System for Mars Exploration," RPI Technical Report MP-18, Rensselaer Polytechnic Institute, Troy, N.Y., January 1971.

Baer, S.R., and Benoit, G.L., "Chromatographic Test Facility," RPI Technical Report MP-19, Rensselaer Polytechnic Institute, Troy, N.Y., March 1971.

Rieback, D.J., "Preliminary Design of an Automatic Device for the Location of the Pole Star and/or True Pole of Mars," RPI Technical Report MP-20, Rensselaer Polytechnic Institute, Troy, N.Y., May 1971.

Simon, R.L., "Design of a Toroidal Wheel for a Martian Roving Vehicle, RPI Technical Report MP-21, Rensselaer Polytechnic Institute, Troy, N.Y., May 1971.

Benoit, G.L., "Reduction of Chromatographic Data and Evaluation of a GC Model," RPI Technical Report MP-22, Rensselaer Polytechnic Institute, Troy, N.Y., June 1971.

Frederick, D.K., et al., "Analysis and Design of a Capsule Landing System and Surface Vehicle Control System for Mars Exploration," RPI Technical Report MP-23, Rensselaer Polytechnic Institute, Troy, N.Y., July 1971.

Pavarini, C., Baker, J., and Goldberg, A., "An Optimal System Design Process," RPI Technical Report MP-24, Rensselaer Polytechnic Institute, Troy, N.Y., Nov. 1971.

Frederick, D.K., et al., "Analysis and Design of a Capsule Landing System and Surface Vehicle Control System for Mars Exploration," RPI Technical Report MP-25, Rensselaer Polytechnic Institute, Troy, N.Y., July 1 to Dec. 31, 1971.

Zuraski, G.D., "Laser Range Measurement for a Satellite Navigation Scheme and Mid-Range Path Selection and Obstacle Avoidance," RPI Technical Report MP-26, Rensselaer Polytechnic Institute, Troy, N.Y., June 1972.

Keba, P.S., and Woodrow, P.T., "Comparison of Two Gas Chromatograph Models and Analysis of Binary Data," RPI Technical Report MP-27, Rensselaer Polytechnic Institute, Troy, N.Y., July 1972.

Frederick, D.K., et al., "Analysis and Design of a Capsule Landing System and Surface Vehicle Control System for Mars Exploration," RPI Technical Report MP-28, Rensselaer Polytechnic Institute, Troy, N.Y., July 1, 1971 to June 30, 1972.

Boheim, S.L., and Purdon, W.C., "Path Selection System Simulation and Evaluation for a Martian Roving Vehicle," RPI Technical Report MP-29, Rensselaer Polytechnic Institute, Troy, N.Y., December 1972.

Frederick, et al., "Analysis and Design of a Capsule Landing System and Surface Vehicle Control System for Mars Exploration," RPI Technical Report MP-30, Rensselaer Polytechnic Institute, Troy, N.Y., July 1, 1972 to Dec. 31, 1972.

RPI TECHNICAL REPORTS (Continued)

Meisch, A.J., "Binary Chromatographic Data and Estimation of Adsorbent Porosities," RPI Technical Report MP-31, Rensselaer Polytechnic Institute, Troy, N.Y., July 1972.

Pfeifer, W.J., "Gradient Estimates from Stereo Measurements for a Martian Vehicle," RPI Technical Report MP-32, Rensselaer Polytechnic Institute, Troy, N.Y., May 1973.

Burger, Paul A., "Stochastic Estimates of Gradient from Laser Measurements for an Autonomous Martian Roving Vehicle," RPI Technical Report MP-33, Rensselaer Polytechnic Institute, Troy, N.Y., May 1973.

Herb, G.T., "Laser Scanning Methods and a Phase Comparison, Modulated Laser Range Finder for Terrain Sensing on a Mars Roving Vehicle," RPI Technical Report MP-34, Rensselaer Polytechnic Institute, Troy, N.Y., May 1973.

Frederick, D.K., et al., "Analysis and Design of a Capsule Landing System and Surface Vehicle Control System for Mars Exploration," RPI Technical Report MP-35, Rensselaer Polytechnic Institute, July 1, 1972 to June 30, 1973.

Woodrow, P.T., "Preliminary Numerical Analysis of Improved Gas Chromatograph Model," RPI Technical Report MP-36, Rensselaer Polytechnic Institute, Troy, N.Y., Sept. 1973.

Palumbo, D.L., "Design of a Laser Rangefinder for Martian Terrain Measurements," RPI Technical Report MP-37, Rensselaer Polytechnic Institute, Troy, N.Y., May 1973.

Ryder, Alan G., "Dynamic Evaluation of RPI's 0.4 Scale Unmanned Martian Roving Vehicle Model, RPI Technical Report MP-38, Rensselaer Polytechnic Institute, December 1973.

Frederick, D.K., et al., "Analysis and Design of a Capsule Landing System and Surface Vehicle Control System for Mars Exploration," Rensselaer Polytechnic Institute, RPI Technical Report MP-39, February 1974.

Woodrow, P.T., "Analysis of Chromatograph Systems Using Orthogonal Collocation," RPI Technical Report MP-40, Rensselaer Polytechnic Institute, Troy, N.Y., May 1974.

Lavoie, R.C., "Composition Dependent Effects in Gas Chromatography," RPI Technical Report MP-41, Rensselaer Polytechnic Institute, Troy, N.Y., May 1974.

Campbell, R.S. and Simonds, R.R., "Path Selection System Development and Evaluation for a Martian Roving Vehicle," RPI Technical Report MP-42, Rensselaer Polytechnic Institute, Troy, N.Y., May 1974.

Pavarini, Carl, "System Design Optimization for a Mars-Roving Vehicle and Perturbed-Optimal Solutions in Nonlinear Programming," RPI Technical Report MP-43, Rensselaer Polytechnic Institute, Troy, N.Y., June 1974.

Frederick, D.K., et al., "Analysis and Design of a Capsule Landing System and Surface Vehicle Control System for Mars Exploration," Rensselaer Polytechnic Institute, RPI Technical Report MP-44, July 1, 1973 to June 30, 1974.

RPI TECHNICAL REPORTS (Continued)

Reed, Martin A., "Recognition of Three Dimensional Obstacles by an Edge Detection Scheme, RPI Technical Report MP-45, Rensselaer Polytechnic Institute, Troy, N.Y., May 1974.

D'Angelo, Kenneth R., "Parameter Estimation for Terrain Modeling from Gradient Data," RPI Technical Report MP-46, Rensselaer Polytechnic Institute, Troy, N.Y., May 1974.

APPENDIX B

RPI Papers and Presentations

Shen, C.N., and P. J. Cefola, "Adaptive Trajectory Control for Mars Entry Based on Sensitivity Analysis," AIAA 68-835, AIAA Guidance, Control and Flight Dynamics Conference, Pasadena, Calif., August 1968. (Accepted for publication in the AIAA Journal).

Cefola, P.J. and Shen, C.N., "Vector-Matrix Second Order Sensitivity Equation with Application to Mars Entry," AIAA Journal, 7, No. 8, 1633 (1969).

Shen, C.N., and Cefola, P.J., "Adaptive Control for Mars Entry Based on Sensitivity Analysis," AIAA Journal, 7, No. 6, 1145 (1969).

Shen, C.N., and Janosko, R., "On-Line Parameter Updating of the Martian Atmosphere with Minimal Storage," Proceedings of the Second Hawaii International Conference on System Sciences at the University of Hawaii, January 1969.

Broniarek, C.A. and Sandor, G. N., "Nonlinear Vibration Analysis of Four-Wheel Surface Vehicle with Flydraulic Driving System," presented at and published in the Proceedings of the Second International Congress on the Theory of Machines and Mechanisms, Zakopane, Poland, Sept. 24-27, 1969, Vol. 2, pp. 45-55.

Shen, A.N., and Yong, K., "On-Line Tracking of Space Vehicles Using Modified Sequential Estimation," Proceedings 3rd Hawaii International Conference on System Science, 1970.

Sandor, G.N., and Rayfield, W.P., "Dragster on Mars," ASME News, Hudson Mohawk Section, Vol. 7, No. 3, January-February, 1970, pp. 3-7.

Janosko, R.E., and Shen, C.N., "Consecutive Tracking of Landmarks: by an Active Satellite and then by a Martian Roving Vehicle," Proceedings 3rd Hawaii International Conference on System Science, 1970.

Duke, J.C., and Shen, C.N., "Optimal Filtering for Nonlinear Parameter Updating of the Martian Atmosphere," Proceedings of the Symposium for International Federation Automatic Control, Kyoto, Japan, August 1970.

Rayfield, W.P., and Sandor, G.N., "Rensselaer's Roving Vehicle for Mars," presented at the First Western Space Congress, Santa Maria, Calif., October 27-29, 1970, published in Proceedings, pp. 838-855.

Chen, H.M., and Shen, C.N., "Surface Navigation System and Error Analysis for Martian Rover," Proceedings of the Fourth Hawaii International Conference on System Sciences, January 1971.

Rayfield, W.P., and Sandor, G.N., "Design of a Roving Vehicle for Mars," Invited Paper, presented at the ASME Design Engineering Conf., New York, N.Y., April 19-22, 1971.

Duke, J.S., and Shen, C.N., "On-Line Parameter Updating for Mars Stratosphere and Troposphere," Proceedings of the AIAA-Joint Automatic Control Conference at St. Louis, Mo., August 1971.

Cefola, P.J., and Shen, C.N., "A Parameter Dependent Spacecraft Guidance Boundary Value Problem," AIAA Journal, Vol. 9, #10, pp 1975-1979, October 1971.

Sandor, G.N., "Rensselaer's Roving Vehicle for Mars: Lessons for Possible Clinical Applications," Medical Society of N.Y., 16th Annual Convention, Feb. 1972.

RPI Papers and Presentations (continued)

Sandor, G.N., "Motorized Wheel Chair Can Even Climb Stairs," (German), Medical Tribune, an international weekly, German language issue for West Germany, Vol. 7, No. 11, Fri., Mar. 17, 1972, published in Wiesbaden, pp. 1 & 48; and also in the German language issue of the same weekly published in Baden for Switzerland, Vol. 5, No. 11, Fri., Mar. 17, 1972, pp. 1 & 20.

Sandor, G.N., "Wheel Chair Can Elevate to Eye Level," Chronic Disease Management Vol. 6, No. 4, April 1972, p. 18.

Yerazunis, S., Moore, J.W., and Wehe, R. L., "Unmanned Exploration of Mars: A NASA-University Experiment in Engineering Education," American Chemical Society Industrial-Academic Cooperation Symposium, Boston, April 1972 (with Cornell and JPL).

Janosko, R.E., and Shen, C.N., "A Simplified Satellite Navigation System for an Autonomous Mars Roving Vehicle," Proceedings of the Fifth Congress of International Federation of Automatic Control at Paris, France, June 1972.

Broniarek, C.A., and Sandor, G.N., "On Surface Vehicle Body Motion with Gyroscopic Storage of Kinetic Energy," Mechanism and Machine Theory, Vol. 7, No. 2, Summer 1972, pp. 141-154.

Pavarini, C., Smith, E.J., Van Denburg, N., "System Modeling and Optimal Design of a Mars Roving Vehicle," Proceedings of IEEE Conference on Decision and Control, New Orleans, La., December 1972.

Shen, C.N., and Burger, P., "Stochastic Estimates of Gradients from Laser Measurements for an Autonomous Martian Roving Vehicle," Proceedings of 3rd IFAC Symposium, The Hague, June 1973.

Sandor, G.N., "Unmanned Martian Roving Vehicle Inspires Stairclimbing Wheel Chair," New York State Journal of Medicine, Dec. 15, 1973, Vol. 73, No. 24, pp. 2880-2883.

Shen, C.N., and D'Angelo, R.P., "Parameter Estimation for Terrain Modeling from Gradient Data," 7th Hawaii International Conference on System Sciences, Hawaii, January 1974.

Burr, A.A. and Sandor, G.N., "Teaching Problem-Solving at Rensselaer," invited paper, Journal of Engineering Education, February 1974, Vol. 64, No. 5, pp. 357-359. (Describes RPI's NASA Mars Rover Design Project).

Reed, M., Sanyal P., and Shen, C.N., "A Practical Obstacle Detection System for the Mars Rover," Proceedings of the Milwaukee Symposium on Automatic Controls, March 1974, Milwaukee, Wisconsin.

Sandor, G.N., "Seven Dangers of Designer Overspecialization and How to Avoid Them by Designer Education," Invited ASME Paper No. 74-DE-35, 1974 Design Engineering Conference, Chicago, April 1-4, 1974, to be preprinted by the ASME in full and to be published in abstract in Mechanical Engineering, Journal of the ASME. (Educational Aspects of RPI's NASA Mars Rover Design Project as Conducted in EDL - (RPI's Engineering Design Laboratory, George N. Sandor, Director.))

Sandor, G. N., "Seven Dangers of Designer Overspecialization and How to Avoid Them by Designer Education," Electromechanical Design, March 1974.

Lashmet, P.K. and Woodrow, P.T., "Simulation of Pulsed, Distributed Systems Using Orthogonal Collocation," Salt Lake City Meeting, American Institute of Chemical Engineers, August 1974.

Lashmet, P.K., Benoit, G.L. and Woodrow, P.T., "Evaluation of a Gas Chromatograph Model," Atlantic City Meeting, American Chemical Society, September 1974.

RPI Papers and Presentations (Continued)

Sandor, G.N., Hassel, David R. and Marino, Philip F., "Modern Mechanisms Make Manless Martian Mission Mobile -- "Spin-Off" Spells Stairclimbing Self-Sufficiency for Earthbound Handicapped", Proceedings of 9th Aerospace Mechanisms Symposium, 18-1 to 18-17, John F. Kennedy Space Center, October 1974.

Shen, C. N. and J. S. Sher, "Simulation of the Range Data and The Picture Enhancing Scheme for the Mars Rover", ACM 1975 Computer Science Conference, Washington, D.C., February 1975.

Shen, C.N. and Audbur Thompson, "Computer Results of Two Dimensional Spline Function in Terrain Modeling Optimization", ACM 1975 Computer Science Conference, Washington, D. C., February 1975.

Shen, C.N. and Mark Friedman, "The Effect of Laser Measurement Reflection Error on Range Data Processing", Milwaukee Symposium on Automatic Computation and Control, Milwaukee, Wisconsin, April 1975.

Shen, C.N. and R. V. Sonalkar, "Mars Obstacle Detection by Rapid Estimation Scheme From Noisy Laser Rangefinder Readings",Milwaukee Symposium on Automatic Computation and Control, Milwaukee, Wisconsin, April 1975.

Shen, C.N. and M. Friedman, "Measurement Scanning Schemes for Terrain Modeling", 6th Annual Pittsburgh Conference on Modeling and Simulation, Pittsburgh, Pa., April 1975.

Shen, C. N., Leung, K.L, Yerazunis, S., "Classification of Terrain Models for Martian Vehicle," 6th Annual Pittsburgh Conference on Modeling and Simulation, Pittsburgh, Pa., April 1975.

Frederick, D.K., "Path Selection System Simulation and Evaluation for a Martian Roving Vehicle", 6th Annual Pittsburgh Conference on Modeling and Simulation, Pittsburgh, Pa., April 1975.

Woodrow, P.T. and Lashmet, P.K., "A Formulation Consideration for Orthogonal Collocation Procedures", AICA International Symposium on Computer Methods for Partial Differential Equations, Bethelehem, Pa., June 1975.

Woodrow, P.T. and Lashmet, P.K., "Zero-Derivative Boundary Conditions for Pulsed Distributed Systems", AICA International Symposium on Computer Methods for Parial Differential Equations, Bethlehem, Pa., June 1975.